SPERMATOGONIAL STEM CELLS AND THEIR ENDOCRINE AND PARACRINE REGULATION IN ZEBRAFISH

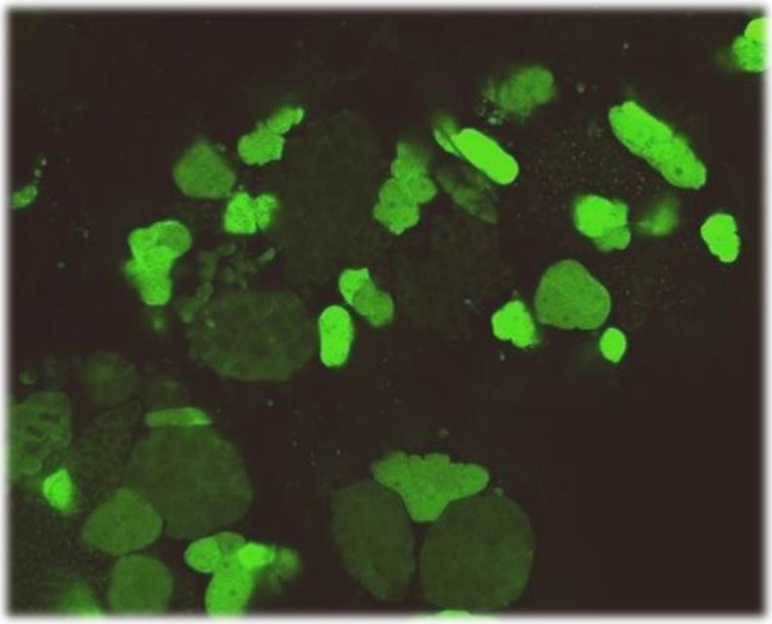

RAFAEL HENRIQUE NÓBREGA

Promotion Committee

Promotor: Prof. dr. S.J.L. van den Heuvel

Co-Promotors: Dr. R.W. Schulz

Dr. J. Bogerd

Members: Prof. dr. A. Akhmanova

Prof. dr. M.R. Egmond

Prof. dr. D.J. van der Horst

Prof. dr. R. Male

Prof. dr. D.G. de Rooij

Prof. dr. A.P.N. Themmen

Paranymphs: H.J.G. van de Kant

J.C.M. Granneman

Printed by: Wöhrmann Print Service. Zutphen

Layout and cover: Rafael Henrique Nóbrega

Image cover: Dr. Rüdiger W Schulz. Testis from a trasgenic *vasa::egfp* zebrafish examined under a confocal scanning laser microscope (CSLM).

The research described in the present thesis was perfomed at Division of Developmental Biology, Departament of Biology, Sicence Faculty, University of Utrecht, The Netherlands.

SPERMATOGONIAL STEM CELLS AND THEIR ENDOCRINE AND PARACRINE REGULATION IN ZEBRAFISH

SPERMATOGONIALE STAMCELLEN, EN HUN PARACRIENE EN ENDOCRIENE REGULATIE IN DE ZEBRAVIS

(met een samenvatting in het Nederlands)

PROEFSCHRIFT

ter verkrijging van de graad van doctor aan de Universiteit Utrecht op gezag van de rector magnificus, prof.dr.G.J. van der Zwaan, ingevolge het besluit van het college voor promoties in het openbaar te verdedigen op dinsdag 2 december 2014 des middags te 12.45 uur

door

Rafael Henrique Nóbrega

geboren 31 mei 1981 te Campinas, Brazilië

PROMOTOR: PROF.DR. S.J.L. VAN DEN HEUVEL

COPROMOTOREN: DR. R.W. SCHULZ

DR. J. BOGERD

This thesis was (partly) accomplished with financial support from Brazilian funding agencies (CNPq/FAPESP), the European Union (LIFECYCLE project FP7-222719), and the Norwegian Research Council (project no. 159045).

TABLE OF CONTENTS

CHAPTER 1 **07**
General Introduction

CHAPTER 2 **29**
Histological and Stereological Evaluation of Zebrafish (*Danio Rerio*)
Spermatogenesis with an Emphasis on Spermatogonial Generations

CHAPTER 3 **73**
Spermatogonial Stem Cell Niche and Spermatogonial Stem Cell
Transplantation in Zebrafish

CHAPTER 4 **121**
Studies in Zebrafish Reveal Unusual Cellular Expression Patterns
of Gonadotropin Receptor Messenger Ribonucleic Acids in the
Testis and Unexpected Functional Differentiation of the Gonadotropins

CHAPTER 5 **162**
Proteolytically Activated, Recombinant Anti-Müllerian Hormone
Inhibits Androgen secretion, Proliferation, and Differentiation
of Spermatogonia in Adult Zebrafish Testis Organ Cultures

CHAPTER 6 **208**
Fsh Promotes Zebrafish Spermatogonial Proliferation
and Differentiation Through Igf3, a New Igf Family Member

CHAPTER 7 **253**
Summarizing Discussion

SUMMARY **269**

SAMENVATTING **270**

ACKNOWLEDGEMENTS **273**

CURRICULUM VITAE **276**

CHAPTER 1

GENERAL INTRODUCTION

1. **General Introduction**

1.1 Spermatogenesis –*an overview*

Spermatogenesis is a stem cell-driven developmental process, in which a single, diploid spermatogonium, the spermatogonial stem cell (SSC) produces many haploid, motile gametes, the spermatozoa. This process can be divided in three phases. The first one is the mitotic or spermatogonial phase. In this phase, the main increase in germ cell number occurs during successive rounds of mitotic duplication of the spermatogonia. Interestingly, the number of spermatogonial generations (and hence the number of mitotic divisions they undergo before differentiating into spermatocytes) varies between but not within species. For example, the number of spermatogonial generations can be as little as 2 (humans) and as much as 14 (guppy), but in many species, 5-8 generations are found (Schulz et al., 2010)**.** In this phase, a peculiar behavior upon the spermatogonial division is seen in all animals. At the end of the mitoses leading towards the production of sperm cells, incomplete cytoplasm division (cytokinesis) occurs, and the two new spermatogonia remain interconnected by a cytoplasmic bridge, instead of forming two individual, single cells (Figure 1A,B). However, the cytoplasmic bridges are not present in the descendants from a given SSC, which enters a self-renewal pathway, where two, single, isolated daughter cells are generate at the end of mitosis. Therefore, cytoplasmic bridges can be a marker of SSC differentiation, and these bridges are formed during all subsequent germ cell divisions (Figure 1B). Therefore, all differentiating descendants from a given SSC form a clone whose members stay interconnected by cytoplasmic bridges, through which their developmental steps are synchronized (Figure 1A). These

bridges are broken when spermatogenesis is completed and germ cells leave the germinal epithelium as spermatozoa.

When entering the second phase, meiosis, the spermatogonia differentiate into spermatocytes that go through the two meiotic divisions. These are characterized by reshuffling of the paternal and maternal genetic information via crossing over during the first meiotic division and the reduction to a haploid genome during the second meiotic division.

During the third phase, spermiogenesis, the haploid spermatids emerging from meiosis differentiate – without further proliferation – into flagellated spermatozoa. The morphological changes in germ cells taking place during spermiogenesis are quite similar among different species (e.g. reduction in cytoplasmic volume and organelles, maximum DNA condensation, differentiation of a flagellum). However, the final shape of the spermatozoa can differ between species and sometimes provides taxonomic clues.

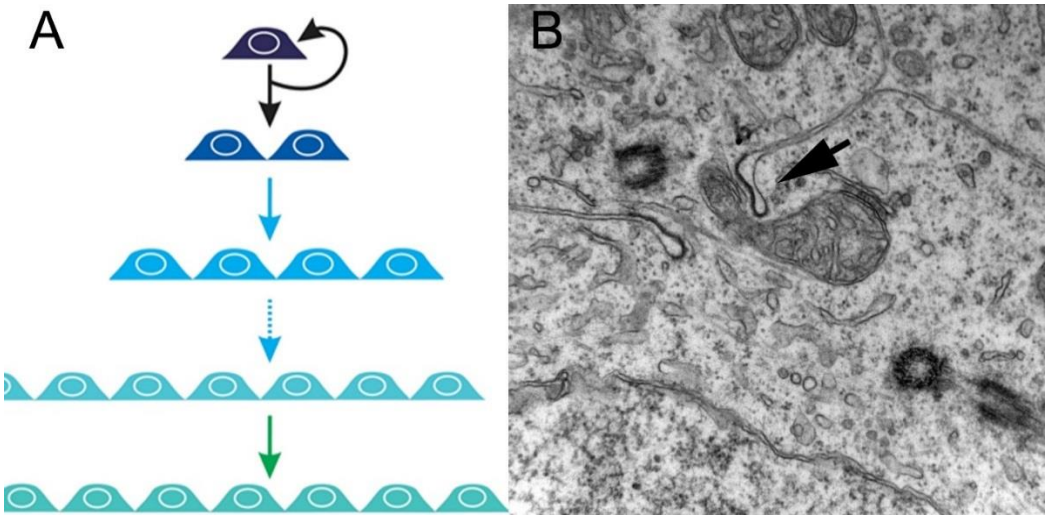

Figure 1. Mitotic or spermatogonial phase. **A.** Clones of spermatogonia are seen in different colors. The clones of spermatogonia are interconnected by cytoplasmic bridges due to the incomplete cytokinesis at the end of each mitosis. The mitotic divisions are

responsible for the geometric increase in the number of germ cells before meiosis. **B.** Electron microscopy detail of a cytoplasmic bridge (**arrow**) connecting two daughter cells resulting from a spermatogonial division. Nóbrega, personal illustration and data.

Figure 2 illustrates the morphological features of each germ cell during the three (proliferative, meiotic and spermiogenic) phases of spermatogenesis, from undifferentiated type A spermatogonia (A_{und}*) until spermatozoon (SZ).

Following the general vertebrate scheme, testes are composed of two compartments, the interstitial (or intertubular) tissue and the seminiferous (or spermatogenic) tubules. The interstitial compartment contains the steroid-producing Leydig cells, blood/lymphatic vessels, macrophages and mast cells, neural and connective tissue elements, including the peritubular myoid cells; the connective tissue elements are continuous with the tunica albuginea, the testis organ wall. Part of the wall of the seminiferous tubules is a basement membrane that is formed by two cell types, the Sertoli cells in the seminiferous tubules, and the peritubular myoid cells in the interstitial compartment. The somatic Sertoli cells and germ cells are the only two cell types within the seminiferous tubules and together form the germinal epithelium. In this epithelium, germ cells survival and development depends on the constant and intimate contact with Sertoli cells.

Although many features are conserved in vertebrate spermatogenesis, the Sertoli cell-germ cell relationship differs between anamniotes vertebrates (fishes and amphibians) showing the so-called cystic type of spermatogenesis on the one hand, and the non-cystic type in amniote vertebrates (reptiles, birds, and mammals).

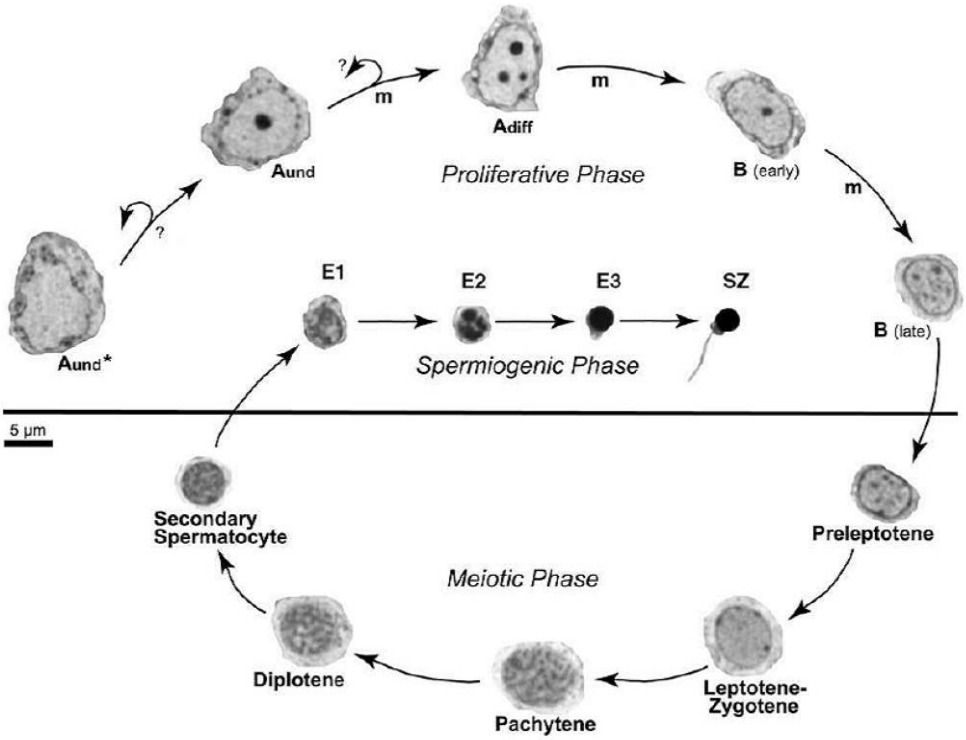

Figure 2. Step-by-step representation of zebrafish spermatogenesis from type A undifferentiated spermatogonia to spermatozoa, throughout the three phases of the spermatogenic process: proliferative or spermatogonial, meiotic or spermatocytary and spermiogenic. The spermatogonial micrographs show the most characteristic features of each cell type, although there is a range of their morphology and size. Type A undifferentiated* spermatogonia (**A_{und}***) (stem cell?); type A undifferentiated spermatogonia (**A_{und}**); type A differentiated spermatogonia (**A_{diff}**); type B spermatogonia (**B**); self-renewal (**curved arrows**); mitosis (**m**); early spermatids (**E1**); intermediate spermatids (**E2**); final spermatids (**E3**); and spermatozoa (**SZ**). **A_{und}*** and **A_{und}**are single cells, whereas **A_{diff}**, **B (early)** and **B (late)** are grouped. The first question mark (**?**) indicates a doubt if **A_{und}*** and **A_{und}** are separated by a mitosis or represent different stages of the same cell cycle(see also Fig. 4), while the second question mark indicates uncertainty as regards the "stemness" of **A_{und}**.

In amniote vertebrates, the germinal epithelium in the adult testis is composed of a fixed number of "immortal" Sertoli cells, which support successive waves of spermatogenesis. During these waves, a given Sertoli cell supports at the same time different developmental stages of germ cells (i.e. cells belonging to different germ cell clones). For example, the Sertoli cell basis contacts spermatogonia, whereas lateral parts contact spermatocytes and early spermatids, and adluminal parts late spermatids

(Figure 3A). In this type of spermatogenesis, it is interesting to mention that Sertoli cells proliferate until puberty when only spermatogonia and a few early spermatocytes are present in the germinal epithelium.

On the other hand, in anamniote vertebrates, the germinal epithelium is composed of spermatogenic cysts. The cyst as morpho-functional unit (Callard 1996) is formed by a dynamic group of Sertoli cells surrounding and supporting one or sometimes two germ cell clones. Different clones being in different stages of development generate the typical histological picture of fish testes, where the tubular compartment contains differently sized groups of germ cells in different stages of spermatogenesis (Figure 3B). There are two main differences compared to the testis of amniote vertebrates. First, within the spermatogenic tubules, cytoplasmic extensions of Sertoli cells form cysts that either envelope a single germ cell clone derived from a single stem cell spermatogonium (Figure 3B), or sometimes contacts two different clones at the two sides off a cytoplasmic extension, as shown by recent electron-microscopy observations (book chapter submitted for publication), while in amniote testes, there are – depending on the species – at least 5 different germ cell clones in different stages of development that are taken care of by a single Sertoli cell. The second main difference between anamniote and amniote vertebrates is that cyst-forming Sertoli cells retain their capacity to proliferate also in adults, while Sertoli cells are considered post-mitotic under normal conditions in the amniote testis (Schulz et al., 2005).

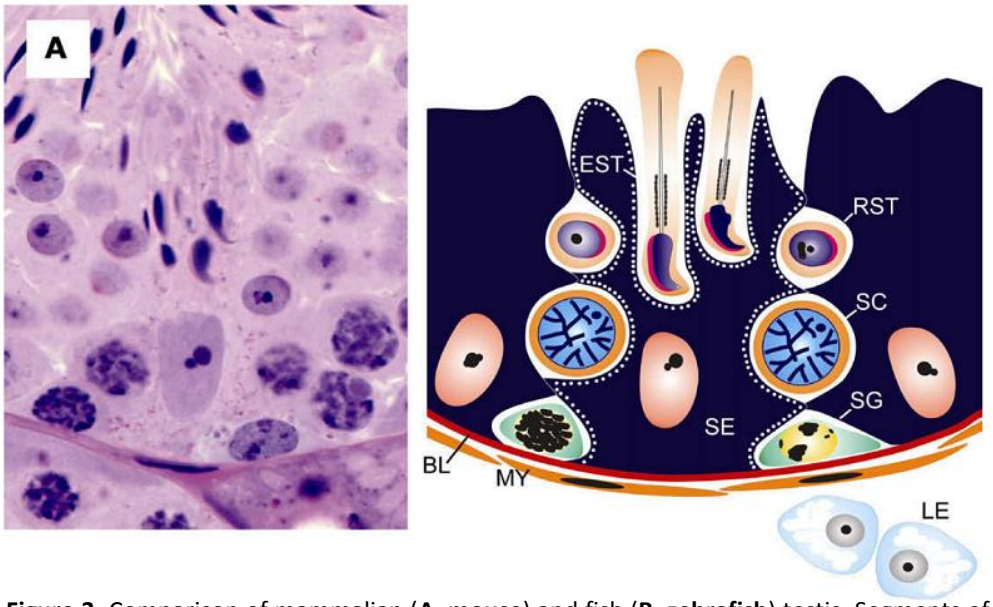

Figure 3. Comparison of mammalian (**A, mouse**) and fish (**B, zebrafish**) testis. Segments of spermatogenic tubules are shown to illustrate the differences in Sertoli/germ cell relation between cystic (**B**) and non-cystic (**A**) spermatogenesis. The germinal epithelium contains Sertoli (**SE**) and germ cells, delineated by a basal lamina (**BL**) and peritubular myoid cells (**MY**). The interstitial Leydig cells (**LE**) and blood vessels (**BV**) are shown. **A:** spermatogonia (**SG**); spermatocyte (**SC**); round spermatid (**RST**); and elongated spermatid (**EST**).

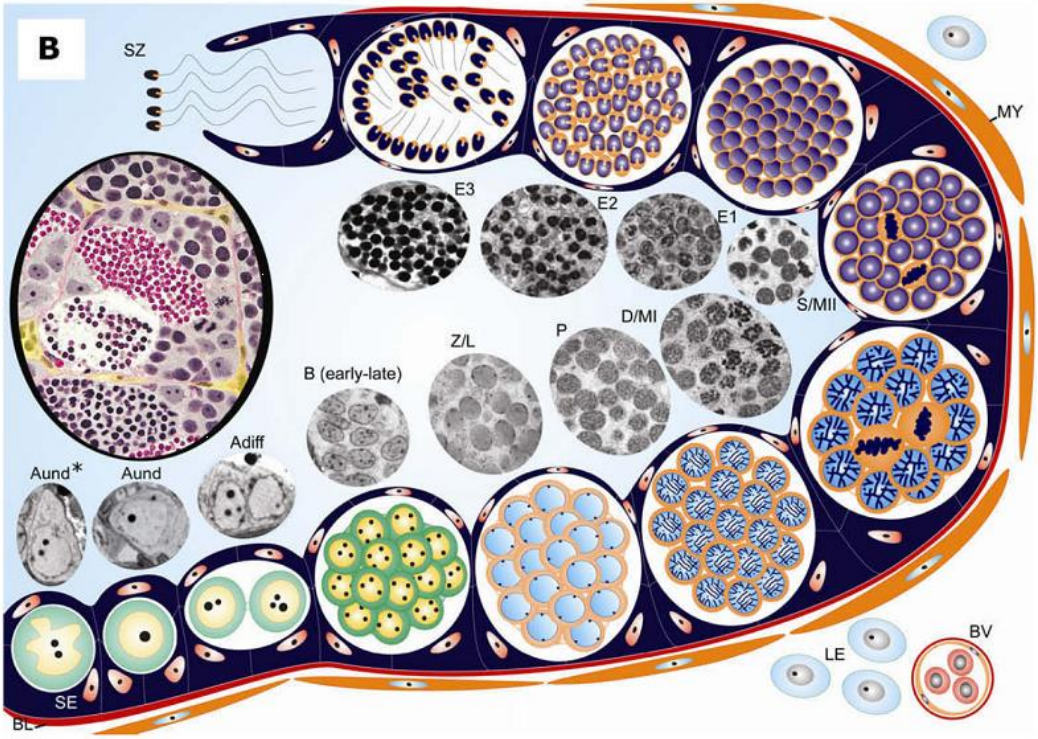

Figure 3. Continuation. Comparison of mammalian (**A, mouse**) and fish (**B, zebrafish**) testis. **B:** type A undifferentiated spermatogonia ($\mathbf{A_{und}}$); type A differentiated spermatogonia ($\mathbf{A_{diff}}$); type B spermatogonia [**B (early-late)**]; leptotenic/zygotenic primary spermatocytes (**L/Z**); pachytenic primary spermatocytes (**P**); diplotenic spermatocytes/metaphase I (**D/MI**); secondary spermatocytes/metaphase II (**S/MII**); early (**E1**), intermediate (**E2**) and final spermatids (**E3**); spermatozoa (**SZ**).

The structural differences in the Sertoli-germ cell relation between anamniote and amniote result in a more simple situation in fish (anamniote) compared to mammals (amniote). However, the basic functions are the same, only that these functions in fish are exerted more in a sequential manner while this is all at the same time in amniote vertebrates. Moreover, compared to invertebrates, vertebrates are characterized by the fact that the endocrine system has developed as the master control system over spermatogenesis, and that the somatic cells are the main targets for the most important reproductive hormones and help translating these signals into local regulation (as will be addressed in more detail further below).

1.2 Spermatogonial stem cells (SSCs) and SSC niche

Spermatogenesis relies on the activity of spermatogonial stem cells (SSCs), which are capable to either self-renew to produce more stem cells, or/and differentiate to daughter cells committed to spermatogenesis (De Rooij and Russell, 2000; De Rooij, 2001 and 2006a,b, Ehmcke et al., 2006; Yan, 2006). The proper balance between SSC self-renewal and differentiation is essential to assure the continuous homeostasis of spermatogenesis. If one of the processes is favored over the other, a seminona (testicular cancer) or a depletion of spermatogenesis is observed (Figure 4).

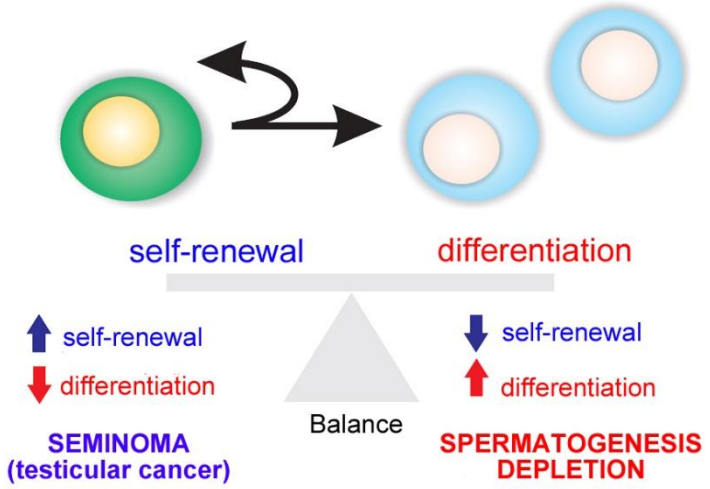

Figure 4. Balance between SSC self-renewal and differentiation. A seminoma (testicular cancer) or a depletion of spermatogenesis is observed if one of process is favored over the other.

The above process is valid for vertebrates showing continuous spermatogenesis, while in seasonally reproducing species a regulated switch is made between preferentially self-renewal at the beginning versus preferentially differentiation at the end of reproductive season.

SSCs are maintained in a specialized environment, denominated niche, which provides the factors and interactions relevant for regulating SSC activities, e.g. cell cycle quiescence, maintenance of the undifferentiated state, proliferation towards self-renewal, or apoptosis (De Rooij, 2001 and 2006a,b; Yan, 2006) (see Figure 5 for a schematic representation of the niche in mammals). The niche is defined as the microenvironment that maintains the undifferentiated state of the stem cell by preventing its differentiation, and is usually composed by three elements: 1) the supporting cells; 2) the stem cells; and 3) the surrounding extracellular matrix (Figure 5) (Spradling et al., 2001; Fuchs et al., 2004; Smith, 2006). In mammals, the testicular stem cell niche lies along the basement membrane (matrix) of the seminiferous epithelium, in contact with the Sertoli cells (supporting cells),

which maintain the fate of the spermatogonial stem cells by physical and paracrine interactions with these cells (McLean 2005; De Rooij, 2006b; Yan, 2006; Hess et al., 2006; Cooke et al., 2006). Besides the Sertoli cells, peritubular myoid cells and Leydig cells may also contribute to the niche characteristics via soluble factors. Moreover, it has become clear that mammalian SSCs are located preferably in those areas of the seminiferous tubules close to the interstitial tissue where Leydig cells and blood vessels reside (Chiarini-Garcia et al., 2001; 2003; Yoshida et al., 2007; De Rooij and Griswold, 2012) (Figure 5).

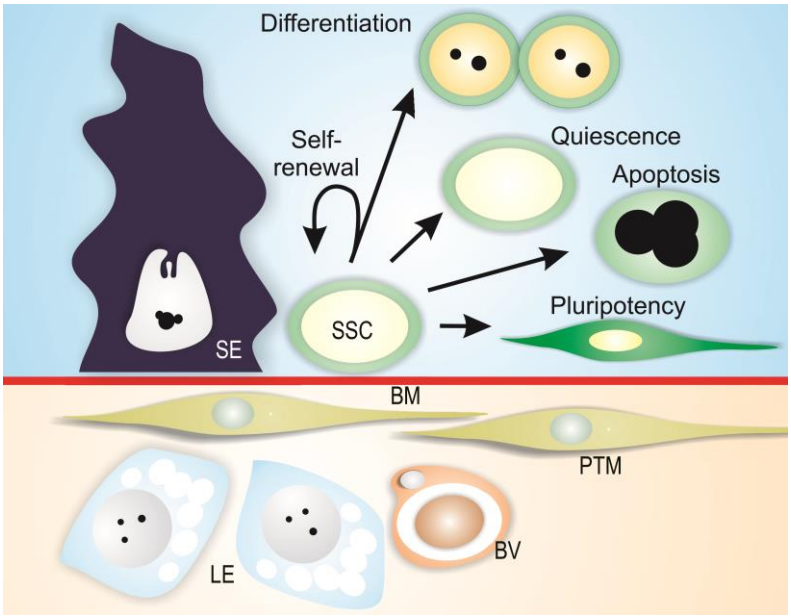

Figure 5. Mammalian testicular SSC niche. Spermatogonial stem cells (**SSCs**) reside along the basement membrane (**BM**) near interstitial Leydig cells (**LE**) and blood vessels (**BV**), and are – as all germ cells – in close contact with Sertoli cells (**SE**). In this microenvironment, physical and paracrine interactions regulate SSC activity (quiescence, pluripotency, self-renewal, or apoptosis). Peritubular myoid cells (**PTM**) are also depicted in the figure.

In submammalian animals, information on SSCs and their niche is scarce, and next to mammals, most information appears to be available for fish. In fish (and other anamniotes), SSCs are completely enveloped by Sertoli cells, therefore, not contacting the basement membrane, in contrast to the situation for amniote SSCs (Schulz et al., 2010). Clear morphological or molecular markers have not been identified yet for SSCs in any vertebrate but the general view is that SSCs are single cells and part of a population referred to as type A undifferentiated spermatogonia (A_{und}) (De Rooij & Russell, 2000; Schulz et al., 2010). There is a functional assay for SSCs though, which is based on their capacity to re-start, after transplantation, spermatogenesis in the testis of a recipient animal, in which endogenous spermatogenesis had been stopped experimentally. Transplantation assays exist for certain mammalian species and are being developed for fish now (Majhi et al., 2009, Lacerda et al., 2010). Although a morphological characteristic of SSCs is that they are single germ cells, i.e. not connected via cytoplasmic bridges to other germ cells, it is not clear if all single type A_{und} spermatogonia indeed have stem cell capacity (Schulz et al., 2010). In zebrafish, for example, two types of single, undifferentiated spermatogonia, type A_{und}* and the type A_{und} spermatogonia are found (Figure 3B) (Schulz et al., 2010). The type A_{und}* shows the most undifferentiated characteristics, such as a large nucleus with little heterochromatin, a high volume of the cytoplasm, a convoluted nuclear envelope and – particularly relevant – darkly staining material on the cytoplasmic side of the invaginations of the convoluted nuclear envelope. Such patches are known as “nuage” in the primordial germ cells, the earliest (embryonic) generation of germ cells. The other type of single spermatogonia shows a smooth nuclear envelope and

less/no nuage and we refer to these cells as type A_{und} spermatogonia (see Figure 3B).

1.3 Endocrine and paracrine regulation of SSC fate

In vertebrates, the pituitary gonadotropins Fsh (follicle-stimulating hormone) and Lh (luteinizing hormone) control testicular development and function by regulating the activity of local signaling systems, involving sex steroids and growth factors (Pierce and Parson, 1981; McLachlan et al., 1996), small RNAs (Panneerdoss et al., 2012) and epigenetic switches (Shirakawa et al., 2013).

In rodents, FSH can modulate the production of Sertoli cell growth factors that are relevant either for SSC self-renewal, or for SSC differentiation (De Rooij and Griswold, 2012). Among the growth factors, the glial cell line-derived neurotrophic factor (GDNF) secreted by Sertoli cells play an important role in SSC self-renewal (Meng et al., 2000), while activin A and bone morphogenetic protein 4 (BMP4), also produced by Sertoli cells (Loveland and Robertson, 2005), promote differentiation (Nagano et al., 2003) (Table 1). Growth factors produced by Leydig and peritubular myoid cells can also modulate SSC self-renewal or differentiation (Oatley et al., 2009) (Table 1). For example, colony-stimulating factor 1 (CSF1) secreted by Leydig and some peritubular myoid cells (Oatley et al., 2009) stimulate self-renewal (Table 1).Table 1 summarizes the most relevant growth factors for SSC self-renewal and differentiation in mammals (De Rooij and Griswold, 2012).

Table 1. Growth factors and their role on SSC self-renewal or differentiation. The production site in the testis is also mentioned. Modified from De Rooij and Griswold, 2012.

Growth Factor	Self-renewal or Differentiation	Production site
GDNF (Glial cell line-derived neurotrophic factor)	**Self-renewal**	**Sertoli cells**
FGF2 (Fibroblast growth factor 2)	**Self-renewal**	**Sertoli cells**
CXCL12 (Chemokine(C-X-C motif) ligand 12)	**Self-renewal**	**Peritubular and Leydig cells**
BMP4 (Bone morphogenetic protein 4)	**Differentiation**	**Sertoli cells**
INHBA (Activin A)	**Differentiation**	**Sertoli cells**

Androgens do not seem to be required for SSC self-renewal or differentiation in rodents (Zhou and Griswold, 2008), but can inhibit spermatogonial differentiation under certain conditions (Shetty et al., 2001; 2006). This might support the preferential location of SSC close to the interstitial compartment in rodents, where the locally high concentration of androgens near to the interstitium might prevent spermatogonial differentiation.

Likewise, gonadotropic hormones (Fsh and Lh) are important for testis development and spermatogenesis in fish. Despite an overall similarity, evolution seems to have taken a different path in teleost fish with respect to the gonadotropic hormones and their biological activities. Early in teleost evolution, the genomic environment of the hormone-specific *lhb*

gene has changed and syntenic homology was lost to tetrapod gonadotropins but also to teleost *fshb* genes (Kanda et al., 2011). Moreover, Leydig cells express not only the receptor for Lh (typically seen in all vertebrates) but also the receptor for Fsh (Ohta et al., 2007; García-López et al., 2009 and 2010; Chauvigné et al., 2012). Therefore, Fsh can regulate Leydig cell functions, including stimulation of androgen (Ohta et al., 2007; García-López et al., 2009 and 2010). In this context, interesting studies have reported that elevated circulating levels of androgens and Fsh coincided with active spermatogonial proliferation in male Chinook salmon, and Fsh is stimulates spermatogonial proliferation in juvenile Japanese eel (Ohta et al., 2007) and androgen production in several fish species (Planas et al., 1993; Ohta et al., 2007; García-López et al., 2009,2010). Therefore, Fsh might be the main gonadotropin regulating the spermatogonial phase in fish. Previous work in immature Japanese eel (*Anguilla japonica*) showed that Fsh can induce full spermatogenesis, and the stimulatory effect of Fsh on spermatogenesis can be fully explained by the Fsh-triggered production of androgens in Leydig cells (Ohta et al., 2007). This is the main difference between fish and mammals, where androgens seem to be required for SSC differentiation in fish (Miura et al., 1991; Ohta et al., 2007), while in mammals not (Zhou and Griswold, 2008). Considering the fact that Fsh regulates growth factor production in Sertoli cells (De Rooij and Griswold, 2012), and that catfish, zebrafish and eel Sertoli cells express the receptor for Fsh (Ohta et al., 2007; García-López et al., 2009, 2010), it is supposed that these cells would have some significant role in the process as well, next to being indirectly activated via Leydig cell-derived androgens. Therefore, it is also reasonable to speculate that Fsh might have a role on the balance

between SSC self-renewal and differentiation in fish through Sertoli cell growth factor production or androgen release by Leydig cells.

In this context, two growth factors had emerged as potential candidates on SSC self-renewal and differentiation in Japanese eel juvenile when work on this thesis started (Figure 6):1) Pd-ecgf (platelet-derived endothelialcell growth factor), also described as "spermatogonial stem cell renewal factor", stimulated self-renewal (Miura et al., 2003); and 2) Amh (anti-Müllerian hormone), a member of the Tgf-β (transforming growth factor beta) family, also described as "spermatogenesis preventing substance", blocked spermatogonial differentiation (Miura et al., 2002). Figure 6 illustrates the most relevant growth factors acting on SSC fate in fish as was known when the work started on this thesis. Figure 6 also shows that in eel estradiol-17β (E2) stimulated SSC self-renewal through PD-ECGF, while androgen (11-ketotestosterone, 11-KT) stimulated spermatogonial proliferation by increasing activin B mRNA and down-regulation of *amh* (Miura et al., 2002, 2003). In rainbow trout, other factors have been identified, such as Igf-1 (insulin-like growth factor 1) stimulating spermatogonial proliferation and differentiation (Loir and Le Gac, 1994). Next to the Igf1 effects in trout, there are the (different) Igf1 effects in eel. In trout, Igf1 has effects by itself which is not the case in eel. In eel, it has a permissive effect on the androgen-mediated stimulation (Nader et al., 1999).

Similar to the situation in mammals/rodents, these data indicated that also in fish, a range of different growth factors regulate SSC proliferation and differentiation behavior, according to changes in the physiological requirements. This also indicates that fish can serve as valid model to further elucidate the endocrine and paracrine regulation of vertebrate spermatogenesis, in particular because full spermatogenesis can be studied

in tissue culture system in fish (Miura et al., 2002; Leal at al., 2009), which is not feasible in mammals.

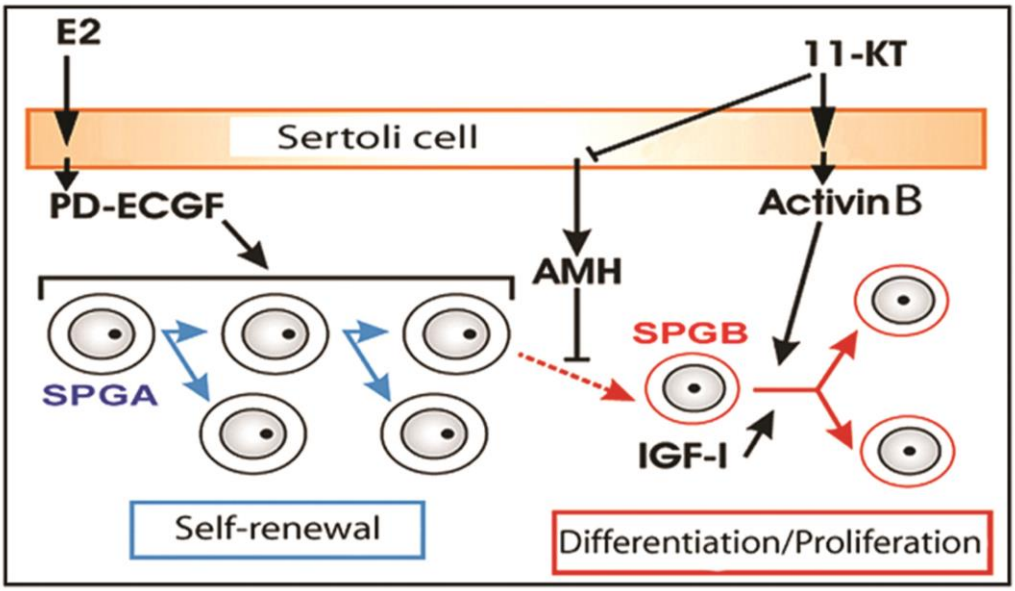

Figure 6. Drawing illustrating the role of some growth factors on SSC activity in fish. Type A undifferentiated spermatogonia (SPGA, which include SSC), type B spermatogonia (SPGB) are shown. Estrogen-17β (E2), platelet-derived endothelial growth factor (PD-ECGF), 11-ketotestosterone (11-KT), anti-Müllerian hormone (AMH), insulin-like growth factor (IGF1), stimulatory signal (→) and inhibitory signal (⊥). Modified from Miura and Miura (2003).

1.4 Aims and outline of the thesis

To characterize the location of the SSC niche, and to obtain further information on the endocrine and paracrine regulation of SSC self-renewal and/or differentiation, the non-cystic spermatogenesis in mammals is a relatively complex experimental system, because a Sertoli cell is associated with several different stages of germ cell development at any given time (Hess and França, 2007). Therefore, in this thesis, we decided to make use of the cystic mode of spermatogenesis in fish (Schulz et al., 2010) as an alternative model to study this question, for several reasons. One is that

among the fish, the zebrafish is the model of choice because of the genomic info and genetic models available, and because its short generation time and larger size over other models in fish (e.g. medaka). Moreover, and this is related to the second reason, a functional testis tissue culture system been available for zebrafish, allowing to study all stages of spermatogenesis (Leal et al., 2009). And finally, zebrafish spermatogenesis belongs to the non-restricted spermatogonial distribution type, which is also found in salmonids, which was the financial background of this work: use of zebrafish model to study spermatogenesis-related problems relevant in salmonid aquaculture. Zebrafish has become an excellent vertebrate model for basic and biomedical studies due to several advantageous characteristics, such as: easy handling, storage at high densities, external fertilization with high progeny, and finally, fully sequenced genome that allows forward and reverse genetic approaches (McGonnell and Fowkes, 2006).

In **Chapter 2**, morphological and morphometrical studies were carried out to characterize zebrafish spermatogenesis, focusing on the spermatogonial generations and Sertoli cell number per cyst, where important information was missing. Furthermore, based on the slow cell cycle speed of stem cells, first BrdU (bromodeoxyuridine) label-retaining studies were carried out to identify zebrafish SSC candidates. Such studies were further developed in **Chapter 3**, allowing also to define the preferential intratubular localization (niche) of these cells in the zebrafish testis, data that were moreover confirmed by transplantation assays. Finally, **Chapter 3** also investigated the expression of selected growth factor genes during the first steps of spermatogenic recovery following exposure to a cytotastic drug (busulfan) that depletes spermatogenesis. Two growth factors showed an interesting regulation in this context, Amh (which was

down-regulated), and a new member of the Igf family, Igf3, which was strongly up-regulated.

Chapter 4, 5 and 6 studied the endocrine and paracrine regulation of the spermatogonial phase, including the SSCs. **Chapter 4** evaluated the role of recombinant zebrafish gonadotropic hormones, Fsh and Lh, on zebrafish testicular functions. Gene expression and steroid release were analyzed using zebrafish testicular explants and injections in vivo. **Chapter 5** concentrated on the Tgfβ family member Amh. These studies showed that recombinant Amh had an inhibitory role on spermatogonial proliferation and differentiation and inhibited Fsh-stimulated androgen production. Finally, recombinant zebrafish Fsh down-regulated *amh* transcript levels.

Finally, **Chapter 6** studied the biological functions of a new Igf family member, Igf3, in zebrafish testis. Igf3 promoted spermatogonial proliferation towards meiosis, and its expression is induced by Fsh. **Chapter 7** summarizes, discusses and integrates the main results obtained from this thesis.

Reference List

CALLARD, GV. (1996).Endocrinology of Leydig cells in nonmammalian vertebrates. In: Payne, A.H., Hardy, M.P., Russell, L.D. (Eds.), The Leydig Cell.: Cache River Press Vienna, IL, USA, pp. 308-331.

CHAUVIGNÉ F, ZAPATER C, GASOL JM, CERDÀ J. (2014). Germ-line activation of the luteinizing hormone receptor directly drives spermiogenesis in a nonmammalian vertebrate. *Proc Natl Acad Sci U S A. 2014* Jan 28;111(4):1427-32. doi: 10.1073/pnas.1317838111. Epub 2014 Jan 13.

CHIARINI-GARCIA H, HORNICK JR, GRISWOLD MD, RUSSELL LD. (2001). Distribution of type A spermatogonia in the mouse is not random. *Biol Reprod* 65:1179-1185.

CHIARINI-GARCIA H, RAYMER A, RUSSELL L. (2003). Non-random distribution of spermatogonia in rats: evidence of niches in the seminiferous tubules. *Reprod* 126:669-680.

COOKE PS, HESS RA, SIMON L, SCHLESSER HN, CARNES K, TYAGI G, HOFMANN M-C, MURPHY KM. (2006). The transcription factor Ets-related molecule (ERM) is essential for spermatogonial stem cell maintenance and self-renewal. *Animal Reprod* 3(2):98-107.

DE ROOIJ DG AND GRISWOLD MD. (2012). Questions about spermatogonia posed and answered since 2000. *J Androl* 33, 1085-1095.

DE ROOIJ DG, RUSSELL LD. (2000). All you wanted to know about spermatogonia but were afraid to ask. *J Androl* 21:776-798.

DE ROOIJ DG. (2001). Proliferation and differentiation of spermatogonial stem cells. *Reprod* 121:347-354.

DE ROOIJ DG. (2006a). Rapid expansion of the spermatogonial stem cell tool box. *Proc Natl Acad Sci* 103(21):7939-7940.

DE ROOIJ DG. (2006b). Regulation of spermatogonial stem cell behavior in vivo and in vitro. *Animal Reprod* 3(2):130-134.

EHMCKE J, WISTUBA J, SCHLATT S. (2006). Spermatogonial stem cells: questions, models and perspectives. *Human Reprod Update* 12(3):275-282.

FUCHS E, TUMBAR T, GUASCH G. (2004). Socializing with the neighbors: stem cells and their niche. *Cell* 116:769-778.

GARCIA-LOPEZ A, BOGERD J, GRANNEMAN JC, VAN DIJK W, TRANT JM, TARANGER GL, SCHULZ RW. (2009). Leydig cells express follicle-stimulating hormone receptors in African catfish. *Endocrinol* 150(1):357-65.

GARCIA-LOPEZ A, DE JONGE H, NOBREGA RH, DE WAAL PP, VAN DIJK W, HEMRIKA W, TARANGER GL, BOGERD J, SCHULZ RW. (2010). Studies in zebrafish reveal unusual cellular expression patterns of gonadotropin receptor messenger ribonucleic acids in the testis and unexpected functional differentiation of the gonadotropins. *Endocrinol* 151(5):2349-60.

HESS RA, COOKE PS, HOFMANN M-C, MURPHY KM. (2006). Mechanistic insights into the regulation of the spermatogonial stem cell niche. *Cell Cycle* 5(11):1164-1170.

HESS RA, FRANÇA LR. (2007). Spermatogenesis and cycle of the seminiferous epithelium. In: Cheng CY (ed). Molecular mechanisms in spermatogenesis, Landes Bioscience, pp. 1-15.

KANDA S, OKUBO K, OKA Y. (2011). Differential regulation of the luteinizing hormone genes in teleosts and tetrapods due to their distinct genomic environments--insights into gonadotropin beta subunit evolution. *Gen Comp Endocrinol.* 173:253-258.

LACERDA SM, BATLOUNI SR, COSTA GM, SEGATELLI TM, QUIRINO BR, QUEIROZ BM, KALAPOTHAKIS E, FRANÇA LR.(2010). A new and fast technique to generate offspring after germ cells transplantation in adult fish: The nile tilapia (*Oreochromis niloticus*) model. *PLoS One* 20;5(5):e10740.

LEAL MC, DE WAAL PP, GARCIA-LOPEZ A, CHEN SX, BOGERD J, SCHULZ RW. (2009). Zebrafish primary testis tissue culture: An approach to study testis function ex vivo. *Gen Comp Endocrinol* 162(2):134-8.

LOIR M, LE GAC F. (1994). Insulin-like growth factor I and II binding and action on DNA synthesis in rainbow trout spermatogonia and spermatocytes. *Biol. Reprod.* 51, 1154-1163.

LOVELAND KL AND ROBERTSON DM (2005). The TGF b superfamily in Sertoli cell biology. In: Griswold, M and M Skinner. (Eds.),. *Sertoli Cell Biology*. Maryland Heights, Missouri: Elsevier Science: 227–247.

MAJHI SK, HATTORI RS, YOKOTA M, WATANABE S, STRUSSMANN CA. (2009). Germ cell transplantation using sexually competent fish: An approach for rapid propagation of endangered and valuable germlines. *PLoS One* 4(7):e6132.

MCGONNELL IM, FOWKES RC. (2006). Fishing for gene function – endocrine modelling in the zebrafish. *J Endocrinol* 189:425-439.

MCLACHLAN RI, WREFORD NG, O'DONNELL L, DE KRETSER DM, ROBERTSON DM. (1996) The endocrine regulation of spermatogenesis: independent roles for testosterone and FSH. J *Endocrinol.;*148:1–9.

MCLEAN DJ. (2005). Spermatogonial stem cell transplantation and testicular function. *Cell Tissue Res* 322:21-31.

MENG X, LINDAHL M, HYVONEN ME, PARVINEN M, DE ROOIJ DG, HESS MW, RAATIKAINEN-AHOKAS A, SAINIO K, RAUVALA H, LAKSO M, PICHEL JG, WESTPHAL H, SAARMA M, SARIOLA H. (2000). Regulation of cell fate decision of undifferentiated spermatogonia by GDNF. *Science* 287:1489-1493.

MIURA T, MIURA C, KONDA Y, YAMAUCHI K. (2002). Spermatogenesis-preventing substance in Japanese eel. *Development* 129:2689-2697.

MIURA T, MIURA CI. (2003). Molecular control mechanisms of fish spermatogenesis. *Fish Physiol Biochem* 28:181-186.

MIURA T, OHTA T, MIURA CI, YAMAUCHI K. (2003). Complementary deoxyribonucleic acid cloning of spermatogonial stem cell renewal factor. *Endocrinol* 144:5504-5510.

MIURA T, YAMAUCHI K, TAKAHASHI H, NAGAHAMA Y. (1991a). Hormonal induction of all stages of spermatogenesis in vitro in the male Japanese eel (*Anguilla japonica*). *Proc. Natl. Acad. Sci. USA* 88, 5774-5778.

MIURA T, YAMAUCHI K, TAKAHASHI H, NAGAHAMA Y. (1991b). Involvement of steroid hormones in gonadotropin-induced testicular maturation in male eel (*Anguilla japonica*). *Biomed. Res.* 12, 241-248.

NADER MR, MIURA T, ANDO N, MIURA C, YAMAUCHI K. (1999). Recombinant human insulin-like growth factor I stimulates all stages of 11-ketotestosterone-induced spermatogenesis in the Japanese eel, *Anguilla japonica*, in vitro. *Biol. Reprod.* 61, 944-947.

NAGANO M, RYU BY, BRINSTER CJ, AVARBOCK MR, BRINSTER RL. (2003). Maintenance of mouse male germ line stem cells in vitro. *Biol Reprod* 68, 2207-2214.

OATLEY JM, OATLEY MJ, AVARBOCK MR, TOBIAS JW, BRINSTER RL. (2009). Colony stimulating factor 1 is an extrinsic stimulator of mouse spermatogonial stem cell self-renewal. *Development* 136(7):1191-9.

OHTA T, MIYAKE H, MIURA C, KAMEI H, AIDA K, MIURA T. (2007). Follicle-stimulating hormone induces spermatogenesis mediated by androgen production in Japanese eel, *Anguilla japonica*. *Biol Reprod* 77(6):970-7.

PANNEERDOSS S, CHANG YF, BUDDAVARAPU KC, CHEN HI, SHETTY G, WANG H, CHEN Y, KUMAR TR, RAO MK. (2012) Androgen-Responsive MicroRNAs in Mouse Sertoli Cells. PLoS ONE 7(7): e41146. doi:10.1371/journal.pone.0041146

PIERCE JG, PARSONS TF. (1981). Glycoprotein hormones: structure and function. *Annu Rev Biochem.*;50:465–495.

PLANAS JV, SWANSON P, DICKHOFF WW. (1993). Regulation of testicular steroid production in vitro by gonadotropins (GTH I and GTH II) and cyclic AMP in coho salmon (*Oncorhynchus kisutch*). *Gen Comp Endocrinol* 91(1):8-24.

SCHULZ RW, DE FRANÇA LR, LAREYRE JJ, LEGAC F, CHIARINI-GARCIA H, NÓBREGA RH & MIURA T (2010). Spermatogenesis in fish. *Gen Comp Endocrinol* 165, 390-411.

SCHULZ RW, MENTING S, BOGERD J, FRANCA L, VILELA DAR, GODINHO, HP. (2005). Sertoli cell proliferation in the adult testis: Evidence from two fish species belonging to different orders. Biol. Reprod. 73, 891-898.

SHETTY G, WENG CC, MEACHEM SJ, BOLDEN-TILLER OU, ZHANG Z, PAKARINEN P, HUHTANIEMI I, MEISTRICH ML. (2006). Both testosterone and FSH independently inhibit spermatogonial differentiation in irradiated rats. *Endocrinol*;147:472–482.

SHETTY G, WILSON G, HUHTANIEMI I, BOETTGER-TONG H, MEISTRICH ML. (2001) Testosterone inhibits spermatogonial differentiation in juvenile spermatogonial depletion mice. *Endocrinol*;142:2789–2795.

SHIRAKAWA T, YAMAN-DEVECI R, TOMIZAWA S, KAMIZATO Y, NAKAJIMA K, SONE H, SATO Y, SHARIF J, YAMASHITA A, TAKADA-HORISAWA Y, YOSHIDA S, URA K, MUTO M, KOSEKI H, SUDA T AND OHBO K. (2013), An epigenetic switch is crucial for spermatogonia to exit the undifferentiated state toward a Kit-positive identity. *Development*140, 3565-3576.

SMITH A. (2006). A glossary for stem-cell biology. *Nature*. 441, doi:10.1038/nature04954.

SPRADLING A, DRUMMOND-BARBOSA D, KAI T. (2001). Stem cells find their niche. *Nature* 414:98-104.

YAN W. (2006). Molecular mechanisms of spermatogonial fate control: lessons from gene knockouts. *Biol Reprod* doi:10.1095/biolreprod.106.051946.

YOSHIDA S, SUKENO M, NABESHIMA Y. (2007). A vasculature-associated niche for undifferentiated spermatogonia in the mouse testis. *Science* 21;317(5845):1722-6.

ZHOU Q, GRISWOLD MD. (2008) Regulation of spermatogonia. In: StemBook [Internet]. Cambridge (MA): Harvard Stem Cell Institute; 2008-. Available from: http://www.ncbi.nlm.nih.gov/books/NBK27035/

CHAPTER 2

Histological and Stereological Evaluation of Zebrafish (*Danio rerio*) Spermatogenesis with an Emphasis on Spermatogonial Generations

Leal MC, Cardoso ER, Nóbrega RH, Batlouni SR, Bogerd J, França LR, Schulz RW.

Biol Reprod. 2009 Jul;81(1):177-87. doi: 10.1095/biolreprod.109.076299. Epub 2009 Apr 1.

ABSTRACT

The zebrafish has become an important vertebrate model for basic and biomedical research including the research field of biology of reproduction. However, very few morphological and stereological data are available as regards zebrafish testis structure and spermatogenesis. In this careful histomorphometric evaluation of the testis, we studied spermatogonial cells using molecular markers, determined the combined duration of meiotic and spermiogenic phases, and examined the formation of the Sertoli cell barrier (tight junctions). We found at least 9 spermatogonial generations and propose a morphology-based nomenclature for spermatogonial generations that is compatible with the one used in higher vertebrates. The number of germ cells per cyst increased dramatically (1 to ~1360 cells) from undifferentiated spermatogonia type A to early spermatids. The combined duration of meiotic and spermiogenic phases is approximately 6 days, one of the shorter ones among the teleost fish investigated to date. The number of Sertoli cells per cyst increased 9-fold during the maturational cycle of spermatogenic cysts and stabilized in the meiotic phase at a ratio of approximately 100 early spermatids per Sertoli cell (Sertoli cell efficiency). Similar to mammals, Sertoli cell proliferation ceased in the meiotic phase, coinciding with the formation of tight junctions between Sertoli cells. Hence, the events taking place during puberty in the germinal epithelium of mammals seem to recapitulate the "life history" of each individual spermatogenic cyst in zebrafish.

testis, teleost fish, spermatogenesis, spermatogonia, Sertoli cell barrier, zebrafish.

INTRODUCTION

The zebrafish (*Danio rerio*; family cyprinidae, order cypriniformes), is a small freshwater teleost fish (~5cm in length) originally from Central Asia [1]. Easy handling; high number of progeny; transparent embryos and forward and reverse genetics approaches have contributed to the importance of this model species in basic and biomedical research. Also reproductive physiology [2], integrative physiology in general [3], as well as more applied research fields such as ecotoxicology [4] or aquaculture [5], increasingly make use of the zebrafish model.

Spermatogenesis is a complex and highly coordinated process by which diploid spermatogonia produce millions of spermatozoa daily [6]. This process is fueled by spermatogonial stem cells, which have the potential for both self-renewal and for differentiating into spermatogonia committed to sperm development [7-9]. In fish, as in other anamniote vertebrates, spermatogenesis occurs in cysts which are formed when a single spermatogonium is completely surrounded by the cytoplasmic projections of one or two Sertoli cells [10]. As in all animals, the cells resulting from differentiating mitotic divisions of single spermatogonia remain interconnected by cytoplasmic bridges that synchronize developmental processes among the members of the same germ cell clone [11**,** 12**].** Thus, in this cystic type of spermatogenesis, a given Sertoli cell is in contact with only one germ cell clone. This is the main difference in relation to the non-cystic spermatogenesis, as occurs in amniote vertebrates (reptiles, birds and mammals), where several clones at different stages of development are distributed along basal, lateral, and adluminal surfaces of a Sertoli cell [6, 13, 14]. Apart from the cystic arrangement, the spermatogenic process in teleost fish is very similar to that of mammals [15].

With regard to the biology of male reproduction, zebrafish were studied to assess the effects of endocrine disruptors [2, 16], or the production of reproductive pheromones [17]. However, few quantitative data are available regarding the basic aspects of testis morphology and spermatogenesis in zebrafish. Histological and stereological investigations are adequate approaches to a better understanding of the spermatogenic process and testis function in fish [18, 19]. Such an evaluation allows the determination of the dynamics in the numbers of germ cells and Sertoli cells per each type of spermatogenic cyst, provides information on the number of spermatogonial generations, on the magnitude of germ cell loss occurring during spermatogenesis, and on the Sertoli cell efficiency.

Our long-term aim is to further our understanding of the regulation of spermatogenesis. We hypothesize that in the cystic mode of spermatogenesis Sertoli cell functions related to supporting a given stage of spermatogenesis can be studied undisturbed by germ cells in other stages of development, in contrast to non-cystic spermatogenesis where several germ cell clones are in contact with a given Sertoli cell. A basis required for such studies, as well as for other fields, like reproductive toxicology, is a thorough description of zebrafish spermatogenesis, including quantitative data that allow a better understanding of spermatogenesis. Such data has not been published yet, and the main objectives of the present study were to perform a comprehensive stereological study of the different types of spermatogenic cysts (the number of germ cells and Sertoli cells per spermatogonial, spermatocyte and spermatid cysts). While the different stages of meiosis and spermiogenesis are relatively easy to differentiate, the successive spermatogonial generations are not. Therefore, we devoted particular attention to the mitotic phase of spermatogenesis, propose a

nomenclature for the different spermatogonial generations, and have started with a molecular characterization of the spermatogonia. Based on these data we are able to estimate the number of spermatogonial generations, the magnitude of germ cell loss, as well as Sertoli cell number and efficiency. We also determined the duration of the combined meiotic and spermiogenic phases at 27^{o}C through the incorporation of 5'bromo-2'-deoxyuridine (BrdU). Finally, the permeability of the Sertoli cell barrier was assessed during the spermatogenic phases by using an electron dense tracer, lanthanum nitrate.

MATERIALS AND METHODS

Animals, Sampling, Biometry and Testis Structure

Thirty sexually mature zebrafish, outbred animals and Tübingen AB strain (TABs), were used for histology and stereology (TABs), analysis of the duration of spermatogenesis (TABs) and Sertoli cell barrier analysis (outbred). The animals were anesthetized, weighed and the testis dissected out, weighed and fixed by immersion (see below). The gonado-somatic index (GSI) was obtained by the formula GSI = (testes weight/body weight) x100. All procedures used followed approved guidelines for the ethical treatment of animals and national laws. Experimental protocols were submitted to, and approved by, the Utrecht University and Federal University of Minas Gerais (CETEA) committees for animal experimentation and care.

Testis stereology

For histological and stereological analysis, testes were fixed in 4% buffered (PBS) glutaraldehyde at 4^{o}C overnight. The tissue was dehydrated and embedded in 2-hydroxyethyl methacrylate. In a pilot study, we determined the nuclear diameter of the different germ cell types to determine the section thickness that avoids counting the same nucleus twice, using the procedure described previously [20]. According to these results, testes were serially sectioned at 2 and 3 µm thickness; histological sections were stained with 1% toluidine blue. The total number of germ cells and Sertoli cells per spermatogonial, spermatocyte, and spermatid cysts was counted on serial sections, using in total thirteen zebrafish. This evaluation was performed after selecting cysts entirely encompassed by serial sections. At least five cysts were analyzed per each germ cell type in each fish. The Sertoli cell efficiency was estimated from the ratio of germ cells to Sertoli cells, per each cyst type.

For a high resolution light microscopy analysis of the spermatogonial compartment and to differentiate morphologically the spermatogonial generations, small fragments of zebrafish testes (n=5) were fixed by immersion in 5% glutaraldehyde in 0.05M sodium cacodylate buffer (pH 7.2–7.4) for at least 24 h. After fixation, the material was rinsed three times in the same buffer, postfixed in an osmium-ferrocyanide, dehydrated, embedded in araldite, sectioned for light microscopy (1 µm thick) and stained with toluidine blue.

The individual Leydig and germ cell volumes (µm^3) were obtained from the nuclear volume and the proportion (%) between nucleus and cytoplasm of each cell type evaluated, which were determined as described previously [20].

Germ cell loss (apoptosis) was analyzed qualitatively and quantitatively, and expressed as a percentage of apoptotic cells per cyst. These apoptotic cells were morphologically characterized as darker stained cells, as it is typical in this condition for cells embedded in plastic and stained with toluidine blue [19].

Immunocytochemical and in situ hybridization experiments

Testis tissue from adult males (outbred or TABs) was fixed in 4% paraformaldehyde in PBS overnight at 4ºC. For immunocytochemistry, the tissue was rinsed briefly in PBS, before being immersed in PBS containing 20% (w/v) sucrose for 1 day at 4ºC. Tissue was then frozen in Neg50 (Richard-Allan Scientific, Kalamazoo, MI). Cryo-sections (10 µm thick) were used to detect Vasa [21] or Ziwi [22] protein, using previously described antisera raised in rabbit.

Rabbit anti-Vasa was used at a dilution of 1:200 and incubated overnight at room temperature, before incubating with a goat anti rabbit antiserum labeled with FITC (Invitrogen, Carlsbad, CA; A11008; diluted 1:200) for 90 minutes at room temperature. The buffer also contained 1 µg/ml of propidium iodide to label DNA. The sections were analyzed with a confocal laser scanning microscope, using 488 and 536 nm as excitation wavelengths for FITC and propidium iodide, respectively. Detection of Ziwi protein, and staining of DNA by DAPI, was done as described by Houwing et al. [22].

For *in situ* hybridization, paraformaldehyde-fixed tissue was dehydrated and embedded in paraffin, according to conventional techniques. Sections of 5 µm thickness were used for the detection of mRNA encoding

proliferating cell nuclear antigen (pcna), a protein involved in DNA synthesis and repair [23] and shown to be predominantly expressed in rapidly proliferating spermatogonia in Japanese eel [24].

The zebrafish *pcna* mRNA sequence (http://www.ncbi.nlm.nih.gov/entrez/viewer.fcgi?db=nuccore&id=18859222) was used to design specific primers. A zebrafish *pcna* PCR product (634 bp) was generated using primers 1039 and 1040 (Supplemental Table 1) and zebrafish testis cDNA as template, gel purified and served as template for digoxigenin (DIG) labeled cRNA probe synthesis by *in vitro* transcription. For cRNA synthesis, 300 ng of PCR product was incubated at 37^{o}C for 2.5 h in a 20 µl reaction volume, containing 4 µl 5×T3/T7 RNA buffer (Invitrogen), 2 µl 0.1 M DTT, 1 µl (29.7 units/µl) RNAguard RNase inhibitor (GE Healthcare, Fairfield, CT, USA), 2 µl 10×DIG RNA labeling mix (Roche, Mannheim, Germany), and either 2 µl (50 units/µl) T3 RNA polymerase (Epicentre, Madison, WI, USA; for sense probe) or 2 µl (50 units/µl) T7 RNA polymerase (Epicentre; for anti-sense probe).

Duration of spermatogenesis (meiotic and spermiogenic phases)

To estimate the combined duration of meiotic and spermiogenic phases at 27^{o}C, 16 animals (TABs) were exposed to 5'-bromo-2'-deoxyuridine (BrdU) dissolved in water (3mg/mL) for approximately 15 hours. The animals (n=2 per time point investigated) were sampled at 1 hour, and 1, 2, 3, 4, 5, 6, and 7 days after the exposure was terminated.

BrdU incorporation was detected following a protocol modified from van de Kant and de Rooij [25]. Zebrafish testes were fixed for 5 hours at room temperature in freshly prepared methacarn (60% [v/v] absolute

ethanol, 30% chloroform, and 10% glacial acetic acid) and embedded in Technovit 7100 (Heraeus Kulzer, Wehrheim, Germany). Five µm thick sections were subjected to antigen retrieval (1% [v/v] periodic acid in water at 60ºC for 30 min) and peroxidase blocking (1% [v/v] H_2O_2 in phosphate buffer saline [PBS] for 10 min). Thereafter, slides were incubated at room temperature for 1 hour with mouse anti-BrdU (BD Bioscience, San Jose, CA, USA; 1:80 diluted in PBS containing 1% [w/v] bovine serum albumin [BSA; Sigma-Aldrich, St. Louis, MO, USA]), and then for an additional hour with biotinylated horse anti-mouse (Vector, Burlingame, CA USA; 1:100 diluted in PBS containing 1% [w/v] BSA). Revelation of immunostaining was done using avidin-biotin complex incubation for 1 hour (Vector) followed by DAB (Dako, Glostrup, Denmark) substrate development for 20 seconds. Nuclei were counterstained with haematoxylin Gills #3 (Sigma-Aldrich) for 30 seconds. For a negative control, the primary antibody (mouse anti-BrdU) was replaced by the same concentration of normal mouse IgG (BD Bioscience).

Sertoli Cell Barrier

To investigate the presence and timing of formation of the Sertoli cell barrier (tight junctions between Sertoli cells) during spermatogenesis, lanthanum nitrate ($La(NO_3)_3$) was prepared by slowly adding drops of 0.01N NaOH to 2% $La(NO_3)_3$ (Vetec, Rio de Janeiro, Brazil) until the solution reached pH 7.8. This opalescent solution was mixed with an equal volume of cacodylate-buffered glutaraldehyde to make a fixative containing 1% lanthanum and 2% glutaraldehyde in 0.1M cacodylate at pH 7.8 or 7.3.

The testes from outbred animals were pre-fixed for two minutes in the fixative containing lanthanum, and then small pieces (2-3 mm^3) were fixed by immersion in the same fixative for 5 hours at room temperature. The material was rinsed overnight in the same lanthanum solution without glutaraldehyde at 4^oC (pH 7.8 or 7.3 according to the fixative pH). The samples were post-fixed for 8h in 1% OsO4 in 0.1M cacodylate buffer containing 1 % lanthanum at pH 7.8 or 7.3 (according to the fixative pH). After overnight staining in 0.5% aqueous uranyl acetate, the material was dehydrated in alcohol, embedded in araldite and documented using a Jeol 100 CX-II transmission electron microscope (80 kV).

Statistical analysis

All quantitative data are presented as the mean ± SEM and analyzed via analysis of variance (Student-Newman-Keuls test). The analysis was performed by using the software STATISTICA 3.11 for Windows (StatSoft, Inc., Tulsa, OK, USA). The significance level in comparisons was considered to be $p<0.05$.

RESULTS

Biometry and testis structure

The mean testes weight of zebrafish was 4.7 ± 0.2 mg, resulting in a GSI of 1.0 ± 0.05%. The testes are paired and elongated organs that stretch dorsally through the length of the body cavity, and are connected to the dorsal body wall via the mesorchium. The testes join caudally to form a single spermatic duct that terminates on the urogenital papilla. The anastomosing seminiferous tubules (arrows on Fig. 1A and inset) empty

dorsally into the main testicular efferent duct (Fig. 1B) that continues caudally as a single spermatic duct. Different types of germ cell cysts (from spermatogonia to spermatids) are distributed along the seminiferous epithelium (Fig. 2A-N and supplemental Fig. 1).

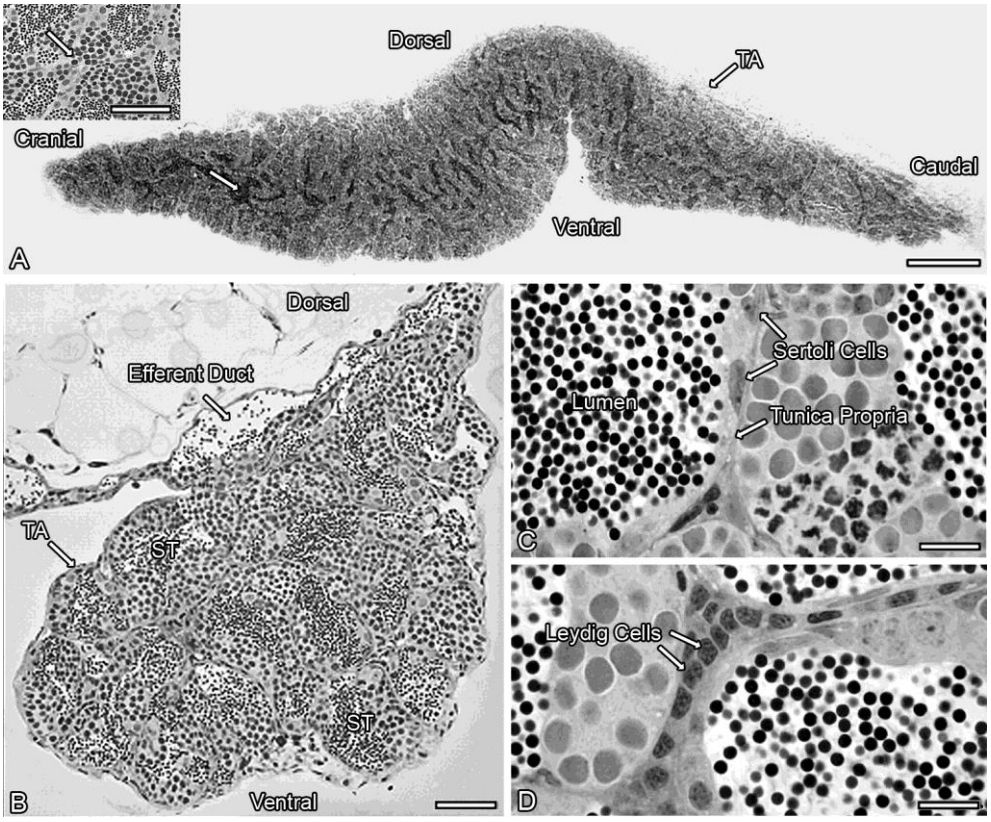

Figure 1. (**A**) Longitudinal section of a zebrafish testis showing the dorsal-ventral and caudal-cranial axis. The tunica albuginea (TA) externally surrounds the testis. The seminiferous tubules sometimes show an anastomosing pattern (arrow and arrow-inset). (**B**) Cross section of zebrafish testis showing the tunica albuginea (TA), the efferent duct, and seminiferous tubules (ST). (**C**) Tubular compartment of the testis showing tunica propria surrounding the seminiferous tubule, Sertoli cells often in the basal region of spermatogenic cysts, and lumen containing spermatozoa. (**D**) Intertubular compartment showing a cluster of Leydig cells. Scale bars are 400µm (**A**), 50µm (inset to **A** and **B**), or 10µm (**C** and **D**).

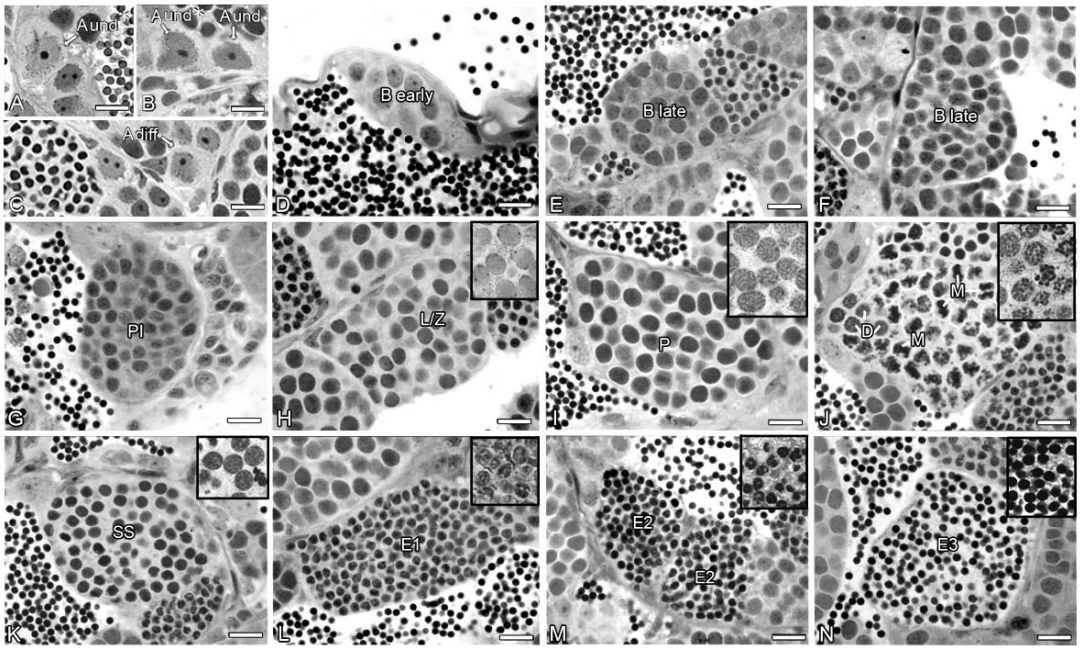

Figure 2. Different germ cell cysts observed during the spermatogenic process in zebrafish from a type A undifferentiated* spermatogonium to spermatids before spermiation. (A) The most undifferentiated type A spermatogonia (A_{und*}; probable stem cell; refer to Fig. 3 for a more detailed account on spermatogonia); (B) type A undifferentiated spermatogonia (A_{und*}) and type A undifferentiated spermatogonium (A_{und}; stem cell capacity?); (C) type A differentiated spermatogonia (A_{diff}); (D) early type B spermatogonia (B_{early}); (E-F) late type B spermatogonia (B_{late}); (G-J) primary spermatocytes in pre-leptotene (Pl), in the transition of leptotene to zygotene (L/Z), pachytene (P), diplotene (D), and meiotic figures from the first meiotic division (M); (K) secondary spermatocytes (SS); (L-N) spermatids at initial (E1), intermediate (E2), and final (E3) steps of development. Scale bars represent 10µm (or 5 µm for the insets in H-N).

Number of Germ cells and Sertoli cells per Cyst

All stereological data are presented in Table 1. The total number of Sertoli cells per cyst increased gradually and significantly from type A undifferentiated spermatogonium to pachytene spermatocytes cysts, and shows a strong trend toward stabilization from diplotene spermatocytes to mature spermatids (Tab. 1). The number of germ cells per cyst increased geometrically, as expected, from type A undifferentiated

spermatogonia to early spermatids, showing a reduction of 7% of the expected theoretical number from intermediate to final spermatid cysts (Tab. 1).

The data obtained for the number of spermatogonia and early spermatocytes per cyst allowed us to estimate that nine generations of spermatogonia are present in zebrafish – one generation of type A undifferentiated spermatogonia (please see below for morphological details on two forms of type A undifferentiated spermatogonia that both are found as single germ cells in early cysts), three generations of type A differentiating spermatogonia, and five generations of type B (early: B1 – B3; late: B4 and B5) spermatogonia. Because the nuclear morphology among the different generations of type B spermatogonia was very similar, the criteria used to distinguish each generation of this cell type were the decreasing cell size and the increasing number of spermatogonia per cyst. Regarding the Sertoli cell efficiency for spermatids, approximately 100 spermatids were found per each Sertoli cell. Considering the theoretical number expected and the number obtained, we can estimate that the total germ cell loss during spermatogenesis was ~38%. Using the deviation from theoretical number of germ cells for each generation, germ cell loss (by apoptosis) occurs in two steps, in the final spermatogonial generation and during the first meiotic prophase (B5 to diplotene), and then during the second meiotic division (secondary spermatocytes to early spermatids; Tab. 1). Although only ~62% of the germ cells complete spermatogenesis in zebrafish, apoptotic germ cells are rarely detected in adult zebrafish.

TABLE 1. Stereology of the different germ cell cysts in zebrafish (n = 8; mean ± SEM).

			Germ cells					
Cyst type*	No. of Sertoli cells per cyst	No. of germ cells per cyst†	Nuclear diameter (μm)	Nuclear volume (μm^3)‡	Cytoplasm volume (μm^3)§	Cell volume (μm^3)	Cyst volume (μm^3)¶	No. of germ cells (cyst) per Sertoli cell
SPG_1–A_{und}	1.2 ± 0.1[a]	1.0 ± 0[a]	8.6 ± 0.1[a]	336 ± 16 (0.50)[a]	342 ± 18[a] (0.50)	677 ± 34[a]	677 ± 34[a]	0.8 ± 0.1[a]
SPG_2–$A_{diff}1$	2.1 ± 0.1[b]	2.0 ± 0[b]	6.6 ± 0.1[b]	150 ± 4 (0.51)[b]	147 ± 6[b] (0.49)	297 ± 9[b]	593 ± 18[a]	1.0 ± 0.1[a]
SPG_3–$A_{diff}2$	2.7 ± 0.1[b]	3.7 ± 0[c] [4]	6.0 ± 0.1[c]	112 ± 1 (0.52)[c]	105 ± 3[c] (0.48)	216 ± 4[c]	790 ± 14[a]	1.4 ± 0.1[a]
SPG_4–$A_{diff}3$	3.9 ± 0.2[c]	7.2 ± 0.1[c] [8]	5.7 ± 0.1[d]	99 ± 1 (0.55)[c]	81 ± 3[c,d] (0.45)	180 ± 3[c,d]	1318 ± 24[a]	1.8 ± 0.1[a]
SPG_5–B1	5.1 ± 0.2[d]	14 ± 0.3[c] [16]	5.6 ± 0.1[d]	92 ± 1 (0.58)[c,d]	66 ± 4[d,e] (0.42)	158 ± 5[d,e]	2159 ± 69[a]	2.7 ± 0.1[a]
SPG_6–B2	5.4 ± 0.1[d]	28 ± 1[c] [32]	5.3 ± 0.1[e]	76 ± 1 (0.60)[d,e]	51 ± 2[e,f] (0.40)	128 ± 2[e,f]	3624 ± 90[a]	5.3 ± 0.1[a,b]
SPG_7–B3	6.2 ± 0.1[e]	55 ± 1[c,d] [64]	5.1 ± 0.1[e,f]	71 ± 0.5 (0.61)[d,f]	45 ± 1[e,g] (0.39)	116 ± 2[f,g]	6473 ± 190[a,b]	9 ± 0.3[b,c]
SPG_8–B4	9.3 ± 0.2[f]	113 ± 3[d] [128]	5.0 ± 0.1[f]	64 ± 1 (0.61)[e,f,g]	41 ± 2[e,h] (0.39)	105 ± 2[f,g]	11 949 ± 429[b,c]	12 ± 0.2[c]
SPG_9–B5	11.2 ± 0.4[g]	208 ± 8[e] [256]	4.7 ± 0.1[g]	53 ± 1 (0.64)[f,h]	29 ± 1[f,g,h,i] (0.36)	82 ± 1[f,g,h]	16 945 ± 755[c,d]	19 ± 1.1[d]
Pl	11.9 ± 0.2[h]	423 ± 9[f] [512]	4.4 ± 0.1[h]	45 ± 1 (0.61)[g,h,i]	29 ± 2[f,g,h,j] (0.39)	74 ± 3[g,h,i]	31 325 ± 1283[e]	36 ± 0.8[e]
L/Z	12.0 ± 0.3[g,h]	395 ± 12[f]	5.1 ± 0.1[e,f]	70 ± 1 (0.59)[e,f,h]	48 ± 3[e,i,j] (0.41)	117 ± 4[e,f,g,h,i]	46 087 ± 1163[f]	33 ± 0.6[e,f]
P	12.8 ± 0.2[i]	377 ± 19[f]	6.0 ± 0.1[c]	112 ± 2 (0.60)[c,d]	76 ± 1[d,e] (0.40)	188 ± 2[c,e]	71 585 ± 3602[g]	30 ± 1.5[f]
D	13.0 ± 0.4[i,j]	397 ± 8[f]	5.2 ± 0.1[e,f]	74 ± 2 (0.61)[d,g,h]	48 ± 3[e,i,j] (0.39)	122 ± 4[e,f,g,h]	48 608 ± 1539[f]	31 ± 1.2[e,f]
S	13.8 ± 0.4[j,k,l]	768 ± 26[g] [1024]	3.9 ± 0.1[i]	31 ± 1 (0.59)[i,j]	21 ± 1[g,h,i] (0.41)	52 ± 2[h,i,j]	38 808 ± 1362[h]	56 ± 1.7[g]
E1	14.3 ± 0.4[k]	1353 ± 45[h] [2048]	3.0 ± 0.1[j]	14 ± 0.2 (0.60)[j,k]	9 ± 1[i,j] (0.40)#	22 ± 1[j]	29 465 ± 1183[e]	94 ± 2.34[h]
E2	14.1 ± 0.3[k]	1299 ± 23[h,i]	2.5 ± 0.1[k]	8 ± 0.3 (0.61)[k]	5 ± 0.3[i,j] (0.39)	14 ± 1[j]	17 616 ± 773[c,d]	92 ± 2.3[h]
E3	13.1 ± 0.2[i,l]	1262 ± 13[i]	2.1 ± 0.1[l]	5 ± 0.1 (0.60)[k]	3 ± 0.1[i,j] (0.40)	8 ± 0.1[j]	10 771 ± 185[b,c]	96 ± 1.6[h]

* SPG_1–A_{und}, primary spermatogonia; SPG_2–$A_{diff}1$, SPG_3–$A_{diff}2$, SPG_4–$A_{diff}3$, different generations of type A differentiated spermatogonia; SPG_5–B1, SPG_6–B2, different generations of type B early spermatogonia; SPG_7–B3, SPG_8–B4, SPG_9–B5, different generations of type B late spermatogonia; Pl, preleptotene primary spermatocytes; L/Z, leptotene/zygotene primary spermatocytes; P, pachytene spermatocytes; D, diplotene spermatocytes; S, secondary spermatocytes; E1, initial spermatids; E2, intermediate spermatids; E3, final (mature) spermatids.

† Values in brackets indicate the theoretical number of germ cells formed after mitotic and meiotic divisions.

‡ Values in parentheses are the percentage of nucleus in the cell.

§ Values in parentheses are the percentage of cytoplasm in the cell.

¶ Sertoli cells not included.

Flagellum included.

[a-l] Different superscript letters indicate that mean values differ significantly ($P < 0.05$).

Germ cell and Leydig cell Stereology and Cyst Volume

While the total number of germ cells increased per cyst during spermatogenesis, the opposite was observed for the nuclear diameter, and for the nuclear, cytoplasmic, and cellular volumes (Tab. 1). The trend was broken by a gradual but transient increase of these parameters in primary spermatocytes (from preleptotene to pachytene spermatocytes). Based on the total number of germ cells per cyst and the individual volume of each germ cell type, we determined the total cyst volume that showed a strong and steady increase from type A undifferentiated spermatogonium to pachytene spermatocytes, decreasing from this maximum to 85% in late spermatid cysts (Tab. 1).

The Leydig cells nuclear, cytoplasmic and cell volumes were 53 ± 0.9, 52 ± 0.7, and 105 ± 1.6 μm^3, respectively. Leydig cells are not randomly distributed in the interstitial space but often form clusters, sometimes in the form of ring-like structures around blood vessels (supplemental Fig. 3). Although not properly quantified, these clusters appeared to be larger in the periphery of the testis.

Spermatogonia Morphology, Spermatocytes, and Spermiogenesis

Two types of A undifferentiated spermatogonia can be differentiated in zebrafish testes based on morphological criteria. They are referred to as type A undifferentiated* (A_{und*}) and type A undifferentiated (A_{und}) (Fig. 3).

Both cell types differ from all later stages in that they are completely enveloped as single cell by Sertoli cells and are the largest germ cells (~ 677 μm^3) with a large nucleus (diameter 8.6 µm) containing poorly condensed chromatin and 1 or 2 compact nucleoli. Specific for type A_{und}*

spermatogonia is that their nuclear envelope has an irregular outline that is not found in type A_{und} spermatogonia, and that the ratio between cytoplasm and nucleus is higher in type A_{und*} than in all other spermatogonia, including type A_{und} (Fig. 3).

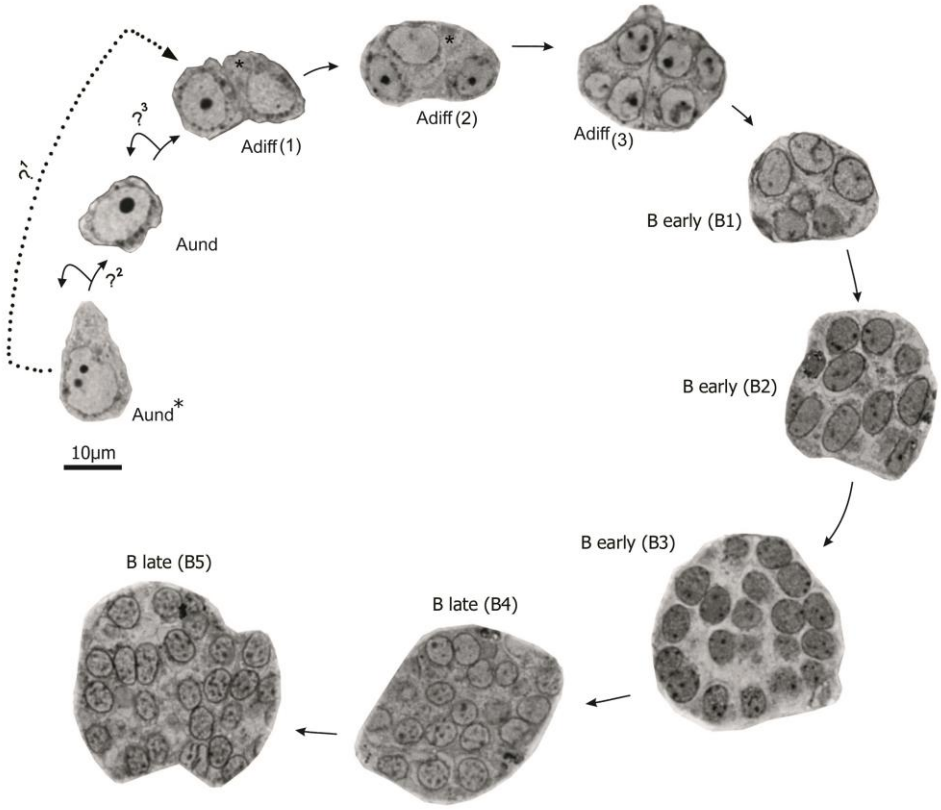

Figure 3. Nine spermatogonial generations in zebrafish. The terminology addressing the different spermatogonial generations was based on morphological features, such as nuclear shape, heterochromatin amount, nucleolar characteristics, and number of germ cells in a cyst. Using high resolution light microscopy applied to 1 µm thick araldite-embedded sections, we propose to differentiate five types of spermatogonia: type A undifferentiated* (A_{und}*), type A undifferentiated (A_{und}), type A differentiated (A_{diff} 1, 2, and 3), type B early (B1-B3) and type B late (B4 and B5). The first question mark ($?^1$) indicates a doubt as regards a possible, asymmetric division of A_{und}* (stippled line leading to a pair of spermatogonia). The second question mark ($?^2$) indicates the doubt whether or not type A_{und}* is separated from type A_{und} by a mitosis. The third question mark ($?^3$) indicates uncertainty as regards the "stemness" of A_{und}. The asterisk indicates spermatogonia

showing the cytological charcateristics of type A_{und}* cells in small cysts with otherwise type A_{diff} spermatogonia, an observation possibly indicating asymmetrical division of A_{und}* (stippled line).

The type A differentiated (A_{diff}) spermatogonia are very similar to the undifferentiated type. However, as these cells result from mitoses with incomplete cytokinesis, they are grouped (2, 4, or 8) within the cyst, and are smaller than the type A_{und} spermatogonia. The nucleus of type A_{diff} spermatogonia is more dense and smaller, the nuclear envelope acquires a regular round shape, and 2 or 3 small nucleoli are found that assume eccentric positions (Fig. 3; supplemental Fig. 1). Moreover, heterochromatin starts to appear as flecks along the nuclear envelope (Fig. 3). When analyzed by high resolution light microscopy, we have sometimes observed small cysts of type A spermatogonia, in which one of the germ cells showed morphological characteristics of type A_{und*} spermatogonia, while the other cells showed the characteristics of type A_{diff} spermatogonia (Fig. 3; asterisk in cysts with $A_{diff}1$ and $A_{diff}2$).

The type B early spermatogonia have an elongated/round nucleus with one or two small nucleoli. A major difference to type A spermatogonia is the increased amount of heterochromatin that is distributed as round clumps throughout the nucleus or associated with the nuclear envelope (Fig. 3 and supplemental Fig. 1).

In the type B late spermatogonia, the number of germ cells inside the cyst increases (Tab. 1). The nucleus is round, smaller than in the early type B spermatogonia, dense and the heterochromatin (round clumps and associated with the nuclear envelope) reaches maximum density (Fig. 3 and supplemental Fig. 1).

Spermatocytes at the different phases of meiosis can be identified by nuclear characteristics, such as size, chromosome condensation and meiotic figures of the chromosomes (e.g. metaphase I or II) (Fig. 2G-K; Tab. 1). Leptotene/zygotene spermatocytes have a larger, more round nucleus compared to the last generation of type B spermatogonia, showing a clear chromatin with small spots of heterochromatin bordering the nuclear envelope (Fig. 2H). Pachytene spermatocytes are the largest cell type among the spermatocytes. Their nucleus is denser and contains chromosomes as bold lines from the periphery to the central part of the nucleus (Fig. 2I). Diplotene spermatocytes are always found together with metaphasic figures (metaphase I) (Fig. 2J). In this cell type, the chromosomes reach their maximum degree of condensation. Secondary spermatocytes are rare because they quickly enter into meiosis II. They have a round nucleus with a dense chromatin (Fig. 2K).

Spermiogenesis in zebrafish is marked by a striking reduction in the cellular volume (Tab. 1). We propose to differentiate three types of spermatids in zebrafish spermiogenesis: early (Fig. 2L), intermediate (Fig. 2M), and final spermatids (Fig. 2N). This classification is based on the increasing nuclear compaction and space between the spermatids (reflecting the loss of cytoplasmic bridges and the flagellum formation; Fig. 2L-N).

Immunocytochemical and in situ hybridization experiments

Our studies on molecular markers showed that antibodies against zebrafish Vasa and Ziwi intensely labeled single type A undifferentiated spermatogonia and, in the case of Ziwi, also small cysts with type A differentiated spermatogonia (supplemental Fig. 2A-B). Vasa protein was

also present at intermediate levels in differentiating spermatogonia, and at low levels in spermatocytes, while spermatids and spermatozoa remained unlabeled. In the case of Ziwi, the labeling became very weak in late type B spermatogonia and spermatocytes, and was not detected in haploid germ cells. The *in situ* hybridization for *pcna* mRNA, on the other hand, provided an intense labeling of more differentiated spermatogonia (supplemental Fig. 2C-D).

Duration of spermatogenesis (meiotic and spermiogenic phases)

The most advanced germ cells that carried a BrdU label after different periods following BrdU exposure at 27^{o}C are shown in Fig. 4. One hour after the termination of exposure (i.e. ~16 hours after the start of contact with BrdU), the most advanced germ cells labeled were identified as early pachytene spermatocytes (Fig. 4A). At 1, 2, and 3 days after BrdU exposure, the most advanced cells labeled were late pachytene spermatocytes (Fig. 4B-D), implying that it took less than one day to form pachytene from preleptotene spermatocytes. Four days after exposure, labeled spermatids were identified, while after 5 days we noticed the first labeled spermatozoa in the tubular lumen (Fig. 4E-F). After 6 and 7 days of exposure we regularly found labeled spermatozoa in the lumen of the seminiferous tubules (Figure 4G-H). Also, after 7 days spermatozoa were found in the lumen of the efferent duct system (Fig. 4I). Based on these observations, we can estimate that the combined duration of meiotic and spermiogenic phases are very short in this species and lasts approximately 6 days (15 hour of incubation + 5 days after incubation).

Sertoli and Leydig cells were also labeled (Figure 4J-K), indicating that both cell types are able to proliferate in sexually mature animals.

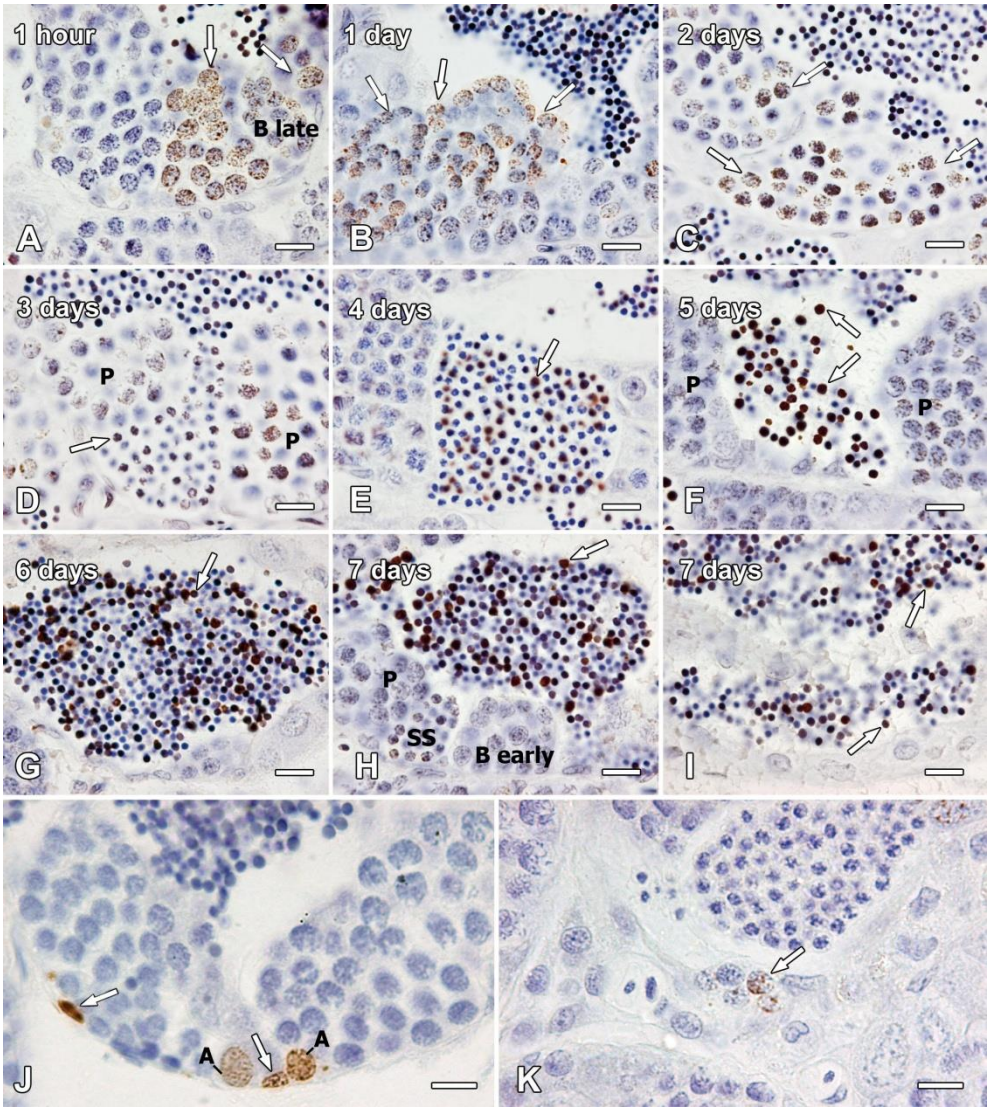

Figure 4. Proliferating (BrdU-positive) somatic and germ cells in adult zebrafish testis. The following labeled cells were observed at different time periods after BrdU exposure: **(A-C)** at 1 hour, 1 and 2 days, primary spermatocytes (pachytene - arrows); **(D-E)** at 3 and 4 days, spermatids (arrows); **(F)** at 5 days, spermatozoa (arrows) during spermiation; **(G-H)** at 6 and 7 days, spermatozoa (arrows) in the lumen of the seminiferous tubules; **(I)** at 7 days, spermatozoa (arrows) in the lumen of the efferent duct; **(J)** at 1 hour, Sertoli (arrow) and **(K)** Leydig cell (arrow). **A**, type A spermatogonium; **B early**, early type B spermatogonia;

B late, late type B spermatogonia; **P**, pachytene primary spermatocytes; **SS**, secondary spermatocytes. Scale bars are 10µm (**A**-**H**) or 20µm (**J** and **K**).

Sertoli Cell Barrier

During spermatogenesis, lanthanum can be found inside spermatogonial and early meiotic cysts (leptotene/zygotene spermatocytes) (Fig. 5A-B).

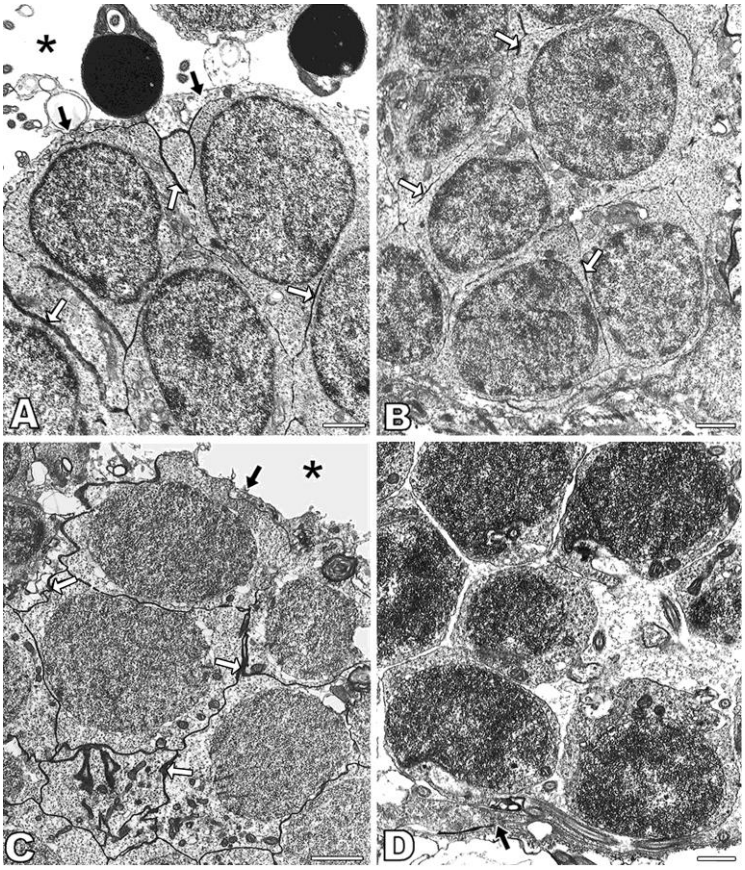

Figure 5. Transmission electron microscopy of zebrafish testis sections using lanthanum as a tracer to investigate the permeability of the Sertoli cell barrier at different stages of spermatogenesis. The barrier is not observed in cysts containing type B spermatogonia (**A**) or primary spermatocytes cysts at the inititial stages of meiosis (leptotene/zygotene) (**B**-**C**), since lanthanum is present between the germ cells (white arrows). (**D**) Lanthanum is found at the level of tight junctions between Sertoli cells in spermatid cysts (arrow). Note that the tracer is not present between the germ cells. The asterisks indicate the lumina of

spermatogenic tubules, where lanthanum has never been found. The arrows in A and C indicate the Sertoli cell cytoplasm. Scale bars are 1µm (**A** and **B**), 2µm (**C**), or 0.5µm (**D**).

On the other hand, lanthanum was not found inside early spermatid cysts (Fig. 5C-D), demonstrating that the Sertoli cell barrier (tight junctions) is established at the beginning of spermiogenesis, obstructing, therefore, the entry of lanthanum into the cyst lumen. Lanthanum has never been found in the lumen of spermatogenic tubules.

DISCUSSION

Testis structure and distribution of spermatogonia

The zebrafish testicular parenchyma shows the typical vertebrate pattern with the germinal and interstitial compartments. As in other fishes and amphibians, the seminiferous tubules contain spermatogenic cysts formed by Sertoli cells that envelope a group of synchronously developing germ cells, which are derived in a clonal manner from one stem cell. The morphology of the different germ cell types observed for zebrafish is in general similar to what is described for most species of teleost fish [18, 19, 26-29], including the absence of acrosomes in spermatozoa [15].

Regarding the distribution of spermatogonia along the germinal compartment, two testis types have been described in fish: restricted and unrestricted [27-29]. In the restricted type (a derived character), undifferentiated type A spermatogonia are confined to the distal end of seminiferous tubules, near the tunica albuginea. In the unrestricted type (a primitive character), these spermatogonia are found at random sites along the seminiferous tubule throughout the testis. An intermediate type appears to exist in a number of orders (e.g. *gadiformes*: [30]; *perciformes*: [18];

pleuronectiformes: [31]), where undifferentiated type A spermatogonia show a preferential, but not exclusive, location close to the tunica albuginea. We have found that undifferentiated type A spermatogonia in zebrafish were distributed along the entire germinal compartment. The zebrafish testis belongs, therefore, to the unrestricted type. Moreover, zebrafish testes contain anastomosing tubules, which is another primitive feature previously described in the orders *cypriniformes, characiformes, salmoniformes*, and others [29].

Sertoli cell number

In the present study, the number of Sertoli cells per cyst was quantified using serial sections. The final number of Sertoli cells in mammals is established at puberty, when Sertoli cells cease proliferating and differentiate terminally [6]. Since a Sertoli cell's capacity to support germ cells is limited, Sertoli cell number limits testis size and determines the spermatogenic capacity [32]. Data on the Sertoli cell number for teleosts with external fertilization are only available for *Oreochromis niloticus* [18-20] and zebrafish (this study). In both species, the number of Sertoli cells per cyst increased (4-fold in tilapia, 9-fold in zebrafish) and tended to stabilize in the meiotic phase, attaining a ratio of ~92 and ~95 spermatids per Sertoli cell in tilapia and zebrafish, respectively. During spermatogenesis in guppies (*Poecilia reticulata*), a species with internal fertilization, it was observed that the number of Sertoli cells per cyst also increased considerably (~30-fold from ~4 to ~130 Sertoli cells per cyst) from a cyst with a single, undifferentiated spermatogonium until the initial phase of the spermiogenesis, when almost 24000 spermatids per cyst were

found (i.e. ~170 spermatids per Sertoli cell; [33]). We conclude that it is a typical feature of adult teleost spermatogenesis that Sertoli cell number increases per cyst during its development. Detailed studies in tilapia and African catfish [18, 19] showed that the vast majority of dividing (i.e. incorporating ^{3}H-thymidine or BrdU) Sertoli cells were associated with expanding spermatogonial cysts. It may not seem surprising therefore that we have found proliferating Sertoli cells in the testes of young adult zebrafish. However, tilapia and catfish show life-long somatic and testis growth, unlike birds or mammals, and unlike zebrafish. However, a certain growth of both body and testis takes place after the zebrafish have completed puberty (first reproduction) at ca. 12 weeks of age. At this point we are unable to determine if the observed Sertoli cell proliferation represents remaining growth until final testis size will have been reached, or if during cystic spermatogenesis a certain loss of Sertoli cells occurs that requires compensatory proliferation. The scarce literature available on Sertoli cells in teleosts speculates that, after spermiation, these cells can degenerate or become integrated into the epithelium of the spermatic ducts [10, 28, 34]. Similar to what was observed in tilapia [18, 19], and despite analyzing several hundreds of cysts in zebrafish, Sertoli cells with the morphological characteristics of apoptosis were not observed. One explanation may be that the very high phagocytotic activity of Sertoli cells [35] removes apoptotic Sertoli cells quickly, so that they do not accumulate to a noticeable degree. Alternatively, Sertoli cells may be “recycled” after spermiation to contribute to the formation/growth of a new/still developing cyst.

Sertoli cell efficiency and germ cells loss

Considering that the number of spermatids per Sertoli cell in zebrafish, tilapia, and guppies (90 to 170) [18-20, 33], the Sertoli cell efficiency is quite high in fish with their cystic arrangement of the spermatogenic process, 10-20 times higher than in mammals [6, 36, 37]. Despite the great range in the number of spermatids per cyst in tilapia, zebrafish and guppies (~650, ~1300, and ~24000; respectively), the efficiency of the Sertoli cells in these three species of teleost fish is relatively similar. Moreover, experimentally induced changes in Sertoli cell numbers led to corresponding changes in germ cell numbers in tilapia [20], suggesting that, like in mammals [37], the number of Sertoli cells is the main factor determining the magnitude of the sperm production.

Germ cell apoptosis constitutes a normal process during spermatogenesis [38], and can occur in different developmental phases. In mammals, it is considered mainly to function in density regulation of spermatogonia, and to eliminate cells with chromosomal damage (meiotic phase), while cell loss during spermiogenesis is less prominent [37]. The quantitative significance of germ cell loss becomes clear when considering that in mammals only 2-3 spermatozoa out of 10 theoretically possible cells are produced from type A1 spermatogonia [7, 37]. In the present study, we found that instead of the theoretically expected 2048 mature spermatids, approximately 1300 were formed. Hence, 6 out of 10 possible cells reached final stages of development, which contributes to the high efficiency of fish spermatogenesis. We speculate that the tailored proliferation of Sertoli cells is a relevant factor for the high survival rate of germ cells in the fish testis.

Apoptosis is mainly found during spermiogenesis in tilapia (~25% vs. ~10%), whereas in zebrafish there is a greater loss (~20% vs. 10%)

during the spermatogonial phase. In both species about 10% apoptosis occurred during meiosis. In guppies [33] and Atlantic cod [30], the main loss of germ cells occurred in the spermatogonial phase. These findings suggest that, while the total losses are quite similar among fish species, apoptosis can occur during different stages along the spermatogenic process, which may reflect differences in the fine regulation of this process. The frequency with which apoptotic cells are observed in sections was surprisingly low, despite the overall loss of ~40% of germ cells. We ascribe this apparent discrepancy to the high phagocytotic efficiency of zebrafish Sertoli cells [35]. However, our understanding of the process of apoptosis and its regulation in fish is still incipient, and only a few species of teleost fish have been investigated in this regard.

Spermatogonial generations

Knowing the precise number of spermatogonial divisions is fundamental to understand the regulation of spermatogenesis. Previous reports stated that the number of spermatogonial generations in teleosts varies from 4-6 in zebrafish [39, 40] up to 14 in guppy [33], and intermediate values are observed in other teleost species [18, 26, 40]. Stereological analysis of spermatogenic cysts, as done by serial sections in the present study, is a laborious but powerful approach to establish the number of cells per cyst, which allows deducing the number of spermatogonial generations. This permitted calculating that nine generations of spermatogonia (type A undifferentiated spermatogonia, 3 generations of type A differentiating, and 5 generations of type B spermatogonia) are present in zebrafish. Ando and collaborators [40] reported 4 or 5 generations

of spermatogonia in zebrafish, but the conclusion was based on counting spermatids in single sections where the cysts showed the maximum diameter. The difference in results may be based on the fact that this approach assumes a spherical shape of spermatid cysts and would lead to an underestimation of cell numbers if the actual shape was irregular or elongated, which is not unusual in zebrafish according to our observations.

Spermatogonial morphology in fish has been described on the light [19, 28, 30, 31, 33, 41, 42] and electron microscopy level [41-43]. However, there is no consensus about the terminology used to address the different spermatogonial generations in this group of vertebrates. This difficulty is in part due to the cystic mode of spermatogenesis, so that – different from the situation in reptiles, birds and mammals – there are no stages (specific cellular associations) in the seminiferous epithelium of fish. Two types of spermatogonia have been described in fish considering basically the size and number of cells within the cysts. For example, single, larger spermatogonia were designated primary spermatogonia or type A spermatogonia; smaller and grouped spermatogonia (in pairs or more), on the other hand, were referred to as secondary or type B spermatogonia [44, 45]. However, close morphofunctional analysis reveals cells with significant differences in morphology and kinetics among the secondary or type B spermatogonia, some generations being more similar to the type A undifferentiated spermatogonia, others more similar to the more differentiated types of smaller spermatogonia in medium-sized or large groups. Hence, the first generations of grouped spermatogonia in small cysts share a number of characteristics with the single spermatogonia in fish as well as with the type A spermatogonia in rodents. Therefore, based on similar criteria (e.g. nuclear and nucleolar features; presence, amount, and distribution of

heterochromatin) used to discriminate between different types of spermatogonia in rodents [46], we evaluated zebrafish testes with high resolution light microscopy, and proposed a nomenclature for spermatogonial generations that is in line with established systems in higher vertebrates. In this way, we have described the following sequence of spermatogonial generations: undifferentiated type A spermatogonia (A_{und*} and A_{und})→ type A differentiated (A_{diff}) → type B early (B_{early}) → type B late (B_{late}). A_{und*} and A_{und} are single cells with a large nucleus containing poorly condensed chromatin and 1 or 2 nucleoli. A_{und}* spermatogonia have an irregular nuclear envelope that is not found in type A_{und}. A_{diff} are grouped (~2, 4, or 8) within the cyst, and their nucleus is denser than in the previous spermatogonial generation with heterochromatin as flecks along the nuclear envelope. The type B early (theoretically 16 to 32 cells; we counted 14-28 cells) have an elongated/round nucleus with one or two small nucleoli. A major difference to type A spermatogonia is the increased amount of heterochromatin that is distributed as round clumps throughout the nucleus or associated with the nuclear envelope. In the type B late spermatogonia (~55 to 208 cells), the nucleus is round, smaller, more dense and the heterochromatin forms round clumps associated with the nuclear envelope.

This morphological classification is standardized and reproducible for the zebrafish, and can be applied to other fish species as well, except perhaps for the absolute values of the cell/nuclear sizes while the relative changes of these parameters are found also in other species [20, 33]. Therefore, this categorization may provide a basis for standardizing the nomenclature used for spermatogonia in fish. Moreover, this classification parallels the nomenclature in mammals, mainly as regards the amount of heterochromatin, which is expected to simplify comparative approaches.

Especially in mice this approach has been used extensively [46, 47]. Finally, the present classification has the flexibility to allow for adjustments if required by future results, for example as regards the molecular and/or functional characterization of the different developmental stages of germ cells, such as indicated by the expression analysis of stage-specific proteins/mRNAs (suppl. Fig. 2), or by the capacity of germ cells to colonize a recipient's testis after transplantation (stemness) [48, 49].

The co-existence of undifferentiated and differentiated spermatogonia type A in the same cyst is intriguing in the context of stemness of spermatogonia. We were able to make this observation since the high resolution approach allowed identifying cell membranes and cyst borders on the light microscopy level. Future work will have to evaluate the ratio between equal/unequal division of type A_{und*} spermatogonia (e.g. stem cell self-renewal versus differentiation fate), and the regulation of this balance, for instance as regards the orientation of the mitotic spindle pole such as described in Drosophila testis [50], or as regards factors (e.g. glial cell line-derived neurotrophic factor) secreted by Sertoli cells in rodents (see [51] for review). In addition, an intriguing question to be investigated in fish refers to the "stemness" of a subset of differentiating spermatogonia, as has been recently described for mouse testis under certain injury conditions [52].

Meiotic and postmeiotic cells.

Compared to the studies on tilapia [18, 19], where the same methods were used as here, the size of germ cells in zebrafish is ~3-fold smaller in practically all of the spermatogenic phases, notwithstanding that a similar

pattern was found as regards the morphological changes during spermatogenesis in zebrafish, tilapia and guppies [33]. A noticeable exception in guppies is that the maximum diameter among primary spermatocytes was observed in zygotene cells.

In general, volume changes of meiotic and postmeiotic germ cells in zebrafish and tilapia were similar to those observed in mammals [37]. However, in mammals, diplotene spermatocytes show the maximum volume [37]. We do not have an explanation for the shift to pachytene in teleosts (zygotene in guppies) at present. It seems reasonable to expect the maximum cell volume in diplotene spermatocytes that have accumulated the genetic and cytoplasmic material required for the two upcoming fast meiotic divisions and the formation of spermatids [37]. Clearly, this aspect of teleost spermatogenesis deserves further studies. With pachytene spermatocytes being the biggest cell type in the meiotic phase, it is not surprising that pachytene cysts also show the maximum average volume of spermatogenic cysts. Cyst volume decreased progressively during spermiogenesis. This may reflect the remarkable nuclear condensation and elimination of cell organelles and cytoplasm during spermiogenesis [18, 19, 37, 53, 54]. Moreover, apoptotic loss of germ cells also occurs during this stage (see above).

Leydig cells

We are not aware of studies on the individual volume of Leydig cells in teleosts other than for tilapia [20, 48]. Similar to the germ cells, Leydig cells in tilapia were 3- to 4-fold bigger than observed here in zebrafish. In mammals, Leydig cell volume can vary from ~400 μm^3 in ovine and wild-

boars [55, 56] to ~5000 μm^3 in horses [57], most species ranging between 1000 and 2000 μm^3 [56, 58]. Hence, the volume of Leydig cell ranges at the low end of this comparative scale. As in other fish [12], Leydig cells formed groups or clusters with extensive plasma membrane contact zones. Although we did not quantify this aspect, it seems that Leydig cell clusters were larger/contained more cells close to the tunica albuginea than in central areas of the testis.

Duration of spermatogenesis (meiotic and spermiogenic phases)

A number of studies dealt with the duration of spermatogenesis in teleosts [18, 39, 59-63]. Determining the duration of spermatogenesis in mammals is classically based on the fact that the different germ cell generations form specific, recurrent cell associations, known as stages of the seminiferous epithelium. The determination of their relative frequencies enables the total duration of the differentiation process from stem cells to spermatozoa to be deduced [6, 37, 56, 58, 64]. In cystic spermatogenesis, however, this approach is not feasible. It is possible, however, to determine the duration of the meiotic and spermiogenic phases, i.e. from pre-leptotene/leptotene up to spermatozoa. This period is identical to the time required for an S-phase marker, such as BrdU, which is incorporated during the final round of DNA synthesis, to appear in spermatozoa. Using this approach, we found that the combined duration of the meiotic and spermiogenic phases is about 6 days in zebrafish. This is similar to the duration found in an Indian fresh-water perch *Colisa fasciata* [65], while a period of three weeks was the longest found among teleosts in black mollies *Poecilia sphenops* [61]. In general, fish germ cells proceed faster through

meiosis/spermiogenesis than mammalian germ cells, which take three to seven weeks [37, 56].

Different from the homoeothermic mammals, the duration of spermatogenesis in fish varies depending on the water/body temperature [66]. Studies describing the effects of temperature on the duration of spermatogenesis in fish [59, 60], or reptiles [67], showed that in general elevated temperatures accelerate germ cell development. The fact that zebrafish usually reproduce in temperatures close to 30ºC can explain, at least in part, the short duration of the meiotic and spermiogenic phases. The short duration, a high number of spermatogonial generations, and a high efficiency of the Sertoli cell jointly allow the prediction that the daily sperm production per volume unit of the zebrafish testicular parenchyma will be rather high.

Sertoli cell barrier

Experimental evidence of the Sertoli cell barrier ("blood testis barrier") became available when certain dyes were incapable of reaching meiotic and postmeiotic germ cells in the mammalian seminiferous epithelium [68, 69]. The use of electron-dense tracers, such as lanthanum, showed in mice [70, 71] that tight junctions between neighboring Sertoli cells in the seminiferous epithelium prevented the passage of the tracer. The Sertoli cell barrier has been demonstrated in all other classes of vertebrates (birds: [72]; reptiles: [73]; amphibians: [74]; fish: [75, 76]). It appears that the effective seclusion of the genetically and immunologically distinct meiotic and postmeiotic cells is an important, evolutionary conserved principle in spermatogenesis.

In fish, depending on the species, the establishment of the tight junctions between Sertoli cells occurs in cysts containing primary spermatocytes [75] or spermatids [12, 77, 78]. In zebrafish, lanthanum was detected among spermatogenic cells until the beginning of the meiotic prophase, but was excluded from cysts containing early spermatids, demonstrating that the Sertoli cell barrier is established at the end of meiotic phase. Interestingly, we have never observed lanthanum in the lumen of spermatogenic tubules, even though it was able to enter cycts containing germ cells up to the stage of leptotene/zygotene spermatocytes. Therefore, we consider it possible that future analysis will provide evidence for tight junctions among adluminal Sertoli cells (i.e. separating the lumen of spermatogenic tubules from the lumen of spermatogenic cysts) being established already shortly after cyst formation. The formation of tight junctions among Sertoli cells at the basal part of the germinal epithelium, on the other hand, appears to depend on the stage of development of the germ cells. This situation suggests that not only in mammals but also in zebrafish, the germinal epithelium is polarized. As regards the establishment of the microenvironment required for germ cell development, other structures besides the Sertoli cell barrier may be involved, such as the capillary endothelium, the basal lamina, and peritubular myoid cells [78].

In conclusion this is the first detailed study using morphological, stereological, and molecular approaches on spermatogenesis in zebrafish. Also, we are proposing a new nomenclature for the spermatogonial generations in zebrafish, which will allow further comparisons with other fishes but also with higher vertebrates such as mammals. The new results obtained for the zebrafish in the present study contribute to the characterization of the testicular function in this important teleost model

species, which may be of great value in future studies on the regulation of spermatogenesis.

ACKNOWLEDGEMENTS

The authors would like to thank R.F. Ketting and S. Houwing (Hubrecht Laboratory, Utrecht, The Netherlands) for providing antibody against zebrafish Ziwi.

REFERENCES

1. Engeszer RE, Patterson LB, Rao AA, Parichy DM. Zebrafish in the wild: A review of natural history and new notes from the field. Zebrafish 2007; 4:21-40.
2. McGonnell IM, Fowkes RC. Fishing for gene function – endocrine modeling in the zebrafish. J Endocrinol 2006; 189:425-439.
3. Briggs JP. The zebrafish: a new model organism for integrative physiology. Am J Physiol Regul Integr Comp Physiol 2002; 282:R3-9.
4. Aleström P, Holter JL, Nourizadeh-Lillabadi R. Zebrafish in functional genomics and aquatic biomedicine. Trends Biotechnol 2006; 24:15-21.
5. Dahm R, Geisler R. Learning from small fry: the zebrafish as a genetic model organism for aquaculture fish species. Mar Biotechnol 2006; 8:329-345.
6. Hess RA, França LR. Structure of the Sertoli Cell In: Skinner MK, Griswold MD (eds), Sertoli Cell Biology. Elsevier Academic Press; 2005: 19-40.
7. De Rooij DG, Russell LD. All you wanted to know about spermatogonia but were afraid to ask. J Androl 2000; 21:776-798.
8. De Rooij DG. Regulation of spermatogonial stem cell behavior in vivo and in vitro. Anim Reprod 2006b; 3:130-134.

9. Ehmcke J, Wistuba J, Schlatt S. Spermatogonial stem cells: questions, models and perspectives. Hum Reprod Update 2006; 12:275-282.
10. Pudney J. Comparative cytology of the non-mammalian vertebrate Sertoli cell. In: Russell LD, Griswold MD (eds), The Sertoli Cell. Clearwater, FL: Cache River Press; 1993: 612-657.
11. Pudney J. Comparative cytology of the Leydig cell. In: Payne AH, Hardy MP, Russell LD (eds). The Leydig Cell, Vienna, IL: Cache River Press; 1996: 98-142.
12. Loir M, Sourdaine P, Mendis-Handagama SMLC, Jégou B. Cell-cell interactions in the testis of teleost and elasmobranchs. Micr Res Tech 1995; 32:533-552.
13. Jones RC, Lin M. Spermatogenesis in birds. Oxf Rev Reprod Biol 1993; 15:233-264.
14. Gribbins KM, Elsey RM, Gist DH. Cytological evaluation of the germ cell development strategy within the testis of the American alligator, *Alligator mississippiensis*. Acta Zool (Stockholm) 2006; 87:59-69.
15. Nóbrega RH, Batlouni SR, França LR. An overview of functional and stereological evaluation of spermatogenesis and germ cell transplantation in fish. Fish Physiol Biochem 2009; 35:197-206.
16. Nash JP, Kime DE, Van der Ven LT, Wester PW, Brion F, Maack G, Stahlschmidt-Allner P, Tyler CR. Long-term exposure to environmental concentrations of the pharmaceutical ethynylestradiol causes reproductive failure in fish. Environ Health Perspect 2004; 112:1725-1733.
17. Van den Hurk R, Schoonen WG, van Zoelen GA, Lambert JG. The biosynthesis of steroid glucuronides in the testis of the zebrafish, *Brachydanio rerio*, and their pheromonal function as ovulation inducers. Gen Comp Endocrinol 1987; 68:179-188.

18. Vilela DAR, Silva SGB, Peixoto MTD, Godinho, HP, França LR. Spermatogenesis in teleost: insights from the Nile tilapia (*Oreochromis niloticus*) model. Fish Physiol Biochem 2003; 28:187-190.
19. Schulz RW, Menting S, Bogerd J, França LR, Vilela DAR, Godinho HP. Sertoli cell proliferation in the adult testis – Evidence from two fish species belonging to different orders. Biol Reprod 2005; 73:891-898.
20. Matta SLP, Vilela DAR, Godinho HP, França LR. The goitrogen 6-n-propyl-2-thiouracil (PTU) given during testis development increases Sertoli and germ cell numbers per cyst in fish: the tilapia (*Oreochromis niloticus*) model. Endocrinology 2002; 143:970-978.
21. Braat AK, van de Water S, Goos H, Bogerd J, Zivkovic D. Vasa protein expression and localization in the zebrafish. Mech Dev 2000; 95:271-274.
22. Houwing S, Kamminga LM, Berezikov E, Cronembold D, Girard A, van den Elst H, Filippov DV, Blaser H, Raz E, Moens CB, Plasterk RH, Hannon GJ, Draper BW, Ketting RF. A role for Piwi and piRNAs in germ cell maintenance and transposon silencing in zebrafish. Cell 2007; 129:69-82.
23. Essers J, Theil AF, Baldeyron C, van Cappellen WA, Houtsmuller AB, Kanaar R, Vermeulen W. Nuclear dynamics of PCNA in DNA replication and repair. Mol Cell Biol 2005; 25:9350-9359.
24. Miura C, Miura T, Yamashita M. PCNA protein expression during spermatogenesis of the Japanese eel (*Anguilla japonica*). Zool Sci 2002; 19:87-91.
25. Van de Kant HJG, de Rooij DG. Periodic acid incubation can replace hydrochloric acid hydrolysis and trypsin digestion in immunogold-silver staining of bromodeoxyuridine incorporation in plastic sections and allows the PAS reaction. Histochem J 1992; 24:170-175.
26. Miura T. Spermatogenic cycle in fish. In: Knobil E, Neill JD (eds), Encyclopedia of Reproduction. San Diego: Academic Press; 1999: 4:571-578.

27. Grier HJ, Linton JR, Leatherland JF, De Vlaming VL. Structural evidence for two different testicular types in teleost fishes. Amer J Anat 1980; 159:331-345.
28. Grier HJ. Cellular organization of the testis and spermatogenesis in fishes. Amer Zool 1981; 21:345-357.
29. Parenti LR, Grier HJ. Evolution and phylogeny of gonad morphology in bony fishes. Integr Comp Biol 2004; 44:333-348.
30. Almeida FFL, Kristoffersen C, Taranger GL, Schulz RW. Spermatogenesis in Atlantic cod (*Gadus morhua*): A novel model of cystic germ cell development. Biol Reprod 2008; 78:27-34.
31. Garcia-Lopez A, Martinez-Rodriguez G, Sarasquete C. Male reproductive system in Senegalese sole *Solea senegalensis* (Kaup): anatomy, histology and histochemistry. Histol Histopathol 2005; 20:1179-1189.
32. Petersen C, Soder O. The Sertoli cell--a hormonal target and ‘super' nurse for germ cells that determines testicular size. Horm Res 2006; 66:153-161.
33. Billard R. La spermatogenèse de *Poecilia reticulata*. I – Estimation du nombre de générations goniales et rendement de la spermatogenèse. Ann Biol Anim Bioch Biophys 1969; 9:251-271.
34. Van den Hurk R, Peute J, Vermeij JAJ. Ultrastructural study of the testis of the black molly (*Mollienisia latipinna*) I. The intratesticular efferent duct system. Proc Kon Ned Akad Wet Ser 1974; 77:460-469.
35. Leal MC, Feitsma H, Cuppen E, França LR, Schulz RW. Completion of meiosis in male zebrafish (*Danio rerio*) despite lack of DNA mismatch repair gene *mlh1*. Cell Tissue Res 2008; 332:133-139.
36. Sharpe RM. Regulation of Spermatogenesis. In: Knobil E, Neill JD (eds), The Physiology of Reproduction. New York: Raven Press; 1994: 1363-1434.
37. França LR, Russell LD. The testis of domestic animals. In: Martínez-García F, Regadera J (eds), Male reproduction: a multidisciplinary overview. Madrid: Churchill Communications; 1998: 198-219.

38. Baum JS, St George JP, McCall K. Programmed cell death in the germ line. Semin Cell Dev Biol 2005; 16:245-259.
39. Ewing HH. Spermatogenesis in the zebrafish, *Brachydanio rerio*. Anat Rec 1972; 172:308.
40. Ando N, Miura T, Nader MR, Miura C, Yamauchi K. A method for estimating the number of mitotic divisions in fish testes. Fisheries Sci 2000; 66:299-303.
41. Billard R. A quantitative analysis of spermatogenesis in the trout, *Salmo trutta fario*. Cell Tiss Res 1983; 230:495-502.
42. Lo Nostro FL, Grier H, Meijide FJ, Guerrero GA. Ultrastructure of the testis in *Synbranchus marmoratus* (Teleostei, Synbranchidae): the germinal compartment. Tissue Cell 2003; 35:121-132.
43. Quagio-Grassiotto I, Carvalho ED. The ultrastructure of *Sorubim lima* (Teleostei, Siluriformes, Pimelodidae) spermatogenesis: premeiotic and meiotic periods. Tissue Cell 1999; 31:561-567.
44. Billard R. Ultrastructural changes in the spermatogonia and spermatocytes of *Poecilia reticulata* during spermatogenesis. Cell Tissue Res 1984; 237(2):219-226.
45. Selman K, Wallace RA. Gametogenesis in *Fundulus heteroclitus*. Am Zool 1986; **26:**173-192.
46. Chiarini-Garcia H, Meistrich ML. High-resolution light microscopic characterization of spermatogonia. In: Hou SX, Singh SR (eds), Germline stem cells. Methods in Molecular Biology, Humana Press, Springer Science; 2008; 450:95-107.
47. Chiarini-Garcia H, Russell LD. Characterization of mouse spermatogonia by transmission electron microscopy. Reproduction 2002; 123:567-577.
48. Lacerda SMSN, Batlouni SR, Silva SBG, Homem CSP, França LR. Germ cells transplantation in fish: the Nile-tilapia model. Anim Reprod 2006; 3:146-159.

49. Shikina S, Ihara S, Yoshizaki G. Culture conditions for maintaining the survival and mitotic activity of rainbow trout transplantable type A spermatogonia. Mol Reprod Dev 2008; 75:529-537.
50. Fuller MT, Spradling AC. Male and female Drosophila germline stem cells: two versions of immortality. Science 2007; 316:402-404.
51. De Rooij DG. Proliferation and differentiation of spermatogonial stem cells. Reproduction 2001; 121:347-354.
52. Nakagawa T, Nabeshima Y, Yoshida S. Functional identification of the actual and potential stem cell compartments in mouse spermatogenesis. Dev Cell 2007; 2:195-206.
53. Grier HJ. Sperm development in the teleost *Oryzias latipes*. Cell Tissue Res 1976; 168:419-431.
54. Sprando RL, Heidinger RC, Russell LD. Spermiogenesis in the bluegill (*Lepomis macrochirus*): A study of cytoplasmic events including cell volume changes and citoplasmic elimination. J Morph 1988; 198:165-177.
55. Lunstra DD, Schanbacher BD. Testicular function and Leydig cell ultraestructure in long-term bilateral cryptorchid rams. Biol Reprod 1988; 38:211-220.
56. Almeida FFL, Leal MC, França LR. Testis morphometry, duration of spermatogenesis and spermatogenic efficiency in the wild boar (*Sus scrofa scrofa*). Biol Reprod 2006; 75:792-799.
57. Johnson L, Neaves WB. Age related changes in the Leydig cell population, seminiferous tubules and sperm population in stallions. Biol Reprod 1981; 24:703-712.
58. Leal MC, França LR. The seminiferous epithelium cycle length in the black tufted-ear marmoset (*Callithrix penicillata*) is similar to humans. Biol Reprod 2006; 74:616-624.

59. Egami N, Hyodo-Taguchi Y. An autoradiographic examination of rate of spermatogenesis at different temperatures in the fish, *Oryzias latipes*. Exp Cell Res 1967; 47:665-667.
60. Billard, R. Influence de la température sur la durée et l`efficacé de la spermatogenèse du guppy, *Poecilia reticulata*. C R Acad (Paris) 1968; 206:2287-2290.
61. De Felice DA, Rasch EM. Chronology of spermatogenesis and spermiogenesis in Poeciliid fishes. J Exp Zool 1969; 171:191-208.
62. Silva M, Godinho HP. Timing of some events of the gametogenesis in the male Nile tilapia, *Sarotherodon niloticus*. Arch Anat Mic 1983; 72:231-237.
63. Sinha GM, Mondal SK, Ghosal SK. Meiosis and spermiogenesis in a freshwater teleost fish, *Channa punctatus* (Bloch): An estimation of their duration by autoradiographic method. Cytol 1983; 48:87-93.
64. França LR, Ogawa T, Avarbock MR, Brinster RL, Russell LD. Germ cell genotype controls cell cycle during spermatogenesis in the rat. Biol Reprod 1998; 59:1371-1377.
65. Sinha GM, Mondal SK, Midya T, Ghosal SK. Chronology of meiosis and spermiogenesis in a fresh-water teleost fish, *Colisa fasciata* (Bloch and Schneider). Z Mikrosk Anat Forsch 1979; 93:442-448.
66. Billard R. Spermatogenesis and spermatology of some teleost fish species. Reprod Nutr Dévelop 1986; 26:877-920.
67. Licht P, Basu SL. Influence of temperature on lizard testes. Nature 1967; 213:672-674.
68. Setchell BP. The blood-testicular fluid barrier in sheep. J Physiol 1967; 189:63-65.
69. Dym M, Fawcett DW. The blood-testis barrier in the rat and the physiological compartimentation of the seminiferous epithelium. Biol Reprod 1970; 3:308-326.

70. Fawcett DW, Leak LV, Heidger PM Jr. Electron microscopic observations on the structural components of the blood-testis barrier. J Reprod Fertil Suppl 1970; 10:105-122.
71. Ross MH. Sertoli-Sertoli junctions and Sertoli-spermatid junctions after efferent ductule ligation and lanthanum treatment. Am J Anat 1977; 148:49-55.
72. Bergmann M, Schindelmeiser J. Development of the blood testis barrier in the domestic fowl (*Gallus domesticus*). Inter J Androl 1987; 10:482-488.
73. Baccetti B, Bigliardi E, Vegni Talluri M, Burrini AG. The Sertoli cell in lizards. J Ultrastruct Res 1983; 85:11-23.
74. Franchi E, Camatini M, de Curtis I. Morphological evidence of a permeability barrier in urodele testis. J Ultrastruct Res 1982; 80:253-263.
75. Abraham M, Rahamim E, Tibika H, Golenser E, Kieselskin M. The blood-testis barrier in *Aphanius dispar* (Teleostei). Cell Tissue Res 1980; 211:207-214.
76. Silva S, Godinho HP. Barreira hemotesticular em *Oreochromis niloticus* (peixe-teleósteo). Rev Bras Ciên Morfol 1989; 6:9-13.
77. Billard R. La spermatogenèse de *Poecilia reticulata* III. Ultrastructure des cellules de Sertoli. Ann Biol Anim Bioch Biophys 1970; 10:37-50.
78. Abraham M. The male germ cell protective barrier along phylogenesis. Int Rev Cytol 1991; 130:111-190.

Legends to Supplemental Figures

Supplemental Table 1: Primers used to generate a DNA template for DIG-labelled cRNA probe synthesis

Primer	Nucleotide sequence (5' → 3')
1039[a]	T3Rpps-CAGGAGAAAGTGTCCGACTATGAGATGAAA
1040[b]	T7Rpps-AACCACAGCAGACACTGAGTAATAAAATGCAT

[a]Primer 1039 contains the T3 RNA polymerase promoter sequence (underlined) at its 5'-end (T3Rpps; 5'-TTTACCTGTTATTAACCCTCACTAAAGGG-3').
[b]Primer 1040 contains the T7 RNA polymerase promoter sequence (underlined) at its 5'-end (T7Rpps; 5'-TTTACCTGTAATACGACTCACTATAGGG-3').

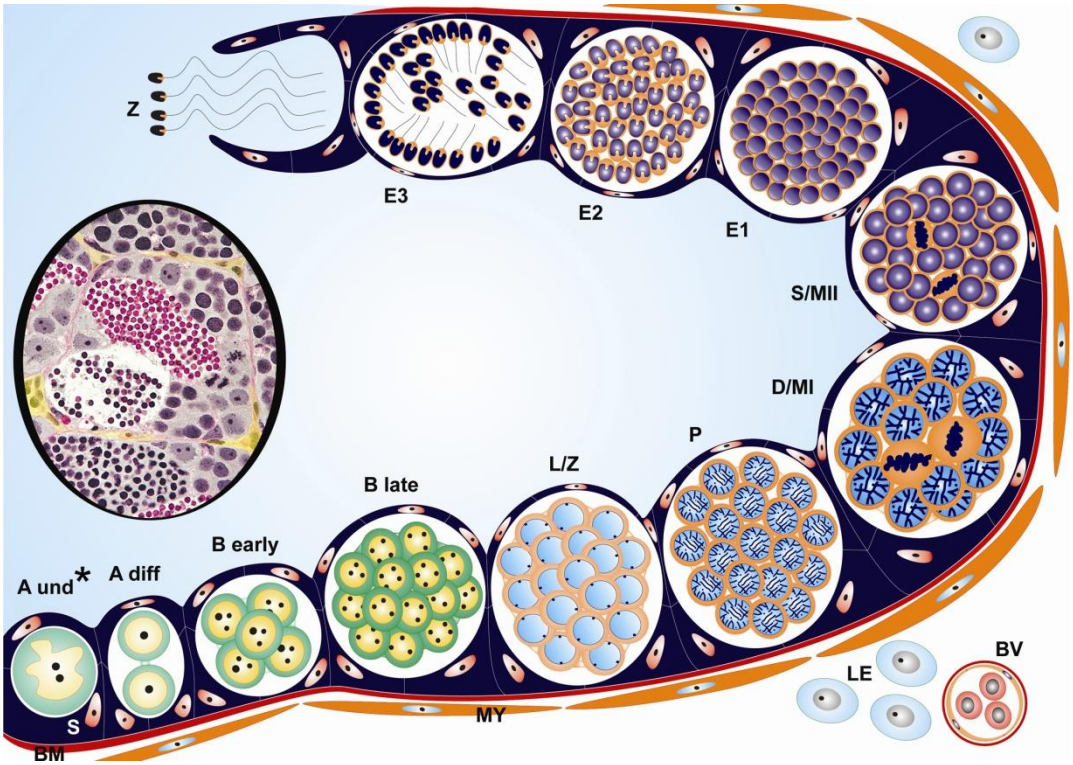

Supplemental Figure 1: Schematic drawing illustrating the progression of zebrafish spermatogenesis from the most undifferentiated type A spermatogonium (A_{und*}) to spermatozoa (Z). Spermatogenesis takes place within cysts that are distributed along the basement membrane (BM) of the seminiferous epithelium. Cysts are formed when Sertoli cells (S) surround completely a single spermatogonium type A_{und*}. Cells resulting from the incomplete mitosis of differentiating type A spermatogonia remain connected by cytoplasmic bridges, developing in a clonal fashion according to the following sequence: type A differentiated spermatogonia (A_{diff}) → type B early spermatogonia (B_{early}) → type B late spermatogonia (B_{late}) → leptotene/zygotene spermatocytes (L/Z)→ pachytene spermatocytes (P) → diplotene spermatocytes/metaphase I (D/MI) → secondary spermatocytes/metaphase II (S/MII) → early spermatids (E1) → intermediate spermatids (E2) → late spermatids (E3) → spermatozoa (Z). As spermatogenesis progresses germ cell number increases within the cyst. Consequently, the number of Sertoli cells per cyst also increases until diplotenic cysts. Note that in cystic spermatogenesis, a given Sertoli cell is usually in contact with only one germ cell clone. The diagram also illustrates the peritubular myoid cells (MY), and Leydig cells (LE) near interstitial blood vessels (BV). The inset shows a histological cross section of a seminiferous tubule with spermatogenic cysts in different stages of germ cell development in the germinative compartment. The interstitial compartment containing Leydig cells and other elements is colored in yellow.

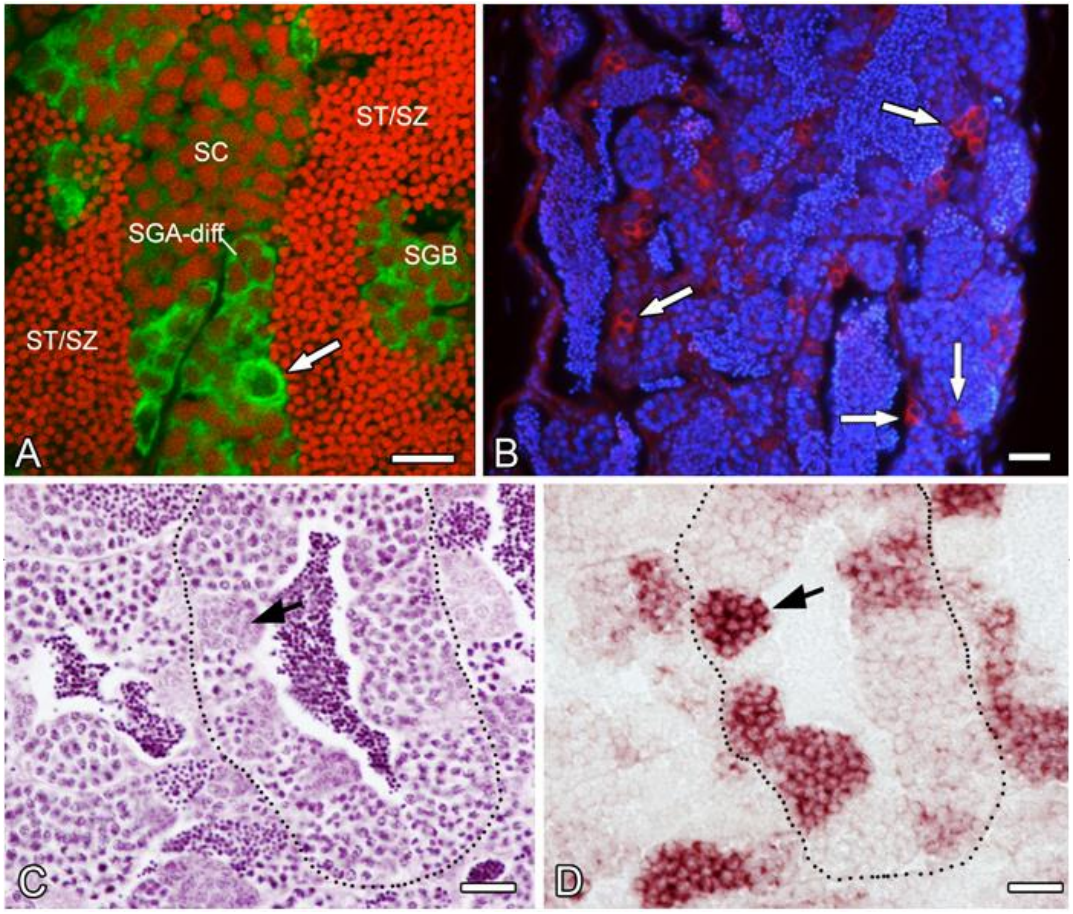

Supplemental Figure 2: Vasa and Ziwi protein and *pcna* mRNA localization in zebrafish testis. An intense labeling for Vasa and Ziwi protein is found in type A spermatogonia (**A-B**, white arrows). *pcna* mRNA is mainly found in cysts with type B spermatogonia (black arrow). Adjacent sections were stained with hematoxilin (**C)** or with *pcna* anti-sense cRNA probe (**D**). The stippled line indicated the circumference of a spermatogenic tubule. Differentiating type A spermatogonia (SGA-diff); Type B spermatogonia (SGB); spermatocytes (SC); spermatids/spermatozoa (ST/SZ). Scale bars are 25µm (**A, C** and **D**), or 50µm (**B**).

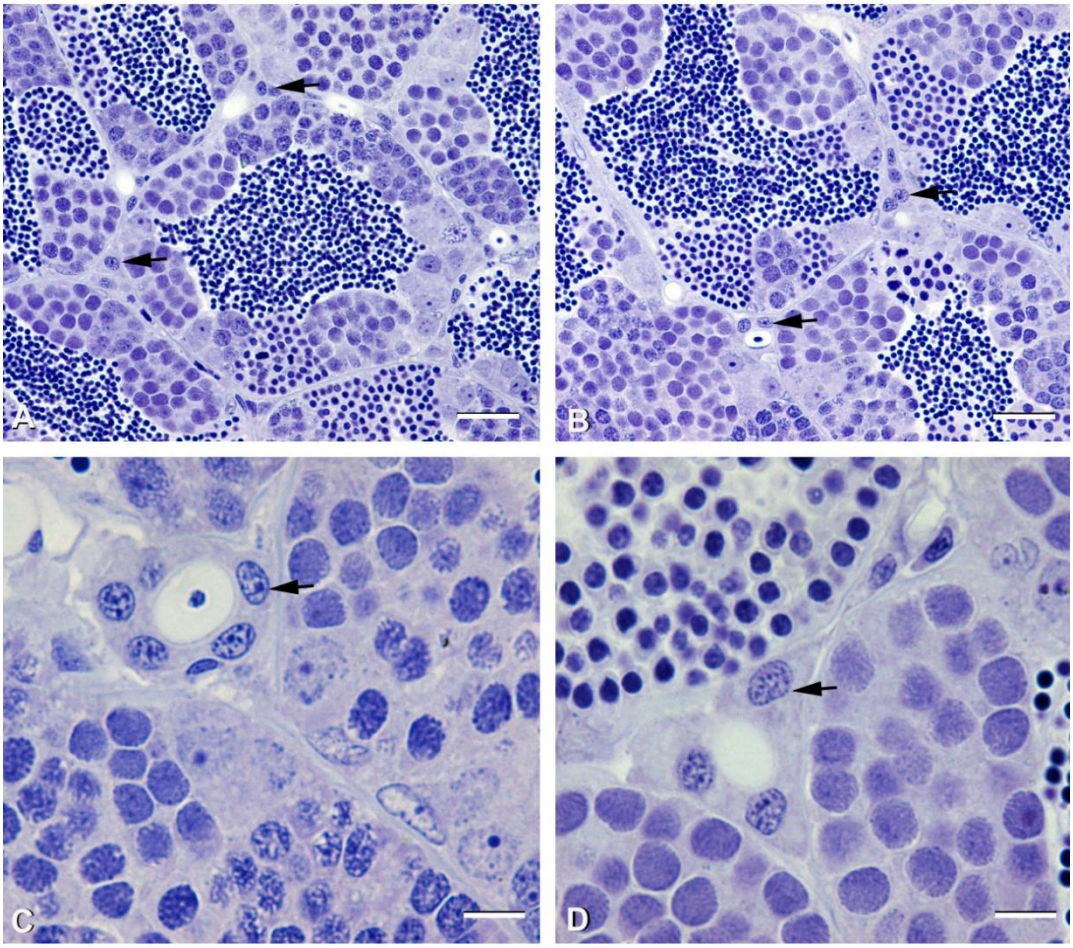

Supplemental Figure 3: Histological sections of zebrafish testis showing Leydig cells in the intertubular space (arrows) **(A-B)**. They often form clusters, sometimes in the form of ring-like structures around blood vessels (arrows) **(C-D)**. Scale bars are 20µm (**A** and **B**) or 10µm (**C-D**).

CHAPTER 3

Spermatogonial Stem Cell Niche and Spermatogonial Stem Cell Transplantation in Zebrafish

Nóbrega RH, Greebe CD, van de Kant H, Bogerd J, de França LR, Schulz RW.

PLoS One. 2010 Sep 20;5(9). pii: e12808. doi: 10.1371/journal.pone.0012808.

ABSTRACT

Spermatogonial stem cells (SSCs) are the foundation of spermatogenesis, and reside within a specific microenvironment in the testes called "niche" which regulates stem cell properties, such as, self-renewal, pluripotency, quiescence and their ability to differentiate. Here, we introduce zebrafish as a new model for the study of SSCs in vertebrates. Using 5'-bromo-2'-deoxyuridine (BrdU), we identified long term BrdU-retaining germ cells, type A undifferentiated spermatogonia as putative stem cells in zebrafish testes. Similar to rodents, these cells were preferentially located near the interstitium, suggesting that the SSC niche is related to interstitial elements and might be conserved across vertebrates. This localization was also confirmed by analyzing the topographical distribution of type A undifferentiated spermatogonia in normal, *vasa::egfp* and *fli::egfp* zebrafish testes. In the latter one, the topographical arrangement suggested that the vasculature is important for the SSC niche, perhaps as a supplier of nutrients, oxygen and/or signaling molecules among other factors. We also developed an SSC transplantation technique for both male and female recipients as an assay to evaluate the presence, biological activity, and plasticity of the SSC candidates in zebrafish. We demonstrated donor-derived spermato- and oogenesis in male and female recipients, respectively, indicating the stemness of type A undifferentiated spermatogonia and their plasticity when placed into an environment different from their original niche. Similar to other vertebrates, the transplantation efficiency was low, and might be attributed to the "pro-differentiation" testicular microenvironment created after busulfan depletion in the recipients, which may have favored differentiation rather than self-renewal of the transplanted SSCs.

INTRODUCTION

Spermatogenesis is a cellular developmental process by which self-renewing spermatogonial stem cells (SSCs) differentiate into millions of sperm daily [1], [2]. To sustain this process continuously throughout the male reproductive life span, SSCs reside within a specific microenvironment in the testes called "niche" which regulates their properties, such as, self-renewal, pluripotency, quiescence and their ability to differentiate [3]-[5]. Despite of its crucial importance on SSC fate, the cellular and molecular composition of SSC niche remain unknown for several species of vertebrates. In rodents, SSC niche has recently been identified within regions of the seminiferous tubules which are adjacent to the interstitial compartment, preferentially along the branches of the interstitial blood vessels [6]-[8]. Apparently, the cellular and molecular environment near the interstitial compartment promotes SSC renewal, and when SSCs leave these areas, the changes in the environment promote their differentiation [5]. The proximity of SSC niche near the interstitium perhaps might be attributed due to the vascular supply of oxygen, nutrients, or hormones, such as follicle-stimulating hormone (FSH) or luteinizing hormone (LH) which influence Leydig and Sertoli cell functions on SSC self-renewal and also on SSC retention and homing in the niche [5], [9]-[11]. For example, FSH induces the secretion of GDNF (glial cell-line derived neurotrophic factor), an extrinsic stimulator of SSC self-renewal, produced by Sertoli cells [3].

Currently, the only means to study SSCs and their niche is by exploiting the stem cells' functional properties, such as slow-cycling and quiescent nature through the label-retaining cell (LRC) approach, or by

studying SSC functionality and plasticity by transplantation assays. In this context, transplantation techniques developed by Brinster and collaborators [12], [13] has enabled tremendous progress in the phenotypic and functional investigations of SSCs. Nowadays, SSC transplantation approaches have been developed for a number of species including also teleost fish [14], [15]. These data have allowed broad implications for understanding the regulation of spermatogenesis, stem cell biology, etiology of male infertility [16]-[20], and also in biotechnology, such as, conservation of valuable genetic stocks, preservation of endangered species, and also as new option for transgenesis [14], [15], [17].

In zebrafish (*Danio rerio*), histological studies have described two subtypes of type A undifferentiated spermatogonia in the testes, designated as A_{und*} and A_{und} [21]. It is still unknown if these two subtypes are separated by mitosis, or if they represent different stages of the same cell cycle [2]. Moreover, there is no information on the spermatogonial stem cell niche in the zebrafish testis, or on the stemness of A_{und*}/A_{und}.

In the current study, we identified the putative SSCs and their niche by identifying the LRCs in zebrafish testes and using a transgenic zebrafish expressing enhanced green fluorescent protein under the control of the germ cell specific *vasa* promoter (*vasa::egfp*) [22]. Furthermore, we also evaluated the spatial relationship between blood vessels and the SSC niche, using testes expressing enhanced green fluorescent protein under the control of the endothelial cell specific *fli* promoter (*fli::egfp*) [23]. To confirm the biological activity (reestablishment of function and plasticity) of the potential SSCs, we developed a transplantation assay in zebrafish. Finally, we characterized the hormonal and genetic recipient's testicular

microenvironment prior transplantation that might have influenced the behavior of the transplanted SSCs.

MATERIAL AND METHODS

Animals

Sexually mature zebrafish males and females, and sexually mature transgenic zebrafish males expressing enhanced green fluorescent protein under the control of the germ cell-specific *vasa* promoter (*vasa::egfp*) [22] or the endothelial cell-specific *fli* promoter (*fli::egfp*) [23] were used. Animal housing and experimentation were consistent with Dutch and Brazilian national regulations and were approved by the Utrecht University and Federal University of Minas Gerais animal use and care committees, respectively.

Topographical distribution of type A undifferentiated spermatogonia in zebrafish seminiferous tubules

Testes from males (n=5) were fixed in 4% buffered glutaraldehyde at 4^{o}C overnight, dehydrated, and embedded in Technovit 7100 (Heraeus Kulzer, Wehrheim, Germany, http://www.kulzer-technik.de), sectioned and stained according to conventional histological procedures [21], [24]. The topographical distribution of early spermatogonia was recorded by examining if type A undifferentiated spermatogonia were adjacent to the interstitial compartment, or contacting one or more tubules (intertubule). The position of 500 type A undifferentiated spermatogonia was counted per animal and expressed as percentage of the total number evaluated; to determine if the distribution of these cells follows a random pattern, the

tubular perimeters adjacent to the interstitium, or intertubule were measured using Image J software (National Institutes of Health, Bethesda, Maryland, USA, http://rsbweb.nih.gov/ij), and the values were expressed as percentage of the total tubular perimeter (n= 50 tubules/animal).

Identification and quantification of label retaining cells (LRCs) in zebrafish testes

To estimate the cell cycle duration of type A undifferentiated spermatogonia, 10 males were exposed to BrdU (Sigma-Aldrich, St. Louis, MO, USA, http://www.sigmaaldrich.com) dissolved in water (4mg/ml) for approximately 4 and 10 h. To identify the LRC population, 25 males were pulsed with BrdU dissolved in water (4 mg/ml) for 10 h/day during 3 consecutive days. Animals (n=5) were sacrificed immediately after the third BrdU pulse, and after 1, 2, 3 and 4 weeks of chase. Testes were fixed, embedded, and sectioned as described above. BrdU incorporation was detected by immunohistochemistry as described previously [25]. Quantification of LRCs was achieved by determining the percentage of labeled cells out of 1000 cells (labeled and non-labeled). The spatial distribution of LRCs was determined by counting the number of labeled cells situated near the interstitium, or in the intertubule, or near the testicular capsule after 3-4 weeks of chase. The values were expressed as percentage of positive-BrdU cells in the mentioned regions.

Whole-mount analysis of *vasa::egfp* testes under confocal laser scanning microscopy (CLSM) and examination of *fli::egfp* testes

Testes from transgenic *vasa::egfp* [22] or *fli::egfp* [23] zebrafish were fixed in 2% buffered paraformaldehyde for 2 h. For whole-mount

examination, *vasa::egfp* testes were permeabilized with 0.2% PBT (0.2% Triton X-100 in PBS) for 10 min, and subsequently stained in DAPI (Invitrogen Molecular Probes, Carlsbad, CA, USA, www.invitrogen.com) for 5 min, followed by two rinses in PBS for 10 min. *vasa::egfp* testes (n=5) were analyzed by CLSM 510 Meta (Zeiss, Jena, Germany, www.zeiss.de/lsm) using 358 nm and 488 nm as excitation wavelengths for DAPI and GFP, respectively. *fli::egfp* testes were frozen in Tissue-Tek (Sakura Finetek Europe B.V., Leiden, Netherlands, http://www.sakura.eu) and cryosectioned at 10 µm, permeabilized in 0.2% PBT for 10 min, stained with DAPI (Invitrogen) for 5 min, and mounted with a coverslip using an anti-fading Vectashield mounting medium (Vector Laboratories, Burlingame, CA, USA, http://www.vectorlabs.com). Sections were examined under fluorescence microscopy using filters for DAPI and FITC visualization.

Depletion of endogenous spermatogenesis in zebrafish male recipients for SSC transplantation

To deplete endogenous spermatogenesis, we first examined the effect of different temperatures. Overall, the speed of spermatogenesis in teleost fish is significantly influenced by temperature [26]. Hence, males were kept in water at 20°C (n=15), 27°C (n=12), 30°C (n=7), or 35°C (n=12) for at least one week. Then, animals received one single intraperitoneal injection of ^{3}H-thymidine (Amersham/GE Healthcare, Piscataway, NJ, USA, http://www.gehealthcare.com) (2 µCi/g/BW), and were sacrificed at 2 h, 12 h, 1, 2, 3, 4, 5 and 6 days after thymidine injection. Testes were weighed for calculating the gonadosomatic index (GSI = testes weight/body weight x100), fixed, embedded and sectioned as

above, and prepared for autoradiographic analysis to estimate the duration of meiosis and spermiogenesis as described previously [14], [27]. Based on these results (Figure S1), temperature of 35°C was chosen as optimal to deplete endogenous zebrafish spermatogenesis. Then, 60 zebrafish males were kept at 35°C for at least one week, and received a single intraperitoneal dose of 30 or 40 mg/Kg/BW of busulfan (Sigma). Testes from males (n=6) were sampled 2, 4, 6, 10 and 12 days after the injection, weighed, fixed, embedded, sectioned and stained as above. As control group, males (n=30) received a single intraperitoneal injection of dimethyl sulfoxide and sampled at the same reported periods. To evaluate the optimal dose and the best window of depletion, frequency of spermatogenic cysts, germ cell apoptosis, and Sertoli cell only phenotype were determined for each sampled period. Results were expressed as percentage of the total number of counted structures.

Preparation of zebrafish female recipients for SSC transplantation

Ovoposition was induced according to usual procedures (http://zfin.org). To evaluate if females after ovoposition may be suitable recipients for SSC transplantation, ovaries (n=5) were fixed, embedded, and sectioned as above, and stained with PAS to determine the number of postovulatory follicles (POFs)/mm^2 of tissue. POFs consisting for a great part of granulosa cells remaining after ovulation, were considered as a space potentially available for transplanted SSCs. The number of POFs/mm^2 from preovulatory females was also evaluated as a control.

Donor cell preparation and SSC transplantation into male and female zebrafish recipients

Testes from males (n=10) were digested with 0.2% collagenase and 0.12% dispase [28]. The obtained cell suspension was immediately submitted to FACS (Fluorescence Activated Cell Sorting) using an inFlux cell sorter (BD Bioscience, San Jose, CA, USA, *www.bdbiosciences.com*). *Vasa* is highly expressed in type A undifferentiated spermatogonia, but expression decreases during meiosis and spermiogenesis [21]. Since type A undifferentiated spermatogonia are the largest germ cell type in zebrafish testes (~10 µm nuclear diameter [21]), FACS settings were adjusted to sort a cell population displaying large size and high intensity of fluorescence, which should enrich type A undifferentiated spermatogonia. To validate the enrichment, the cell fraction obtained by FACS was analyzed under fluorescence microscopy, or fixed, embedded, sectioned, and stained as above to determine the percentage of germ cell type. For SSC transplantation, the FACS-enriched cell fraction was suspended in L-15 medium (Sigma), 5% trypan blue and 10% calf serum. SSCs were transplanted into testes or ovaries through the genital pores, using a glass capillary needle coupled to a peristaltic pump (Figure S2). To optimize this procedure, zebrafish male and female genital pores were analyzed morphologically (diameter and angle) to adjust the settings for the glass capillary needle (Figure S2). The transplantation route was standardized and tested by injecting trypan blue (Figure S2).

SSC transplantation analysis

Recipients were sacrificed 2 and 3 weeks (males) or 3 and 4 weeks (females) after transplantation. The gonads were fixed in 2% buffered paraformaldehyde for 2 h, permeabilized, and stained with DAPI before analysis by CLSM, as described above. As positive control, Vasa protein

expression was examined by GFP immunodection in *vasa::egfp* gonad sections or by Vasa immunocytochemistry in wild-type males [29]. The PCR detection of donor-derived germ cells in male and female recipients was carried out as described previously [30], using a system that detects both *gfp* and *yfp*.

Characterization of 11-ketotestosterone (11-KT) plasma levels in busulfan-depleted male zebrafish and 11-KT release by depleted testes *in vitro*

Males (n=19) were sampled 10 days after busulfan (40 mg/kg) treatment. A blood sample was collected for quantification of 11-ketotestosterone (11-KT) plasma levels, as described previously [31]. As controls, 11-KT plasma levels were also quantified in zebrafish kept at 27°C (n=7), or at 35°C (n=11). In other experiments, carried out at the same time, but published separately [31], 11-KT plasma levels were measured 2 h after a single injection of recombinant zebrafish Fsh or hCG. Results are expressed as ng 11-KT/ml of plasma. To evaluate testicular 11-KT release in tissue culture, testes were collected from adult zebrafish kept at 27ºC (control) (n=7), or from busulfan-treated zebrafish (n=7). The two testes of a given fish were incubated in parallel, such that one of them (randomly chosen left or right) served as control (basal) for the contralateral one, which was incubated in the presence of 1 µM of the adenylate cyclase activator forskolin [31]. After incubation the medium was processed for the quantification of 11-KT [32]. Results were expressed as ng 11-KT/mg of tissue.

Gene expression in spermatogenesis-depleted testes in busulfan-treated zebrafish

Testes from males kept at 27ºC (control) (n=7), or at 35ºC (n=5), or treated with busulfan (n=12) were snap frozen in liquid nitrogen and stored at -80ºC until RNA extraction. Total RNA was extracted from testes using the RNAqueous®-Micro Kit (Ambion, Austin, TX, USA, http://www.ambion.com). Further processing to determine the threshold cycle (Cq) values of the reference endogenous control gene *elongation factor 1-alpha* (*ef1α*), as well as of *insulin-like 3 (insl3)* [33], *steroidogenic acute regulatory protein* (*star*), and *cytochrome P450, family 17, subfamily A, polypeptide 1* (*cyp17a1*), *androgen receptor* (*ar*), *anti-Müllerian hormone* (*amh*), *gonadal soma-derived growth factor (gsdf), insulin growth factor 1a (igf1a)* and *1b (igf1b)* [34], and germ cell genes *piwil1* (spermatogonia), and *synaptonemal complex protein 3 (sycp3l)* (spermatocytes) by qPCR analysis was performed as reported [31], [35], [36]. No significant differences (P>0.05) were found among the mean *β-actin1* and *ef1α* Cq values in the different groups (Figure S3) thus validating *β-actin1* and *ef1α* as a suitable references for the current experiments. Then, relative mRNA levels of the selected genes were normalized to *β-actin1* and *ef1α*, and expressed as fold of relative control (27°C) mRNA levels. Nomenclature of zebrafish proteins, mRNAs and genes are according to ZFIN (http://zfin.org) rules.

Statistical analysis

Significant differences between two groups were identified using Student test (paired and unpaired) (P<0.05), and comparisons of more than

two groups were performed with one-way ANOVA followed by Student-Newman-Keuls test ($P<0.05$), using Graph Pad Prism 4.0 (Graph Pad Software, Inc., San Diego, CA, USA, http://www.graphpad.com) for all statistical analysis.

RESULTS

Characterization of SSC candidates and their niche in zebrafish testes

The topographical distribution found for type A spermatogonia showed that 75% of undifferentiated spermatogonia are situated adjacent to the interstitial compartment (Figure 1A,C,D) which represents only 1/3rd of the total perimeter of the spermatogenic tubules (Figure 1B). Quantification of the mitotic index of these cells suggested that type A undifferentiated spermatogonia have a long-lasting cell cycle of at least 10 h (Figure 1E). To confirm the existence of a slow-cycling cell population (stem cell candidates), a pulse with BrdU was given and the testes were examined after a long period of chase (up to 4 weeks); putative stem cells are considered to be part of the LRC population. Apart from some somatic elements, type A undifferentiated spermatogonia (10%) were the only BrdU retaining germ cells after 3-4 weeks of chase (Figure 2A). Intriguingly, 76% of them were situated adjacent to the interstitium, and only 20% or 5% adjacent to the intertubular area or the testicular capsule, respectively (Figure 2B,C-H). A similar pattern was found in *vasa::egfp* testes examined under CLSM where the strongest expression of *vasa* was observed adjacent the interstitium (Figure 3 and Video S1). To further study the spatial relation between the vasculature and undifferentiated spermatogonia, testes of transgenic zebrafish expressing GFP in endothelial cells (*fli::egfp*) were analyzed.

Capillaries surround the seminiferous tubules (Figure 3F), and type A undifferentiated spermatogonia were often found in close association with endothelial cells (Figures 2E-inset; 3G-I). A combination of the above results is illustrated schematically in Figure S4, showing a hypothetical spermatogonial stem cell niche in zebrafish.

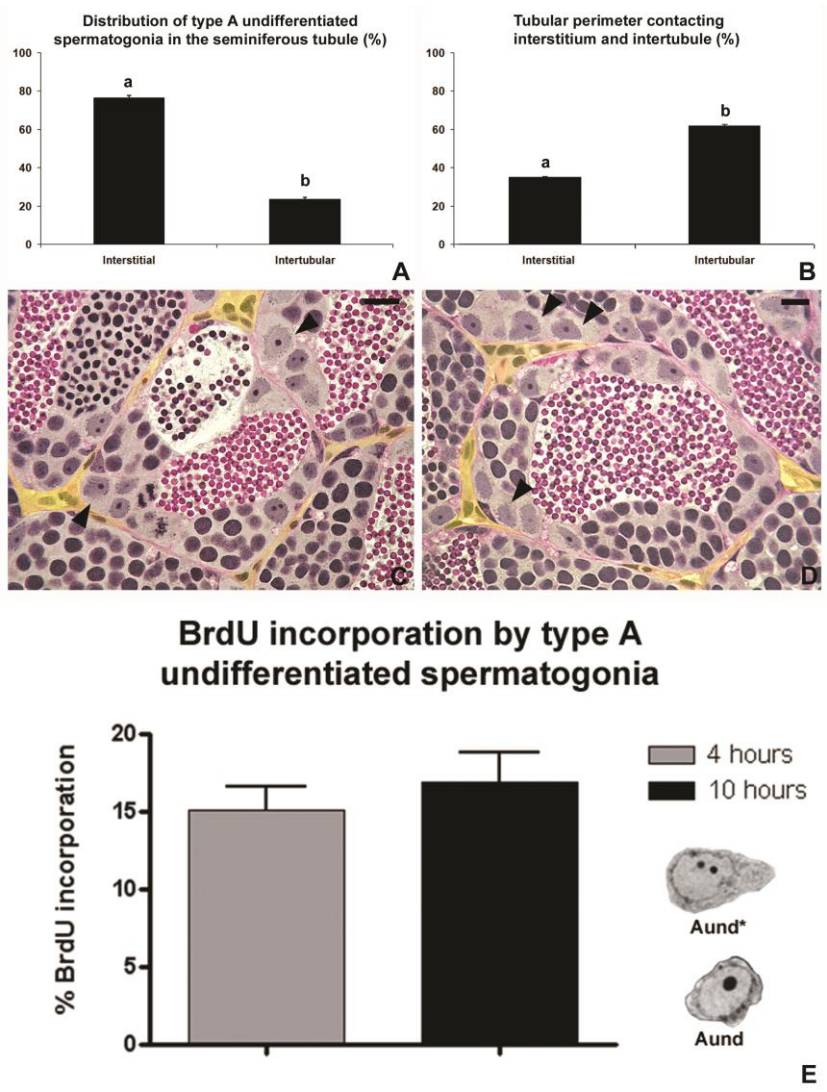

Figure 1. Topographical distribution of type A undifferentiated spermatogonia in zebrafish testes. **A.** Quantification of type A undifferentiated spermatogonia which

are situated near the interstitium or in the intertubular area. Note that ~76% of type A undifferentiated spermatogonia are preferentially located near the interstitium. **B.** Tubular perimeter of the regions contacting the interstitium and intertubule. **A,B.** Bars represent the mean ± SE which are expressed as percentage. Different letters mean significant differences between the groups. **C,D.** Histological sections of the zebrafish seminiferous tubules. Note that most of type A undifferentiated spermatogonia (arrowheads) are distributed near the interstitium which is coloured by yellow. Staining: PAS (Periodic Acid Schiff)/Ferric Hematoxylin/Metanil Yellow. Scale bar = 10 µm. **E.** Index of labeled type A undifferentiated spermatogonia after 4 and 10 hours of BrdU (4mg/ml) exposure in the water. Bars represent the mean± SE which are expressed as percentage. There is no significant difference between 4 and 10 hours of exposure.

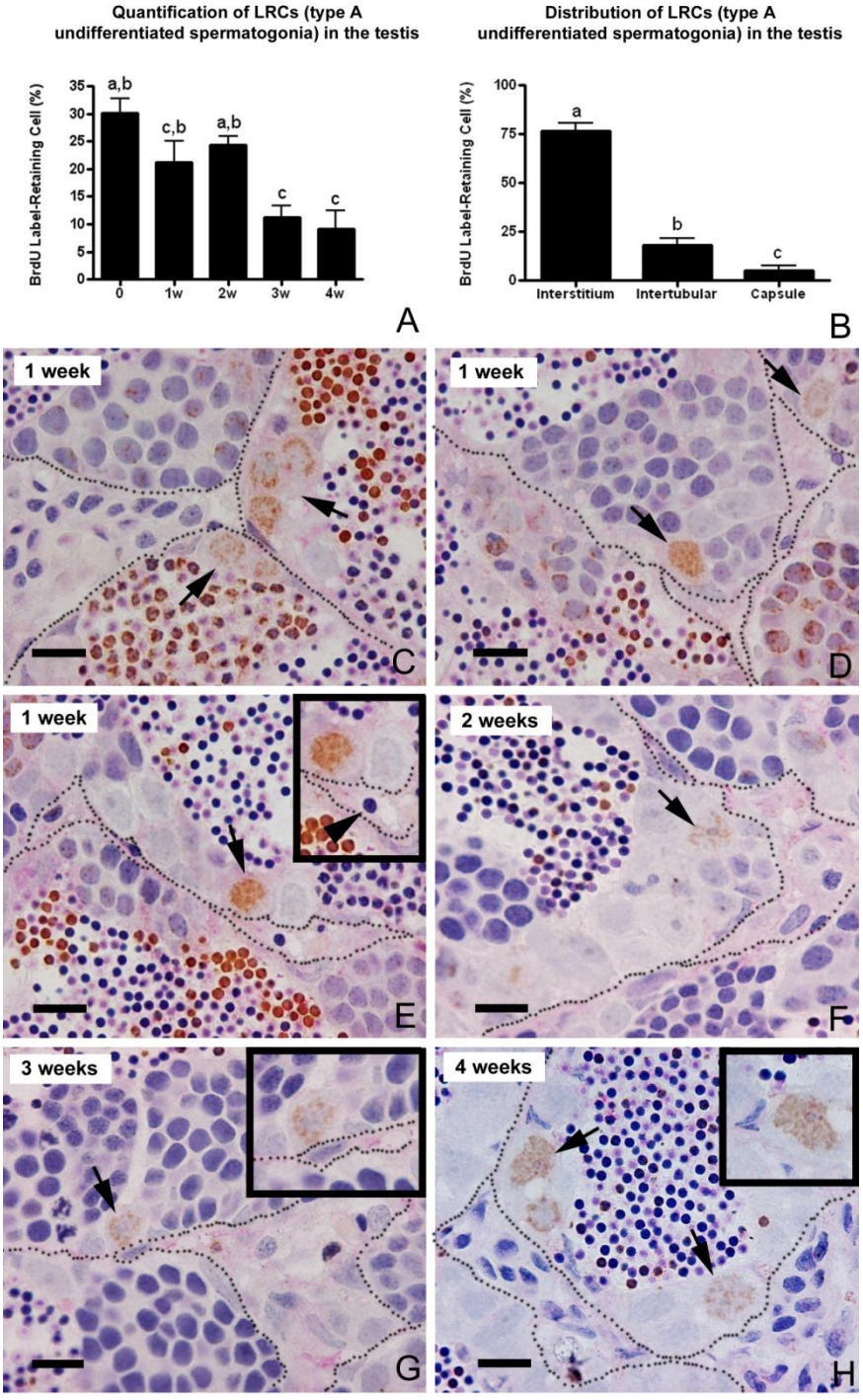
Quantification of LRCs (type A undifferentiated spermatogonia) in the testis
BrdU Label-Retaining Cell (%)
35
30
25
20
15
10
5
0
a,b
c,b
a,b
c
c
0
1w
2w
3w
4w
A
Distribution of LRCs (type A undifferentiated spermatogonia) in the testis
BrdU Label-Retaining Cell (%)
100
75
50
25
0
a
b
c
Interstitium
Intertubular
Capsule
B
1 week
C
1 week
D
1 week
E
2 weeks
F
3 weeks
G
4 weeks
H

Figure 2. Identification of BrdU LRC in zebrafish testes. **A.** Quantification of label-retaining germ cells (type A undifferentiated spermatogonia) immediately after BrdU pulse (0), and after 1, 2, 3 and 4 weeks of chase. **B.** Distribution of LRC (type A undifferentiated spermatogonia) in the zebrafish testes after 3-4 weeks of chase. Note that most of the SSC candidates are situated near the interstitium. **A,B.** Bars represent the mean ± SE which are expressed as percentage. Different letters mean significant differences ($p<0.05$) between the groups. **C-H.** BrdU immunodetection with PAS staining after 1 (**C-E**), 2 (**F**), 3 (**G**), and 4 (**H**) weeks of chase. Note that BrdU immunostaining is diluted as a consequence of the spermatogenesis progression during the weeks. Only the slow-cycling cells (stem cells candidates) are able to retain the BrdU label for long period. LRCs are indicated by arrows. Some of LRC are near to blood vessels (**arrowhead**) (**E**). Insets are high magnification of the LRCs (type A undifferentiated spermatogonia). The interstitium is delimited by spotted lines. Scale bars = 10 µm.

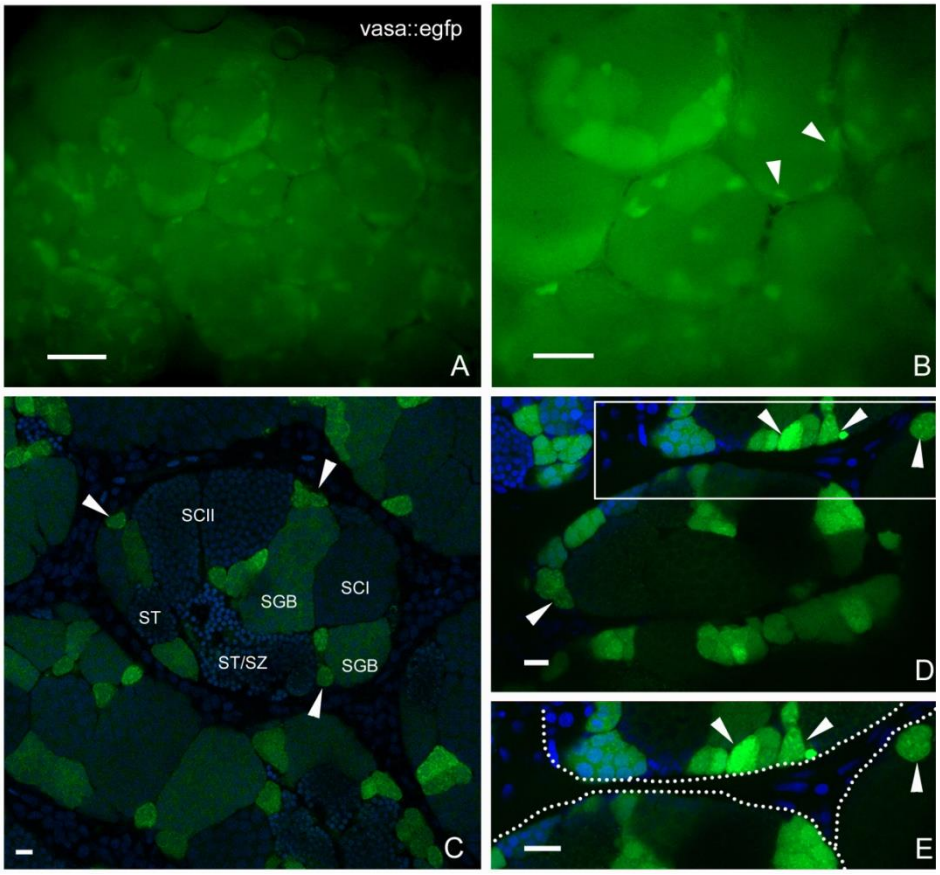

Figure 3. Legend in the next page.

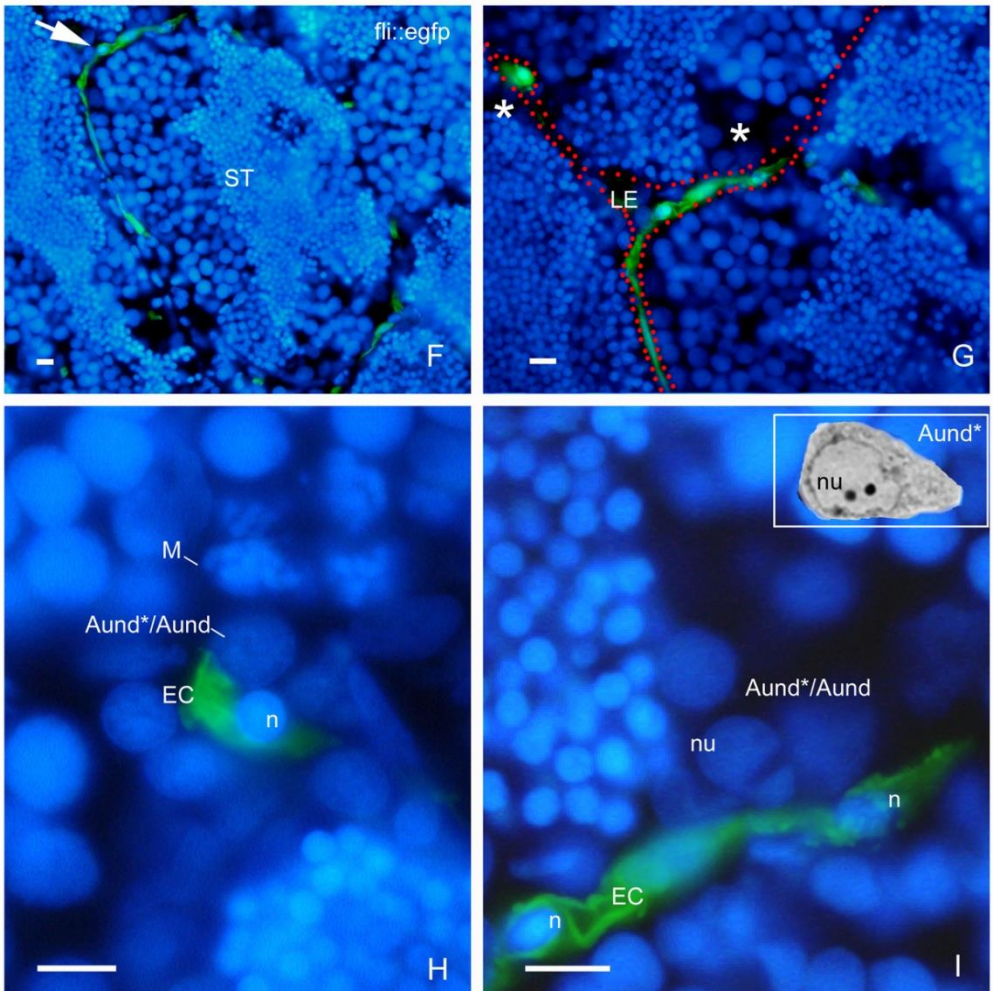

Figure 3. Whole-mount of *vasa::egfp* testes analyzed under fluorescence (**A,B**) and CLSM (**C-E**). **A,B.** Most of the brightest and small spots (type A undifferentiated spermatogonia) (arrowheads) are adjacent the triangle/lozenge dark areas (interstitium). Scale bars = 0.1 mm and 0.5 mm, respectively. **C-E.** Vasa is highly expressed in type A undifferentiated spermatogonia, and is gradually decreased during the spermatogenesis. A_{und*}/A_{und} (arrowheads), type B spermatogonia (SGB), primary spermatocytes (SCI), secondary spermatocytes (SCII), spermatids (ST), spermatids and spermatozoa (ST/SZ). Note that most of A_{und*}/A_{und} (arrowheads) are situated near the interstitium (**D**, dark areas; **E**, delimited by spotted lines). **E** is a high magnification of the square in **D**. Scale bars = 10 µm. **F-I:** Cryosections of *fli::egfp* testes stained with DAPI (nuclear staining) and analyzed under fluorescence microscopy. The arrow in **F** shows a blood vessel

(green) surrounding the circumference of a seminiferous tubule (ST). Interstitium (delimited with red dotted lines), Leydig cells (LE) and group of type A spermatogonia (asterisks) are shown in **G**. **H,I.** A_{und*}/A_{und} are near the endothelial cell (EC) nuclei (n). Note a metaphase figure (**M**) in **H**. Nucleolus (nu) of type A undifferentiated spermatogonia is shown in **I**. Compare the similar morphology of A_{und*} (inset) with the cells found near the endothelial cell. Scale bars = 10 µm.

Preparation of male and female recipients for SSC transplantation

Zebrafish were exposed to different temperatures to optimize the treatment with busulfan (Figure 4A, Figure S1). Higher temperatures accelerated spermatogenesis (Figure S1), whereas at 35^{o}C, spermatogenesis did no longer progress beyond metaphase I and showed abnormalities, such as massive apoptosis, absence of sperm, and a significant decrease of the gonadosomatic index (Figure 4A,E; Figure S1). Both doses of busulfan (30 or 40 mg/Kg/BW) tested at 35^{o}C induced germ cell apoptosis (Figure 4D-H) and a progressive GSI decrease, which reached its lowest value 10 days after injection (Figure 4B,C). However, only the higher dose suppressed efficiently endogenous spermatogenesis, resulting in 88% of the spermatogenic tubules showing a Sertoli cell only appearance, i.e. all germ cells were missing (Figure 4D,I). After only 2 more days at 35^{o}C, endogenous spermatogenesis had started to recover in these animals (Figure 4D). To prepare female zebrafish recipients for SSC transplantation, ovoposition was induced; since a pilot study indicated a high mortality among females when applying the combination of high temperature and busulfan. The increased number of POFs showed that ovoposition created spaces and “free” somatic cells (follicle cells from POFs), potentially suitable for receiving injected germ cells, and to support transplanted SSCs development, respectively (Figure S5).

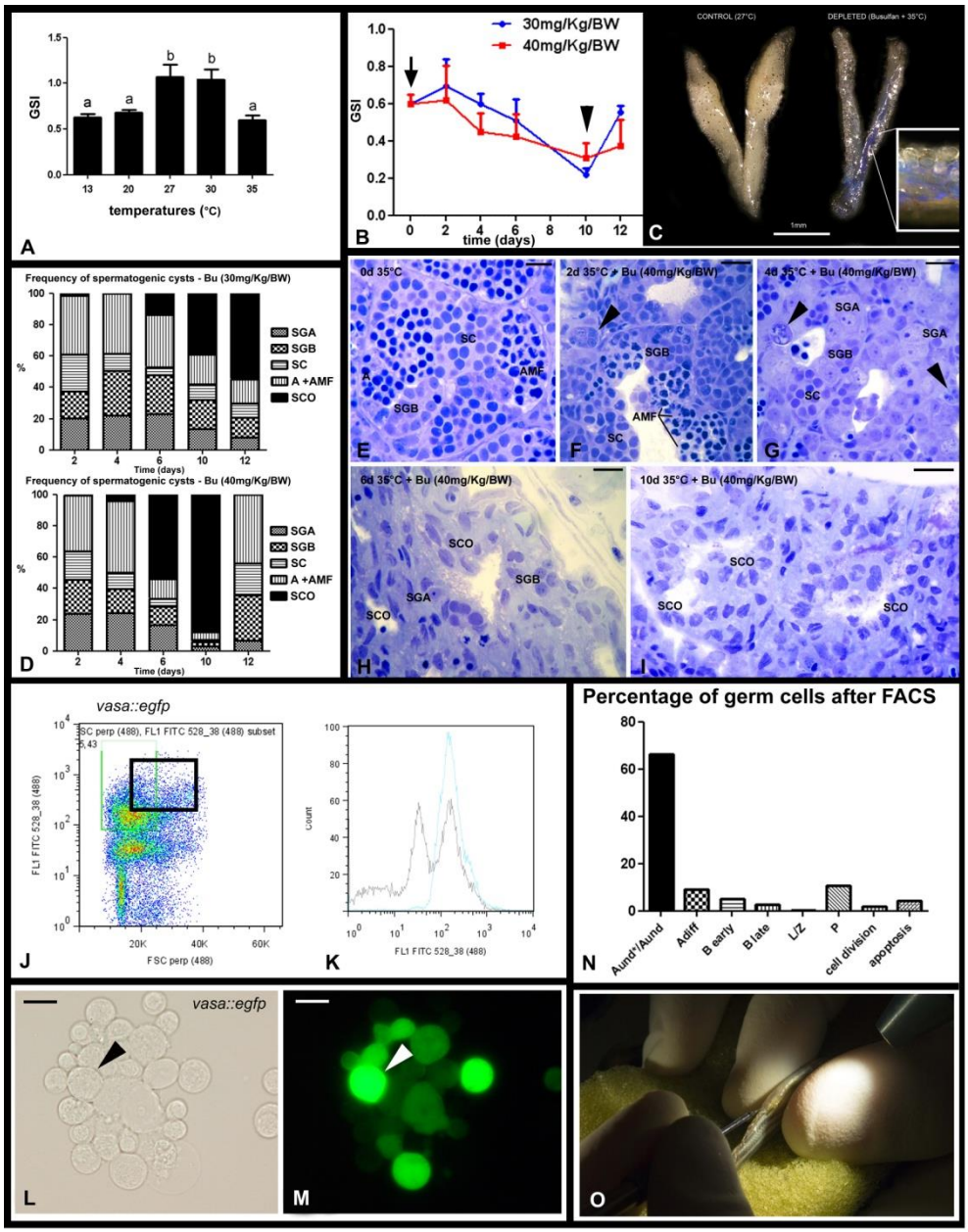

Figure 4. Depletion of endogenous spermatogenesis in male recipients for SSC transplantation. **A.** Effects of different temperatures on zebrafish GSI (gonadosomatic index). Bars represent mean ± SE. Different letters indicate significant differences ($p<0.05$) between groups. **B.** Effects of two single doses of

busulfan (30 or 40 mg/Kg) on zebrafish GSI. The arrow indicates the day of injection (day 0), whereas the arrowhead shows that the lowest GSI is observed at 10 days after injection. Dots represent mean±SE. **C.** Testes from control (27^{o}C, left) and busulfan-depleted animals. Inset shows a high magnification of the depleted testis after in vivo injection via the urogenital pore of a solution containing trypan blue. **D.** Frequency of spermatogenic cysts after a single dose of 30 or 40 mg/Kg busulfan. Type A spermatogonia (SGA), type B spermatogonia (SGB), spermatocytes (SC), apoptosis and abnormal metaphase I figures (A+AMF), Sertoli cell only (SCO). Bars represent means expressed as percentage. **E-I.** Histological sections of testes collected at 0 (**E**), 2 (**F**), 4 (**G**), 6 (**H**), and 10 (**I**) days after a single injection of 40 mg/Kg busulfan at 35^{o}C. Note that busulfan induced spermatogonial apoptosis (arrowheads) after 4 days of injection. Apoptosis (A), type A spermatogonia (SGA), type B spermatogonia (SGB), spermatocytes (SC), abnormal metaphase I figures (AMF), and Sertoli cell only (SCO) tubules. Scale bars = 10 µm. **J.** Testicular cell suspensions were obtained from *vasa::egfp* testes and subjected to FACS. Dot plot shows the total testicular suspension from which a population of large cells (forward scatter, FSC; abscissa), showing an intense fluorescence (FL1 FITC; ordinate) was sorted (black square). **K.** Histogram shows an enrichment of the sorted cells after FACS. Blue line (sorted cells), black line (total testicular cell suspension). FL1 FITC (x axis) means intensity of fluorescence, and counts (y axis), the number of events. **L,M.** Fraction of sorted cells under normal light (**L**) and under fluorescence (**M**). Arrow indicates a large cell carrying high fluorescence. Scale bars = 10 µm. **N.** Histogram showing the percentage of germ cells in the sorted fraction. Despite of the contamination with other germ cell types (cell clumping before FACS), there is an enrichment of type A undifferentiated spermatogonia (A_{und*}/A_{und}) population, which might contain SSC candidates. Undifferentiated type A spermatogonia (most primitive) (A_{und*}), undifferentiated type A spermatogonia (A_{und}), differentiating type A spermatogonia (A_{diff}), type B early spermatogonia (B_{early}), type B late spermatogonia (B_{late}), leptotene/zygotene (L/Z) and pachytene (P) spermatocytes. Bars represent means expressed as percentage. **O.** Germ cell transplantation into zebrafish genital pore using a glass capillary needle.

Donor cell isolation and male and female transplantation

Using *vasa::egfp* transgenic zebrafish as donors, a testicular cell suspension was obtained and subsequently submitted to FACS, in order to enrich transplantable SSC (Figure 4J,K) by sorting for big cells carrying high fluorescence (Figure 4L,M). Indeed, after sorting, we observed an enrichment of type A undifferentiated spermatogonia (Figure 4K-N). The

sorted cells (8.10^3-4.10^4 cells/µl) were injected through the genital pore (Figure 4O, Figure S2). Since females have a prominent belly, direct injections into ovaries (via lateral body wall) were also successfully performed (Figure S2). After transplantation, zebrafish recipient males and females were placed in water of 27^{o}C.

Male and female transplantation analysis

After two weeks of transplantation, donor cells colonized the recipient's seminiferous epithelium, and formed clusters, which were situated near the interstitial compartment (Figure 5A,B). Using CLSM, we found that these clusters were composed of ~8 cells/cyst (Figure 5C,D; Video S2). Three weeks after transplantation, donor-derived cysts had increased in number and size, and were found at different stages of spermatogenesis (e.g. differentiating type A spermatogonia, type B spermatogonia and spermatocytes) along the recipient's seminiferous epithelium (Figure 5E,F; Video S3). Donor type A undifferentiated spermatogonia (A_{und*} and A_{und}) were also found in the recipient seminiferous epithelium (Figure 5E,F). The *vasa* expression pattern in donor-derived germ cells was the same as observed *in vasa::egfp* testes immunostained for GFP (Figure S6A), or in wild-type testes immunostained for Vasa (Figure S6B). The transplantation efficiency was considered not high (30%) as colonization and donor-derived spermatogenesis was observed in about 3 out of 10 recipients. With regard to SSC transplantation into females, cell clusters derived from transplanted SSC were found in recipient ovaries after three weeks of transplantation (Figure 6A, Video S4). Small GFP-positive oocytes at an early stage of oocyte development were also found in recipient females (Figure 6B,C). Surprisingly, these male-derived germ cells

progressed into oocyte development, and gave rise to advanced oocytes after one month of transplantation (Figure 6D-F; Video S5). Clusters of GFP-positive cells, possibly clones of oogonia, were also found near male-derived oocytes (Figure 6G,H). The presence of GFP-positive cells in both transplanted males (three weeks after transplantation) and females (one month after transplantation) was also confirmed by PCR analysis (Figure S7).

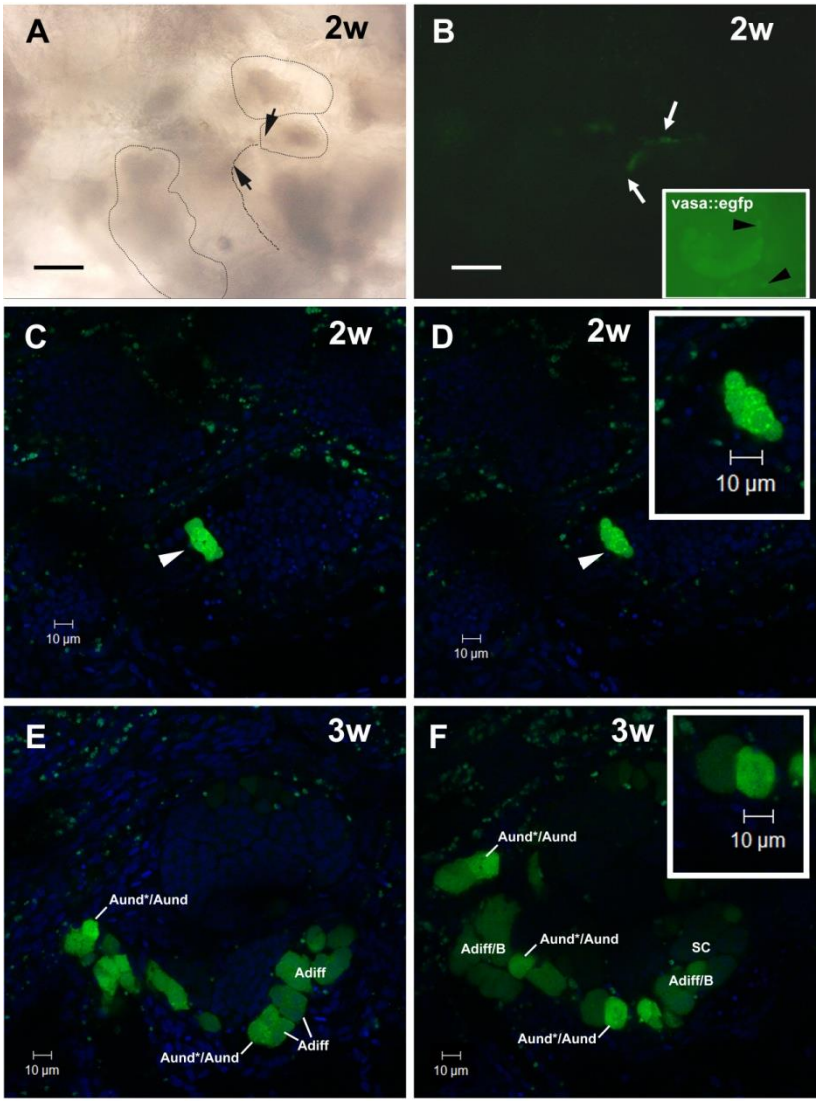

Figure 5. SSC transplantation into male zebrafish recipients. **A,B.** Recipient testes after two weeks (2w) of transplantation analyzed by light (**A**) and fluorescence (**B**) microscopies. Seminiferous tubules are delimited by stippled lines. Arrows indicate the same area in **A** and **B**. Donor cells formed clusters situated near the interstitium in a similar way as observed in *vasa::egfp* testes (see arrowheads in the inset). Nuclei (blue) are stained with DAPI. Scale bars = 50 µm. **C,D.** CLSM analysis of recipient testes after two weeks (2w) of transplantation. Arrowheads indicate a donor-derived cyst composed of ~8 cells. **Inset.** High magnification of donor-derived cyst. Nuclei (blue) are stained with DAPI. **E,F.** Recipient testes after 3 weeks (3w) of transplantation analyzed under CLSM. Donor-derived cysts increased their number and size, being found at different stages of spermatogenesis. Type A undifferentiated spermatogonia (A_{und*}/A_{und}), type A differentiating spermatogonia (A_{diff}), type B spermatogonia (B), and spermatocytes (SC). **Inset** shows a high magnification of type A undifferentiated spermatogonia. Nuclei (blue) are stained with DAPI.

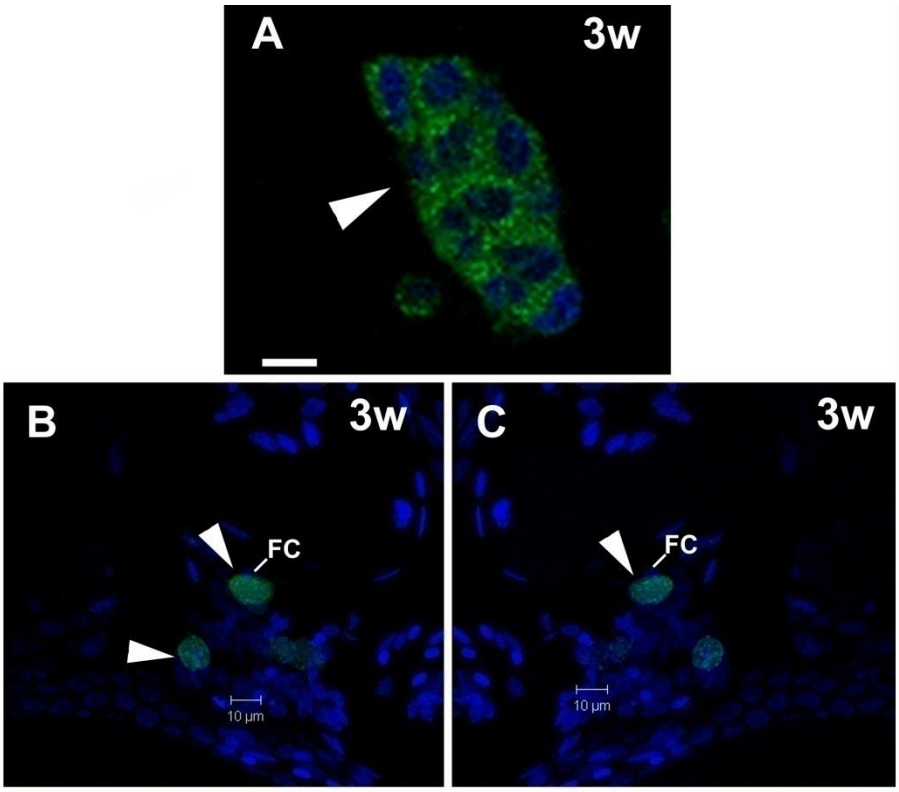

Figure 6. Legend in the next page.

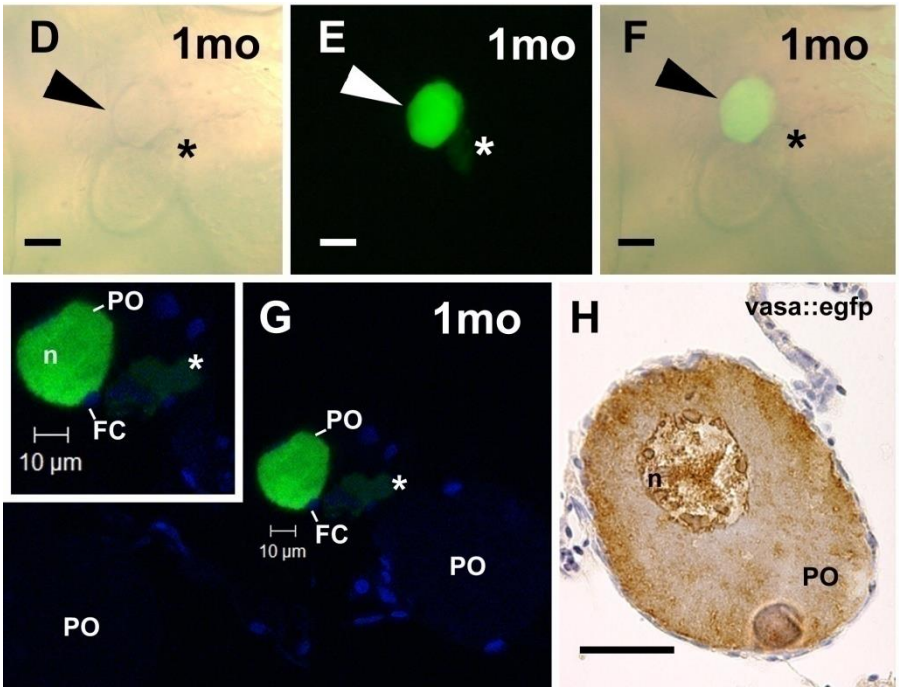

Figure 6. SSC transplantation into female zebrafish recipients analyzed under CLSM. **A.** A GFP cell cluster-derived from transplanted SSC after three weeks (3w) of transplantation. Nuclei (blue) are stained with DAPI. Scale bar = 10 µm. **B,C.** Arrowhead indicates an early donor-derived oocytes surrounded by follicle cells (FC) after three weeks (3w) of transplantation. Nuclei (blue) are stained with DAPI. **D-F.** Arrowhead indicates an advanced GFP oocyte, which was originated from transplanted SSC into zebrafish ovaries after one month (1mo) of transplantation. Note a small GFP cell cluster (asterisk) near the donor-derived oocyte. Light (**D**) and fluorescence (**E**) microscopies, and overlay of both (**F**). Scale bars = 25µm. **G.** The same oocyte in **D-F** examined under CLSM. A green donor-derived perinucleolar oocyte (PO), endogenous perinucleolar oocyte (PO), small GFP cell cluster (asterisk), and nucleus (n) are shown. **Inset.** High magnification of advanced donor-derived oocyte. Nuclei (blue) are stained with DAPI. **H.** Perinucleolar oocyte from *vasa::egfp* ovaries immunostained for gfp. Compare similar *vasa* expression pattern between donor-derived oocyte and perinucleolar oocyte from *vasa::egfp* ovaries. Scale bar = 25 µm.

Hormonal characterization and gene expression in busulfan-depleted zebrafish

The relatively low efficiency of colonization after transplantation, triggered studies on the recipient's testicular microenvironment prior to transplantation. The plasma levels of 11-KT were ~3 times higher in fish kept at 35^{o}C (with or without busulfan injection) than in non-treated zebrafish kept at 27^{o}C (Figure 7A). The temperature-induced elevation of 11-KT plasma levels were similar to the stimulatory effect of hCG (10 IU/g) or recombinant zebrafish Fsh (100 ng/g) [31]. Also, testicular 11-KT release in primary culture was higher from tissue of males exposed to 35^{o}C and busulfan than from testis tissue of control males kept at 27^{o}C, in particular with regard to basal release (7-fold higher), while the difference in forskolin-stimulated androgen did not reach statistical significance (Figure 7B).

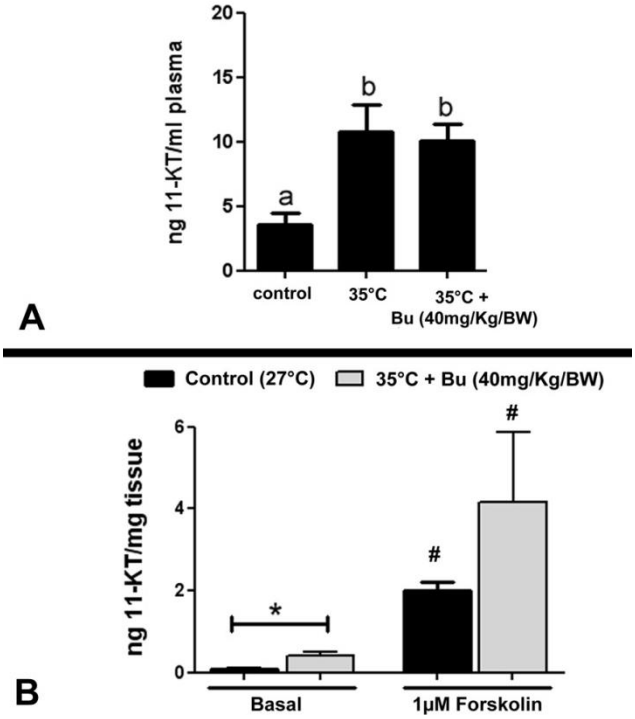

Figure 7. Characterization of male recipients prior SSC transplantation. **A.** 11-KT plasma levels (ng/ml plasma) from zebrafish kept at 27°C (control) (n=7), 35°C (n=11), and busulfan-depleted animals (n=19). Bars represent the mean±SE. Different letters mean significant differences ($p<0.05$) between the groups. **B.** In vitro 11-KT (ng/mg testis) release from control (27°C) (n=7) and busulfan-depleted testes [35°C + Bu (40 mg/Kg/BW)] (n=7) in basal and 1µM forskolin-induced. Bars represent the mean±SE. * means significant differences ($p<0.05$) between control and depleted in the same experimental condition (Student unpaired t-test). # indicates significantly higher ($p<0.05$) than the respective basal release (Student paired t-test).

Quantifying the expression of selected genes revealed that transcript levels of steroidogenesis and androgen signaling genes (*star, ar, cyp17a1*) had increased 3-fold in busulfan-depleted testes (Figure 7C). In most cases, exposure to 35^{o}C alone did not change gene expression. These are two interesting exceptions. The transcript levels of *amh* were significantly down-regulated at 35^{o}C and in busulfan-depleted testes, while *igf1b* transcript levels were strongly up-regulated. Expression of germ cell-specific genes, such as, *piwil1* and *sycp3l* significantly decreased only on busulfan-treated animals (Figure 7C), while *gsdf* and *insl3* mRNA levels did not change among the groups (Figure 7C).

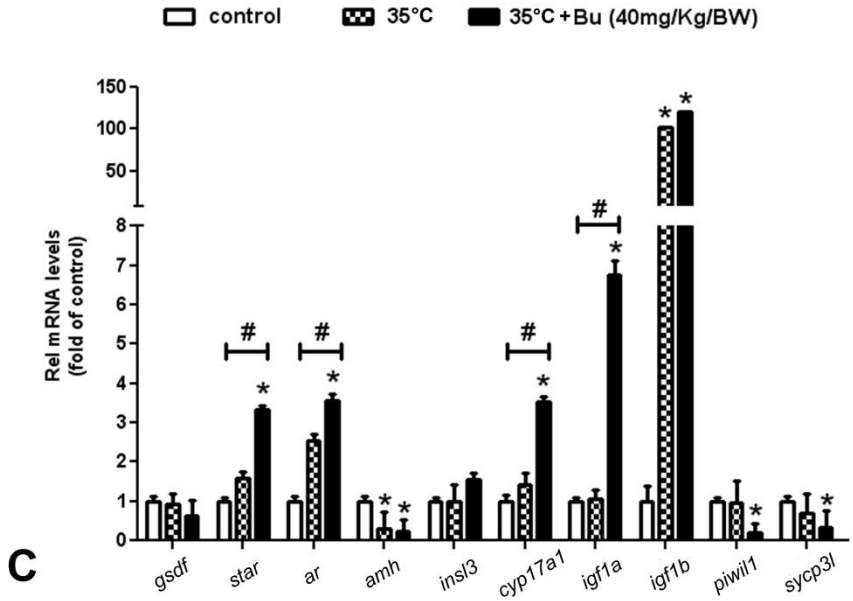

C

Figure 7C. Relative mRNA levels of *gsdf, star, amh, insl3, cyp17a, igf1a, igf1b, piwil1* and *sycp3l* from control (27°C) (n=7), 35°C (n=4), and busulfan-depleted testes [35°C + Bu (40 mg/Kg/BW)] (n=12). Bars represent the mean±SE of relative mRNA levels normalized to *β-actin1* or *ef1α*, and expressed as fold of relative control (27°C) mRNA levels. * and # are significantly different ($p<0.05$) from control levels (Student unpaired t-test) and among the groups (ANOVA), respectively.

DISCUSSION

Using a BrdU pulse-chase, we identified the LRC population in zebrafish testis. Within this category of testicular cells, somatic cells were found (e.g. Sertoli and interstitial cells), but type A undifferentiated spermatogonia (A_{und*} and A_{und}) were the only germ cells able to retain the label after 3-4 weeks of chase, constituting therefore the putative SSCs. The BrdU dilution kinetics for type A undifferentiated spermatogonia in zebrafish testis showed an initial, rapid decline that stabilized at 3-4 weeks. Applying mathematical modeling analysis to hematopoietic stem cells (HSCs) [37], a similar biphasic profile of BrdU dilution was described. The initial, rapid decline was attributed to the faster turnover of activated cells, while the subsequent, decelerated decline resulted from the slow turnover of quiescent cells. This suggested the presence of a heterogeneous population of HSCs which can be activated or deactivated according to the systemic needs [37]. In our zebrafish data, the second decelerated decline was not evident since the number of slow-cycling retaining cell (10%) stabilized after 3 weeks of chase. This might be interpreted as reflecting the presence of two subpopulations of single type A undifferentiated spermatogonia, one being a more rapidly dividing, "active" population (related to differentiation and indicated by the rapid decline), the other one being a slow-cycling, "reserve" population (related to self-renewal and indicated by the

stabilization). The latter population showed the morphological characteristics of type A_{und*} spermatogonia, and the former may be part of the type A_{und} spermatogonia. Also in the human testis, two types of single A spermatogonia (pale and dark) are present, and might play distinct roles as "reserve" versus "active" stem cell, respectively [38], [39].

The LRC assay also revealed the precise location of stem cells, and consequently the characterization of the neighboring cells that form the stem cell niche [40]-[42]. As in rodents [6], [7], we found that slow-cycling BrdU-labeled type A undifferentiated spermatogonia (stem cells candidates) were preferentially situated in regions of the seminiferous tubules opposite to the interstitial compartment. This observation suggests that elements of the SSC niche are probably conserved across vertebrates. The preferential location of SSC close to the interstitial compartment in rodents may be related to a locally high concentration of androgens which inhibit spermatogonial differentiation [9]. 11-KT is the main androgen in zebrafish [35] and other teleost fish, and is able to support full spermatogenesis in testis tissue culture of juvenile Japanese eel (*Anguilla japonica*) [43] or adult zebrafish [36]. Moreover, induction of androgen insufficiency in adult male zebrafish inhibited the differentiation of type A to type B spermatogonia [44]. Although the possible role(s) of androgen signaling in regulating zebrafish SSC activity still have to be clarified, the available evidence in fish strongly suggests that, different from mammals, androgens stimulate spermatogonial differentiation [2]. On the other hand, estrogens stimulate SSC self-renewal in Japanese eel [45], so that Leydig cells may be relevant as a source for aromatizeable androgens, thereby contributing directly and/or indirectly to the zebrafish SSC niche. Moreover, Leydig cell paracrine signaling might influence SSC behavior, since colony stimulating

factor 1 (Csf1) produced by Leydig and myoid cells is an extrinsic stimulator of SSC self-renewal in mice [10].

Endothelial cells support the expansion of normal and malignant stem cells not only by delivering oxygen and nutrients, but also by the paracrine release of endothelial cell growth factors and trophogens, which are referred as "*angiocrine factors*" [46]. Thus, endothelial cells have been pointed out as an important element of the stem cell niche in several systems, including the rodent SSC niche [8], [47]. In the zebrafish model, the distribution of SSC candidates (A_{und*} and A_{und}) close to blood vessels might indicate an involvement of endothelial cells in regulating SSC function. While there is no information on angiocrine signaling in the zebrafish testis, it has been shown that platelet-derived endothelial cell growth factor (PD-ECGF) induced SSC self-renewal in Japanese eel [48], [49].

The functional capacity of the identified SSC candidates in zebrafish was investigated by transplantation assays. In this assay, SSC candidates were transplanted into zebrafish in which endogenous spermatogenesis had been depleted by busulfan, similar to the technique developed for rodents and others species [12]-[15], [17]. Apparently and similar to tilapia [14], zebrafish spermatogenesis is more sensitive to busulfan treatment under elevated temperatures (35^{o}C), resulting in 88% of spermatogenic tubules showing Sertoli cells only after 10 days of treatment. Interestingly, spermatogenesis recovered quickly after having passed the nadir of busulfan-induced depletion. It has been shown previously that the proliferation of undifferentiated spermatogonia is greatly enhanced when the number of differentiating spermatogonia is reduced following busulfan exposure [50], which might explain why spermatogenesis recovered much

faster in recipients that seemed most vulnerable to busulfan, as seen in zebrafish, and recently shown in different strains of mice (BALB and C3H) [51]. It has been also demonstrated that differentiated spermatogonia can act as "potential stem cells", shifting their nature of transit-amplifying cell population to self-renewal in order to rapidly recover spermatogenesis in depleted testes [52]. Further studies are required to address the existence of "potential stem cells" in zebrafish testes and their involvement in the spermatogenesis recovery after busulfan treatment. However, based on the BrdU dilution kinetics, and the fast recovery, we can assume a functional heterogeneity within the zebrafish SSC candidates.

The treatment with busulfan induced an increase in androgen plasma levels as well as an increase in testicular androgen release. This might reflect the suppression of the negative feedback on gonadotropin release. In rat, the negative feedback on FSH release exerted by germ cells via inhibin is transiently eliminated after busulfan treatment [53], explaining the increase in circulating FSH levels between 6 and 10 weeks after busulfan injection [54], [55]. In mammals, androgen plasma levels were not elevated in busulfan-treated animals [53]-[55]. However, in fish, also Leydig cells express the receptor for Fsh [56], [57] including zebrafish [31], and Fsh is strongly steroidogenic in several species [31], [56], [57]. Hence, we attribute the increased androgen levels after busulfan treatment to higher Fsh plasma levels. Consistent with the elevated androgen production, busulfan treatment increased the mRNA levels of transcripts encoding proteins involved in steroidogenesis, such as *star* and *cyp17a1*. The down-regulation of *amh* mRNA expression in busulfan-depleted testes also seems coherent with higher androgen levels, since androgens down-regulated *amh* expression in juvenile Japanese eel testis and stimulated spermatogonial differentiation

towards meiosis [58]. Thus, down-regulation of *amh* might contribute to an environment that favours spermatogonial differentiation in busulfan-depleted zebrafish testis. With regards to the expression of *igf* gene family members, a strong up-regulation in particular of *igf1b* mRNA levels has been observed. This is interesting in the context of ongoing work showing that recombinant zebrafish Fsh increases *igf1b* levels in adult testis tissue culture (unpublished data). Taken together, our data suggest that busulfan treatment might create a microenvironment in zebrafish testes where the balance of the factors favored spermatogonial differentiation rather than SSC self-renewal. While this might facilitate the fast recovery after the severe loss of germ cells induced by busulfan, the "pro-differentiation" environment may also influence the behavior of transplanted cells. Thus, transplanted SSCs may differentiate rather than self-renew, possibly limiting the efficiency of donor-colonization (30%) in the recipient seminiferous tubules as observed for other vertebrates [59]. Future studies will aim at weakening the pro-differentiation environment, for example by an estrogen treatment [44] of the recipients.

Despite of the limited efficiency, we have taken important steps towards the development and standardization of SSC transplantation assay to confirm the "stemness" of SSC candidates in zebrafish. Transplantation of a FACS-enriched fraction of A_{und*} and A_{und} into busulfan-depleted testes showed that stem cell candidates were able to colonize, self-renew, and to differentiate in the recipient seminiferous tubules. This confirms the presence of stem cells in the transplanted pool of type A undifferentiated spermatogonia. Moreover, spermatogonial colonization started from regions within the recipient's seminiferous tubules which are adjacent to the interstitial compartment, the putative SSC niche in zebrafish testes. This

might indicate that the SSC niche creates a cellular and molecular environment which is optimal for colonization and development of transplanted SSCs. Since zebrafish have been used as a suitable model for understanding the mechanisms of testicular germ cell tumors [60], and most of the tumors have their defect unknown, standard experimental design including reciprocal transplantation of germ cells from affected donors to wild-type testes and vice versa could be applied to evaluate whether the defect is on Sertoli cells or intrinsic to the germ cells. Another important application of germ cell transplantation is transgenesis through the male germ line using transplantation of transfected germ cells [3], [17]. This might be an option to create transgenic animals in a shorter time than the conventional methods [17].

Finally, we have demonstrated the plasticity of the transplanted spermatogonia by placing the SSC candidates into a different microenvironment, i.e. into an ovary. SSC candidates were able to colonize recipient ovaries and differentiate into female germ line cells. Recently, it has been shown in mammals the existence of a subset of spermatogonia within the SSC population which express the novel orphan G-protein coupled receptor (GPR125), and this subset is capable to be reprogrammed to pluripotency, originating the derivatives of the ecto, meso, and endoderm layers [61]-[63]. Due to this property, this population is referred as multipotent adult spermatogonial-derived stem cells [61]-[63]. Further studies are required to examine the expression of GPR125 in zebrafish testes, and to extend SSC pluripotency for different organs.

CONCLUSION AND/OR SUMMARY

We present in the current work characteristics of zebrafish SSC candidates (A_{und*} and A_{und}), their niche, and their functional capability to both self-renew and differentiate in recipient testes, as well as their remarkable plasticity in recipient ovaries. To our knowledge, this is the first work to report on a SSC niche in fish. As in rodents, SSC location in zebrafish was characterized within areas of the seminiferous tubules which are opposite to the interstitial compartment, suggesting the influence of interstitial elements on SSC self-renewal and maintenance. We developed and standardized SSC transplantation techniques in male and female zebrafish, showing donor-derived spermatogenesis and male-derived oocytes, respectively, after transplantation. Thus, we introduced SSC transplantation in zebrafish as a promising technique for the study of SSCs.

ACKNOWLEDGMENTS

The authors would like to acknowledge Wytske van Dijk for technical assistance during radio immuno assays (RIAs); Ger Arkesteijn for technical assistance with FACS; Henk Schriek and Co Rootselaar for assistance during the *in vivo* experiments and maintaining the zebrafish stocks; and Teresa Bowman for the donation of *fli::egfp* transgenic zebrafish.

REFERENCES

1.Hess RA, Franca LR. (2008) Spermatogenesis and cycle of the seminiferous epithelium. Adv Exp Med Biol 636: 1-15. 10.1007/978-0-387-09597-4_1.

2.Schulz RW, Franca LR, Lareyre JJ, LeGac F, Chiarini-Garcia H, et al. (2010) Spermatogenesis in fish. Gen Comp Endocrinol 165(3): 390-411.

10.1016/j.ygcen.2009.02.013.

3.Oatley JM, Brinster RL. (2008) Regulation of spermatogonial stem cell self-renewal in mammals. Annu Rev Cell Dev Biol 24: 263-286. 10.1146/annurev.cellbio.24.110707.175355.

4.de Rooij DG. (2006) Regulation of spermatogonial stem cell behavior in vivo and in vitro. Anim Reprod v.3(n.2): 130-134.

5.de Rooij DG. (2009) The spermatogonial stem cell niche. Microsc Res Tech 72(8): 580-585. 10.1002/jemt.20699.

6.Chiarini-Garcia H, Hornick JR, Griswold MD, Russell LD. (2001) Distribution of type A spermatogonia in the mouse is not random. Biol Reprod 65(4): 1179-1185.

7.Chiarini-Garcia H, Raymer AM, Russell LD. (2003) Non-random distribution of spermatogonia in rats: Evidence of niches in the seminiferous tubules. Reproduction 126(5): 669-680.

8.Yoshida S, Sukeno M, Nabeshima Y. (2007) A vasculature-associated niche for undifferentiated spermatogonia in the mouse testis. Science 317(5845): 1722-1726.10.1126/science.1144885.

9.Meistrich ML, Shetty G. (2003) Suppression of testosterone stimulates recovery of spermatogenesis after cancer treatment. Int J Androl 26(3): 141-146.

10.Oatley JM, Oatley MJ, Avarbock MR, Tobias JW, Brinster RL. (2009) Colony stimulating factor 1 is an extrinsic stimulator of mouse spermatogonial stem cell

self-renewal. Development 136(7): 1191-1199. 10.1242/dev.032243.

11.Hofmann MC. (2008) Gdnf signaling pathways within the mammalian spermatogonial stem cell niche. Mol Cell Endocrinol 288(1-2): 95-103. 10.1016/j.mce.2008.04.012.

12.Brinster RL, Zimmermann JW. (1994) Spermatogenesis following male germ-cell transplantation. Proc Natl Acad Sci U S A 91(24): 11298-11302.

13.Brinster RL, Avarbock MR. (1994) Germline transmission of donor haplotype following spermatogonial transplantation. Proc Natl Acad Sci U S A 91(24): 11303-11307.

14.Lacerda SMSN, Batlouni SR, Silva SBG, Homem CSP, França LR. (2006) Germ cell transplantation in fish: The nile tilapia model. Anim Reprod 2: 146-159.

15.Majhi SK, Hattori RS, Yokota M, Watanabe S, Strussmann CA. (2009) Germ cell transplantation using sexually competent fish: An approach for rapid propagation of endangered and valuable germlines. PLoS One 4(7): e6132. 10.1371/journal.pone.0006132.

16.McLean DJ. (2005) Spermatogonial stem cell transplantation and testicular function. Cell Tissue Res 322(1): 21-31. 10.1007/s00441-005-0009-z.

17.Dobrinski I. (2006) Transplantation of germ cells and testis tissue to study mammalian spermatogenesis. Anim Reprod v.3(n.2): 135-145.

18.Krawetz SA, De Rooij DG, Hedger MP. (2009) Molecular aspects of male fertility. International Workshop on Molecular Andrology. EMBO Rep 10(10):

1087-1092. 10.1038/embor.2009.211.

19.Wu X, Schmidt JA, Avarbock MR, Tobias JW, Carlson CA, et al. (2009) Prepubertal human spermatogonia and mouse gonocytes share conserved gene expression of germline stem cell regulatory molecules. Proc Natl Acad Sci U S A 106(51): 21672-21677. 10.1073/pnas.0912432106.

20.Sadri-Ardekani H, Mizrak SC, van Daalen SK, Korver CM, Roepers-Gajadien HL, et al. (2009) Propagation of human spermatogonial stem cells in vitro. JAMA 302(19): 2127-2134. 10.1001/jama.2009.1689.

21.Leal MC, Cardoso ER, Nóbrega RH, Batlouni SR, Bogerd J, et al. (2009) Histological and stereological evaluation of zebrafish (*Danio rerio*) spermatogenesis with an emphasis on spermatogonial generations. Biol Reprod 81(1): 177-187. 10.1095/biolreprod.109.076299.

22.Krovel AV, Olsen LC. (2002) Expression of a vas::EGFP transgene in primordial germ cells of the zebrafish. Mech Dev 116(1-2): 141-150.

23.Lawson ND, Weinstein BM. (2002) In vivo imaging of embryonic vascular development using transgenic zebrafish. Dev Biol 248(2): 307-318.

24.Quintero-Hunter I, Grier H, Muscato M. (1991) Enhancement of histological detail using metanil yellow as counterstain in periodic acid schiff's hematoxylin staining of glycol methacrylate tissue sections. Biotech Histochem 66(4): 169-172.

25.van de Kant HJ, de Rooij DG. (1992) Periodic acid incubation can replace hydrochloric acid hydrolysis and trypsin digestion in immunogold--silver staining

of bromodeoxyuridine incorporation in plastic sections and allows the PAS reaction. Histochem J 24(3): 170-175.

26.Nóbrega RH, Batlouni SR, Franca LR. (2009) An overview of functional and stereological evaluation of spermatogenesis and germ cell transplantation in fish. Fish Physiol Biochem 35(1): 197-206. 10.1007/s10695-008-9252-z.

27.Schulz RW, Menting S, Bogerd J, Franca LR, Vilela DA, et al. (2005) Sertoli cell proliferation in the adult testis--evidence from two fish species belonging to different orders. Biol Reprod 73(5): 891-898. 10.1095/biolreprod.105.039891.

28.Sakai N. (2006) In vitro male germ cell cultures of zebrafish. Methods 39(3): 239-245. 10.1016/j.ymeth.2005.12.008.

29.Braat AK, van de Water S, Goos H, Bogerd J, Zivkovic D. (2000) Vasa protein expression and localization in the zebrafish. Mech Dev 95(1-2): 271-274.

30.Rehbein H, Bogerd J. (2007) Identification of genetically modified zebrafish (*Danio rerio*) by protein- and DNA-analysis. Journal für Verbraucherschutz und Lebensmittelsicherheit 2(2): 122-125. Available: http://dx.doi.org/10.1007/s00003-007-0179-6 via the Internet.

31.García-López A, de Jonge H, Nóbrega RH, de Waal PP, van Dijk W, et al. (2010) Studies in zebrafish reveal unusual cellular expression patterns of gonadotropin receptor mRNAs in the testis and unexpected functional differentiation of the gonadotropins. Endocrinology accepted.

32.Schulz RW, van der Sanden MC, Bosma PT, Goos HJ. (1994) Effects of gonadotrophin-releasing hormone during the pubertal development of the male African catfish (*Clarias gariepinus*): Gonadotrophin and androgen levels in plasma. J Endocrinol 140(2): 265-273.

33.Good-Avila SV, Yegorov S, Harron S, Bogerd J, Glen P, et al. (2009) Relaxin gene family in teleosts: Phylogeny, syntenic mapping, selective constraint, and expression analysis. BMC Evol Biol 9: 293. 10.1186/1471-2148-9-293.

34.Zou S, Kamei H, Modi Z, Duan C. (2009) Zebrafish IGF genes: Gene duplication, conservation and divergence, and novel roles in midline and notochord development. PLoS One 4(9): e7026. 10.1371/journal.pone.0007026.

35.de Waal PP, Wang DS, Nijenhuis WA, Schulz RW, Bogerd J. (2008) Functional characterization and expression analysis of the androgen receptor in zebrafish (*Danio rerio*) testis. Reproduction 136(2): 225-234. 10.1530/REP-08-0055.

36.Leal MC, de Waal PP, García-López A, Chen SX, Bogerd J, et al. (2009) Zebrafish primary testis tissue culture: An approach to study testis function ex vivo. Gen Comp Endocrinol 162(2): 134-138. 10.1016/j.ygcen.2009.03.003.

37.Glauche I, Moore K, Thielecke L, Horn K, Loeffler M, et al. (2009) Stem cell proliferation and quiescence--two sides of the same coin. PLoS Comput Biol 5(7): e1000447. 10.1371/journal.pcbi.1000447.

38.Schulze C. (1979) Morphological characteristics of the spermatogonial stem cells in man. Cell Tissue Res 198(2): 191-199.

39.Schulze C. (1988) Response of the human testis to long-term estrogen treatment: Morphology of Sertoli cells, Leydig cells and spermatogonial stem cells. Cell Tissue Res 251(1): 31-43.

40.Szotek PP, Chang HL, Brennand K, Fujino A, Pieretti-Vanmarcke R, et al. (2008) Normal ovarian surface epithelial label-retaining cells exhibit stem/progenitor cell characteristics. Proc Natl Acad Sci U S A 105(34): 12469-12473. 10.1073/pnas.0805012105.

41.Chan RW, Gargett CE. (2006) Identification of label-retaining cells in mouse endometrium. Stem Cells 24(6): 1529-1538. 10.1634/stemcells.2005-0411.

42.Kuwahara R, Kofman AV, Landis CS, Swenson ES, Barendswaard E, et al. (2008) The hepatic stem cell niche: Identification by label-retaining cell assay. Hepatology 47(6): 1994-2002. 10.1002/hep.22218.

43.Miura T, Yamauchi K, Takahashi H, Nagahama Y. (1991) Hormonal induction of all stages of spermatogenesis in vitro in the male Japanese eel (*Anguilla japonica*). Proc Natl Acad Sci U S A 88(13): 5774-5778.

44.de Waal PP, Leal MC, García-López A, Liarte S, de Jonge H, et al. (2009) Oestrogen-induced androgen insufficiency results in a reduction of proliferation and differentiation of spermatogonia in the zebrafish testis. J Endocrinol 202(2): 287-297. 10.1677/JOE-09-0050.

45.Miura T, Miura C, Ohta T, Nader MR, Todo T, et al. (1999) Estradiol-17beta stimulates the renewal of spermatogonial stem cells in males. Biochem Biophys Res Commun 264(1): 230-234. 10.1006/bbrc.1999.1494.

46.Butler JM, Kobayashi H, Rafii S. (2010) Instructive role of the vascular niche in promoting tumour growth and tissue repair by angiocrine factors. Nat Rev Cancer 10(2): 138-146. 10.1038/nrc2791.

47.Nikolova G, Strilic B, Lammert E. (2007) The vascular niche and its basement membrane. Trends Cell Biol 17(1): 19-25. 10.1016/j.tcb.2006.11.005.

48.Miura T, Ohta T, Miura CI, Yamauchi K. (2003) Complementary deoxyribonucleic acid cloning of spermatogonial stem cell renewal factor. Endocrinology 144(12): 5504-5510. 10.1210/en.2003-0800.

49.Miura C, Kuwahara R, Miura T. (2007) Transfer of spermatogenesis-related cDNAs into eel testis germ-somatic cell coculture pellets by electroporation: Methods for analysis of gene function. Mol Reprod Dev 74(4): 420-427. 10.1002/mrd.20653.

50.van Keulen CJ, de Rooij DG. (1974) The recovery from various gradations of cell loss in the mouse seminiferous epithelium and its implications for the spermatogonial stem cell renewal theory. Cell Tissue Kinet 7(6): 549-558.

51.Kanatsu-Shinohara M, Ogonuki N, Miki H, Inoue K, Morimoto H, et al. (2009) Genetic influences in mouse spermatogonial stem cell self-renewal. J Reprod Dev 10.1262/jrd.09-153N.

52.Nakagawa T, Nabeshima Y, Yoshida S. (2007) Functional identification of the actual and potential stem cell compartments in mouse spermatogenesis. Dev Cell 12(2): 195-206. 10.1016/j.devcel.2007.01.002.

53.O'Shaughnessy PJ, Hu L, Baker PJ. (2008) Effect of germ cell depletion on levels of specific mRNA transcripts in mouse Sertoli cells and Leydig cells. Reproduction (135): 839-850.

54.Gomes WR, Hall RW, Jain SK, Boots LR. (1973) Serum gonadotropin and testosterone levels during loss and recovery of spermatogenesis in rats. Endocrinology 93(4): 800-809.

55.Morris ID, Bardin CW, Musto NA, Thau RB, Gunsalus GL. (1987) Evidence suggesting that germ cells influence the bidirectional secretion of androgen binding protein by the seminiferous epithelium demonstrated by selective impairment of spermatogenesis with busulphan. Int J Androl 10(5): 691-700.

56.Ohta T, Miyake H, Miura C, Kamei H, Aida K, et al. (2007) Follicle-stimulating hormone induces spermatogenesis mediated by androgen production in Japanese eel, *Anguilla japonica*. Biol Reprod 77(6): 970-977. 10.1095/biolreprod.107.062299.

57.García-López A, Bogerd J, Granneman JC, van Dijk W, Trant JM, et al. (2009) Leydig cells express follicle-stimulating hormone receptors in African catfish. Endocrinology 150(1): 357-365. 10.1210/en.2008-0447.

58.Miura T, Miura C, Konda Y, Yamauchi K. (2002) Spermatogenesis-preventing substance in Japanese eel. Development 129(11): 2689-2697.

59.Honaramooz A, Behboodi E, Megee SO, Overton SA, Galantino-Homer H, et al. (2003) Fertility and germline transmission of donor haplotype following germ cell transplantation in immunocompetent goats. Biol Reprod 69(4): 1260-1264.

10.1095/biolreprod.103.018788.

60.Neumann JC, Dovey JS, Chandler GL, Carbajal L, Amatruda JF. (2009) Identification of a heritable model of testicular germ cell tumor in the zebrafish. Zebrafish 6(4): 319-327. 10.1089/zeb.2009.0613.

61.Seandel M, Falciatori I, Shmelkov SV, Kim J, James D, et al. (2008) Niche players: Spermatogonial progenitors marked by GPR125. Cell Cycle 7(2): 135-140.

62.de Rooij DG, Mizrak SC. (2008) Deriving multipotent stem cells from mouse spermatogonial stem cells: A new tool for developmental and clinical research. Development 135(13): 2207-2213. 10.1242/dev.015453.

63.Dym M, He Z, Jiang J, Pant D, Kokkinaki M. (2009) Spermatogonial stem cells: Unlimited potential. Reprod Fertil Dev 21(1): 15-21.

Supplemental Figures

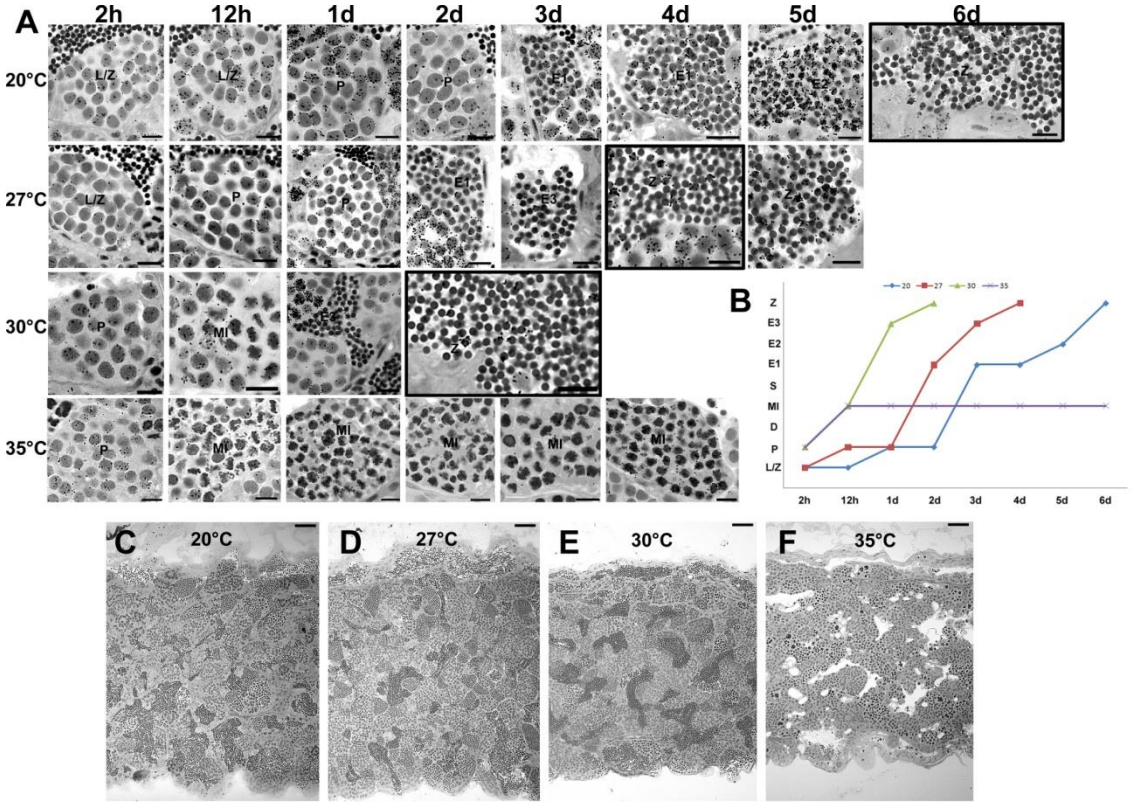

Figure 1. Effects of different temperatures on zebrafish spermatogenesis. **A.** More advanced labeled germ cell after 2h, 12h, 1d, 2d, 3d, 4d, 5d, 6d of ^{3}H-thymidine injection in zebrafish males kept at 20°C, 27°C, 30°C, and 35°C. Leptotene/zygotene (L/Z) and pachytene (P) spermatocytes, metaphase I (MI), initial spermatids (E1), intermediate spermatids (E2), final spermatids (E3) and spermatozoa (Z). Scale bars = 10µm. Cells were considered labeled when four to five or more grains were present over the nucleus in the presence of low-to-moderate background (i.e., very few grains per histological field observed under oil immersion). Black squares indicate the time in which labeled spermatozoa were found in the lumen of zebrafish testes at different temperatures. **B.** Histogram showing the combined duration of meiotic and spermiogenic phases at different temperatures. Spermatogenesis did not progress beyond the first meiotic division at 35°C. X axis represents the time, whereas y axis the ^{3}H-thymidine labeled germ cell [Leptotene/zygotene (L/Z), pachytene (P) and diplotene (D) spermatocytes, metaphase I (MI), initial spermatids (E1), intermediate spermatids (E2), final spermatids (E3) and spermatozoa (Z)]. **C-E.** Histological sections of zebrafish testes at 27°C, 30°C, and 35°C. Sperm free and a massive germ cell apoptosis is seen in zebrafish testes at 35°C. Scale bars = 50µm.

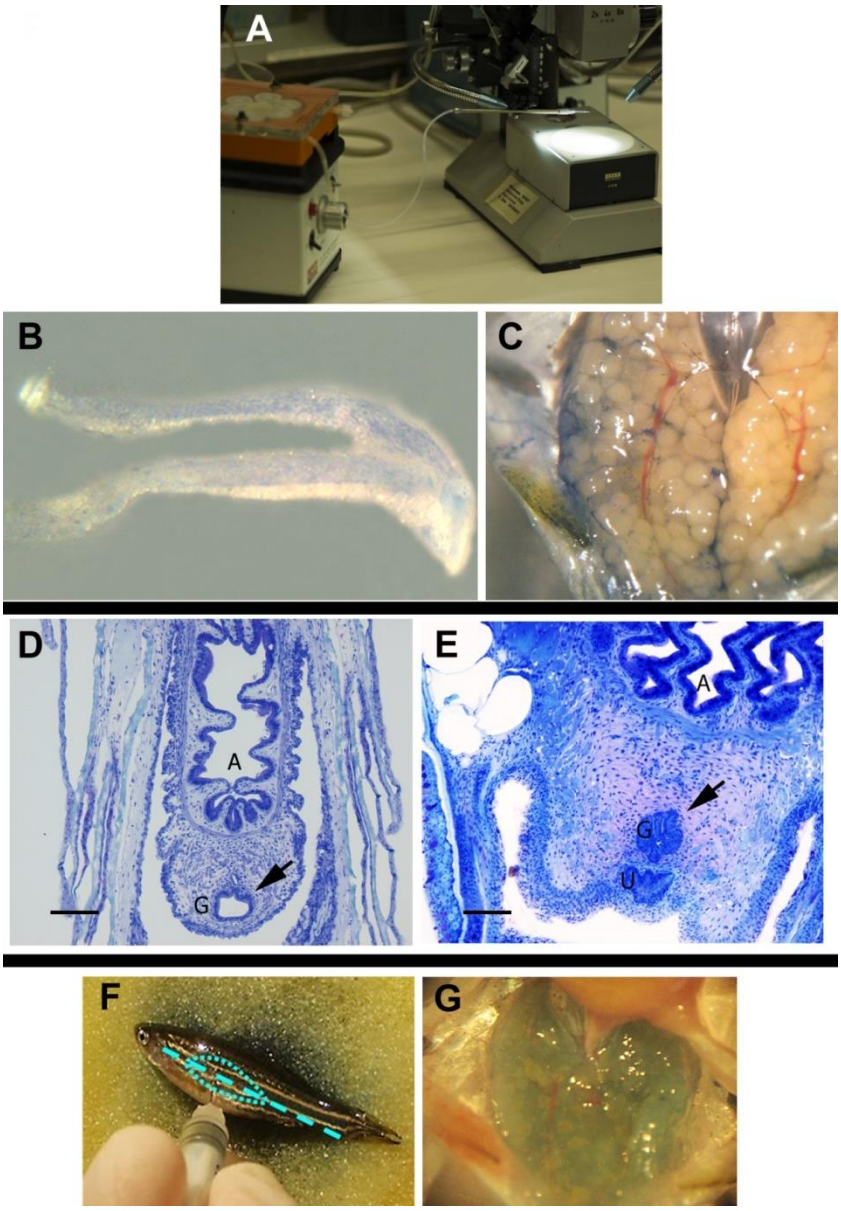

Figure 2. A. Transplantation device, in which a glass capillary needle is coupled to a peristaltic pump. **B,C.** Standardization of transplantation via using trypan blue to monitor the efficiency of the injections. Note trypan blue inside the testis (**B**) and ovaries (**C**). **D,E.** Genital pore histological sections stained with toluidine blue (male – **D**, female – **E**). Genital pore measurements: 120x80 µm dimensions, 63° angle (female); 75x50 µm dimensions, 60° angle (male). Anus (A), genital pore (G, arrow), and urethra (U). Scale bars = 100 µm. **F.** Ovary cell transplantation

throughout injections into the lateral body wall (indicated by stippled line). **G.** Trypan blue was used to monitor the specificity of the injection. Note trypan blue inside the ovaries.

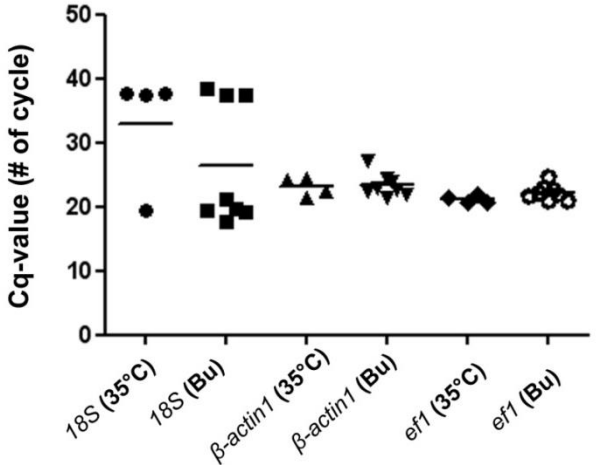

Figure 3. Scatter plot to check the stability of *18S* rRNA, *β-actin1* and *ef1α* mRNAs as a housekeeping gene in 35°C (n=4), and depleted testes (35°C + busulfan 40mg/Kg/BW) (n=12). Each dot in the scatter plot represents the average Cq-value of duplicate measurements for each fish in the different experimental condition. Stability was seen only between *β-actin1* and *ef1α*. Control (27°C) was not shown, but followed the same pattern.

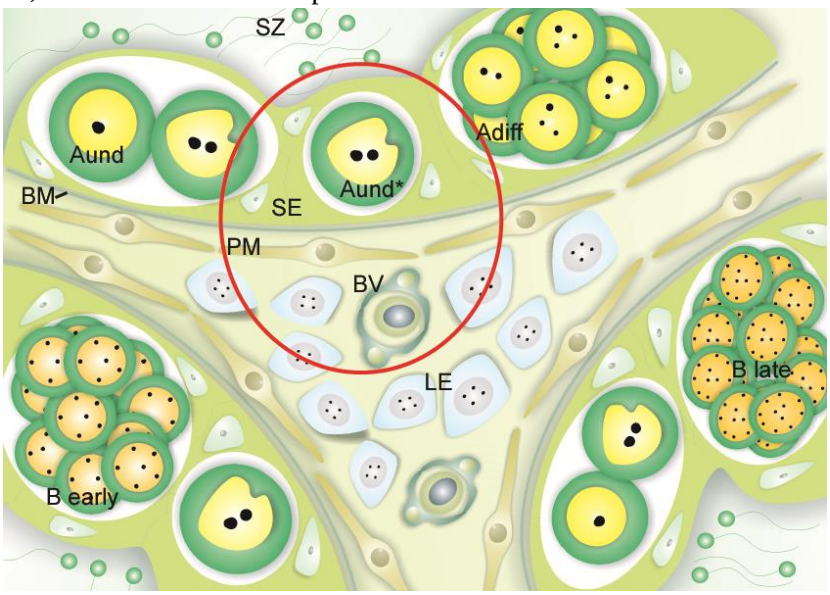

Figure 4. The hypothetical SSC niche in zebrafish testes. SSC niche is indicated by

a red circled line. The niche is constituted by elements of the interstitial compartment (**IC**) such as, basement membrane (**BM**), peritubular myoid cells (**PM**), Leydig cells (**LE**), blood vessels (**BV**) and other interstitial elements. Type A undifferentiated spermatogonia (Aund*/Aund), type A differentiated spermatogonia (**Adiff**), type B early spermatogonia (**B early**) and type B late spermatogonia (**B late**) and spermatozoa (**SZ**) are illustrated. Sertoli cells (**SE**) are also shown.

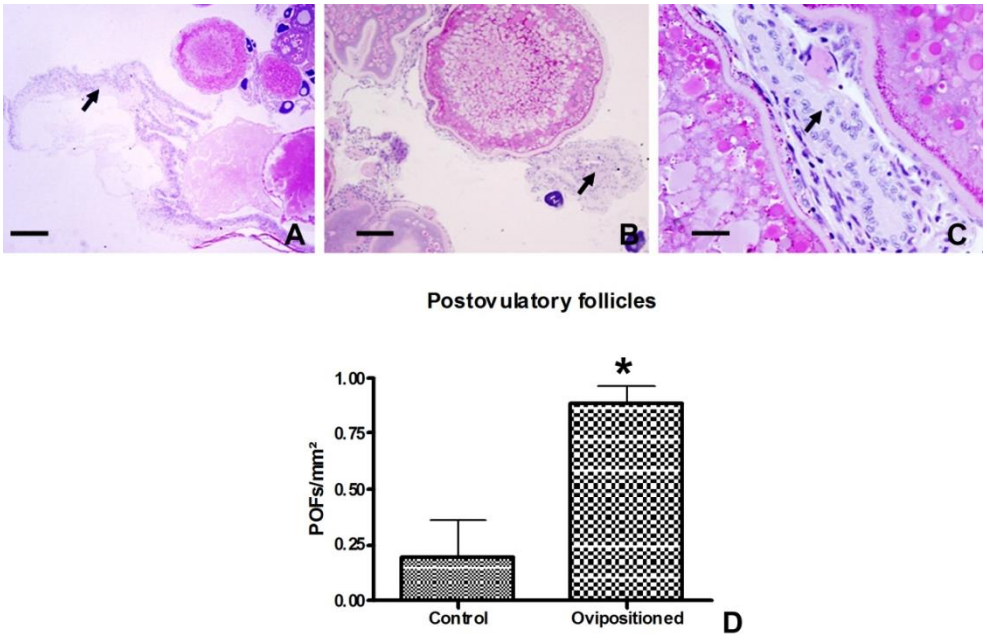

Figure 5. Preparation of female zebrafish recipients for SSC transplantation. **A-C.** Ovaries histological sections of ovoposition-induced females stained with PAS (Periodic acid Schiff). Arrows indicate postovulatory follicles after ovoposition. Note in **C** the available follicle cells which can support the transplanted SSC development. Scales bars = 250µm (A), 100µm (B), 25µm (C). **D.** Number of postovulatory follicles (POFs)/mm^2 of ovary in control (n=5) and ovopositioned females (n=5). Bars represent the mean± SE. * means significant differences ($p<0.05$) between the groups (Student unpaired t-test).

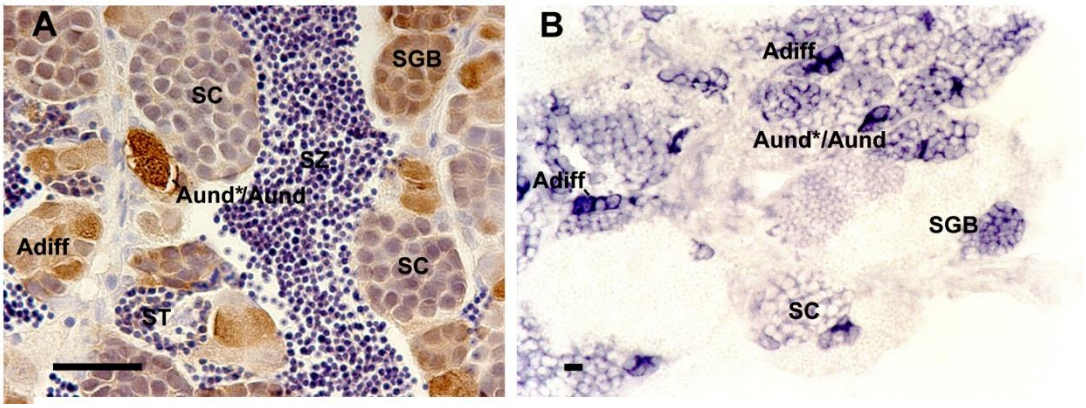

Figure 6. Vasa expression pattern during male germ cell development using gfp immunodetection in sections of vasa::egfp testes (**A**), or vasa immunodetection in cryosections of wild-type testes (**B**). Type A undifferentiated spermatogonia (Aund*/Aund), type A differentiating spermatogonia (Adiff), type B spermatogonia (B), spermatocytes (SC), spermatids (ST), spermatozoa (SZ). Scale bars = 25µm (**A**) and 10 µm (**B**).

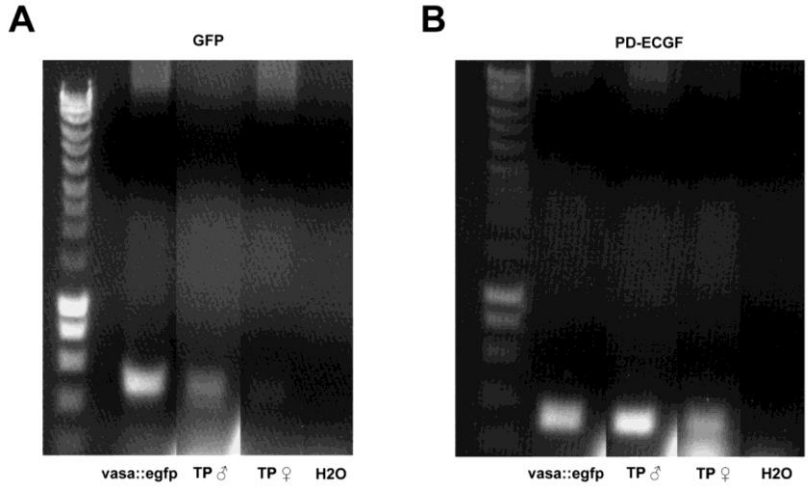

Figure 7. PCR analysis for GFP detection using primers located in the YFP gene, 2% agarose gel containing ethidium bromide, showing the detection of a faint background band. **A.** vasa::egfp testes were used as a positive control. TP ♂ transplanted male after 3 weeks of transplantation, TP ♀ transplanted female after 1 month of transplantation, H20 water as negative control. Bands at left side are DNA markers from SMART ladder (Eurogentec). **B.** PCR detection using primers located in the PD-ECGF (plated-derived endothelial cell growth factor) gene as

positive control for genomic DNA in the different individuals, 2% agarose gel containing ethidium bromide, showing the detection of a faint background band. Bands at left side are DNA markers from SMART ladder.

Supplemental online video

Video 1. Z stack from vasa::egfp testis showing the distribution of vasa positive cells in the zebrafish seminiferous tubules.

Video 2. Z stack from wild-type zebrafish testis 2 weeks after SSC transplantation. Note a donor-derived cyst composed of ~8 cells in the seminiferous epithelium.

Video 3. Z stack from wild-type zebrafish testis 3 weeks after SSC transplantation. SSCs were able to colonize recipient testis and differentiate into daughter cells committed with the spermatogenic process. Donor-derived cysts at different stages of zebrafish spermatogenesis were found in recipient seminiferous epithelium.

Video 4. Z stack from ovaries fragments 3 weeks after SSC transplantation into female zebrafish ovaries. Small cell clusters-derived from SSC were seen in female ovaries.

Video 5. Z stack from ovaries fragments 1 month after SSC transplantation. SSCs were able to colonize female ovaries and differentiate into female germ cell line. Note a male-derived oocyte in the female recipient ovary.

CHAPTER 4

Studies in Zebrafish Reveal Unusual Cellular Expression Patterns of Gonadotropin Receptor Messenger Ribonucleic Acids in the Testis and Unexpected Functional Differentiation of the Gonadotropins

García-López A, de Jonge H, Nóbrega RH, de Waal PP, van Dijk W, Hemrika W, Taranger GL, Bogerd J, Schulz RW.

Endocrinology. 2010 May;151(5):2349-60. doi: 10.1210/en.2009-1227. Epub 2010 Mar 22.

ABSTRACT

This study aimed to improve, using the zebrafish model, our understanding of the distinct roles of pituitary gonadotropins FSH and LH in regulating testis functions in teleost fish. We report, for the first time in a vertebrate species, that zebrafish Leydig cells as well as Sertoli cells express the mRNAs for both gonadotropin receptors (*fshr* and *lhcgr*). Although Leydig cell *fshr*expression has been reported in other piscine species and may be a common feature of teleost fish, Sertoli cell *lhcgr* expression has not been reported previously and might be related to the undifferentiated gonochoristic mode of gonadal sex differentiation in zebrafish. Both recombinant zebrafish (rzf) gonadotropins (*i.e.* rzfLH and rzfFSH) stimulated androgen release *in vitro* and *in vivo*, with rzfFSH being significantly more potent than rzfLH. Forskolin-induced adenylate cyclase activation mimicked, whereas the protein kinase A inhibitor H-89 significantly reduced, the gonadotropin-stimulated androgen release. Therefore, we conclude that both FSH receptor and LH/choriogonadotropin receptor signaling are predominantly mediated through the cAMP/protein kinase A pathway to promote steroid production. Despite this similarity, other downstream mechanisms seem to differ. For example, rzfFSH up-regulated the testicular mRNA levels of a number of steroidogenesis-related genes both *in vitro* and *in vivo*, whereas rzfLH or human chorionic gonadotropin did not. Although not fully understood at present, these differences could explain the capacity of FSH to support both steroidogenesis and spermatogenesis on a long-term basis, whereas LH-stimulated steroidogenesis might be a more acute process, possibly restricted to periods during which peak steroid levels are required. Both zebrafish gonadotropin receptors show overlapping cellular expression in the testis and share downstream signaling steps, but the biological activities of each gonadotropin still differ substantially, in particular with regard to modifying testicular gene expression levels.

INTRODUCTION

The pituitary gonadotropins LH and FSH play critical roles in regulating male reproduction across vertebrates (1, 2, 3). In mammals, the specific activities of both gonadotropins are clearly defined, given the highly specific interactions between each hormone and its respective receptor, LH/choriogonadotropin receptor (Lhcgr) and FSH receptor (Fshr). In addition, Lhcgr and Fshr expression in mammalian testis is restricted to Leydig and Sertoli cells, respectively (1, 2, 4). Hence, LH predominantly controls Leydig cell steroidogenesis, whereas FSH regulates Sertoli cell functions (2, 4, 5, 6).

In teleost fish, conversely, the biological activities of FSH and LH seem to be broader because both are strong steroidogenic hormones (7, 8, 9, 10, 11, 12, 13, 14, 15, 16). Our present concept on how gonadotropins develop their bioactivity in fish testis is mainly based on a groundbreaking study in coho salmon, *Oncorhynchus kisutch*, showing LH binding to Leydig cells (indicating the presence of Lhcgr) and FSH binding to Sertoli cells (indicating the presence of Fshr), although FSH binding to Leydig cells could not be unequivocally demonstrated or clearly excluded (17). Recently, Fshr protein (Japanese eel, *Anguilla japonica*) (18) and mRNA (African catfish, *Clarias gariepinus*) (7) have been demonstrated in teleost Leydig cells, findings compatible with a direct trophic effect of FSH on Leydig cell functioning, including the regulation of steroid release (7). Thus, a revision of the concept of gonadotropin mode of action in fish testis is required. For instance, in the presence of Fshr in both Leydig and Sertoli cells, FSH alone may regulate the activities of both cell types during early-

mid spermatogenesis, when plasma LH levels are very low or undetectable in seasonally reproducing species (19, 20, 21).

Another distinctive feature of teleost gonadotropin bioactivity is the limited hormone-binding selectivity that the gonadotropin receptors exhibit (7, 14, 16, 17, 22, 23, 24, 25, 26). This may lead to receptor cross-activation, most probably LH interaction with Fshr (see references above), especially during the spawning season when LH reaches peak plasma levels (19, 20,21, 27). The physiological relevance of this phenomenon (if any) is unknown at present.

To understand how gonadotropins modulate gonadal functions, knowledge about the identity and the relevant characteristics of the gonadotropin target cells is imperative. This information is still missing in zebrafish, *Danio rerio*, an important vertebrate model species. Thus, the first objective of the present report was to identify the cell types expressing either the *fshr* or the *lhcgr* mRNA in zebrafish testis. We then set out to produce recombinant zebrafish (rzf) gonadotropins for studies on their biological activities regarding testicular androgen release and expression of selected testicular genes.

MATERIAL AND METHODS

Animals

Sexually mature zebrafish from the Tübingen AB strain, either wild type or transgenic [expressing enhanced green fluorescent protein (EGFP) under the control of the germ cell-specific *vas* promoter; *vas::EGFP* (28)], and outbred fish were used. Animal housing (29) and experimentation were

consistent with Dutch national regulations and were approved by the Utrecht University Animal Use and Care Committee.

Cellular localization of gonadotropin receptor gene expression in zebrafish testis

The localization of *lhcgr* and *fshr* mRNA expression in zebrafish testis was investigated by *in situ* hybridization, laser microdissection of testis sections, and fluorescence-activated sorting of testicular cell suspensions.

In situ hybridization for *lhcgr*, *fshr*, and *insulin-like peptide 3* (*insl3*), a Leydig cell-specific transcript (30), was performed on 10-μm-thick cryosections from wild-type Tübingen AB zebrafish testis using digoxigenin-labeled cRNA probes (7). Gene-specific primers used to generate DNA templates for probe synthesis are shown in Supplemental Table 1 (published on The Endocrine Society's Journals Online web site at http://endo.endojournals.org).

Laser microdissection of zebrafish testis sections was carried out using a PALM MicroBeam Instrument (PALM Microlaser Technologies, Bernried, Germany). Two microdissected fractions were analyzed from two independent biological samples for *lhcgr* and *fshr* mRNA abundance: interstitial tissue, identified by 3β-hydroxysteroid dehydrogenase (3β-Hsd) staining of Leydig cells, and intratubular tissue, containing spermatogenic cysts (germ/Sertoli cells units). See Supplemental Materials and Methods and Supplemental Fig. 1 for further details.

Fluorescence-activated cell sorting (FACS) was used to isolate a germ-cell-enriched population from *vas::EGFP* zebrafish testis. Both EGFP

intensity and cell size decrease as spermatogenesis progresses (31), whereas somatic cells are EGFP negative and have variable sizes. This allowed obtaining cell populations enriched in spermatogonia and primary spermatocytes by selecting for cells showing strong EGFP intensity and large size (Supplemental Fig. 1, D and E). Dissociated testicular cells were prepared from two independent batches of 10–12 fish each (32), resuspended in 1 ml D-PBS+ (Invitrogen, Carlsbad, CA), and then immediately subjected to FACS using an inFlux cell sorter (Becton Dickinson Biosciences, Franklin Lakes, NJ). The obtained cell suspension was centrifuged at 50 × *g* for 10 min followed by total RNA extraction using the RNAqueous-Micro kit (Ambion, Austin, TX). Synthesis of cDNA from total RNA samples was performed as described (26).

Primers to detect zebrafish *fshr* mRNA, *lhcgr* mRNA, *piwi-like 1* (*piwil1*) mRNA (predominantly expressed in spermatogonia) (33), *synaptonemal complex protein 3 like* (*sycp3l*) mRNA (expressed by primary spermatocytes) (34, 35), *outer dense fiber 3 like* (*odf3l*) mRNA (expressed by spermatids) (35), *gonadal somatic cell-derived factor* (*gsdf*) mRNA (expressed by Sertoli cells) (36), *insl3* mRNA (expressed by Leydig cells) (30), and the reference endogenous control gene β-*actin1* (Supplemental Table 2) were designed and validated for specificity and amplification efficiency on serial dilutions of testis cDNA (26). All real-time quantitative PCRs (qPCRs) and calculations were performed as described previously (7, 26,37).

Gonadotropins

The rzfFSH and rzfLH proteins used for these experiments were produced as detailed in the Supplemental Materials and Methods and Supplemental Fig. 2. Human chorionic gonadotropin (hCG) was obtained from Organon (Oss, The Netherlands).

In vitro androgen release response to increasing gonadotropins and forskolin concentrations

Testicular tissue was challenged in concentration-response bioassays with either rzfFSH (from 12.5–1000 ng protein/ml), rzfLH (from 100-2000 ng protein/ml), or the adenylate cyclase activator forskolin (from 0.1–25 μM; Sigma-Aldrich, St. Louis, MO). Testis tissue was collected from 12 outbred zebrafish per condition tested, and the two testes from each fish were incubated in parallel, one of them (randomly chosen left or right) serving as control for the contralateral one. Incubations lasted 18 h in a humidified air atmosphere at 25 C in 96-well flat-bottom plates (Corning Inc., Corning, NY) using a final volume of 200 μl culture medium (38).

After incubation, tissue explants were weighed and discarded, while the medium was processed for the quantification of 11-ketotestosterone (11-KT) and 11β-hydroxyandrostenedione (OHA) levels by RIA (39).

Because of the experimental design used (one testis assigned to basal condition and the contralateral one to experimental condition), we obtained data for basal steroid release for all concentrations of the compounds assayed. Homogeneity of basal steroid release among the different replicates was tested by one-way ANOVA. Because no statistically significant differences ($P > 0.05$) were identified, basal steroid release data were compiled into one single basal steroid release condition for each compound

tested. Thereafter, significant differences among the different concentrations of each substance were identified by one-way ANOVA followed by the Student-Newman-Keuls test ($P < 0.05$).

Role of the cAMP/protein kinase A (PKA) pathway on the gonadotropin-mediated stimulation of androgen release *in vitro*

Testis tissue explants were incubated with rzfFSH (250 ng/ml) or rzfLH (1000 ng/ml) in the absence or presence of 100 μM of the PKA inhibitor H-89 (Sigma-Aldrich) (7). Fish origin, batch and age, number of replicates per condition tested, tissue preparation, culture conditions, and analyses performed were the same as described above. For each fish, one testis was incubated with recombinant gonadotropin, whereas the contralateral one was incubated with gonadotropin plus H-89. Significant differences were identified by the Student's paired *t* test ($P < 0.05$).

***In vitro* short-term actions of gonadotropins on testis functions**

The capacities of rzfFSH (100 ng/ml) and rzfLH (500 ng/ml) to modulate the mRNA levels of a number of testicular genes were investigated over a 2-h incubation period. Origin of the fish (n = 8 per condition), tissue preparation, culture conditions, and analyses performed were the same as described above, except that testis explants were saved for gene expression studies.

Total RNA was extracted from testis explants using the RNAqueous-Micro kit (Ambion). Further processing to determine the threshold cycle (Cq) values of the reference endogenous control gene β-*actin1* as well as of *fshr*; *lhcgr*; the Leydig cell genes *insl3*, *steroidogenic acute regulatory*

protein (*star*), and *cytochrome P450, family 17, subfamily A, polypeptide 1*(*cyp17a1*); and the Sertoli cell genes *androgen receptor* (*ar*; expression not detectable in zebrafish Leydig cells by *in situ* hybridization) (37), *anti-Müllerian hormone* (*amh*), and *gsdf* (primer sequences are listed in Supplemental Table 2) by qPCR analysis was performed as reported (26, 37). No significant differences ($P > 0.05$) were found among the mean β-*actin1*Cq values in the different treatment groups (Supplemental Fig. 3A), thus validating β-*actin1* as a suitable reference for the current experiments. Because the two testes from each fish were incubated in parallel, the amounts of androgens released into the incubation media and the relative mRNA expression levels were compared between treated and respective control groups by the Student's paired *t* test ($P < 0.05$). Thereafter, values were expressed as percentage of respective basal levels, and differences between each gonadotropin treatment were identified by the Student's unpaired *t* test ($P < 0.05$).

In vitro medium-term actions of gonadotropins on testis functions

The capacities of rzfFSH (100 ng/ml) and rzfLH (500 ng/ml) to modulate the mRNA levels of a number of testicular genes were investigated in a medium-term organ culture system (38). In addition, the relative contribution of steroid production to gonadotropin-induced changes in gene expression was assessed by including 25 μg/ml of the 3β-Hsd inhibitor trilostane (Chemos, Regenstauf, Germany) in the media. After 2 d incubation in a humidified air atmosphere at 25 C, explants (n = 8 per condition) were processed as above for gene expression analysis. No

significant differences ($P > 0.05$) were found among the mean β-*actin1* Cq values in the different treatment groups (Supplemental Fig. 3B).

Incubation media were recovered after culture and stored at −25 C until 11-KT and/or OHA quantification (39). Pilot studies determined that the 11-KT antibody cross-reacted with trilostane at the concentration used, and therefore, trilostane-containing incubation media were assayed for OHA only. Recovery studies using tritiated androgens showed that 47 ± 1% of total steroids added to culture wells was present in the incubation medium after an overnight equilibration period (n = 8), whereas the remaining steroid was trapped in the agar cylinder. The results obtained were corrected accordingly.

Data were compared between treated and respective control explants by the Student's paired*t* test ($P < 0.05$). Thereafter, values were expressed as percentage of respective basal levels, and differences between treatments (*i.e.* gonadotropin *vs.* gonadotropin plus trilostane) were identified by the Student's unpaired *t* test ($P < 0.05$).

In vivo short-term actions of gonadotropins on testis functions

In this experiment, outbred zebrafish received an ip injection of 100 ng/g body weight rzfFSH or rzfLH or 10 IU/g body weight hCG in a total volume of approximately 5 µl (n = 8 fish per condition). Control fish received a 5-µl PBS injection. Two hours after the injections, fish were euthanized in ice water, the caudal peduncle cut, and a sample of blood collected using heparinized syringes. Samples were then transferred to heparinized tubes and the 11-KT plasma levels quantified (39). Testes were used for gene expression analysis as reported above. No significant

differences ($P > 0.05$) were found among the mean β-*actin1* Cq values in the different treatment groups (Supplemental Fig. 3C).

Significant differences among the different treatments were identified by one-way ANOVA followed by the Student- Newman-Keuls test ($P < 0.05$).

RESULTS

Zebrafish Leydig and Sertoli cells express both *fshr* and *lhcgr* mRNA

A clear *in situ* hybridization signal on interstitial Leydig cells was obtained with *fshr* antisense probe (Fig. 1A). The arrangement of cells stained was characteristic of Leydig cells as observed on histological sections (Fig. 1B) and resembled those obtained with *insl3* antisense probe (Fig. 1D) and with the 3β-Hsd enzyme-histochemical reaction (Fig. 1E). Sertoli and germ cells were negative for *fshr* mRNA by *in situ* hybridization. No signal was obtained for *lhcgr* mRNA. The *fshr* mRNA-positive Leydig cells present were stained with an approximately similar intensity, and no apparent spatial distribution pattern of Leydig cells (*e.g.* rostrocaudal, ventrodorsal, or central *vs.* peripheral in the testis) was observed. Hybridization with sense cRNA probes for *fshr* (Fig. 1C), *lhcgr*, or *insl3* (not shown) did not yield any staining.
Confirmation of *fshr* mRNA expression by interstitial Leydig cells was obtained by qPCR analysis of laser microdissected testis fractions (Fig. 1F).

This analysis also revealed expression of *fshr* mRNA in the intratubular compartment [~3-fold lower than in the interstitial (Leydig cell) fraction]. Moreover, *lhcgr* mRNA expression was found in the interstitial and, remarkably, also in the intratubular samples (~24- and ~18-fold lower

than *fshr* mRNA levels measured in the interstitial compartment, respectively). The purity of the intratubular fraction was confirmed by measuring mRNA levels of the Leydig cell-specific gene *insl3*. Its expression level was approximately 265-fold lower in the intratubular than in the interstitial fraction (Supplemental Fig. 1C). Contamination of the interstitial testis tissue fraction with intratubular Sertoli cells was assessed by measuring the mRNA levels of the Sertoli cell-specific gene *gsdf*. Its expression level in the interstitial fraction was approximately 11-fold lower than in the intratubular fraction (Supplemental Fig. 1C). These data indicated a small degree of Sertoli cell contamination in the interstitial fraction but negligible contamination of the intratubular fraction with interstitial elements. Still, *lhcgr* mRNA levels were even 1.3-fold higher in the intratubular than in the interstitial fraction.

Identification of the intratubular cell type expressing the gonadotropin receptor mRNAs was accomplished by qPCR analysis of a germ-cell-enriched population obtained by FACS of testis cell suspensions prepared from *vas::EGFP* transgenic zebrafish (Fig. 1F). This cell population exhibited abundant *piwi1l* and *sycp3l* mRNA expression in addition to intermediate *odf3l* mRNA levels (*i.e.* the cell population contained mainly spermatogonia and spermatocytes but also spermatids), whereas the levels of the somatic transcripts *gsdf* and *insl3* were at least 60-fold lower than *piwi1l* (Supplemental Fig. 1F), indicating the high purity of the samples obtained. Because both *fshr* and *lhcgr* mRNA levels were very low in the germ cells compared with the whole intratubular compartment (Fig. 1F), we concluded that the intratubular expression of both *fshr* and *lhcgr* genes resided in the only non-germ-cell type in the intratubular compartment, the Sertoli cell.

Altogether, our results indicate that in zebrafish testis, both Leydig and Sertoli cells express both *fshr* and *lhcgr* mRNA, whereas germ cells are devoid of such transcripts.

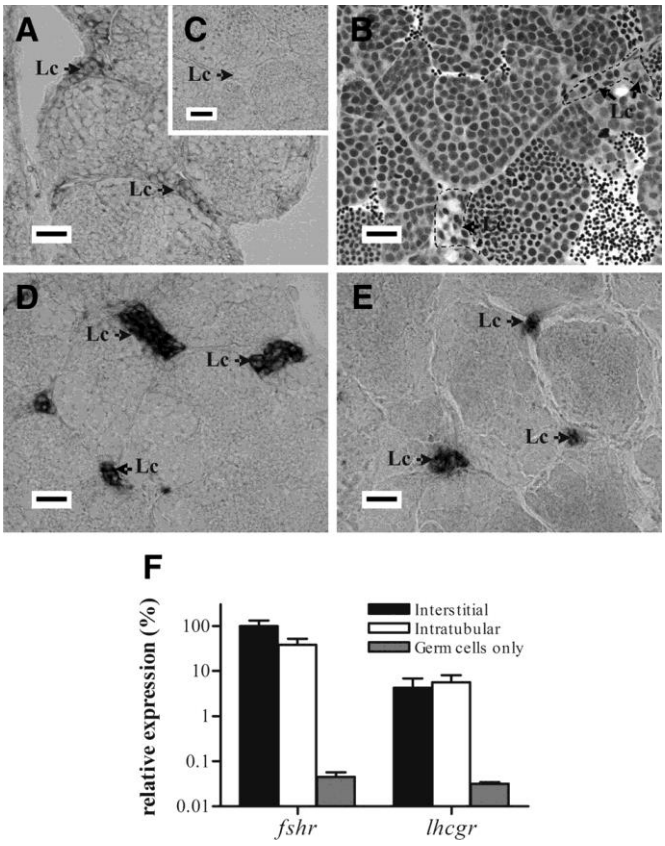

FIG. 1. Cellular localization of *fshr* and *lhcgr* mRNA expression in zebrafish testis. A and C, *In situ* hybridization with either an antisense (A) or a sense (C) riboprobe for zebrafish *fshr*; note the positive staining in Leydig cells (Lc) in the interstitial tissue in A and the absence of signal in C. In both cases, germ cells were devoid of staining. B, Toluidine blue-stained 2-μm-thick plastic section showing groups of Leydig cells (Lc) within the interstitial compartment (*enclosed by broken lines*). D and E, Leydig cells are also identified by their positive staining with an *insl3* antisense cRNA probe (D) and with the 3β-Hsd enzymatic reaction (E). *Scale bars*, 20 μm. F, Relative *fshr* and *lhcgr* mRNA expression levels in two microdissected testis tissue fractions (interstitial and intratubular) and a germ-cell-enriched population obtained from *vas::EGFP* transgenic zebrafish by FACS (germ cells only). Data correspond to values from two experiments, each with duplicate measurements (mean ± SEM), normalized to β-*actin1* mRNA levels, and

expressed as percentage of *fshr* transcript amounts in the interstitial fraction. Note the logarithmic scale.

Recombinant, single-chain zebrafish gonadotropins and forskolin stimulate androgen production in testicular explants

When zebrafish testes were incubated with rzfFSH, androgen secretion increased gradually with the gonadotropin concentrations (Fig. 2A). The lowest rzfFSH concentration tested (12.5 ng/ml) elicited significant elevations of both 11-KT and OHA release (~4.7- and ~3.5-fold above basal levels, respectively). Maximal androgen release (~47-fold for 11-KT and ~84-fold for OHA) was reached at 500 ng/ml rzfFSH. No further increase was observed by doubling the concentration.

For rzfLH (Fig. 2B), 250 ng/ml induced the first significant increase in both 11-KT and OHA secretion (~2.5-and ~1.8-fold above basal levels, respectively). From 250-2000 ng/ml, androgen secretion kept increasing significantly. Higher rzfLH concentrations could not be tested. However, the androgen release induced by 2000 ng/ml rzfLH was similar to those observed in response to maximally effective rzfFSH or forskolin concentrations, suggesting that maximal androgen release had been reached. Incubation with 0.1 μM forskolin, the lowest concentration tested, already induced significant increases in both 11-KT and OHA production by zebrafish testis (~4.0- and ~5.9-fold above basal levels, respectively) (Fig. 2C). The maximal steroidogenic response was obtained with forskolin concentrations between 10 and 25 μM.

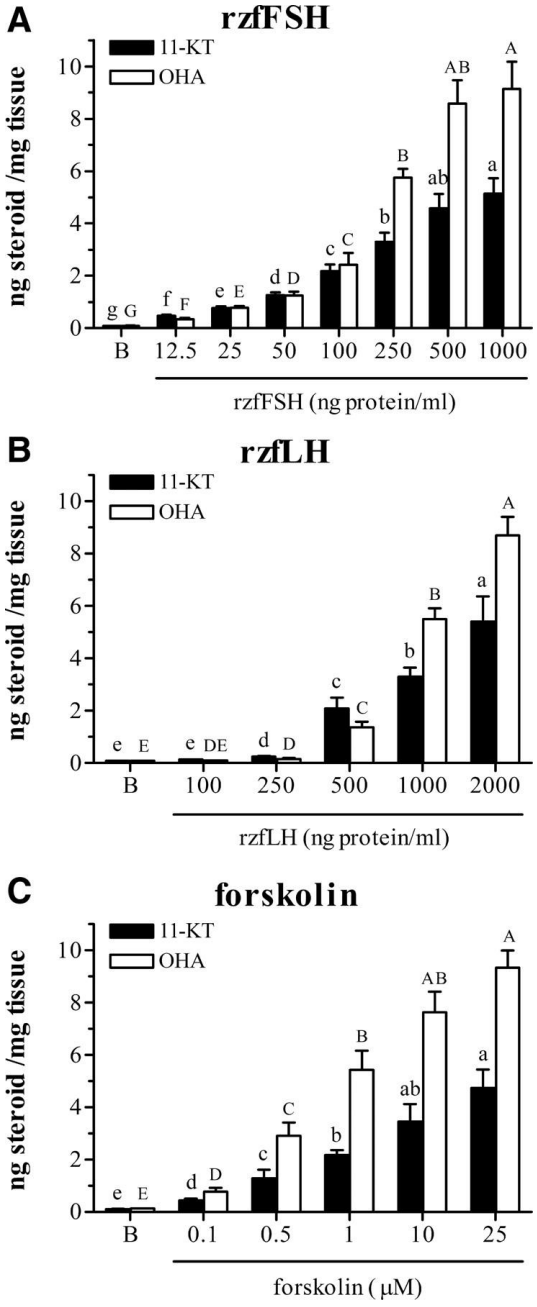

FIG. 2. Stimulation of androgen release by zebrafish testicular explants. Amounts of 11-KT and OHA (mean ± SEM) measured in incubation media after overnight (18 h) exposure to increasing concentrations of zfFSH (panel A), rzfLH (panel B), or the adenylate cyclase activator forskolin (panel C). B, Basal release. Values represent compiled data from two

experiments, each with six replicates per ligand concentration. *Different letters* denote significant differences among groups ($P < 0.05$).

The cAMP/PKA pathway is involved in both the FSH- and LH-stimulated androgen production

When testis tissue was incubated with 250 ng/ml rzfFSH or 1000 ng/ml rzfLH in the presence of 100 μM of the PKA inhibitor H-89, androgen production was strongly reduced (22- to 16-fold) compared with the levels measured in the absence of the inhibitor (Fig. 3). Therefore, for both rzf gonadotropins, the cAMP-PKA pathway is the major mediator of the steroidogenic response. This is further supported by comparing the residual 11-KT release observed in the presence of gonadotropin and H-89 with basal 11-KT release from 49–82 individual testis incubations of fish of the same origin and age (basal release from the dose-response experiments described above; see Fig. 2): all 11-KT release levels were within the basal release range, whereas the values of the precursor OHA showed a somewhat higher dispersion with part of the data being above the basal range (Supplemental Fig. 4).

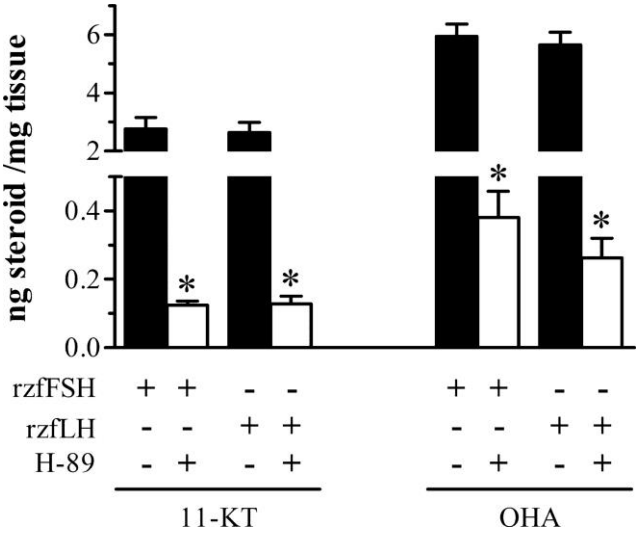

FIG. 3. Effects of the PKA inhibitor H-89 on the gonadotropin-stimulated androgen release by zebrafish testicular explants. Amounts of 11-KT and OHA (mean ± SEM) measured in incubation media after overnight (18 h) exposure to 250 ng/ml rzfFSH or 1000 ng/ml rzfLH alone and in combination with 100 μM H-89. Values represent compiled data from two experiments, each with six to seven replicates per condition. *, Values are significantly different ($P < 0.05$) from the respective gonadotropin-only condition.

The rzf gonadotropins show differential effects on steroidogenesis and testicular gene expression *in vitro* and *in vivo*

Zebrafish testis explants incubated for 2 d with either 100 ng/ml rzfFSH or 500 ng/ml rzfLH displayed a significant up-regulation (5- to 10-fold) of androgen release (Fig. 4). However, we observed significant changes in gene expression levels only in response to rzfFSH. The steady-state mRNA levels of a number of Leydig cell genes (*i.e. insl3*, *star*, and *cyp17a1*) increased (2.5- to 8-fold), whereas *fshr* mRNA levels were reduced to 60% of control values (Fig. 4A). No significant changes were observed for the Sertoli cell genes *amh*, *gsdf*, or *ar* mRNA levels (Fig. 4A). In the presence of the 3β-Hsd inhibitor trilostane, both rzfFSH- and rzfLH-stimulated androgen release was completely abolished (Fig. 4). Although trilostane did not modify the rzfFSH-stimulated *insl3* and *cyp17a1* mRNA overexpression, it prevented rzfFSH-induced *fshr* mRNA down-regulation and further increased *star* mRNA levels (Fig. 4A). The presence of trilostane in combination with rzfLH did not modify the mRNA levels of any of the transcripts analyzed (Fig. 4B).

The short-term culture approach (Fig. 5) provided a picture similar to that obtained in the medium-term study; both rzfFSH and rzfLH stimulated testicular 11-KT release ($P < 0.05$), whereas significant changes in steroidogenesis-related transcripts (*star* and *cyp17a1*) were detected only after rzfFSH treatment. Incubation with rzfLH elicited a 1.8-fold increase in *fshr* mRNA levels, but statistical significance was not reached. Moreover, no significant changes were observed for any of the Sertoli cell genes assayed as compared with basal samples, although *amh* mRNA expression differed statistically between rzfFSH- and rzfLH-treated explants.

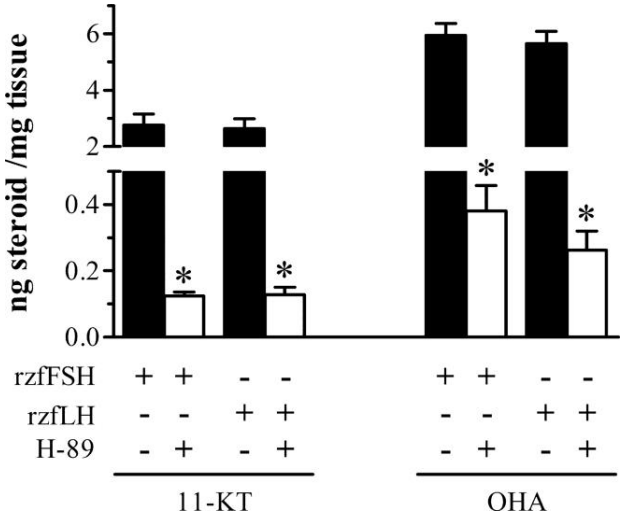

FIG. 4. *In vitro* medium-term (2 d) modulation of androgen release and testicular gene expression by rzf gonadotropins. Amounts of the androgens OHA and 11-KT measured in incubation media and relative mRNA expression levels of several testicular genes (*fshr*, *lhcgr*, *insl3*, *star*, *cyp17a1*,*amh*, *gsdf*, and *ar*) after 2 d exposure to 100 ng/ml rzfFSH (A) or 500 ng/ml rzfLH (B) alone (*black bars*) and in combination with 25 μg/ml of the 3β-Hsd inhibitor trilostane (*white bars*). Data (mean ± SEM) come from an experiment with eight replicates per condition and are expressed as percentage of basal levels, which were set to 100% for each parameter analyzed. Basal androgen release was 237 ± 18 pg OHA/mg tissue and 147 ± 17 pg 11-KT/mg tissue. Gene expression levels were normalized to β-*actin1* mRNA levels. *, Values are significantly different ($P < 0.05$) from the respective basal condition in the absence of recombinant gonadotropin; #, significant difference ($P < 0.05$) between the absence and the presence of trilostane.

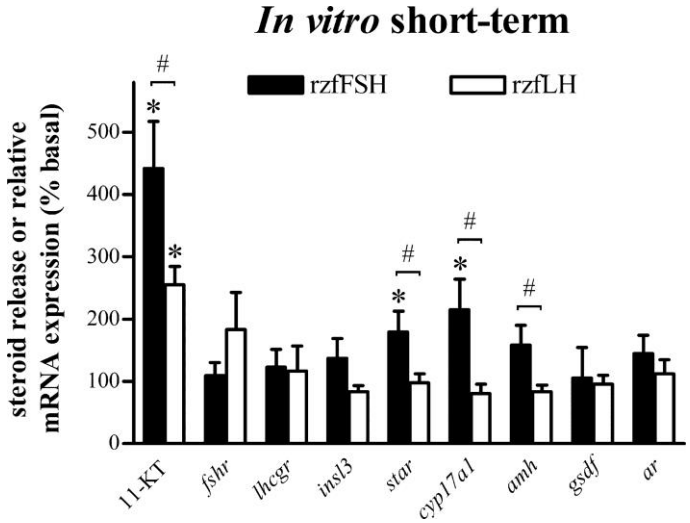

FIG. 5. *In vitro* short-term (2 h) modulation of androgen release and testicular gene expression by rzf gonadotropins. Amounts of androgen (11-KT) measured in incubation media and relative mRNA expression levels of several testicular genes

(*fshr*, *lhcgr*, *insl3*, *star*, *cyp17a1*, *amh*, *gsdf*, and *ar*) after 2 h exposure to 100 ng/ml rzfFSH (*black bars*) or 500 ng/ml rzfLH (*white bars*). Data (mean ± SEM) come from an experiment with eight replicates per condition and are expressed as percentage of basal levels, which were set to 100% for each parameter analyzed. Basal androgen release was 40.0 ± 4.9 pg 11-KT/mg tissue. Gene expression levels were normalized to β-*actin1* mRNA levels. *, Values are significantly different ($P< 0.05$) from the respective basal condition in the absence of recombinant gonadotropin; #, significant difference ($P < 0.05$) between treatment with rzfFSH and rzfLH.

Both recombinant gonadotropins exhibited bioactivity also *in vivo*, as reflected in significantly elevated plasma 11-KT levels and the change in the mRNA levels of several genes expressed in zebrafish testis (Fig. 6). At the dose (100 ng/g body weight) and time after administration (2 h) tested, rzfFSH showed significantly higher steroidogenic potency than rzfLH, although the difference between the two hormones was less pronounced than that observed *in vitro*. Considering changes in gene expression, the rzfFSH treatment up-regulated *insl3*, *cyp17a1*, and *ar* mRNA levels (1.8- to 2.5-fold). *In vivo* administration of rzfLH, conversely, had only minor effects on testicular gene expression.

An interesting exception was the significant 1.7-fold up-regulation of *fshr* mRNA levels. Injection of hCG also elicited a significant increase in plasma 11-KT levels that was intermediate between those observed after the treatments with rzfFSH and rzfLH (Fig. 6). Similar to rzfLH, hCG injection did not change the mRNA levels of the steroidogenesis-related genes (*e.g. star* and *cyp17a1*) or the Leydig cell-specific gene *insl3*, the only exception being the previously unreported down-regulation of *lhcgr* transcription.

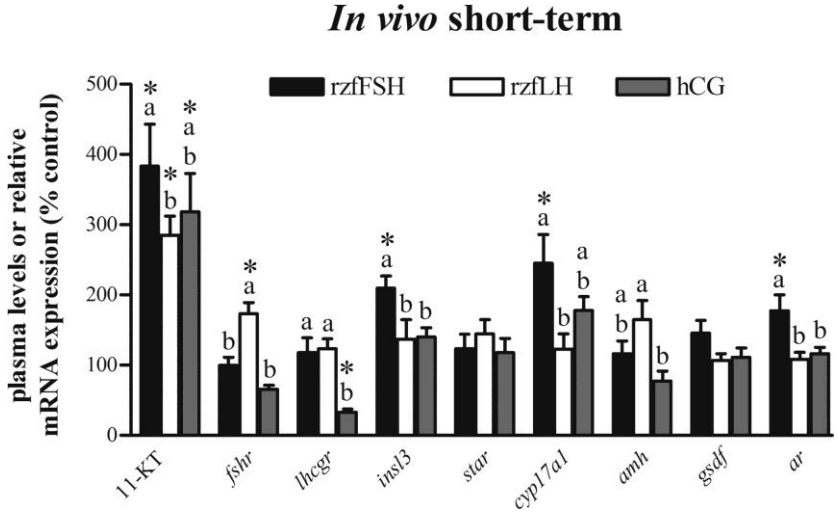

FIG. 6. *In vivo* short-term (2 h) modulation of plasma androgen levels and testicular gene expression by rzf gonadotropins and hCG. Circulating 11-KT concentrations and relative mRNA expression levels of several testicular genes (*fshr*, *lhcgr*, *insl3*, *star*, *cyp17a1*, *amh*, *gsdf*, and *ar*) 2 h after injection with 100 ng/g body weight rzfFSH (*black bars*), rzfLH (*white bars*) or 10 IU/g body weight hCG (*gray bars*). Data (mean ± SEM) come from an experiment with eight fish per condition and are expressed as percentage of control levels, which were set to 100% for each parameter analyzed. Control androgen levels were 3.6 ± 0.9 ng 11-KT/ml plasma. Gene expression levels were normalized to β-*actin1* mRNA levels. *, Values are significantly different ($P < 0.05$) from the basal control condition. *Different letters* denote significant differences among groups ($P < 0.05$).

DISCUSSION

The pituitary gonadotropins LH and FSH, acting via their receptors, Lhcgr and Fshr, are the main factors controlling testis functions across vertebrates, including teleost fish (1, 2, 3, 40). Knowledge about the identity and characteristics of testicular cell types responding to gonadotropic signals, *i.e.* expressing the gonadotropin receptors, is crucial for understanding how gonadotropins regulate testis functions. This information is, however, lacking in most fish species. The available data are restricted to coho salmon, Japanese eel, and African catfish (7, 17, 18), although a complete data set has been reported only for the latter; African catfish

Leydig cells express both *lhcgr* and *fshr* mRNA, whereas Sertoli cells solely express *fshr* mRNA (7). In view of the importance of zebrafish as an experimental model and the essential roles that pituitary gonadotropins play in the regulation of testis physiology, we considered it imperative to identify gonadotropin receptor-expressing cells in the zebrafish testis.

In situ hybridization and qPCR analysis of laser microdissected testicular interstitial tissue showed that, also in zebrafish, the steroid-producing Leydig cells express both *fshr* and *lhcgr* mRNAs. These results support the view that *fshr*/Fshr expression by Leydig cells is a common feature among teleost fish, which is further supported by the strong steroidogenic activity displayed by several piscine FSH proteins (7, 8, 9, 10, 11, 12, 13, 14, 15, 16). Therefore, we propose to explain the steroidogenic activity of FSH-like piscine gonadotropins by a trophic, direct effect on Leydig cells steroid release (7).

qPCR-based analyses of samples obtained by laser microdissection and FACS demonstrated *fshr* expression in zebrafish Sertoli cells, as typically reported in other vertebrates (1, 2, 4) including fish (7, 17, 18). Surprisingly, we also found, for the first time in any vertebrate, *lhcgr* mRNA expression in zebrafish Sertoli cells. This striking testicular expression pattern of *lhcgr* in zebrafish may be related to its undifferentiated gonochoristic mode of gonadal sex differentiation, in which the indifferent gonad initially develops as an ovary-like structure in all individuals, but in future males, developing oocytes soon degenerate and the gonads transform into testes (41, 42, 43). Accordingly, in undifferentiated gonochoristic fish, the default differentiation pathway of the germ-cell-supporting somatic cell precursor (common for both granulosa and Sertoli cells) (44, 45) may be toward granulosa-like cells, which may retain the potential to

transdifferentiate to Sertoli cells (46, 47, 48, 49) and/or may regress, whereas another population of undifferentiated somatic cells differentiates into Sertoli cells (50). Because mammalian as well as salmon granulosa cells (51, 52, 53) express both Fshr and Lhcgr protein and the respective mRNAs, it seems possible that the coexpression of both *fshr* and *lhcgr* mRNA in zebrafish Sertoli cells is related to the transitory female developmental stage observed in this species.

In the present report, we show that rzfFSH was at least 20-fold more potent in stimulating androgen production than rzfLH, whereas both hormones reached similar maximal stimulation levels. This difference in the steroidogenic potency may be related to the higher mRNA expression levels shown by *fshr* in comparison with *lhcgr*, which may lead to a lower abundance of Lhcgr protein on the Leydig cell membrane. This may also represent an adaptive mechanism to balance the constitutive activity of the zebrafish Lhcgr (54) in favor of a tight regulation of Leydig cell steroid release. Functional characterization of zebrafish gonadotropin receptors has shown that the Lhcgr was exclusively activated by LH, whereas both FSH and LH were able to activate the Fshr, which showed a slightly higher preference for FSH (24). Therefore, we conclude that the stimulation of steroid release elicited by rzfFSH was exclusively mediated via Fshr-dependent mechanisms.

Incubation of zebrafish testicular explants with increasing concentrations of the adenylate cyclase activator forskolin resulted in a concentration-dependent stimulation of androgen release, as previously shown in other fish (8, 55, 56, 57). In the current study, forskolin and both recombinant gonadotropins reached similar maximal induction levels, whereas the PKA inhibitor H-89 strongly inhibited gonadotropin-stimulated

androgen release. Together, these data suggest a prominent role for the cAMP/PKA pathway in both Fshr- and Lhcgr-mediated regulation of testicular steroid production (7, 8, 55, 56, 57), although other signaling pathways may have (a quantitatively minor) role in the process, as proposed for other fish (8, 55, 58, 59) and mammalian species (5, 60, 61).

Although both FSH and LH make use of the cAMP/PKA pathway in zebrafish Leydig cells, other downstream mechanisms that the gonadotropins use seem to differ, as demonstrated by analyzing expression levels of steroidogenesis-relevant transcripts; only rzfFSH up-regulated the testicular mRNA levels of *star* and *cyp17a1*. Our results are similar to those recently obtained for Japanese eel where the two gonadotropins showed similar potencies in stimulating testicular androgen release, but only recombinant FSH induced major changes in steroidogenic gene expression (16). Because up-regulation of gene expression is essential for the long-term maintenance of steroid production (60, 62), piscine FSH seems to be the main hormone sustaining Leydig cell steroidogenesis.

The finding that zebrafish (this study) and Japanese eel (16) recombinant LH proteins have limited capacities to support expression of steroidogenesis-related genes may indicate that their bioactivity regarding steroid production relies predominantly on nongenomic mechanisms. Although the present results do not allow identifying such mechanisms, possible explanations could include direct stimulation of the catalytic activity of steroidogenic enzymes, recruitment of mRNAs encoding for steroidogenic enzymes and/or steroidogenic acute regulatory protein from previously produced and stabilized pools, and/or activation (*e.g.* by phosphorylation) of already synthesized but inactive protein pools (60, 62). However, all these assumptions would postulate the use by FSH of yet

unidentified downstream pathways, which may or may not involve the participation of cAMP and/or PKA, to induce the observed up-regulation of steroidogenesis genes expression. As mentioned previously, the latter is essential for the sustained production of steroids, suggesting that the effects exerted by piscine LH on steroidogenesis have a limited duration. This may constitute an additional mechanism in zebrafish Leydig cells to counterbalance the constitutive activity of the Lhcgr (54). Hence, we propose that the LH bioactivity on Leydig cells may be restricted to a transient response of the testicular steroidogenic system, such as described in spawning goldfish, a close relative of the zebrafish, with processes of short duration requiring a quick response in males once they perceive the stimuli from ovulatory females (27, 63). Such events are characterized by the presence of high plasma sex steroid levels, and the two gonadotropins may cooperate to produce the high steroid output required for semen hydration, for stimulating courtship/spawning behavior, and/or for the release of pheromones into the water (7, 27, 63,64).

Although rzfLH did not change the mRNA levels of steroidogenesis-related genes analyzed, it did increase *fshr* mRNA levels in our short-term experiments (2 h). Interestingly, rzfFSH induced a partial down-regulation of *fshr* mRNA levels after 2 d culture, which, together with the short-term LH-induced up-regulation, may represent a regulatory loop to achieve a balanced testicular gonadotropin receptor expression.

The ability of hCG to stimulate steroidogenesis in fish is well known (65) and is explained by its capacity to activate the Lhcgr but not the Fshr in different species, including the zebrafish (23, 54). In our *in vivo* study, hCG elicited downstream effects on zebrafish testis similar to rzfLH (*i.e.* stimulation of androgen release without up-regulating gene expression),

although the effects at thereceptor transcription level were different: *lhcgr* mRNA down-regulation occurred after hCG but not after rzfLH treatment. This could be associated with the long half-life of hCG (65) or the comparatively high concentration used (10 IU to ~715 ng); also, the high specificity of hCG for the Lhcgr of fish is remarkable because piscine (purified or recombinant) LH proteins, although preferring the Lhcgr, also activate the Fshr (7, 22, 24, 52).

The experimental setup involving the 3β-Hsd inhibitor trilostane revealed inhibitory effects of androgens on rzfFSH-induced changes in both *fshr* and *star* mRNA levels. Both genes are situated far upstream in the steroidogenic process (60), and thus, androgen-mediated inhibition may be part of a negative feedback loop to prevent overstimulation of steroidogenesis. This is supported by ongoing studies in our laboratory showing that testicular *star* mRNA levels are down-regulated by exposure to 11-KT (unpublished) as well as by the information available for mammalian models (66, 67).

Further confirmation of the differential roles of FSH and LH on zebrafish Leydig cell functions was obtained in the current study by measuring mRNA levels of the Leydig cell-specific gene *insl3*. Its expression remained unchanged after exposure to rzfLH or hCG but was strongly up-regulated by rzfFSH in a steroid-independent manner. The latter observation agrees with own*in vitro* assays in zebrafish testis showing no effect of increasing concentrations of 11-KT on *insl3* mRNA transcription (unpublished), although it contrasts with previous studies reporting stimulatory effects of androgens on testicular *insl3* expression in amphibians (68). In mammals, although one study has reported that *Insl3* expression was regulated by androgens both in primary cultures of rat Leydig cells and

in the mouse MA-10 tumor Leydig cell line (69), another study using the same cell line concluded that *Insl3* was expressed in a constitutive manner (70). To our knowledge, the present report is the first demonstrating in any teleost species a stimulatory effect of FSH on *insl3* expression, a Leydig cell-specific factor with antiapoptotic effects on meiotic germ cells in mammals (71) but with yet unknown functions in fish.

Although there is substantial evidence supporting the critical nursing functions of Sertoli cells during germ cell proliferation and differentiation in fish spermatogenesis (40), very little is known about the mechanisms by which Sertoli cells relay the gonadotropic signals toward the developing germ cells. Thus, in an attempt to characterize gonadotropin effects on zebrafish Sertoli cells, we measured the mRNA levels of a number of Sertoli cell-specific genes in several bioassays. However, among the genes examined, we found little response to both gonadotropins, the exceptions being the transient increases in *fshr* or *ar* mRNA levels after 2 h *in vivo* rzfLH and rzfFSH treatment, respectively. In general, our candidate gene approach regarding gonadotropin-sensitive Sertoli cell transcripts was of limited success; future studies should therefore include unbiased approaches.

Whether the effects elicited by recombinant hormones (in this and other studies, *e.g.* Refs. 11,13, 16 , and 72, 73, 74, 75, 76) reflect the biological activities of the pituitary hormones could be answered only by comparing highly purified gonadotropins with homologous recombinant proteins, a setting not feasible in zebrafish due to its small size. Nevertheless, different recombinant gonadotropins, including single-chain and/or N-terminal His-tagged molecules (like the hormones used in this study), have been shown to elicit biological effects comparable to

heterodimeric purified native hormones, which has been explained by the receptors' capacity to specifically recognize their ligands even if those are presented in different conformations (77, 78, 79, 80, 81, 82). Moreover, based on structural analysis of human FSH in complex with its receptor (80), the His tag used for purification is pointing away from the major receptor interaction sites, and therefore, it is unlikely to interfere with receptor activation. Whether this applies to fish gonadotropins and their receptors as well remains to be explored with species large enough to allow purification of pituitary hormones for comparative studies. However, our His-tagged, single-chain gonadotropins were able to fully exploit the steroidogenic potency of zebrafish testis tissue (as measured by forskolin incubations), demonstrating their suitability as *bona fide* ligands to entirely activate their receptors.

In summary, the zebrafish testis shows a unique, previously unreported among vertebrates, cellular pattern of *lhcgr* and *fshr* expression, because both Leydig and Sertoli cells express the mRNAs for both receptors. Particularly remarkable is the *lhcgr* expression by Sertoli cells, which may be related to the undifferentiated gonochoristic mode of sex differentiation in zebrafish. In a series of functional bioassays, rzfFSH showed a higher potency in stimulating the testicular steroidogenic system and a higher capacity to alter testicular gene expression profiles than rzfLH. These differences highlight the distinct functional domains of FSH and LH in regulating testis physiology in adult zebrafish, with a role for FSH as the constitutive driving force for both steroidogenesis and spermatogenesis, whereas the function of LH might be seen in context with an acute, additional steroid demand. Moreover, although pharmacological data show that the Fshr can be cross-activated by LH, this does not appear to happen *in*

*vivo*or under culture conditions, because only FSH induced clear changes in the expression of selected testicular genes.

This work was supported by the Norwegian Research Council (Grant 159645/S40 to G.L.T., R.W.S., and J.B.), the National Institutes of Health (Grant DK69711 to J.B.), the Ramón Areces Foundation (Spain; to Á.G.-L), and the National Council for Scientific and Technological Development (Brazil; to R.H.N.).
Current address for Á.G.-L.: Institute of Marine Sciences of Andalucía (High Spanish Council for Scientific Research), Avenida República Saharaui 2, 11510 Puerto Real, Cádiz, Spain.
Disclosure Summary: The authors have nothing to disclose.

First Published Online March 22, 2010
Abbreviations: Cq, Threshold cycle; FACS, fluorescence-activated cell sorting; Fshr, FSH receptor; hCG, human chorionic gonadotropin; 3β-Hsd, 3β-hydroxysteroid dehydrogenase; 11-KT, 11-ketotestosterone; Lhcgr, LH/choriogonadotropin receptor; OHA, 11β-hydroxyandrostenedione; PKA, protein kinase A; qPCR, quantitative PCR; rzf, recombinant zebrafish.

We thank DSM Food Specialties (Delft, The Netherlands) and SenterNovem (The Netherlands) for using their PALM MicroBeam Instrument at the Department of Cell Architecture and Dynamics (Utrecht University), G. Arkesteijn for technical assistance with FACS, Roland Romijn (U-Protein Express B.V.) for assistance in expression and purification of recombinant zebrafish gonadotropins, and H. C. Schriek and J. van Rootselaar (Utrecht University aquarium facility) for taking care of zebrafish stocks.

REFERENCE LIST

1.Pierce JG, Parsons TF 1981 Glycoprotein hormones: structure and function. *Annu Rev Biochem* 50:465–495

2.McLachlan RI, Wreford NG, O'Donnell L, de Kretser DM, Robertson DM 1996 The endocrine regulation of spermatogenesis: independent roles for testosterone and FSH. *J Endocrinol* 148:1–9

3.Kumar TR 2005 What have we learned about gonadotropin function from gonadotropin subunit and receptor knockout mice? *Reproduction* 130:293–302

4.Petersen C, Soder O 2006 The Sertoli cell: a hormonal target and ‘super’ nurse for germ cells that determines testicular size. *Horm Res* 66:153–161

5.Saez JM 1994 Leydig cells: endocrine, paracrine, and autocrine regulation. *Endocr Rev*15:574–626

6.Meng X, Lindahl M, Hyvönen ME, Parvinen M, de Rooij DG, Hess MW, Raatikainen-Ahokas A, Sainio K, Rauvala H, Lakso M, Pichel JG, Westphal H, Saarma M, Sariola H2000 Regulation of cell fate decision of undifferentiated spermatogonia by GDNF. *Science*287:1489–1493

7.García-López A, Bogerd J, Granneman JC, van Dijk W, Trant JM, Taranger GL, Schulz RW 2009 Leydig cells express follicle-stimulating hormone receptors in African catfish.*Endocrinology* 150:357–365

8.Planas JV, Swanson P, Dickhoff WW 1993 Regulation of testicular steroid production *in vitro* by gonadotropins (GTH I and GTH II) and cyclic AMP in cocho salmon (*Oncorhynchus kisutch*). *Gen Comp Endocrinol* 91:8–24

9.Planas JV, Swanson P 1995 Maturation-associated changes in the response of the salmon testis to the steroidogenic actions of gonadotropins (GTH I and GTH II) *in vitro*. *Biol Reprod*52:697–704

10.Kagawa H, Tanaka H, Okuzawa K, Kobayashi M 1998 GTH II but not GTH I induces final maturation and development of maturational competence of oocytes of red seabream *in vitro.Gen Comp Endocrinol* 112:80–88

11.Kamei H, Ohira T, Yoshiura Y, Uchida N, Nagasawa H, Aida K 2003 Expression of a biologically active recombinant follicle stimulating hormone of Japanese eel *Anguilla japonica*using methylotropic yeast, *Pichia pastoris. Gen Comp Endocrinol* 134:244–254

12.Weltzien FA, Norberg B, Swanson P 2003 Isolation and characterization of FSH and LH from pituitary glands of Atlantic halibut (*Hippoglossus hippoglossus* L.). *Gen Comp Endocrinol*131:97–105

13.Aizen J, Kasuto H, Golan M, Zakay H, Levavi-Sivan B 2007 Tilapia follicle-stimulating hormone (FSH): immunochemistry, stimulation by gonadotropin-releasing hormone, and effect of biologically active recombinant FSH on steroid secretion. *Biol Reprod* 76:692–700

14.Zmora N, Kazeto Y, Kumar RS, Schulz RW, Trant JM 2007 Production of recombinant channel catfish (*Ictalurus punctatus*) FSH and LH in S2 *Drosophila* cell line and an indication of their different actions. *J Endocrinol* 194:407–416

15.Molés G, Gómez A, Rocha A, Carrillo M, Zanuy S 2008 Purification and characterization of follicle-stimulating hormone from pituitary glands of sea bass (*Dicentrarchus labrax*). *Gen Comp Endocrinol* 158:68–76

16.Kazeto Y, Kohara M, Miura T, Miura C, Yamaguchi S, Trant JM, Adachi S, Yamauchi K 2008 Japanese eel follicle-stimulating hormone (Fsh) and luteinizing hormone (Lh): production of biologically active recombinant Fsh and Lh by *Drosophila* S2 cells and their differential actions on the reproductive biology. *Biol Reprod* 79:938–946

17.Miwa S, Yan L, Swanson P 1994 Localization of two gonadotropin receptors in the salmon gonad by *in vitro* ligand autoradiography. *Biol Reprod* 59:629–642

18.Ohta T, Miyake H, Miura C, Kamei H, Aida K, Miura T 2007 Follicle-stimulating hormone induces spermatogenesis mediated by androgen production in Japanese eel, *Anguilla japonica. Biol Reprod* 77:970–977

19.Prat F, Sumpter JP, Tyler CR 1996 Validation of radioimmunoassays for two salmon gonadotropins (GTH I and GTH II) and their plasma concentrations throughout the reproductive cycle in male and female rainbow trout (*Oncorhynchus mykiss*). *Biol Reprod*54:1375–1382

20.Gomez JM, Weil C, Ollitrault M, Le Bail PY, Breton B, Le Gac F 1999 Growth hormone (GH) and gonadotropin subunit gene expression and pituitary and plasma changes during spermatogenesis and oogenesis in rainbow trout (*Oncorhynchus mykiss*). *Gen Comp Endocrinol* 113:413–428

21.Sohn YC, Yoshiura Y, Kobayashi M, Aida K 1999 Seasonal changes in mRNA levels of gonadotropin and thyrotropin subunits in the goldfish, *Carassius auratus. Gen Comp Endocrinol* 113:436–444

22.Vischer HF, Granneman JC, Linskens MH, Schulz RW, Bogerd J 2003 Both recombinant African catfish LH and FSH are able to activate the African catfish FSH receptor.*J Mol Endocrinol* 31:133–140

23.Bogerd J, Granneman JC, Schulz RW, Vischer HF 2005 Fish FSH receptors bind LH: How to make the human FSH receptor to be more fishy? *Gen Comp Endocrinol* 142:34–43

24.So WK, Kwok HF, Ge W 2005 Zebrafish gonadotropins and their receptors. II. Cloning and characterization of zebrafish follicle-stimulating hormone and luteinizing hormone subunits: their spatial-temporal expression patterns and receptor specificity. *Biol Reprod*72:1382–1396

25.Sambroni E, Le Gac F, Breton B, Lareyre JJ 2007 Functional specificity of the rainbow trout (*Oncorhynchus mykiss*) gonadotropin receptors as assayed in a mammalian cell line. *J Endocrinol* 195:213–228

26.Bogerd J, Blomenröhr M, Andersson E, van der Putten HH, Tensen CP, Vischer HF, Granneman JC, Janssen-Dommerholt C, Goos HJ, Schulz RW 2001 Discrepancy between molecular structure and ligand selectivity of a testicular follicle-stimulating hormone receptor of the African catfish (*Clarias gariepinus*). *Biol Reprod* 64:1633–1643

27.Kobayashi M, Aida K, Hanyu I 1986 Gonadotropin surge during spawning in male goldfish. *Gen Comp Endocrinol* 62:70–79

28.Krøvel AV, Olsen LC 2002 Expression of a *vas::EGFP* transgene in primordial germ cells of the zebrafish. *Mech Dev* 116:141–150

29.Westerfield M 1995 The zebrafish book. A guide for the laboratory use of zebrafish (*Danio rerio*). Eugene, OR: University of Oregon Press; 1–26

30.Good-Avila SV, Yegorov S, Harron S, Bogerd J, Glen P, Ozon J, Wilson BC 2009Relaxin gene family in teleosts: phylogeny, syntenic mapping, selective constraint, and expression analysis. *BMC Evol Biol* 9:293

31.Leal MC, Cardoso ER, Nóbrega RH, Batlouni SR, Bogerd J, França LR, Schulz RW2009 Histological and stereological evaluation of zebrafish (*Danio rerio*) spermatogenesis with an emphasis on spermatogonial generations. *Biol Reprod* 81:177–187

32.Kurita K, Sakai N 2004 Functionally distinctive testicular cell lines of zebrafish to support male germ cell development. *Mol Reprod Dev* 67:430–438

33.Houwing S, Kamminga LM, Berezikov E, Cronembold D, Girard A, van den Elst H, Filippov DV, Blaser H, Raz E, Moens CB, Plasterk RH, Hannon GJ, Draper BW, Ketting RF 2007 A role for piwi and piRNAs in germ cell maintenance and transposon silencing in zebrafish. *Cell* 129:69–82

34.Iwai T, Yoshii A, Yokota T, Sakai C, Hori H, Kanamori A, Yamashita M 2006 Structural components of the synaptonemal complex, SYCP1 and SYCP3, in the medaka fish *Oryzias latipes. Exp Cell Res* 312:2528–2537

35.Yano A, Suzuki K, Yoshizaki G 2008 Flow-cytometric isolation of testicular germ cells from rainbow trout (*Oncorhynchus mykiss*) carrying the green fluorescent protein gene driven by trout *vasa* regulatory regions. *Biol Reprod* 78:151–158

36.Sawatari E, Shikina S, Takeuchi T, Yoshizaki G 2007 A novel transforming growth factor-β superfamily expressed in gonadal somatic cells enhances primordial germ cell and spermatogonial proliferation in rainbow trout (*Oncorhynchus mykiss*). *Dev Biol* 301:266–275

37.de Waal PP, Wang DS, Nijenhuis WA, Schulz RW, Bogerd J 2008 Functional characterization and expression analysis of the androgen receptor in zebrafish (*Danio rerio*) testis. *Reproduction* 136:225–234

38.Leal MC, de Waal PP, García-López A, Chen SX, Bogerd J, Schulz RW 2009 Zebrafish primary testis tissue culture: an approach to study testis function *ex vivo*. *Gen Comp Endocrinol* 162:134–138

39.Schulz RW, van der Corput L, Janssen-Dommerholt C, Goos HJTh 1994 Sexual steroids during puberty in male African catfish (*Clarias gariepinus*): serum levels and gonadotropin-stimulated testicular secretion *in vitro. J Comp Physiol B* 164:195–205

40.Schulz RW, de França LR, Lareyre JJ, LeGac F, Chiarini-Garcia H, Nobrega RH, Miura T 2010 Spermatogenesis in fish. *Gen Comp Endocrinol* 165:390–411

41.Takahashi H 1977 Juvenile hermaphroditism in the zebrafish, *Brachydanio rerio*. *Bull Fac Fish Hokkaido Univ* 28:57–65

42.Orban L, Sreenivasan R, Olsson PE 2009 Long and winding roads: testis differentiation in zebrafish. *Mol Cell Endocrinol* 312:35–41

43.Maack G, Segner H 2003 Morphological development of the gonads in zebrafish. *J Fish Biol* 62:895–906

44.Albrecht KH, Eicher EM 2001 Evidence that *Sry* is expressed in pre-Sertoli cells and Sertoli and granulosa cells have a common precursor. *Dev Biol* 240:92–107

45.Nakamura S, Aoki Y, Saito D, Kuroki Y, Fujiyama A, Naruse K, Tanaka M 2008*Sox9b*/*sox9a2*-EGFP transgenic medaka reveals the morphological reorganization of the gonads and a common precursor of the female and male supporting cells. *Mol Reprod Dev*75:472–476

46.Wang XG, Orban L 2007 Anti-Müllerian hormone and 11β-hydroxylase show reciprocal expression to that of aromatase in the transforming gonad of zebrafish males. *Dev Dyn*236:1329–1338

47.Guigon CJ, Coudouel N, Mazaud-Guittot S, Forest MG, Magre S 2005 Follicular cells acquire Sertoli cell characteristics after oocyte loss. *Endocrinology* 146:2992–3004

48.Couse JF, Hewitt SC, Bunch DO, Sar M, Walker VR, Davis BJ, Korach KS 1999Postnatal sex reversal of the ovaries in mice lacking estrogen receptors α and β. *Science*286:2328–2331

49.Uhlenhaut NH, Jakob S, Anlag K, Eisenberger T, Sekido R, Kress J, Treier AC, Klugmann C, Klasen C, Holter NI, Riethmacher D, Schütz G, Cooney AJ, Lovell-Badge R, Treier M 2009 Somatic sex reprogramming of adult ovaries to testes by FOXL2 ablation.*Cell* 139:1130–1142

50.Uchida D, Yamashita M, Kitano T, Iguchi T 2002 Oocyte apoptosis during the transition from ovary-like tissue to testes during sex differentiation of juvenile zebrafish. *J Exp Biol*205:711–718

51.Themmen APN, Huhtaniemi IT 2000 Mutations of gonadotropins and gonadotropin receptors: elucidating the physiology and pathophysiology of pituitary-gonad function. *Endocr Rev* 21:551–583

52.Yan L, Swanson P, Dickhoff WW 1992 A two-receptor model for salmon gonadotropins (GTH I and GTH II). *Biol Reprod* 47:418–427

53.Andersson E, Nijenhuis W, Male R, Swanson P, Bogerd J, Taranger GL, Schulz RW2009 Pharmacological characterization, localisation and quantification of expression of

gonadotropin receptors in Atlantic salmon (*Salmo salar* L.) ovaries. *Gen Comp Endocrinol*163:329–339

54.Kwok HF, So WK, Wang Y, Ge W 2005 Zebrafish gonadotropins and their receptors. I. Cloning and characterization of zebrafish follicle-stimulating hormone and luteinizing hormone receptors: evidence for their distinct functions in follicle development. *Biol Reprod* 72:1370–1381

55.Wade MG, Van der Kraak G 1991 The control of testicular androgen production in the goldfish: effects of activators of different intracellular signaling pathways. *Gen Comp Endocrinol* 83:337–344

56.Amiri RM, Maebayashi M, Adachi S, Moberg GP, Doroshov SI, Yamauchi K 1999 In vitro steroidogenesis by testicular fragments and ovarian follicles in a hybrid sturgeon, Bester.*Fish Physiol Biochem* 21:1–14

57.Schulz RW, Liemburg M, García-López A, Dijk W, Bogerd J 2008 Androgens modulate testicular androgen production in African catfish (*Clarias gariepinus*) depending on the stage of maturity and type of androgen. *Gen Comp Endocrinol* 156:154–163

58.Lister A, Van Der Kraak G 2002 Modulation of goldfish testicular testosterone production*in vitro* by tumor necrosis factor α, interleukin-1β, and macrophage conditioned media. *J Exp Zool* 292:477–486

59.Martins RS, Fuentes J, Almeida O, Power DM, Canario AV 2009 Ca^{2+}-calmodulin regulation of testicular androgen production in Mozambique tilapia (*Oreochromis mossambicus*). *Gen Comp Endocrinol* 162:153–159

60.Stocco DM, Wang X, Jo Y, Manna PR 2005 Multiple signaling pathways regulating steroidogenesis and steroidogenic acute regulatory protein expression: more complicated than we thought. *Mol Endocrinol* 19:2647–2659

61.Manna PR, Chandrala SP, Jo Y, Stocco DM 2006 cAMP-independent signaling regulates steroidogenesis in mouse Leydig cells in the absence of StAR phosphorylation. *J Mol Endocrinol* 37:81–95

62.Stocco DM, Clark BJ 1996 Regulation of the acute production of steroids in steroidogenic cells. *Endocr Rev* 17:221–244

63.Kyle AL, Stacey NE, Peter RE, Billard R 1985 Elevation in gonadotrophin concentrations and milt volumes as a result of spawning behavior in the goldfish. *Gen Comp Endocrinol*57:10–22

64.Chen SX, Bogerd J, García-López A, de Jonge H, de Waal PP, Hong WS, Schulz RW2010 Molecular cloning and functional characterization of a zebrafish nuclear progesterone receptor. *Biol Reprod* 82:171–181

65.Mylonas CC, Fostier A, Zanuy S 2010 Broodstock management and hormonal manipulations of fish reproduction. *Gen Comp Endocrinol* 165:516–534

66.Houk CP, Pearson EJ, Martinelle N, Donahoe PK, Teixeira J 2004 Feedback inhibition of steroidogenic acute regulatory protein expression *in vitro* and *in vivo* by androgens.*Endocrinology* 145:1269–1275

67.Eacker SM, Agrawal N, Qian K, Dichek HL, Gong EY, Lee K, Braun RE 2008 Hormonal regulation of testicular steroid and cholesterol homeostasis. *Mol Endocrinol* 22:623–635

68.De Rienzo G, Aniello F, Branno M, Izzo G, Minucci S 2006 The expression level of frog relaxin mRNA (*fRLX*), in the testis of *Rana esculenta*, is influenced by testosterone. *J Exp Biol*209:3806–3811

69.Laguë E, Tremblay JJ 2008 Antagonistic effects of testosterone and the endocrine disruptor mono-(2-ethylhexyl) phthalate on *INSL3* transcription in Leydig cells. *Endocrinology*149:4688–4694

70.Sadeghian H, Anand-Ivell R, Balvers M, Relan V, Ivell R 2005 Constitutive regulation of the *Insl3* gene in rat Leydig cells. *Mol Cell Endocrinol* 241:10–20

71.Kawamura K, Kumagai J, Sudo S, Chun SY, Pisarska M, Morita H, Toppari J, Fu P, Wade JD, Bathgate RA, Hsueh AJ 2004 Paracrine regulation of mammalian oocyte maturation and male germ cell survival. *Proc Natl Acad Sci USA* 101:7323–7328

72.Yu X, Lin SW, Kobayashi M, Ge W 11 July 2008 Expression of recombinant zebrafish follicle-stimulating hormone (FSH) in methylotropic yeast *Pichia pastoris.* Fish Physiol Biochem 10.1007/s10695-008-9244-z

73.Ko H, Park W, Kim DJ, Kobayashi M, Sohn YC 2007 Biological activities of recombinant Manchurian trout FSH and LH: their receptor specificity, steroidogenic and vitellogenic potencies. *J Mol Endocrinol* 38:99–111

74.Kasuto H, Levavi-Sivan B 2005 Production of biologically active tethered tilapia LHβα by the methylotrophic yeast *Pichia pastoris*. *Gen Comp Endocrinol* 140:222–232

75.Hayakawa Y, Morita T, Kitamura W, Kanda S, Banba A, Nagaya H, Hotta K, Sohn YC, Yoshizaki G, Kobayashi M 2008 Biological activities of single-chain goldfish follicle-stimulating hormone and luteinizing hormone. *Aquaculture* 274:408–415

76.Kobayashi M, Morita T, Ikeguchi K, Yoshizaki G, Suzuki T, Watabe S 2006 In vivo biological activity of recombinant goldfish gonadotropins produced by baculovirus in silkworm larvae. *Aquaculture* 256:433–442

77.Ben-Menahem D 2004 Single chain variants of the glycoprotein hormones and their receptors as tools to study receptor activation and analogue design. *J Neuroendocrinol*16:171–177

78.Fidler AE, Lin JS, Lun S, Ng Chie W, Western A, Stent V, McNatty KP 2003 Production of biologically active tethered ovine FSHβα by the methylotrophic yeast *Pichia pastoris*. *J Mol Endocrinol* 30:213–225

79.Legardinier S, Poirier JC, Klett D, Combarnous Y, Cahoreau C 2008 Stability and biological activities of heterodimeric and single-chain equine LH/chorionic gonadotropin variants. *J Mol Endocrinol* 40:185–198

80.Fan QR, Hendrickson WA 2005 Structure of human follicle-stimulating hormone in complex with its receptor. *Nature* 433:269–277

81.Sugahara T, Pixley MR, Minami S, Perlas E, Ben-Menahem D, Hsueh AJ, Boime I1995 Biosynthesis of a biologically active single peptide chain containing the human common α and chorionic gonadotropin β subunits in tandem. *Proc Natl Acad Sci USA* 92:2041–2045

82.Fralish GB, Narayan P, Puett D 2003 Consequences of single-chain translation on the structures of two chorionic gonadotropin yoked analogs in α-β and β-α configurations. *Mol Endocrinol* 17:757–767

SUPPLEMENTAL INFORMATION

Laser micro-dissection

Five μm cryosections from snap-frozen wild-type Tübingen AB strain zebrafish testis tissue were mounted on PALM 1 mm MembraneSlides. Air-dried sections were treated with xylene for 2 min, incubated in the 3β-Hsd staining medium (containing 0.1 mg/ml 5α-androstan-3β-ol-17one, 0.5 mg/ml β-nicotinamide adenine dinucleotide, 0.2 mg/ml nitroblue tetrazolium chloride, and 10% dimethylformamide in 0.1 M phosphate buffer pH 7.4) (1) at 37ºC for 1 h, fixed in 4% formalin for 2 min, counterstained with nuclear fast red for 30 sec, and air-dried. Areas of interest were immediately selected, laser micro-dissected (supplemental Fig. 1, A and B) and pressure-catapulted into 40 μl PALM catapult buffer (20 mM Tris pH 7.4, 1 mM EDTA). Given that both Leydig cells and germinal cysts at different stages of development are randomly distributed along zebrafish testis, Leydig cell groups and intratubular samples were collected over the whole surface of testis tissue sections. Thereafter, samples were digested with 0.25 μg/μl proteinase K (Sigma-Aldrich, St. Louis, MO, USA) in the presence of 0.5 U/μl RNase inhibitor (RNAguard, GE Healthcare, Fairfield, CT, USA) at 55ºC for 1 h. Total RNA extraction, linear amplification, and reverse-transcription to cDNA of laser micro- dissected samples were performed as reported previously (2, 3).

Production of recombinant, single-chain zebrafish gonadotropins

Recombinant zebrafish FSH and LH (rzfFSH and rzfLH) were expressed as single-chain

molecules, following a strategy as described for human FSH (4). The expression constructs comprised the entire mature sequence of the *fsh* subunit (GenBank accession number: NM_205624) or the *lh* subunit (GenBank accession number: NM_205622) followed by a 15-residue linker (GGGSGGGSGGGSGGG) and the mature sequence of the glycoprotein hormone α subunit (GenBank accession number: NM_205687). The respective sequences were amplified with primers introducing a 5' *Bam* HI and a 3' *Not* I restriction site, digested with these enzymes and ligated into a *Bam* HI *Not* I compatible proprietary mammalian expression vector introducing an N-terminal TEV cleavable 6×His tag (U-Protein Express B.V., Utrecht, The Netherlands) (supplemental Fig. 2A). For large scale expression, 1 liter of FreeStyle medium (Invitrogen) supplemented with 0.02% v/v fetal calf serum (Invitrogen) and containing ~$0.5x10^6$ proprietary HEK293-EBNA cells per ml was transiently transfected with 500 μg plasmid DNA using polyethylenimine (Sigma-Aldrich) (5). Four hours after transfection, 0.9% v/v Primatone (Kerry Biosciences, Naarden, The Netherlands) was added to the medium. After five days, the medium was harvested by centrifugation, concentrated, and dialyzed into 20 mM Tris pH 8.0, 500 mM NaCl using a Quickstand hollow fiber with a UFP-10 kDa molecular weight cut-off cartridge (GE Healthcare). Protein solutions were then loaded onto a 1 ml HisTrap FF column (GE Healthcare) and eluted with a gradient of imidazole (0-40 mM) in binding buffer (20 mM Tris pH 8.0, 500 mM NaCl). Peak fractions were analyzed using SDS PAGE and Western blotting (using a commercially available His-tag specific monoclonal antibody as recommended by the manufacturer; Novagen, Darmstadt, Germany) and fractions containing hormone were pooled, dialyzed into 20 mM Tris pH 7.5, 500 mM NaCl, and then loaded on a 2 ml Concanavalin-A Sepharose column (GE Healthcare). Elution was performed using an increasing gradient of α-D-methyl mannopyranoside (0-500 mM) in 20 mM Tris pH 7.5, 500 mM NaCl. Peak fractions were again analyzed by Western blotting (using anti His-tag antibody), pooled and concentrated to a volume less than 5 ml and loaded on a HiLoad 16/60 Superdex 200 pg column (GE Healthcare). Fractions containing pure hormone by Western blotting and Coomassie staining were pooled (supplemental Fig. 2B) and dialyzed against PBS. Four different batches of each recombinant gonadotropin were produced in this way, pooled, and concentrated to 500 ng/μl protein. Protein quantification was performed spectrophotometrically using a NanoDrop ND-1000 instrument (Thermo Fisher Scientific, Waltham, MA, USA).

References

1.Levy HW, Deane HW, Rubin BL 1959 Visualization of steroid-3β-ol-dehydrogenase activity in tissues of intact and hypophysectomized rats. Endocrinology 65:932-943

2.García-López Á, Bogerd J, Granneman JCM, van Dijk W, Trant JM, Taranger GL, Schulz RW 2009 Leydig cells express follicle-stimulating hormone receptors in African catfish. Endocrinology 150:357-365

3.Bogerd J, Blomenröhr M, Andersson E, van der Putten HHAGM, Tensen CP, Vischer HF, Granneman JCM, Janssen-Dommerholt C, Goos HJTh, Schulz RW 2001 Discrepancy between molecular structure and ligand selectivity of a testicular follicle-

stimulating hormone receptor of the African catfish (*Clarias gariepinus*). Biol Reprod 64:1633-1643

4.Fan QR, Hendrickson WA 2005 Structure of human follicle-stimulating hormone in complex with its receptor. Nature 433:269-277

5.Marx PF, Brondijk TH, Plug T, Romijn RA, Hemrika W, Meijers JC, Huizinga EG 2008 Crystal structures of TAFI elucidate the inactivation mechanism of activated TAFI: a novel mechanism for enzyme autoregulation. Blood 112:2803-2809

SUPPLEMENTAL FIGURES

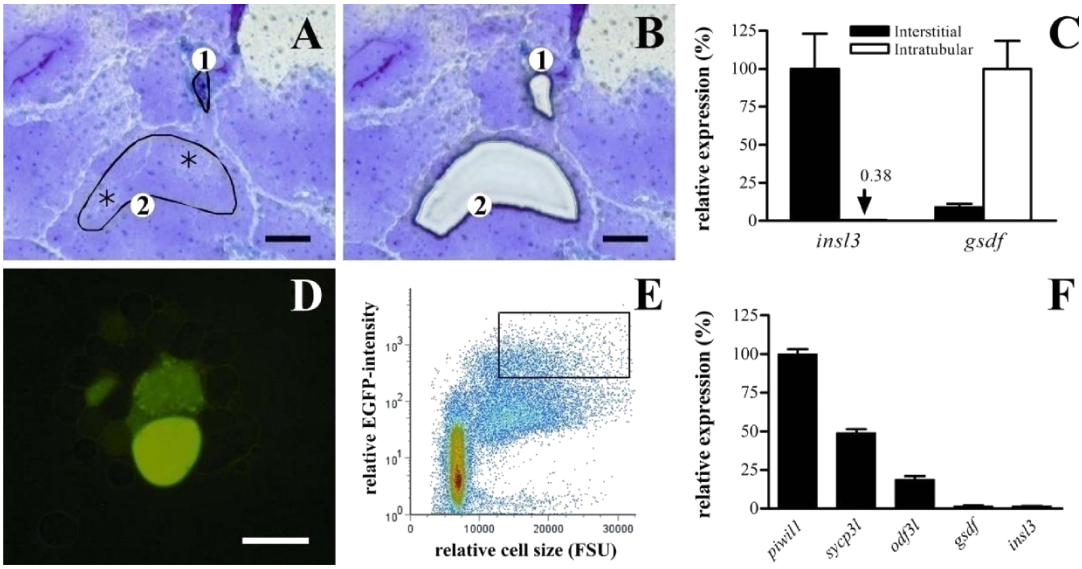

SUPPLEMENTAL FIG. 1. Morphological and molecular characterization of zebrafish laser micro- dissected testis tissue fractions and germ cell-enriched population obtained by FACS. (A-C) Laser micro-dissection process and validation of samples collected. (A) Target areas for micro-dissection were selected and tagged as follows: interstitial (tagged with number 1) containing 3β-HSD positive Leydig cells, and intratubular (tagged with number 2) containing spermatogenic cysts (*i.e.* Sertoli and germ cells; asterisks). (B) After selection, tissue was laser micro-dissected and pressure-catapulted into separate tubes for interstitial and intratubular tissue. (C) Characterization of micro-dissected tissue fractions using the molecular markers *insl3* and *gsdf*. (D-F) FACS process and validation of sample obtained. (D) Fluorescent view of whole cell suspension before flow cytometry showing cells with different EGFP intensities and sizes; the bigger size correlates with higher EGFP intensity. (E) Dot plot diagram showing the whole cell suspension appearance and the sorting window selected to obtain the germ-cell-enriched population according to EGFP intensity and size (FSU: forward scatter units). (F) Characterization of the germ-cell-enriched population obtained using the molecular markers *piwil1*, *sycp3l*, *odf3l*, *gsdf*, and *insl3*. *Scale bars*, 30 μm. Expression levels (C and F) correspond to values from two experiments with duplicate measurements each (mean ± SEM), normalized to zebrafish *β-*

actin1 mRNA levels, and expressed as percentages of mRNA amounts of each transcript in the interstitial (*insl3*) or the intratubular (*gsdf*) fractions (C) or of *piwil1* mRNA levels (F).

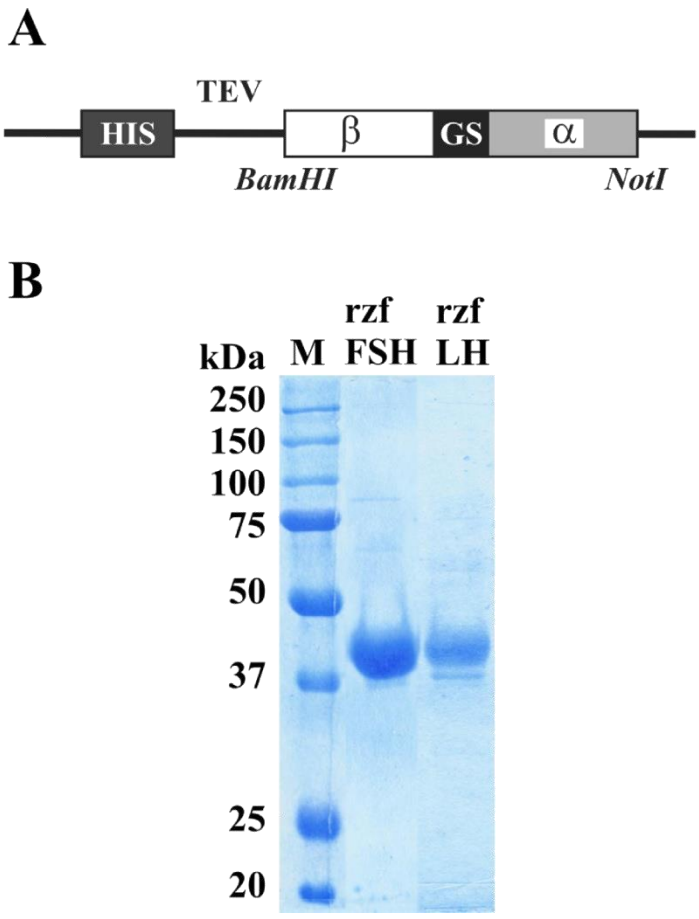

SUPPLEMENTAL FIG. 2. Recombinant, single chain zebrafish gonadotropins used in the current study. (A) Schematic representation of a portion of the zebrafish gonadotropins expression vector construct, including an N-terminal 6×His tag (HIS), a TEV-cleavage site, and each specific β subunit linked to the common α subunit by a 15-residue Gly-Ser linker (GS) between the *BamHI* and *NotI* restriction sites; (B) Characterization by reducing 12% SDS PAGE analysis of affinity-purified recombinant gonadotropins, rzfFSH and rzfLH. M, molecular weight marker.

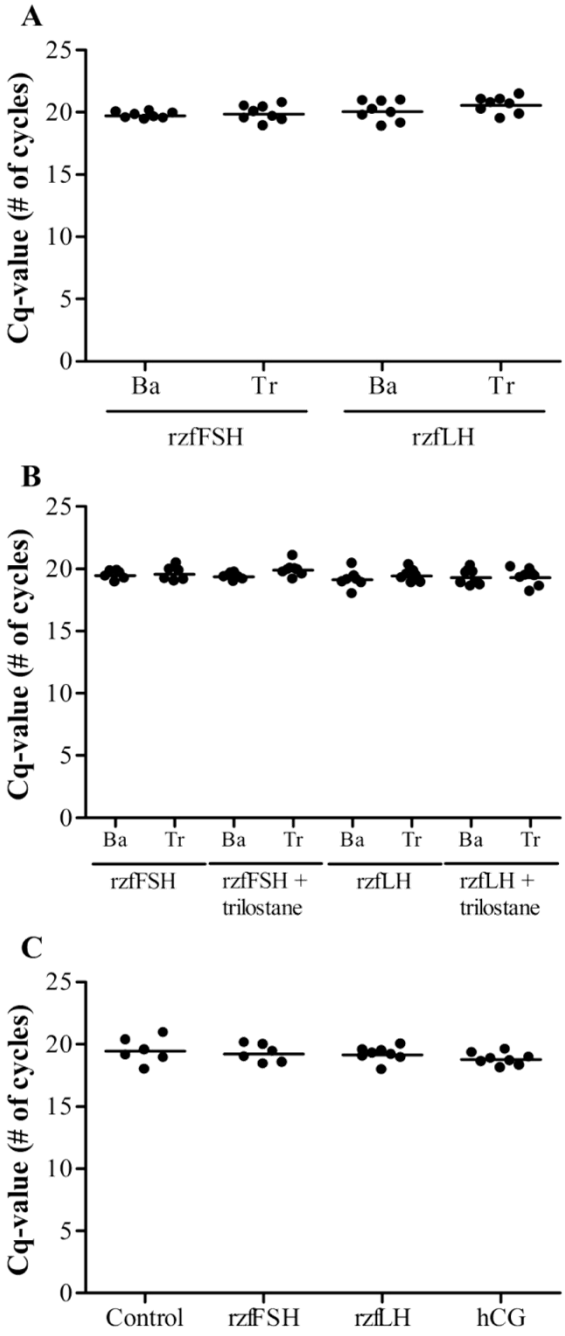

SUPPLEMENTAL FIG. 3. Stability of *β-actin1* mRNA as a reference gene in the different experiments reported in the current study. (A) *In vitro* short-term; (B) *In vitro* medium-term; and, (C) *In vivo* short-term. Each dot in the scatter plots represents the average quantification or threshold cycle (Cq) value of duplicate measurements per sample. For each experiment, no significant differences ($P>0.05$) were found among the mean *β-actin1* mRNA expression levels (horizontal line within each group of dots) in the different treatments. Ba: basal; Tr: treated.

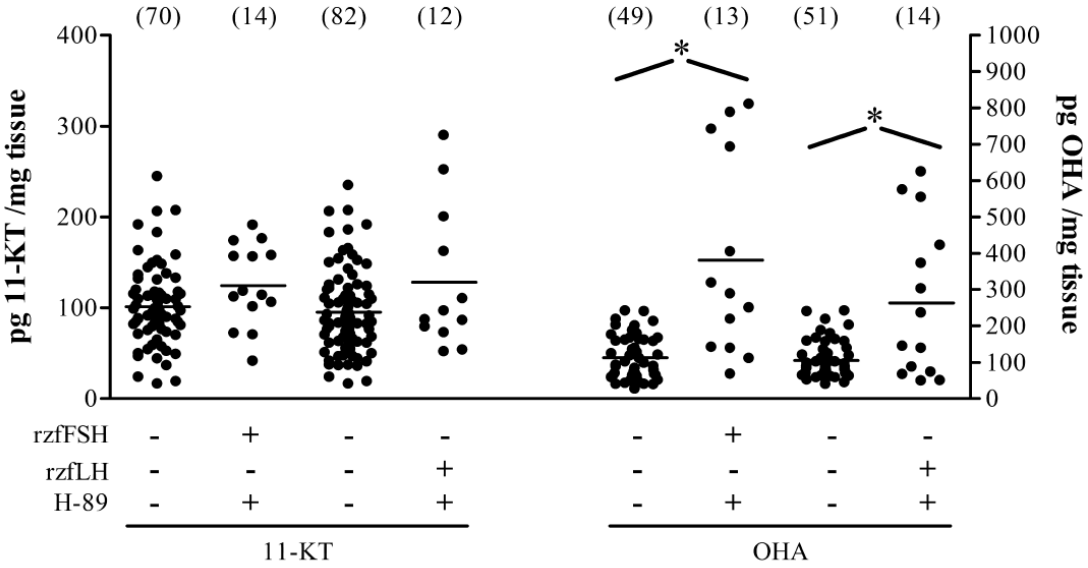

SUPPLEMENTAL FIG. 4. Comparison of basal androgen release with residual androgen release in the presence of the PKA inhibitor H-89 and recombinant zebrafish gonadotropins. Amounts of 11-KT and OHA measured in incubation media after overnight (18 h) exposure to 250 ng/ml recombinant zebrafish Fsh (rzfFSH) or 1000 ng/ml recombinant zebrafish Lh (rzfLH) in combination with 100 µM H-89 (see Fig. 3 of the main text). Basal release data were compiled from the experiments described in Fig. 2 of the main text. Means are indicated by horizontal lines. *Numbers in parenthesis* represent sample size. *, Means are significantly different (P<0.05; Student unpaired t-test).

SUPPLEMENTAL TABLE 1. Primers used to generate DNA templates for DIG-labelled cRNA probe synthesis for *in situ* hybridization.

Target	Primer	Nucleotide sequence (5' → 3')
fshr	2390[a]	T3Rpps- TCAAGACCTCACCTGAACAACAGCAGCTA
	2391[b]	T7Rpps- AGCCCCGTTCTCGGACACCACTATTC
lhcgr	2402[a]	T3Rpps- AGGTCTGCCCTGCTTCTTGTTT
	2403[b]	T7Rpps- AGATGCTCAGGTATCTGAGTTTGGG
insl3	2126[a]	T3Rpps- AGTGAAGATGTGCGAGTGAAGC
	2127[b]	T7Rpps- GTACTGAATCAGTTCATTCATGGTGCA

[a]Primers contain the T3 RNA polymerase promoter sequence (underlined) (T3Rpps; 5'-GGGCGGGTGTTATTAACCCTCACTAAAGGG-3').

[b]Primers contain the T7 RNA polymerase promoter sequence (underlined) (T7Rpps; 5'-CCGGGGGGTGTAATACGACTCACTATAGGG-3').

(5' → 3')

SUPPLEMENTAL TABLE 2. Primers and hydrolysis probe used in the current study to quantify mRNA levels by qPCR[a].

Target	GenBank Accession No.	Primer	Nucleotide sequence (5' → 3')
β-actin1	NM_131031	Fw	TGCTCTGTATGGCGCATTGA
		Rv	GCTCCTCCCCCTGTTAGACAAC
amh	AY721604	Fw	CTCTGACCTTGATGAGCCTCATTT
		Rv	GGATGTCCCTTAAGAACTTTTGCA
		Pr	ATTCCACAGGATGAGAGGCTCCCATCC
ar	EF153102	Fw	ACGTGCCTGGCGTGAAAA
		Rv	CAAACCTGCCATCCGTGAAC
cyp17a1	NM_212806	Fw	GGGAGGCCACGGACTGTTA
		Rv	CCATGTGGAACTGTAGTCAGCAA
fshr	AY278107	Fw	GCATATCTACCGCACTGAGATTTCTT
		Rv	GGAGTACAGCGTCCCATCACTAGT
gsdf	EU378916	Fw	CATCTGCGGGAGTCATTGAAA
		Rv	AGCTTGCCGGAGGACTCTG
insl3	EF685704	Fw	TCGCATCGTGTGGGAGTTT
		Rv	TGGATAGAGACCTCGTTGTGCA
lhcgr	NM_205625	Fw	GCCTTCAGGAAAGACGCTTGTAT
		Rv	CATCCGGTACAAGTTAGCTTTGCT
odf3l	NM_199958	Fw	GATGCCTGGAGACATGACCAA
		Rv	CAAAGGAGAAGCTGGGAGCTTT
piwil1	NM_183338	Fw	GATACCGCTGCTGGAAAAAGG
		Rv	TGGTTCTCCAAGTGTGTCTTGC
star	AF220435	Fw	CCTGGAATGCCTGAGCAGAA
		Rv	ATCTGCACTTGGTCGCATGAC
sycp3l	BC115343	Fw	AGAAGCTGACCCAAGATCATTCC
		Rv	AGCTTCAGTTGCTGGCGAAA

[a]Sequences are shown for the sense (Fw) and antisense (Rv) primers and the TaqMan hydrolysis probe (Pr).

CHAPTER 5

Proteolytically Activated, Recombinant Anti-mullerian Hormone Inhibits a Androgen Secretion, Proliferation, and Differentiation of Spermatogonia in Adult Zebrafish Testis Organ Cultures

K. S. Skaar*, R. H. Nóbrega*, A. Magaraki, L. C. Olsen, R. W. Schulz, and R. Male

**equally contributed*

Endocrinology. 2011 Sep;152(9):3527-40. doi: 10.1210/en.2010-1469. Epub 2011 Jul 12.

ABSTRACT

Anti-Müllerian hormone (Amh) is in mammals known as a TGFβ type of glycoprotein processed to yield a bioactive C-terminal homodimer that directs regression of Müllerian ducts in the male fetus and regulates steroidogenesis and early stages of folliculogenesis. Here, we report on the zebrafish Amh homologue. Zebrafish, as all teleost fish, do not have Müllerian ducts. Antibodies raised against the N- and C-terminal part of Amh were used to study the processing of endogenous and recombinant Amh. The N-terminally directed antibody detected a 27-kDa protein, whereas the C-terminally directed one recognized a 32-kDa protein in testes extracts, both apparently not glycosylated. The C-terminal fragment was present as a monomeric protein, because reducing conditions did not change its apparent molecular mass. Recombinant zebrafish Amh was cleaved with plasmin to N- and C-terminal fragments that after deglycosylation were similar in size to endogenous Amh fragments. Mass spectrometry and N-terminal sequencing revealed a 21-residue N-terminal leader sequence and a plasmin cleavage site after Lys or Arg within Lys-Arg-His at position 263–265, which produce theoretical fragments in accordance with the experimental results. Experiments using adult zebrafish testes tissue cultures showed that plasmin-cleaved, but not uncleaved, Amh inhibited gonadotropin-stimulated androgen production. However, androgens did not modulate *amh* expression that was, on the other hand, down-regulated by Fsh. Moreover, plasmin-cleaved Amh inhibited androgen-stimulated proliferation as well as differentiation of type A spermatogonia. In conclusion, zebrafish Amh is processed to become bioactive and has independent functions in inhibiting both steroidogenesis and spermatogenesis.

INTRODUCTION

Anti-Müllerian hormone (Amh) is a member of the TGFβ superfamily engaged in the regulation of cell proliferation, differentiation, growth, and apoptosis (1, 2). The namesake function of Amh is to induce regression of the Müllerian ducts during male sex differentiation in tetrapod vertebrates (3, 4).

Amh was first isolated as a 123-kDa dimeric glycoprotein secreted from bovine testes and from bovine testes incubation medium (3, 5–7). Recombinant human Amh produced in Chinese hamster ovary cells is processed by cleavage of the 24-amino acid (aa) leader sequence, followed by a second cleavage after the RAQR motif at position 424–427 (8, 9). Functional experiments have revealed that Amh is strongly activated by cleaveage (10, 11). Amh is glycosylated in the N-terminal part of the human and avian protein (12, 13), and the N-terminal region (present as a homodimer after cleavage) enhances the activity of the C-terminal fragment (14). The C-terminal fragment contains the conserved TGFβ domain (2) with highly conserved cysteines involved in forming a cystine-knot structure of the active part (12, 15). A recent report has verified that cleavage is necessary for efficient receptor binding and that the N-terminal proregion is present at receptor interaction but dissociates from the C-terminal homodimer as a consequence of receptor binding (16).

Amh signals through binding to a Amh type II transmembrane receptor (AmhRII) with serine/threonine kinase activity (17). This complex recruits and phosphorylates one of the activin-receptor kinases (ALK) mediating stimulatory (ALK2 and ALK3) or inhibitory (ALK6) effects (17, 18) that involve Smad proteins in the downstream signaling cascade

(19). In the testis, AmhRII is expressed in Sertoli (20) and Leydig (21) cells. In fish, an AmhRII has been identified in medaka (*Oryzias latipes*) (22) and reported from black porgy, *Acanthopagrus schlegeli* (23). In mammalian testes, Amh is highly expressed by immature Sertoli cells until prepuberty, when at the start of meiosis, increasing testosterone levels down-regulate Amh, mRNA and protein levels, that remain low during late puberty and adulthood (24). Amh expression in juvenile males is stimulated by Fsh when the androgen receptor is not activated in Sertoli cells (25). Moreover, Amh is a negative regulator of postnatal Leydig cell differentiation and steroidogenesis. Mice transgenic for human Amh show a decreased number of adult-type, differentiated Leydig cells, low plasma levels of testosterone, and reduced mRNA levels of steroidogenic enzymes, including Cyp17 (21). Also, Amh reduced LH-induced testosterone production by fetal and adult Leydig cells in rodents (26, 27). Amh-deficient mice, on the other hand, showed a remarkable hyperplasia of Leydig cells (28, 29). These observations suggest that in mammals, Amh has a negative regulatory role in the postnatal differentiation and function of Leydig cells.

Teleost fish lack Müllerian ducts, but Amh homologues have been identified in several species, such as Japanese eel (30), zebrafish (31, 32), tilapia (33), medaka (22), sea bass (34), Iberian chub (35), pejerrey (36), and rainbow trout (37, 38). In primary cultures of Japanese eel testis fragments, recombinant eel Amh (originally named spermatogenesis-preventing substance) inhibited 11-ketotestosterone (11-KT), the main androgen in zebrafish (39) and other fish species (40), and induced spermatogenesis by blocking the proliferation of type B spermatogonia (30). In medaka, there is an additional aspect of Amh bioactivity during early gonad differentiation in both sexes: gene knockdown experiments targeting Amh or AmhRII

reduced germ-cell proliferation, and recombinant eel Amh counteracted this effect when added to medaka gonad tissue fragments from *amh* knockdown animals (41). In contrast, the medaka *amhrII/hotei* loss-of-function mutant displayed an increased number of germ cells in both sexes (42). Moreover, male mutants showed premature initiation of meiosis, and 50% underwent sex reversal.

Taken together, there is evidence for effects of Amh on germ-cell proliferation in fish, whereas the quality of the effect differs, being stimulatory during early stages of development (41) but inhibitory at the onset of puberty (30). However, it has remained unexplored whether Amh bioactivity described in mammals, such as the inhibitory effect on Leydig cell function (43), can be observed in fish and may thus be an evolutionary conserved feature. Moreover, it is not known whether Amh has an effect on spermatogenesis in adult animals. In this work, we first have investigated how zebrafish Amh is processed to become bioactive, before testing plasmin-cleaved, recombinant Amh in zebrafish testis cultures. To this end, we have investigated whether Amh modulates steroidogenesis or spermatogenesis in adult zebrafish testis. We also investigated the ontogenesis of *amh* expression and aspects of the endocrine regulation of *amh* expression, and we propose a model on the role of Amh on adult zebrafish testis functions.

MATERIAL AND METHODS

Detailed material and methods are provided in the Supplemental data, published on The Endocrine Society's Journals Online web site at http://endo.endojournals.org. In brief, antisera directed to N-terminal and

C-terminal regions of Amh were raised against peptides and provided as purified rabbit antibodies by BioGenes (Berlin, Germany). The C-terminal-directed antibody was used for immunocytochemical detection of endogenous Amh in adult zebrafish testis. Recombinant zebrafish Amh was produced in stably transfected human embryonic kidney 293 (HEK293) cells and purified from culture medium via a 6xHis tag introduced after Pro33 (AY721604). The presumed proteolytic cleavage site, based on sequence comparison, was optimized from RAQR motif (position 439–442) to RARR using QuickChange II Site-Directed Mutagenesis kit (Stratagene, La Jolla, CA), and the product was named His-Amh-Q441R. Plasmin treatments were conducted as indicated in figure legends. The reaction was stopped with aprotinin (A3428; Sigma, St. Louis, MO) and the extract frozen at −80 C until further use.

Amh in distilled water was deglycosylated using the Enzymatic Carbo Release kit from QA-Bio (Palm Desert, CA) (KE-DG01). N-terminal sequencing using Edman degradation was performed (Proteomics Facility, University of Leeds, Leeds, UK) on SDS-PAGE separated Amh followed by electroblotting onto a sequencing-grade polyvinylidene fluoride membrane. Matrix-assisted laser desorption/ionization-time-of-flight analyses (PROBE Proteomics Facility, University of Bergen) were performed on acetone precipitated purified untreated and plasmin-cleaved peptide-in-gel samples. Untreated and plasmin-cleaved, recombinant zebrafish Amh (10 μg/ml or 140 nM, 70 nM if dimer) were added to primary zebrafish testis organ cultures (as described in Ref. 44) in the presence of recombinant zebrafish Fsh (100–500 ng/ml). Cultures were analyzed for 11-KT in media (44), and testis tissue for expression of selected genes [*cytochrome P450, family 17, subfamily A, polypeptide*

1 (*cyp17a1*),*steroidogenic acute regulatory protein* (*star*), *insulin-like 3 (insl3*), and *androgen receptor* (*ar*)] by real-time quantitative PCR (44). Relative mRNA levels of target genes (*cyp17a1*, *star*,*insl3*, and *ar*) were normalized to *18S* rRNA (reference endogenous control gene) and expressed as fold induction compared with the control groups.

Gonadal *amh* mRNA was quantified as previously (44) in samples collected 4 wk postfertilization (wpf) (after completion of sex differentiation), 8 wpf (pubertal gonad growth ongoing), and 12 wpf (young adults), detailed in Supplemental Methods. To address the endocrine regulation of *amh* expression, adult testis tissue was incubated with androgens or with recombinant zebrafish Fsh in the absence or presence of a protein kinase A inhibitor H89 under different conditions (see Supplemental Methods), before *amh* mRNA levels were quantified as previously (44).

Effects of recombinant zebrafish Amh on spermatogenesis [bromodeoxyuridine (BrdU) incorporation into type A undifferentiated (A_{und}) spermatogonia and frequency of germ-cell types] were analyzed using a previously described tissue culture system (45). Testes were collected from untreated, adult males, and tissue was incubated in the presence of 200 nM 11-KT to test the effect of recombinant zebrafish Amh (10 μg/ml), or testes were collected from adult males exposed for 3 wk to 10 nM estradiol-17β to induce androgen insufficiency and inhibit spermatogenesis (46) before the tissue was incubated in the absence or presence of Amh (10 μg/ml). Incubation conditions, fixation, and morphological and morphometrical analysis of the samples are detailed in the Supplemental Methods.

Significant differences between two groups were identified using Student's *t* test (paired and unpaired) ($P < 0.05$). Comparisons of more than

two groups were performed with one-way ANOVA followed by Student-Newman-Keuls test ($P < 0.05$). GraphPad Prism 4.0 (GraphPad Software, Inc., San Diego, CA) was used for all statistical analysis. Sequence analyses were performed as described in Supplemental Methods.

RESULTS

Amh is processed by proteolytic cleavage

The zebrafish Amh cDNA sequence (AY721604) predicts a 549-aa protein with a molecular mass of 61.1 kDa, including a 21-residue leader sequence, that after cleavage gives a 58.7-kDa protein (Fig. 1A and Supplemental Fig. 1). Two N-glycosylation sites were predicted at N334 (NSST) and N510 (NRSL), where the first site is conserved among fish species and is close to the human Amh glycosylation site (NLSD position 329–332, BC049194) (Supplemental Fig. 1). The predicted C-terminal TGFβ domain (aa 457–549) has seven conserved cysteine residues where C514 is expected to be involved in dimer formation. Human AMH is known to be cleaved after RAQR at position 448–451, which align to a putative cleavage site in zebrafish Amh at position 439–445 (Supplemental Fig. 1B). Immunoblots of testes protein extracts under reducing and nonreducing conditions revealed two fragments probably generated by proteolytic cleavage of the full-length protein: N-27 and C-32 (Fig. 1, B and C). An alternative lysis buffer produced two candidate full-length Amh proteins of 66 and 71 kDa detected with the anti-C antibody (Fig. 1C). A 140-kDa protein detected under nonreducing conditions may represent a dimerized form. We observed no molecular mass shift between reducing and nonreducing conditions of the presumptive processed C-32 form of the

protein. This finding implies that the 32-kDa C-fragment is present as a monomer in zebrafish testes and not as the expected cysteine-bridged dimer typically seen in the TGFβ class of protein (IPR021203; http://www.ebi.ac.uk/interpro).

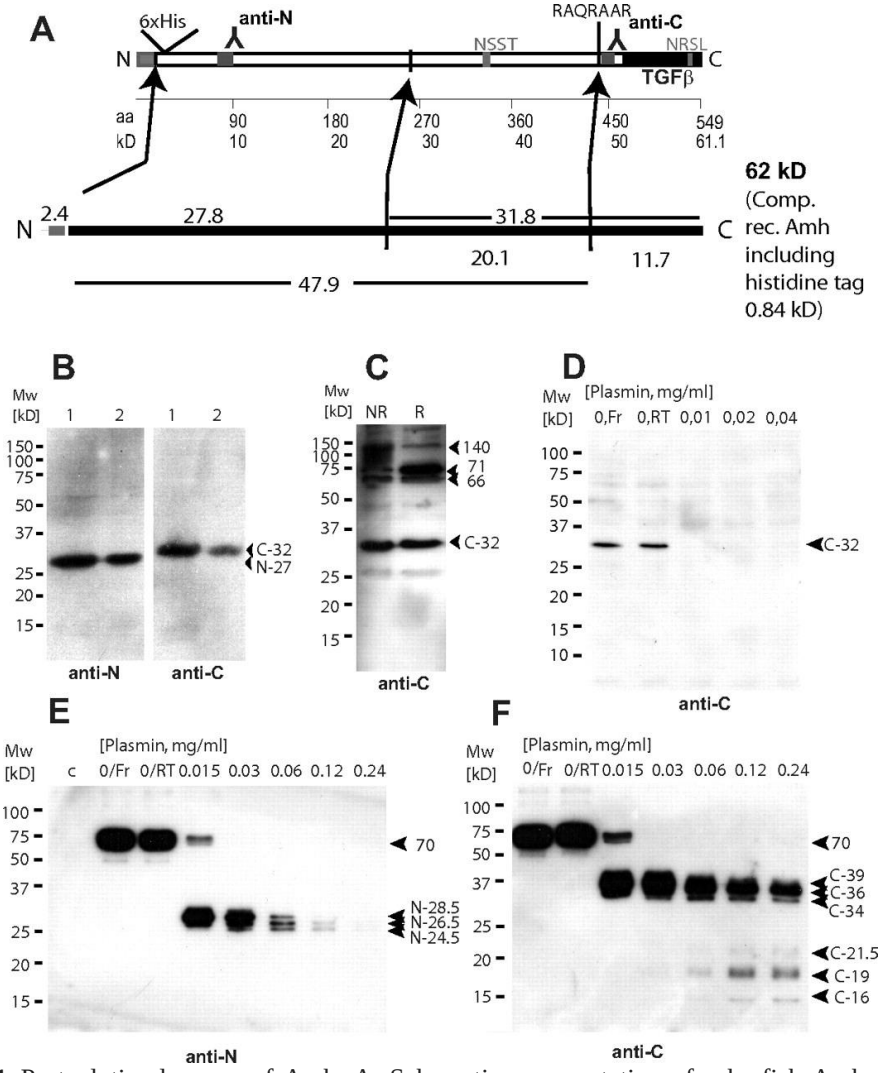

Fig. 1. Proteolytic cleavage of Amh. A, Schematic representation of zebrafish Amh with predicted and experimental cleavage products. Positions of N-terminal leader sequence, peptides used to generate antisera, possible glycosylation sites, and the conserved structural TGFβ domain are indicated. Testis extracts (B–D) and recombinant Amh (E and F) were subjected to immunoblotting with antibodies anti-N (B, *left panel*, and E) and anti-C (B, *right panel*, C, D, and F). Extracts of testes from adult zebrafish males were

homogenized in Ringer solution (extracts 1 and 2; B) or prepared in lysis buffer (C) under reducing (B and C, lane R) or nonreducing conditions (C, lane NR). Testis extracts (D) and concentrated (22×) medium from HEK293 cells secreting recombinant zebrafish Amh (E and F) were cleaved with increasing concentrations of plasmin indicated in milligrams per milliliter. Controls without plasmin are indicated as immediately frozen (0/Fr) or room temperature incubated (0/RT). The c lane (E) contains concentrated (20.5×) medium from nontransfected cells. Testes protein extracts 1 and 2 were made from 5.5- and 12-month-old fish in B and 9-month-old fish in C and D. *Arrows* indicate detected precursor protein and processed forms in kilodaltons. Migration of molecular mass standards are indicated to the *left* in kilodaltons.

Recombinant zebrafish Amh

Recombinant Amh (wild-type sequence) produced in HEK293 cells was recognized as a 70-kDa precursor in cells lysates and in concentrated medium by the two specific antibodies anti-N and anti-C (see Fig. 1, E and F). Treatment with plasmin, a serine protease that cleaves after arginine or lysine (9), gave three cleavage products from the N terminus (N-24.5-26.5-28.5), whereas the C-terminal antibody detected three matching products (C-34-36-39) (Fig. 1, E and F). Increased plasmin concentrations produced several less abundant C-fragments (C-16-19-21.5), all larger than the predicted C-product of 11.7 kDa assuming TGFβ class of maturation (Fig. 1A and Supplemental Fig. 1C).

Amh in testis extracts from zebrafish was apparently cleaved by an endogenious enzyme to give the C-terminal 32-kDa protein. This fragment was susceptible to plasmin treatment, because it was degraded even at low protease concentration and no degradation products were observed (see Fig. 1D).

Recombinant zebrafish Amh optimized for downstream processing

To produce a biologically active recombinant zebrafish Amh designed for simple purification and use in functional experiments, a

strategy used with human recombinant AMH (47) was adapted. The putative protease cleavage motif RAQR at aa position 439–442 was changed to a RARR motif, and a histidine tag was inserted just before proline at position 33 (similar to 47). Medium from stably transfected HEK293 cells producing His-Amh-Q441R revealed both the apparent 70-kDa precursor form and different processed forms (Fig. 2A). Nonreducing conditions gave a 140-kDa protein, suggesting a dimerized form of the 70-kDa protein. A 50-kDa protein (N-50) was detected with anti-N corresponding to the predicted 48-kDa product after cleavage at the RARR site (Fig. 2A). Also, additional fragments were detected, suggesting at least one additional cleavage site.

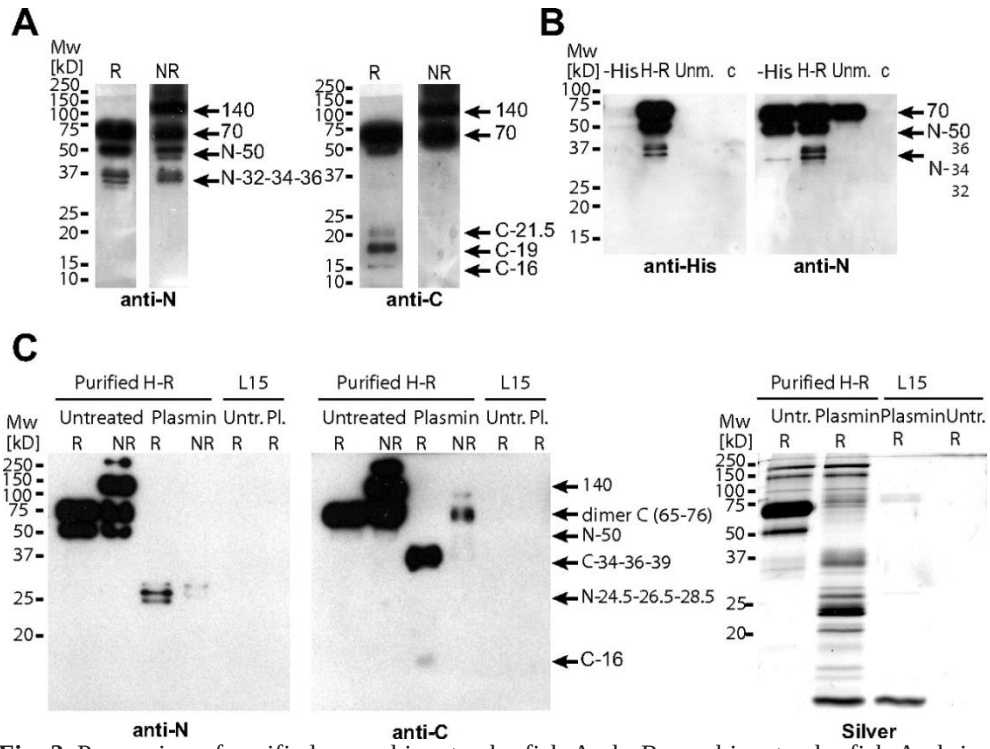

Fig. 2. Processing of purified recombinant zebrafish Amh. Recombinant zebrafish Amh in up-concentrated cell culture medium (A and B) or as purified protein (C) were Western blotted and detected using anti-N, anti-C, or anti-His antibodies under reducing (R) or nonreducing (NR) conditions. Recombinant His-Amh-Q441R (R/H) was analyzed except in B, where unmodified recombinant Amh (Unm) or recombinant Amh with optimized cleavage site RARR but no histidine tag (−His) was included in addition to negative control

(c) culture medium from nontransfected HEK293 control cells. Purified Amh was treated *in vitro* with plasmin (C), untreated refer to no plasmin digestion and L15 represents no protein, *i.e*. purified fractions using culture medium as input during purification. Silver-stained gel (C, *right*) shows purified His-Amh-Q441R, untreated, and plasmin-treated compared with culture medium L15. Medium in A had been concentrated 32.5 times, whereas in B, the −His, R/H, Unm, and c-medium had been concentrated 20, 37.5, 21.4, and 27.3 times the initial volume, respectively.

Three low molecular mass fragments were detected with the C-terminal antibody at reducing conditions, which were similar to fragments seen after plasmin cleavage (compare Figs. 1F and 2A). The inserted histidine tag was recognized by an antihistidine antibody (Fig. 2B) and revealed a pattern similar to the anti-N antibody. The histidine tag was used for purification of the recombinant protein and revealed a 140-kDa possible dimer at nonreducing conditions and a major 70-kDa and a strong 50-kDa product also seen in a silver stained gel (Fig. 2C). Plasmin treatment produced three fragments similar to unmodified recombinant Amh (Fig. 1, E and F), N-24.5-26.5-28.5 detected with anti-N, whereas anti-C detected C-34-36-39 plus a weak C-16. Interestingly, the C-terminal fragments shifted to a higher molecular mass at nonreducing conditions, and C-16 was only detected at reducing conditions (Fig. 2C). The above results show that some of the 70-kDa full-length and the C-terminal C-34-36-39 plasmin products produce putative homodimers linked by a disulfide bridge in the C-terminal half of the protein (Fig. 2C).

Identification of signal peptide and possible site of proteolytic cleavage

The predicted 21-aa leader sequence (Fig. 1 and Supplemental Fig. 1) was verified by N-terminal sequencing (Edman degradation) of purified 70-kDa zebrafish His-Amh. Identification of the six first aa showed that the

signal peptide had been cleaved off between aa C21 and A22 (see Supplemental Figs. 1 and 2A).

Two products from plasmin-treated recombinant Amh, N-28.5 and C-36, were analyzed by mass spectrometry to reveal the cleavage site (Supplemental Fig. 2B). Aligning the fragments from the mass spectrometry analysis indicated cleavage after K269 or R270 in the sequence of the modified protein (K263 or R264 in the native Amh). Theoretically, this cleavage should give an N-fragment of 27.8 kDa (27 kDa without histidine tag) and a C-fragment of 31.8 kDa (Fig. 1 and Supplemental Fig 1).

Zebrafish Amh is glycosylated in human cultured cells but not in zebrafish testes

Mammalian Amh is glycosylated, and two N-glycosylation sites were predicted in the zebrafish protein (Supplemental Fig. 1). In HEK293 cells, recombinant Amh colocalized with disulfide isomerase to the endoplasmic reticulum, which is necessary for the secretory pathway and glycosylation (Supplemental Fig. 3). To examine glycosylation, purified recombinant and endogenous zebrafish Amh were subjected to enzymatic deglycosylation (Fig. 3). Size analysis showed that recombinant Amh was reduced by approximately 5 kDa after treatment with the N-deglycosylation enzyme (anti-N; Fig. 3A). Plasmin fragmentation and immunoblotting revealed both N- and possibly also O-glycosylation but only in the C-terminal half of the protein. The results are in agreement with glycosylation taking place at the conserved NSST site at position 340–343 and possibly at the NRSL site at position 516–519 and that Amh is proteolytically cleaved at KRH263–265 as suggested (Fig. 3). Similar enzyme treatment had no

effect on the molecular masses of the endogenous Amh, suggesting that it is not glycosylated (Fig. 3B).

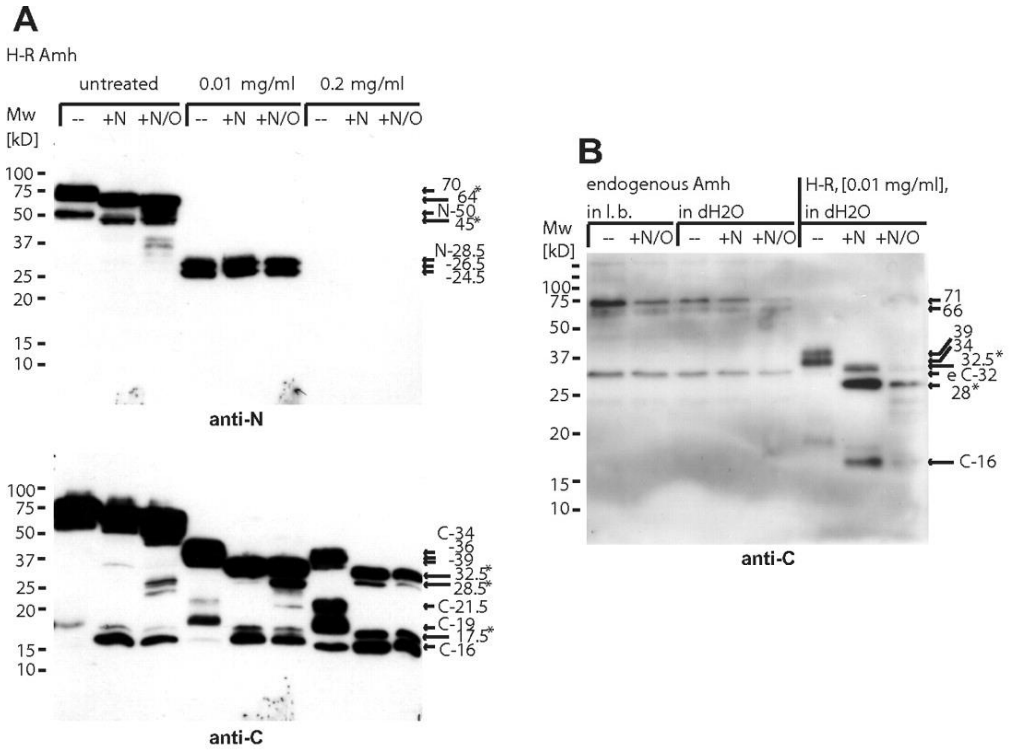

Fig. 3. Glycosylation analyses of Amh. Purified His-Amh-Q441R (A) and endogenous Amh in testes extracts (B) treated with N-deglycosidase (+N) or with N and O-deglycosidases in combination (+N/O) analyzed with immunoblotting using anti-N (A) and anti-C (A and B). Molecular mass shifts are indicated with *asterisks* and fragment sizes in kilodaltons. Recombinant Amh had either been proteolytically cleaved with plasmin (0.01 or 0.2 mg/ml) or were untreated. l.b., Lysis buffer; R/H, His-Amh-Q441R; e, endogenous.

Expression and localization of endogenous Amh and biological activity of recombinant zebrafish Amh

In males, *amh* mRNA levels increased approximately 80-fold from 4 to 8 wpf and another approximately 8-fold from 8 to 12 wpf (see figure 5A). In females, expression levels increased approximately 10-fold from 4 to 8 wpf but then remained constant (see figure 5A). In adult zebrafish testes,

Amh was detected in Sertoli cells surrounding early germ-cell generations, such as type A_{und} (Fig. 4, A–E) and type A differentiated (A_{diff}) spermatogonia (Fig. 4, F and G), the former often located near to the interstitial compartment (Fig. 4, B and C). The Amh-specific staining was much weaker or absent from Sertoli cells surrounding later stages of germ-cell development, such as type B spermatogonia, spermatocytes, and spermatids (Fig. 4, A, D, and F). Preabsorption of the antibody with the peptide fragment used to generate the antiserum abolished the staining (Supplemental Fig. 4), demonstrating the specificity of the immunocytochemical reaction.

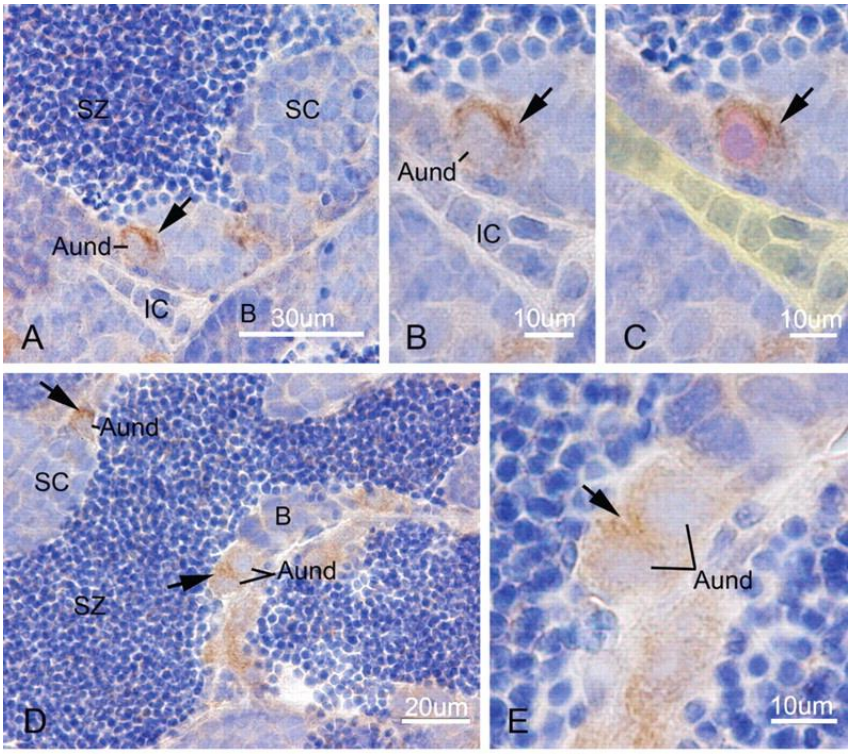

Fig. 4. Immunocytochemical localization of Amh on zebrafish testis sections. A, D, and F, Low magnifications show Amh in Sertoli cells surrounding early stages of germ-cell development (*arrows*), such as type A_{und} spermatogonia and type A_{diff} spermatogonia. Note that Amh staining was much weaker or absent from Sertoli cells surrounding further

advanced germ cells, such as type B spermatogonia (B) and spermatocytes (SC). Interstitial compartment (IC) and sperm (SZ) are also shown.

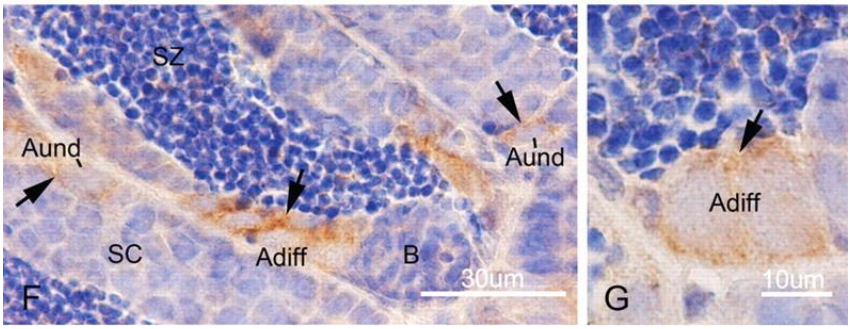

B, C, E, and G, High magnifications of Amh-positive Sertoli cells surrounding one (B and C) or two A_{und} spermatogonia (E), as well as a pair of A_{diff} spermatogonia (G). B and C, Nucleus (*blue*) and cytoplasm (*red*) of type A_{und} spermatogonia are colored in C to illustrate that Amh is restricted to the Sertoli cell cytoplasm. The interstitial compartment (IC) is colored *yellow*.

Testes from adult zebrafish were studied in a primary, short-term tissue culture system to investigate the effect of Amh on gonadotropin-stimulated androgen release. In zebrafish, the pituitary gonadotropin Fsh has a strong steroidogenic potency that exceeds the one of LH, and Leydig cells express the receptor for both gonadotropins, Lh and Fsh (44). Thus, the release of 11-KT, the major androgen in fish, was stimulated using recombinant zebrafish Fsh. Preincubation of zebrafish testes with purified plasmin-treated recombinant zebrafish Amh for 6 or 24 h significantly reduced, or abolished, respectively, Fsh-stimulated androgen release (Fig. 5B). When testing uncleaved recombinant Amh, Fsh-stimulated 11-KT production was not compromised (Fig. 5B, *to the right of dashed line*). Expression analysis revealed that the Fsh-induced up-regulation of *cyp17a1*, *star*, and *insl3* transcript levels was significantly reduced after 24 h of preincubation with Amh (Fig. 5C, Supplemental Fig. 5); expression of *ar* remained unaltered under all conditions. *amh* mRNA in testis tissue

cultures was down-regulated by Fsh treatment, independent of the steroidogenic activity of Fsh (Fig. 5, D and E). Increasing doses of 11-KT did not change *amh* mRNA levels significantly. Moreover, the down-regulatory effect of Fsh is possibly also independent of the cAMP/PKA pathway (Fig. 5, D and E).

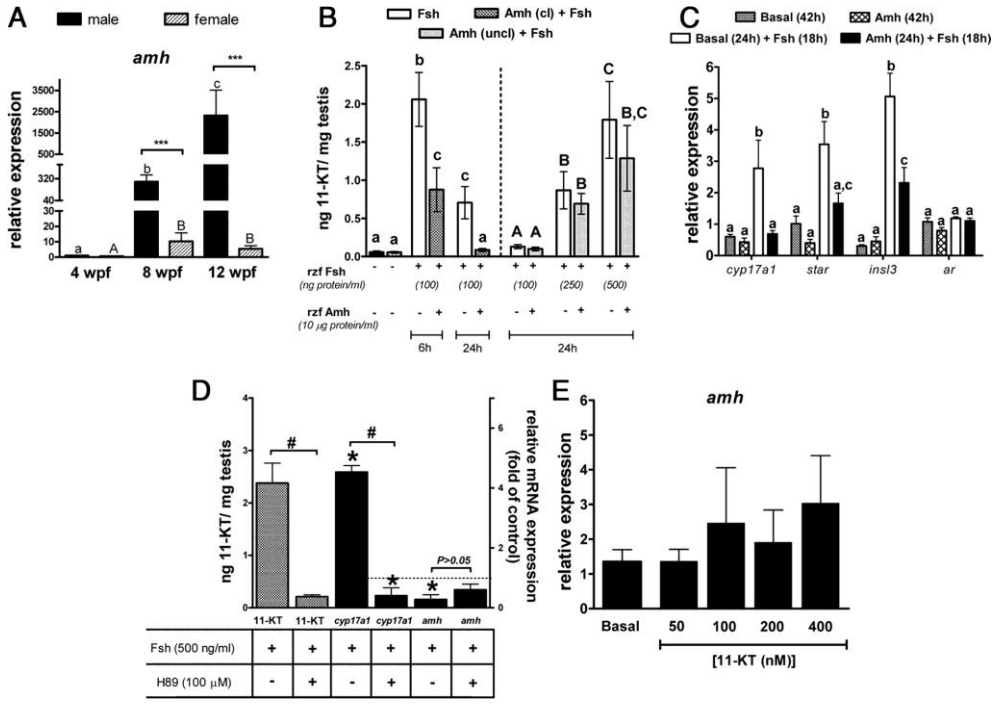

Fig. 5. Amh ontogeny, Amh role on androgen synthesis, and Amh endocrine regulation on zebrafish testes. A, Relative expression of *amh* during 4, 8, and 12 wpf of *vasa::egfp* zebrafish males and females. The individuals were selected according to their enhanced green fluorescent protein expression pattern and shape of the gonad. mRNA levels were determined by quantitative PCR, normalized to the levels of *18S* rRNA, and expressed as relative levels to the *amh* mRNA levels of 4-wpf males. *Bars* indicate mean ± SEM (4 wpf, n = 4♂/3♀; 8 wpf, n = 7♂/6♀; 12 wpf, n = 5♂/6♀). *Small and capital letters* indicate significant differences ($P < 0.05$) during the evaluated period for males and females, respectively. *Asterisks*indicate differences between males and females (***, $P <$ 0.001). B, *Bars* (mean ± SEM) represent the amounts of Fsh-induced 11-KT (ng/mg testis) release in the presence or absence of cleaved (cl) (*left*) or uncleaved (uncl) (*right*) His-Amh-Q441R (10 µg/ml) (rzfAmh) for 6 or 24 h of incubation. The biological activity of uncleaved Amh (to the *right of the vertical dotted line*) was tested using different concentrations (100, 250, and 500 ng/ml) of a different batches of recombinant zebrafish

Fsh (rzfFsh). *Different letters* denote significant differences ($P < 0.05$) between the different experimental groups. C, Relative mRNA expression of *cyp17a1*, *star*, *insl3*, and *ar* in testis tissue incubated in the absence of Amh and Fsh (Basal), in the presence of cleaved Amh (Amh 42 h), in the presence of Fsh (basal 24 h + Fsh 18 h), or preincubated with cleaved Amh before addition of Fsh (Amh 24 h + Fsh 18 h). Gene expression levels (mean ± SEM) were normalized to *18S* rRNA levels (Supplemental Fig. 5). *Different letters* denote significant differences ($P < 0.05$) between the different experimental groups. D, Fsh (500 ng/ml) effects on steroid release (11-KT, *left ordinate*), and mRNA levels of *cyp17a1*, and *amh* (*right ordinate*) in the presence of absence of 100 μM PKA inhibitor H89 for short-term incubation (24 h). *Bars* indicate mean ± SEM (n = 8 for 11-KT; n = 6 for gene expression) nanograms of 11-KT released per milligram of tissue, or fold induction of the control (without Fsh for Fsh only, or without H89 for Fsh + H89). The *dotted line* crossing the ordinate at 1 (*right axis*) indicates no stimulation. *Asterisks*denote significant differences ($P < 0.05$) between control and treated groups using a paired *t* test, whereas a *hash symbol* (#) indicates differences ($P < 0.05$) between Fsh only and Fsh + H89. The down-regulated levels of *amh* by Fsh did not change in the presence of H89 ($P > 0.05$). For each gene, mRNA levels were normalized with the geometric mean of the housekeeping genes (*18S*, *ef1*, and β-*actin*), calibrated with the PCR threshold values as δ CT mean value obtained from all samples, and expressed as fold induction of control. E, The effect of different concentrations of androgens (50, 100, 200, and 400 nM 11-KT) on zebrafish *amh* mRNA levels after 7 d of *in vitro* testis tissue culture. *Bars* (n = 21 for basal; n = 4 for 50 nM; n = 6 for 100 nM; n = 4 for 200 nM; n = 7 for 400 nM) indicate the relative expression of *amh* transcript levels (mean ± SEM), which were normalized to the *18S* rRNA levels. No significant difference ($P > 0.05$) of *amh* expression was found among the different concentrations of androgens.

To examine whether zebrafish Amh prevents androgen-stimulated adult spermatogenesis, akin to the inhibition of the onset of spermatogenesis described in juvenile Japanese eel (30), we incubated adult zebrafish testis tissue (45) for 7 d with 11-KT only (control), or with 11-KT and Amh. All stages of spermatogenesis were present (*i.e.* undifferentiated and differentiated type A spermatogonia, type B spermatogonia, spermatocytes, spermatids, and spermatozoa) (see Fig. 6, A, C, and E) in testes incubated with 11-KT only. Qualitatively, all these stages were also present after incubation with 11-KT and Amh. However, morphometric analysis revealed significant differences. The number of cysts with type A_{und} spermatogonia was higher in testis tissue exposed to Amh, whereas the number of cysts containing type B spermatogonia, spermatocytes, and spermatids was

significantly reduced (Fig. 6, A, D, and F). The increased number of type A_{und} spermatogonia can reflect a block of their differentiation, leading to their accumulation, or an increase in their proliferation. Therefore, we studied BrdU incorporation, which revealed a reduction of the BrdU-labeling index of A_{und}spermatogonia in the presence of Amh (Fig. 6B), excluding the possibility that Amh stimulated the proliferation of A_{und} spermatogonia. The inhibitory effect of Amh on 11-KT-induced proliferation of further advanced germ cells was reflected in the reduced number of BrdU-positive cysts in testis exposed to 11-KT and Amh (Fig. 6, D and F).

Quantitatively clearer results as regards spermatogonia type A_{und} were obtained when using testis tissue for primary cultures from males pretreated with estrogen *in vivo*. Previous studies showed that estrogen treatment blocked differentiation and reduced proliferation of A_{und} but also of A_{diff} spermatogonia (46). Spermatogonial proliferation and differentiation recovered from the estrogen-induced inhibition when testis tissue was cultured *ex vivo* under basal conditions, as indicated by the presence of clones of type B spermatogonia (Fig. 7B), a BrdU-labeling index of spermatogonia type A_{und} of 40% (Fig. 7C), and a high number of BrdU-positive germ cells (Fig. 7E), both single cells and differentiating clones of spermatogonia. This spontaneous recovery was suppressed in the presence of Amh: differentiating germ cells were rare and spermatogonia type A_{und} were frequently present (Fig. 7A), whereas their BrdU-labeling index was reduced more than 3-fold (Fig. 7B). In general, the number of BrdU-positive cells was lower (Fig. 7D). We conclude that Amh reduced proliferation and prevented differentiation of spermatogonia type A_{und}.

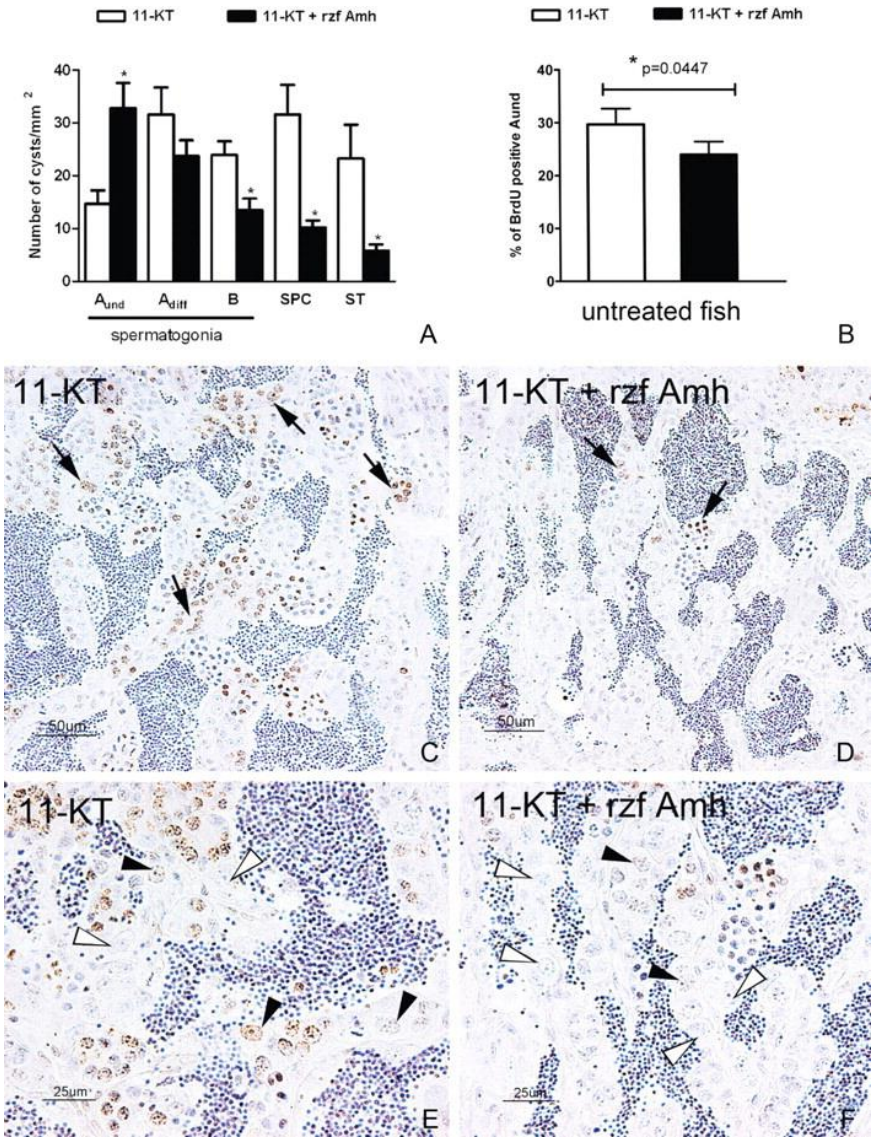

Fig. 6. Biological activity of recombinant zebrafish Amh (rzfAmh) on zebrafish spermatogenesis in testis tissue culture from untreated adult males. A,*Ex vivo* spermatogenesis supported by 11-KT (200 nM; *white bars*) was inhibited by Amh (10 µg/ml; *black bars*). *Bars* indicate the number (mean ±SEM) of cysts/mm^2 of testis containing type A_{und} spermatogonia, type A_{diff} spermatogonia, type B spermatogonia, spermatocytes (SC), and spermatids (ST). B, BrdU-labeling index of type A_{und} spermatogonia from zebrafish testes cultured for 7 d with 11-KT or 11-KT+Amh. *, Values are significantly different ($P < 0.05$) between 11-KT and 11-KT + Amh in A and B. C and D, Low magnifications of zebrafish testis sections immunostained for BrdU (*brown*) and counterstained with hematoxylin. Amh decreased the number of BrdU-positive spermatogenic cysts containing germ cells advanced beyond the stage of type A

spermatogonia (*arrows*) and led to an accumulation of type A_{und} spermatogonia. E and F, High magnifications illustrate that type A_{und} spermatogonia are often BrdU-positive (*black arrowheads*) in tissue incubated with 11-KT, whereas type A_{und}spermatogonia accumulated in the presence of Amh and were then often BrdU-negative (*white arrowheads*).

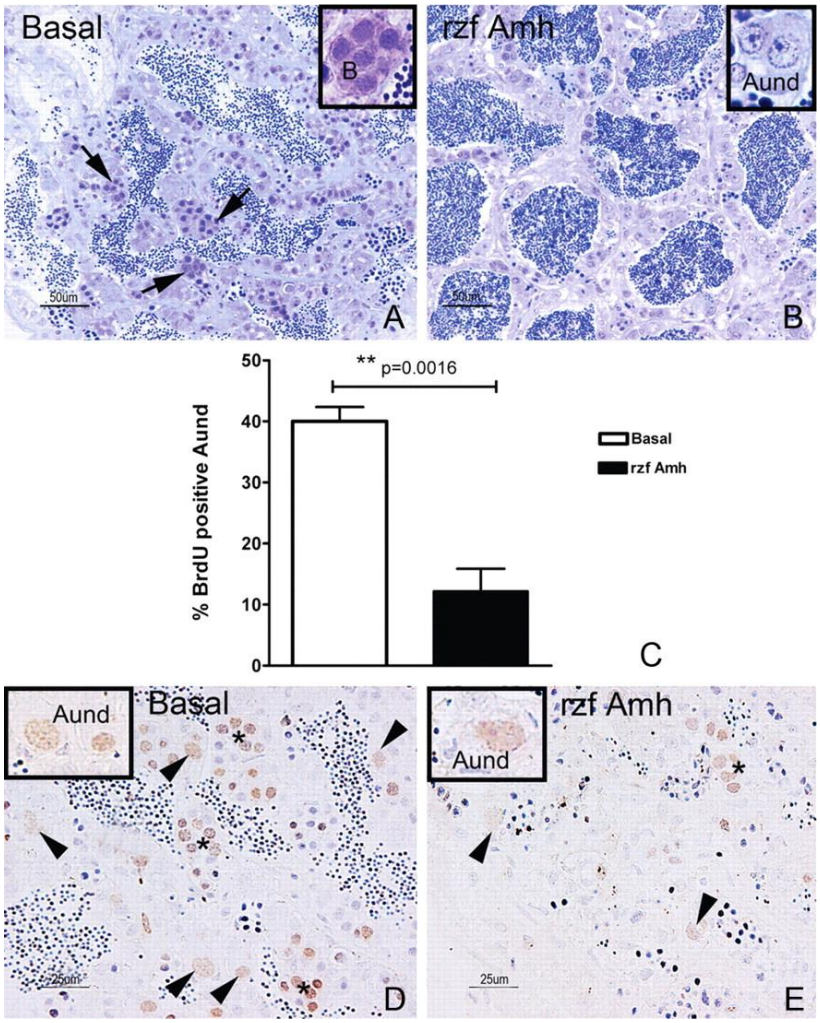

Fig. 7. Biological activity of recombinant zebrafish Amh (rzfAmh) on zebrafish spermatogenesis in testis tissue culture from estrogen pretreated adult males. A and B, Zebrafishtestis sections stained with toluidine blue from adult males, which were first exposed to estrogen *in vivo* to reduce spermatogonial proliferation and differentiation, before *ex vivo* incubation for 7 d with basal medium (A) or Amh (B). In the absence of estrogen, spermatogonial proliferation and differentiation recovered *ex vivo* (*arrows*) in basal medium (A) but not in the presence of Amh (B), where mainly of type A_{und} spermatogonia were found (*inset* in B), whereas several cysts of type B spermatogonia (B) were found in the testes incubated with basal medium (*inset* in A). C, Amh inhibited the proliferation of type A_{und} spermatogonia. *Bars* represent the % of BrdU-positive

A_{und} expressed as mean ±SEM; **, Values between Amh and basal are significantly different. D and E, Zebrafish testis sections immunostained for BrdU showed a decrease in the number of BrdU-positive cysts containing type A_{und} spermatogonia (*arrowheads*) and more advanced germ cells (*asterisks*) in Amh-treated tissue (E) compared with the basal condition (D).

DISCUSSION

This communication focuses on how Amh is processed to a biologically active protein and elucidating its functions in fish. Using zebrafish as model organism, Amh was analyzed in testes extracts and as recombinant protein. We found that zebrafish Amh, proteolytically cleaved to become fully active, near abolished Fsh-stimulated androgen production, inhibited spermatogenesis, and was down-regulated by Fsh but not by androgens.

Endogenous Amh

The endogenous zebrafish protein was detected as a N-27 and a C-32 fragment in contrast to processed endogenous rat Amh, reported to be 48 and 12 kDa, respectively, at reducing conditions (11). The eel homologue was detected as a 30-kDa protein in immature testes using an antiserum against the N-terminal 243 aa of the protein (30). This suggests that Amh is proteolytically processed both in mammals and fish but with different cleavage sites. In human Amh, the C-terminal fragment includes 109 aa and forms a homodimer (2), whereas the zebrafish protein C terminus extends over 280 residues and is a monomer. This is unusual for members of the TGFβ family, because dimerization of a C-terminal fragment is considered a general characteristic of this class of proteins (48). However, the recombinant variant of zebrafish Amh appeared as a disulfide linked dimer

in the range of 65–76 kDa and monomer size of 34, 36, and 39 kDa detected with C-terminal-directed antibodies.

Two endogenous precursor candidate proteins of 66 and 71 kDa were recognized with the anti-C antibody (Figs. 1C and 3B) and a possible dimer of 140 kDa at nonreducing conditions. The eel Amh is 60 kDa at reducing conditions and 120 kDa at nonreducing conditions due to disulfide bonding (37). Full-length zebrafish Amh consists of 549 aa, whereas full-length eel protein consists of 614 aa, coinciding with theoretical molecular masses of 58.7 and 62.6 kDa without signal peptides, respectively.

Proteolytic activation of zebrafish Amh differs from human Amh

Signal peptides of secreted proteins are cleaved off by signal peptidase in the endoplasmatic reticulum (ER) before secretion (49). N-terminal sequencing of the purified recombinant Amh verified cleavage of a 21-residue long signal peptide. The recombinant Amh was further located to ER in the HEK293 cells and colocalized with the ER-protein disulfide isomerase (Supplemental Fig. 3).

Zebrafish His-Amh-Q441R was designed to be *in vivo* processed in the HEK293 cells similar to modified mammalian Amh (47). Although mammalian Amh was cleaved at the optimized site only (47), we never detected the predicted C-terminal 11.7-kDa zebrafish fragment (Supplemental Fig. 1). The N-terminal-directed antibody detected a major 50-kDa protein and several weaker fragments (N-32-34-36). In addition, C-fragments (with C-19 as major product) were found. The pattern of fragments agrees with the occurrence of at least one extra cleavage of zebrafish Amh in HEK293 cells compared with modified human protein. Proteolytic activation of human AMH takes place by cleavage after residue

451 at RAQR/S, although a potential alternative cleavage may occur after R254 at PR/S (50). Human AMH with the optimized RARR451/S cleavage site is spontaneously cleaved in HEK293 cells to give a biologically active protein (51). The sequence variant RAQR451/R needed plasmin cleavage to be activated. Treating zebrafish Amh with plasmin resulted in a different cleavage pattern compared with human AMH, with preference for larger C-fragments than the reported bioactive 25-kDa human homodimer protein.

The predicted plasmin cleavage site (KR264/H) in zebrafish Amh (Supplemental Fig. 1) seems to be in a position similar to the secondary mammalian cleavage site (R254) (50).

Modification by glycosylation

Endogenous and recombinant Amh appeared as 70-kDa proteins, whereas sequence predictions suggested proteins of 58.7 and 59.6 kDa (excluding leader sequences), respectively. Glycosylation of the recombinant protein was evident in HEK293 cells and could explain much of the observed differences (Fig. 3A). The discrepancy between observed and theoretical molecular mass of endogenous Amh remains unclear, because glycosylation was not detected (Fig. 3C). The *in vivo* function of glycosylation remain obscure, but studies of gonadotropins point at a general impact on improved secretion and stability (52, 53).

Deglycosylation of recombinant Amh C-terminal cleavage product C-34-36-39 yielded a 32-kDa product similar to the theoretical size and endogenous nonglycosylated Amh. This suggests that the verified cleavage site KR/H could be a natural cleavage site of zebrafish Amh yielding a 27-kDa N-fragment and a 32-kDa C-fragment. Endogenous protease(s), which have Amh as natural substrate, is/are not known. However, proprotein

convertase 5 has been suggested as the natural protease in rat (11). The proprotein convertases 1 (enzyme commission number 3.4.21.93) and 2 (enzyme commission number 3.4.21.94) cleave proteins at KR-X sites. Further investigations will have to reveal if these proteases are present in zebrafish testes and if they can cleave zebrafish Amh.

Zebrafish Amh, monomer, or dimer?

Based on the gel patterns of recombinant zebrafish Amh under reducing and nonreducing conditions (Fig. 2C), it seems that a cysteine close to the C terminus is involved in dimerization of the protein. The N-terminal fragments failed to form homodimers, in contrast to human AMH (Fig. 4C) (9). Homodimerization of the recombinant Amh C-peptide correlates well to data on mammalian AMH (9) but disagrees with our observation that the endogenous C-32 is present as a monomer in zebrafish testes. Japanese eel Amh was detected as a 120-kDa cysteine-bridged dimer in its full-length form in testes extracts but the cysteine-bridge where absent in a 30-kDa N-terminal part in the recombinant eel Amh variant, suggesting a similar organization as for the recombinant zebrafish Amh (30). The human Amh required cleavage for biological activity to generate the active C-terminal 25-kDa homodimer, the N-terminal part remains in the complex and enhances receptor binding but is lost during receptor activation (16).

Cleaved Amh inhibits Fsh-stimulated androgen production and inhibits spermatogenesis

Teleost fish lack Müllerian ducts but nevertheless express Amh, suggesting that other than the namesake functions can be investigated in fish. In mammals, AMH inhibited Leydig cell differentiation and LH-

stimulated androgen release (27, 43, 54). Our studies revealed for the first time in a lower vertebrate a suppressive role of Amh on gonadotropin-stimulated Leydig cell gene expression (*star*, *insl3*, and *cyp17a1*) and androgen release (Fig. 5). *In vivo* (55) and *in vitro* (27) experiments demonstrated that Amh inhibition of testosterone production also in rodents involved reduced *Cyp17* expression, and low levels of testosterone in Amh-overexpressing mice coincided with decreased expression of steroidogenic genes (21). We conclude that Amh-mediated down-regulation of *star* and *cyp17a1* in Leydig cells is dominant over stimulatory effects of steroidogenic gonadotropin on the expression of these genes and is an evolutionary conserved function of Amh.

Amh reduced Fsh-induced increases in *insl3* mRNA levels. In mammals, INSL3 is required for the testicular descent in embryonic life and acts as a male germ-cell survival factor in adults (56, 57). Transcription factors such as steroidogenic factor 1 and NUR77 (a nuclear receptor subfamily 4 group A member 1) regulate certain steroidogenic enzyme-encoding genes and regulate the *INSL3* promoter in mouse, rat, and humans (58). Hence, although there is no mechanistic information regarding *insl3* regulation in zebrafish, we speculate that Amh modulates *insl3* expression via reduced androgen production.

Amh transcripts are present in Sertoli cells in fish (31, 58). Our work verified this for the first time at the protein level (Fig. 4). Amh was prominently present in Sertoli cells around early spermatogonia, close to the interstitial area, which fits well to other observations we have made on the location of stem cell candidates in the testis (59). Because Sertoli cells contacting later germ-cell generations showed little/no Amh protein, Amh

function may be related to spermatogonial stages of germ-cell development, especially type A spermatogonia.

In prepubertal Japanese eel, Amh inhibited the 11-KT-induced proliferation of type B spermatogonia, thereby inhibiting the onset of spermatogenesis (30). This is in line with AmhrII loss-of-function experiments in medaka that resulted in a germ-cell overproliferation phenotype (42). Our observations verify this in a third and unrelated order of teleost fish, suggesting that Amh-mediated inhibition of spermatogenesis may be a typical aspect of Amh action in fish. In addition, we report for the first time on effects of Amh on adult spermatogenesis. BrdU incorporation analysis showed that although Amh reduced the mitotic index of type A_{und} spermatogonia, that are the germ-cell population containing the spermatogonial stem cells (59), still the number of type A_{und} spermatogonia increased. This apparent contradiction can be explained by the Amh-mediated block of the further differentiation of the slowly (*viz.* low mitotic index) accumulating type A_{und} spermatogonia. Inhibiting differentiation of type A_{und} spermatogonia would also explain the decreased number of more differentiated germ cells observed after Amh exposure. The present data, however, do not allow excluding an independent effect of Amh on later germ-cell stages. Taken together, our studies provide direct evidence for an inhibitory effect of Amh on the proliferation of type A_{und} spermatogonia and moreover for a block of their differentiation. Hence, type A_{und}spermatogonia accumulate while rapidly proliferating type B spermatogonia (and later stages of spermatogenesis) become depleted. In rat testis, the highest levels of expression of AMH and its receptor are in Sertoli cells in epithelial stage VII (60), postulating a relation between AMH signaling and the low mitotic activity of spermatogonia in stage VII. It might therefore be interesting to

examine experimentally the possibility that AMH modulates proliferation/differentiation of spermatogonia also in adult mammals.

Sertoli cell *AMH* expression is high before puberty in mammals (2), is up-regulated by FSH (25), and greatly reduced at the pubertal increase in androgen levels and Sertoli cell androgen receptor expression (2). In zebrafish, however, *amh* expression progressively increased with puberty and adulthood. Two related observations seem important in this regard. First the Amh protein level is high in Sertoli cells contacting type A spermatogonia. And second, these Sertoli cells are not terminally differentiated in fish. Therefore, increasing *amh* expression during ontogenesis can be explained with the increase in the number of spermatogenic cysts containing type A spermatogonia that accompanies pubertal testis growth and the further development toward adulthood (61).

Amh expression patterns during ontogenesis change differently in mammals *vs*. zebrafish and may reflect differences in the regulation of expression. In mammals, Fsh-stimulated androgen hormone excretion and inhibits *Amh* expression, whereas in zebrafish Fsh, down-regulated *amh* expression and androgens had no significant effect. For androgens, we speculate that the cystic mode of spermatogenesis in fish, characterized by undifferentiated Sertoli cells in contact with type A spermatogonia (*i.e*. showing high levels of Amh) also in the adult testis, is a situation incompatible with a mechanism where the pubertal increase in androgen production would induce a testis-wide down-regulation of *amh* expression. The down-regulation triggered by zebrafish Fsh contrasts with the up-regulation observed in mammals (25). We have not examined if cAMP is required in zebrafish in this context, but PKA signaling appears to be of minor relevance. Fsh-mediated down-regulation of *amh* expression fits well

into the spectrum of biological activities of Amh. Two aspects are relevant in this context, namely that Fsh is a potent steroidogenic hormone in fish (58), including zebrafish (44), and that unpublished work in our laboratory shows that the proliferation/differentiation of spermatogonia is stimulated by Fsh in testis tissue culture in an androgen-independent manner (Nobrega, R. H., and R. W. Schulz, unpublished data). Both these effects of Fsh would be counteracted by Amh, so that Fsh-mediated down-regulation of *amh* expression seems an integral component of Fsh-mediated stimulation of zebrafish testis functions.

Despite the different regulatory mechanisms, reduced Amh signaling may permit germ-cell development both in fish (continuously occurring after puberty on the level of individual spermatogenic cysts) and mammals (occurring as a testis-wide event during puberty) and could be the second aspect of evolutionary conserved Amh bioactivity across vertebrates.

The biological activities of Amh in zebrafish are summarized graphically in Fig. 8. Amh effects in zebrafish are consistent with keeping germ cells in an immature state of development. In view of the Fsh-mediated suppression of Amh, we predict that Sertoli cells expressing high levels of Amh may have a limited responsiveness to Fsh. In Leydig cells, Amh inhibits androgen production, so that in the vicinity of Sertoli cells expressing high levels of Amh (*i.e*. contacting type A spermatogonia), androgen levels may be locally lower, resulting in an area were germ-cell differentiation is less likely to occur. In Sertoli cells, yet elusive signaling mechanisms would be activated in response to Amh to prevent differentiation of early spermatogonial generations (Fig. 8). When Sertoli cells expressing high levels of Amh become responsive to Fsh, Amh would be down-regulated, thereby permitting Fsh to stimulate germ-cell

proliferation/differentiation and androgen production. For future work, several aspects are of interest, such as the biological activity of fish Amh as monomeric protein; information on the signaling systems used by Amh to modulate steroidogenesis via Leydig cells, and spermatogenesis via Sertoli cells; or finally, the integration of the mainly inhibitory Amh signaling with presumably existing, stimulatory signaling to achieve a coordinated regulation of testis functions.

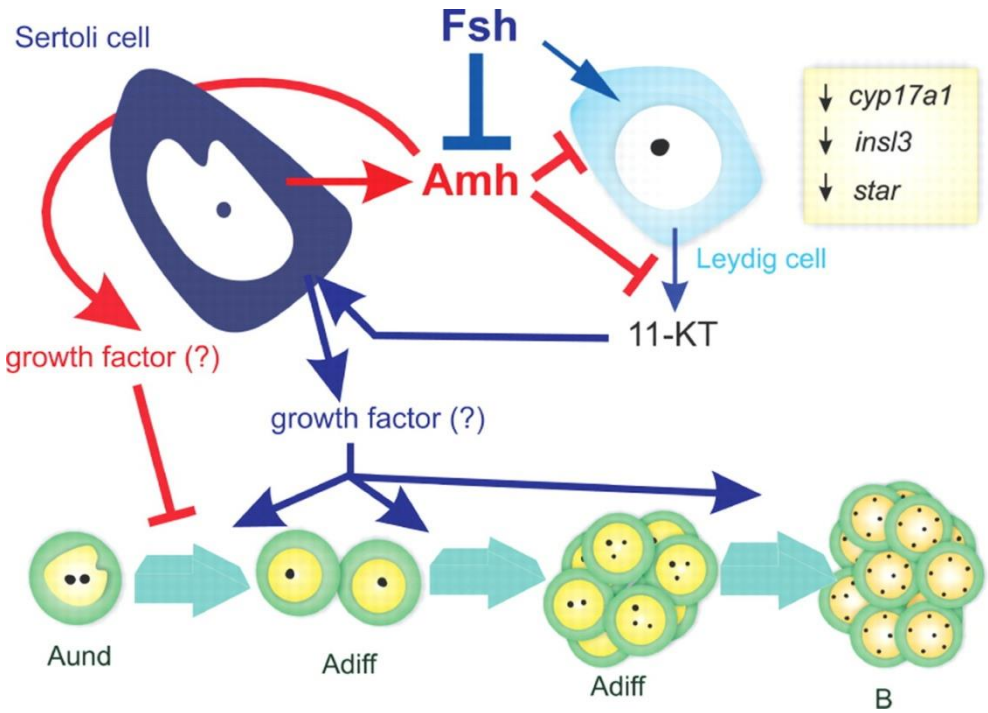

Fig. 8. Amh effects on zebrafish testis functions. Fsh stimulates Leydig cell androgen (11-KT) release but down-regulates Amh expression in Sertoli cells, whereas Amh suppresses Leydig cell androgen (11-KT) production by decreasing the expression of key genes involved in androgen biosynthesis, such as *star* and *cyp17a1*, also in the presence of Fsh. In the absence of Amh, androgens stimulate germ-cell differentiation from type A_{und} spermatogonia into type A_{diff} spermatogonia, and type B spermatogonia (B). The suppressive role of Amh on steroidogenesis might have secondary effects on the expression of other Leydig cell genes, such as *insl3* (partially down-regulated). Similar to the mammalian testis, Amh receptors are expressed by Sertoli cells but not by germ cells in fish (22), so that an autocrine Amh loop might trigger a downstream signaling mechanism in Sertoli cells, which would prevent early spermatogonial differentiation. On the other hand, when Sertoli cells expressing high levels of Amh respond to Fsh, Amh-mediated inhibition

of germ-cell development and androgen production would wane, whereas Fsh-stimulated androgen and possibly growth factor release would stimulate the progression of germ cells toward meiosis.

Abbreviations:

aa	Amino acid
A_{diff}	A differentiated
ALK	activin-receptor kinase
Amh	anti-Müllerian hormone
AmhRII	Amh type II transmembrane receptor
ar	*androgen receptor*
A_{und}	A undifferentiated
BrdU	bromodeoxyuridine
cyp17a1	*cytochrome P450, family 17, subfamily A, polypeptide 1*
ER	endoplasmatic reticulum
HEK293	human embryonic kidney 293
insl3	*insulin-like 3*
11-KT	11-ketotestosterone
PKA	protein kinase A
star	*steroidogenic acute regulatory protein*
wpf	week postfertilization.

Acknowledgments
We thank M. Niere for the help in establishing permanently transfected; W. Telle, E. Langelandsvik, and D. Jensen for excellent technical assistance; Wytske van Dijk and Caaj Douwe Greebe for technical assistance during the *in vitro* Amh biological studies and radio immunoassays; Fernanda Loureiro de Almeida for performing the negative controls of the immunocytochemistry reactions; and Henk Schriek and Co Rootselaar for assistance during the *in vivo* experiments and maintaining the zebrafish stocks.

This work was supported by the Norwegian Research Council Project no. 159045, theEuropean Union LIFECYCLE project no. FP7-222719, and the National Council for Scientific and Technological Development (R.H.N.).
Disclosure Summary: The authors have nothing to disclose.

REFERENCES

1. Moustakas A, Pardali K, Gaal A, Heldin CH 2002 Mechanisms of TGF-beta signaling in regulation of cell growth and differentiation. Immunol Lett 82:85-91

2. Josso N 1986 Anti-mullerian hormone. Clin Endocrinol (Oxf) 25:331-345

3. Josso N 2008 Professor Alfred Jost: the builder of modern sex differentiation. Sex Dev 2:55-63

4. Picard JY, Tran D, Josso N 1978 Biosynthesis of labelled anti-mullerian hormone by fetal testes: evidence for the glycoprotein nature of the hormone and for its disulfide-bonded structure. Mol Cell Endocrinol 12:17-30

5. Picard JY, Josso N 1984 Purification of testicular anti-Mullerian hormone allowing direct visualization of the pure glycoprotein and determination of yield and purification factor. Mol Cell Endocrinol 34:23-29

6. Picard JY, Goulut C, Bourrillon R, Josso N 1986 Biochemical analysis of bovine testicular anti-Mullerian hormone. FEBS Lett 195:73-76

7. Cate RL, Mattaliano RJ, Hession C, Tizard R, Farber NM, Cheung A, Ninfa EG, Frey AZ, Gash DJ, Chow EP, et al. 1986 Isolation of the bovine and human genes for Mullerian inhibiting substance and expression of the human gene in animal cells. Cell 45:685-698

8. Pepinsky RB, Sinclair LK, Chow EP, Mattaliano RJ, Manganaro TF, Donahoe PK, Cate RL 1988 Proteolytic processing of mullerian inhibiting substance produces a transforming growth factor-beta-like fragment. J Biol Chem 263:18961-18964

9. MacLaughlin DT, Hudson PL, Graciano AL, Kenneally MK, Ragin RC, Manganaro TF, Donahoe PK 1992 Mullerian duct regression and antiproliferative bioactivities of mullerian inhibiting substance reside in its carboxy-terminal domain. Endocrinology 131:291-296

10. Nachtigal MW, Ingraham HA 1996 Bioactivation of Mullerian inhibiting substance during gonadal development by a kex2/subtilisin-like endoprotease. Proc Natl Acad Sci U S A 93:7711-7716

11. Lee MM, Donahoe PK 1993 Mullerian inhibiting substance: a gonadal hormone with multiple functions. Endocr Rev 14:152-164

12. Neeper M, Lowe R, Galuska S, Hofmann KJ, Smith RG, Elbrecht A 1996 Molecular cloning of an avian anti-Mullerian hormone homologue. Gene 176:203-209

13. Wilson CA, di Clemente N, Ehrenfels C, Pepinsky RB, Josso N, Vigier B, Cate RL 1993 Mullerian inhibiting substance requires its N-terminal domain for maintenance of biological activity, a novel finding within the transforming growth factor-beta superfamily. Mol Endocrinol 7:247-257

14. Rey R, Lukas-Croisier C, Lasala C, Bedecarras P 2003 AMH/MIS: what we know already about the gene, the protein and its regulation. Mol Cell Endocrinol 211:21-31

15. Vitt UA, Hsu SY, Hsueh AJ 2001 Evolution and classification of cystine knot-containing hormones and related extracellular signaling molecules. Mol Endocrinol 15:681-694

16. di Clemente N, Jamin SP, Lugovskoy A, Carmillo P, Ehrenfels C, Picard JY, Whitty A, Josso N, Pepinsky RB, Cate RL 2010 Processing of anti-mullerian hormone regulates receptor activation by a mechanism distinct from TGF-{beta}. Mol Endocrinol 24:2193-2206

17. Josso N, diClemente N 2003 Transduction pathway of anti-Mullerian hormone, a sex-specific member of the TGF-beta family. Trends Endocrinol Metab 14:91-97

18. Visser JA 2003 AMH signaling: from receptor to target gene. Mol Cell Endocrinol 211:65-73

19. di Clemente N, Josso N, Gouedard L, Belville C 2003 Components of the anti-Mullerian hormone signaling pathway in gonads. Mol Cell Endocrinol 211:9-14

20. Baarends WM, van Helmond MJ, Post M, van der Schoot PJ, Hoogerbrugge JW, de Winter JP, Uilenbroek JT, Karels B, Wilming LG, Meijers JH, et al. 1994 A novel member of the transmembrane serine/threonine kinase receptor family is specifically expressed in the gonads and in mesenchymal cells adjacent to the mullerian duct. Development 120:189-197

21. Racine C, Rey R, Forest MG, Louis F, Ferre A, Huhtaniemi I, Josso N, di Clemente N 1998 Receptors for anti-mullerian hormone on Leydig cells are responsible for its effects on steroidogenesis and cell differentiation. Proc Natl Acad Sci U S A 95:594-599

22. Klüver N, Pfennig F, Pala I, Storch K, Schlieder M, Froschauer A, Gutzeit HO, Schartl M 2007 Differential expression of anti-Mullerian hormone (amh) and anti-Mullerian hormone receptor type II (amhrII) in the teleost medaka. Dev Dyn 236:271-281

23. Wu GC, Chiu PC, Lyu YS, Chang CF 2010 The expression of amh and amhr2 is associated with the development of gonadal tissue and sex change in the protandrous black porgy, *Acanthopagrus schlegeli*. Biol Reprod 83:443-453

24. Rey RA, Musse M, Venara M, Chemes HE 2009 Ontogeny of the androgen receptor expression in the fetal and postnatal testis: its relevance on Sertoli cell maturation and the onset of adult spermatogenesis. Microsc Res Tech 72:787-795

25. Behringer RR, Finegold MJ, Cate RL 1994 Mullerian-inhibiting substance function during mammalian sexual development. Cell 79:415-425

26. Wu X, Arumugam R, Baker SP, Lee MM 2005 Pubertal and adult Leydig cell function in Mullerian inhibiting substance-deficient mice. Endocrinology 146:589-595

27. Miura T, Miura C, Konda Y, Yamauchi K 2002 Spermatogenesis-preventing substance in Japanese eel. Development 129:2689-2697

28. Rodriguez-Mari A, Yan YL, Bremiller RA, Wilson C, Canestro C, Postlethwait JH 2005 Characterization and expression pattern of zebrafish Anti-Mullerian hormone (Amh)

relative to sox9a, sox9b, and cyp19a1a, during gonad development. Gene Expr Patterns 5:655-667

29. Schulz RW, Bogerd J, Male R, Ball J, Fenske M, Olsen LC, Tyler CR 2007 Estrogen-induced alterations in amh and dmrt1 expression signal for disruption in male sexual development in the zebrafish. Environ Sci Technol 41:6305-6310

30. Shirak A, Seroussi E, Cnaani A, Howe AE, Domokhovsky R, Zilberman N, Kocher TD, Hulata G, Ron M 2006 Amh and Dmrta2 genes map to tilapia (*Oreochromis spp.*) linkage group 23 within quantitative trait locus regions for sex determination. Genetics 174:1573-1581

31. Halm S, Rocha A, Miura T, Prat F, Zanuy S 2007 Anti-Mullerian hormone (AMH/AMH) in the European sea bass: its gene structure, regulatory elements, and the expression of alternatively-spliced isoforms. Gene 388:148-158

32. Pala I, Kluver N, Thorsteinsdottir S, Schartl M, Coelho MM 2008 Expression pattern of anti-Mullerian hormone (amh) in the hybrid fish complex of *Squalius alburnoides*. Gene 410:249-258

33. Fernandino JI, Hattori RS, Kimura H, Strussmann CA, Somoza GM 2008 Expression profile and estrogenic regulation of anti-Mullerian hormone during gonadal development in pejerrey *Odontesthes bonariensis*, a teleost fish with strong temperature-dependent sex determination. Dev Dyn 237:3192-3199

34. Vizziano D, Randuineau G, Baron D, Cauty C, Guiguen Y 2007 Characterization of early molecular sex differentiation in rainbow trout, *Oncorhynchus mykiss*. Dev Dyn 236:2198-2206

35. Rolland AD, Lareyre JJ, Goupil AS, Montfort J, Ricordel MJ, Esquerre D, Hugot K, Houlgatte R, Chalmel F, Le Gac F 2009 Expression profiling of rainbow trout testis development identifies evolutionary conserved genes involved in spermatogenesis. BMC Genomics 10:546

36. de Waal PP, Wang DS, Nijenhuis WA, Schulz RW, Bogerd J 2008 Functional characterization and expression analysis of the androgen receptor in zebrafish (*Danio rerio*) testis. Reproduction 136:225-234

37. Borg B 1994 Androgens in teleost fishes. Comp Biochem Physiol C - Pharmacol Toxicol & Endocrinol 109:219-245

38. Shiraishi E, Yoshinaga N, Miura T, Yokoi H, Wakamatsu Y, Abe S, Kitano T 2008 Mullerian inhibiting substance is required for germ cell proliferation during early gonadal differentiation in medaka (*Oryzias latipes*). Endocrinology 149:1813-1819

39. Morinaga C, Saito D, Nakamura S, Sasaki T, Asakawa S, Shimizu N, Mitani H, Furutani-Seiki M, Tanaka M, Kondoh H 2007 The hotei mutation of medaka in the anti-

Mullerian hormone receptor causes the dysregulation of germ cell and sexual development. Proc Natl Acad Sci U S A 104:9691-9696

40. Salva A, Hardy MP, Wu XF, Sottas CM, MacLaughlin DT, Donahoe PK, Lee MM 2004 Mullerian-inhibiting substance inhibits rat Leydig cell regeneration after ethylene dimethanesulphonate ablation. Biol Reprod 70:600-607

41. Garcia-Lopez A, de Jonge H, Nobrega RH, de Waal PP, van Dijk W, Hemrika W, Taranger GL, Bogerd J, Schulz RW 2010 Studies in zebrafish reveal unusual cellular expression patterns of gonadotropin receptor messenger ribonucleic acids in the testis and unexpected functional differentiation of the gonadotropins. Endocrinology 151:2349-2360

42. Leal MC, de Waal PP, Garcia-Lopez A, Chen SX, Bogerd J, Schulz RW 2009 Zebrafish primary testis tissue culture: an approach to study testis function ex vivo. Gen Comp Endocrinol 162:134-138

43. de Waal PP, Leal MC, Garcia-Lopez A, Liarte S, de Jonge H, Hinfray N, Brion F, Schulz RW, Bogerd J 2009 Oestrogen-induced androgen insufficiency results in a reduction of proliferation and differentiation of spermatogonia in the zebrafish testis. J Endocrinol 202:287-297

44. Weenen C, Laven JS, Von Bergh AR, Cranfield M, Groome NP, Visser JA, Kramer P, Fauser BC, Themmen AP 2004 Anti-Mullerian hormone expression pattern in the human ovary: potential implications for initial and cyclic follicle recruitment. Mol Hum Reprod 10:77-83

45. Daopin S, Piez KA, Ogawa Y, Davies DR 1992 Crystal Structure of Transforming Growth Factor-β2: An Unusual Fold for the Superfamily Science 257:369-373

46. Lodish H, Berk A, Zipursky SL, Matsudaira P, Baltimore D, Darnell J eds. 2000 Molecular Cell Biology. 4 ed. New York: Freeman

47. Ragin RC, Donahoe PK, Kenneally MK, Ahmad MF, MacLaughlin DT 1992 Human mullerian inhibiting substance: enhanced purification imparts biochemical stability and restores antiproliferative effects. Protein Expr Purif 3:236-245

48. Papakostas TD, Pieretti-Vanmarcke R, Nicolaou F, Thanos A, Trichonas G, Koufomichali X, Anago K, Donahoe PK, Teixeira J, Maclaughlin DT, Vavvas D 2010 Development of an efficiently cleaved, bioactive, highly pure FLAG-tagged recombinant human Mullerian Inhibiting Substance. Protein Expr Purif 70:32-38

49. Trbovich AM, Sluss PM, Laurich VM, O'Neill FH, MacLaughlin DT, Donahoe PK, Teixeira J 2001 Mullerian Inhibiting Substance lowers testosterone in luteinizing hormone-stimulated rodents. Proc Natl Acad Sci U S A 98:3393-3397

50. Sriraman V, Niu E, Matias JR, Donahoe PK, MacLaughlin DT, Hardy MP, Lee MM 2001 Mullerian inhibiting substance inhibits testosterone synthesis in adult rats. J Androl 22:750-758

51. Houk CP, Pearson EJ, Martinelle N, Donahoe PK, Teixeira J 2004 Feedback inhibition of steroidogenic acute regulatory protein expression in vitro and in vivo by androgens. Endocrinology 145:1269-1275

52. Ivell R, Bathgate RA 2002 Reproductive biology of the relaxin-like factor (RLF/INSL3). Biol Reprod 67:699-705

53. Tremblay JJ, Robert NM 2005 Role of nuclear receptors in INSL3 gene transcription in Leydig cells. Ann N Y Acad Sci 1061:183-189

54. Schulz RW, de Franca LR, Lareyre JJ, Le Gac F, Chiarini-Garcia H, Nobrega RH, Miura T 2010 Spermatogenesis in fish. Gen Comp Endocrinol 165:390-411

55. Nobrega RH, Greebe CD, van de Kant H, Bogerd J, de Franca LR, Schulz RW 2010 Spermatogonial stem cell niche and spermatogonial stem cell transplantation in zebrafish. PLoS One 5

56. Dolle C, Niere M, Lohndal E, Ziegler M 2010 Visualization of subcellular NAD pools and intra-organellar protein localization by poly-ADP-ribose formation. Cell Mol Life Sci 67:433-443

57. Heukeshoven J, Dernick R 1985 Simplified method for silver staining of proteins in polyacrylamide gels and the mechanism of silver staining. Electrophoresis 6:103-112

58. Dunn MJ 1999 Detection of Total Proteins on Western Blots of 2-D Polyacrylamide gels In: Link AJ ed. 2-D Proteome Analysis Protocols. Totowa, New Jersey: Humana Press; 319-329

59. Emanuelsson O, Brunak S, von Heijne G, Nielsen H 2007 Locating proteins in the cell using TargetP, SignalP and related tools. Nat Protoc 2:953-971

Supplemental Material

Supplemental Methods:

Preparation of protein extracts from zebrafish testes

Male zebrafish were anaesthetized in MESAB (0.25 g/l ethyl 3-aminobenzoate methanesulfonate) and decapitated. Testes (3-6) were dissected and immediately transferred to 0.3 ml of either cold Ringer solution (10 mM HEPES, pH 7,4, 3 mM KCl, 3mM NaCl, 3.5 mM MgCl2, 5 mM CaCl2,) or cold lysis buffer (15 mM HEPES pH 7,9, 50 mM KCl, 6.25 mM MgCl2, 5 % (v/v) glycerol, 0.1 % (v/v) Nonidet P40, 1 mM EDTA containing Complete Protease Inhibitor Cocktail, Roche). The testes were homogenised using a pellet pestle motor. The Ringer

homogenate was added to reducing SDS sample buffer, vortexed, boiled for 5 minutes and finally centrifuged at 12000 xg for 2 minutes and the supernatants were recovered. The lysis buffer-homogenate was centrifuged at 12000 xg, 15 minutes at 4 °C. The supernatant was recovered and added to reducing or non-reducing SDS sample buffer. Protein extracts were frozen at -20 °C until further analyses.

Recombinant zebrafish Amh-production

Zebrafish *amh* cDNA (AY721604) was cloned into a pcDNA3.1/V5/His-vector (Invitrogen). Mutations were introduced using QuickChange II Site-directed mutagenesis kit, Stratagene. The presumed cleavage site, based on the human sequence, was optimized changing the RAQR-motif at amino acid position 439-442 to an RARR-motif (1) replacing CAG (Glu) at position 1321-1323 to CGG (Arg) with primers 5'-CAGAAAGAGCCCGGCGAGCAGCGAG and 5'-CTCGCTGCTCGCCGGGCTCTTTCTG. A six histidine-tag was incorporated behind Pro33 (based on the hisitidine tag incorporation in human proline-30 by 1) using primers 5'-GAGCAGGACAACAACCATCACCATCACCATCACCCG AAGGTCAACCCG and 5'-CGGGTTGACCTTCGGGTGATGGTGATGGT GATGGTTGTTGTCCTGCTC. The identities of these mutants were verified by DNA sequencing. Human embryonic kidney (HEK293) were transfected using the calcium phosphate-method and selected for positive cells with G418 (PAA Laboratories, 0.55 mg/ml) 48 hours post transfection. Surviving colonies were picked and tested for recombinant Amh-production by immunocytochemistry and grown at 37 °C in a 5% CO2 in complete medium; Dulbecco's Modified Eagle's Medium (DMEM, Gibco), supplemented with 10 % v/v fetal bovine serum (FBS), and penicillin/streptomycin (BioWhittaker/Cambrex) containing 0.1 mg/ml G418. Cells were adapted to serum-free conditions, first for 24 hours with reduced serum (5%) following serum-free medium for four days incubation. At harvest, media were centrifuged for 2 minutes at 1000 xg to remove cell debris and then frozen at -20 °C until use. Medium was concentrated using Amicon Ultra Centrifugal Devices (Millipore), cutoff 5 kDa, following the manufacturer's recommendations. Samples for SDS-PAGE were added reducing or non-reducing SDS sample buffer while the remaining concentrated medium was frozen at -20 °C. Recombinant zebrafish Amh was purified from medium (70-80 ml) on a 1 ml HisTrap HP Nickel column, using Äkta Explorer system (GE Pharmacia) in 20 mM sodiumdihydrogen phosphate, pH 7.4, 0.2M NaCl, 20 mM imidazole and eluted by gradually increasing the imidazole concentration. Imidazole was removed with a PD10 column (GE), in Leibovitz-15 medium (Gibco) and the protein fraction was kept frozen at -80 °C until further use.

Enzyme treatment of Amh

Recombinant zebrafish Amh in concentrated cultured medium was treated with plasmin (0.015-0.24 mg/ml Sigma P1867) for 1 hour at room temperature. Testes protein extracts were homogenized in Ringer solution based on Tris-HCl (pH 8.5) to achieve optimal conditions for the enzyme and treated with plasmin (0.01-0.04 mg/ml) for 1 hour at room temperature. Reactions were stopped by adding SDS sample buffer and frozen at -20 °C. Purified recombinant His-Amh-Q441R protein to be tested for activity in organ cultures was cleaved using plasmin at concentrations 0.01 mg/ml and 0.2 mg/ml for 2 hours at room temperature. Protein had been diluted in 1x reaction buffer (50 mM sodium phosphate buffer pH 7). The reaction was stopped by adding cell culture tested Aprotinin (A3428, Sigma) at equal concentrations as plasmin and frozen at -80 °C until further use. For deglycosylation recombinant and endogenous zebrafish Amh were dialysed towards distilled water (Slide-A-Lyzer dialysis cassette, cutoff 10 kD, Pierce) and treated with N-deglycosylating PNGase F, and O-deglycosylating O-Glycosidase, Sialidase from the Enzymatic Carbo ReleaseTM Kit from QA-Bio (KE-DG01), following the manufacturer's recommendations.

Protein analysis

Sodium dodecyl sulphate polyacrylamide gel (12.5%) electrophoresis (SDS-PAGE) and immunoblotting with Immobilon-Psq –PVDF membrane (0.2 μm) were performed following standard procedures. Size standard was the Precision Plus Dual Colour and sizes are indicated in kD. Medium had been concentrated 20.5 times (control) and 22 times the volume (recombinant). The SDS-PAGE was performed with 12.5 % polyacrylamide gels, and the proteins were transferred to a 0.2 μm PVDF membrane. For N-terminal sequencing, fractions (300 μl) of untreated and plasmin-treated purified protein (approximately 0.15 mg/ml) from conditioned medium were acetone-precipitated (80% acetone, 3 hours). SDS-PAGE and immunoblotting was performed and the membrane was washed twice in distilled water and exposed to Coomassie stain for membranes (2). The N-terminal sequencing using Edman degradation method was performed by the Proteomics Facility, University of Leeds. Maldi-TOF analyses were performed by the staff at PROBE Proteomics Facility, University of Bergen. Acetone precipitated purified protein was used to prepare peptide-in-gel samples of plasmin-treated (0.01 μg/μl) and untreated Amh. Gels were fixed in 0.518 % (v/v) orto-phosphoric acid and stained with Colloidal/Wita Coomassie (34% (v/v) methanol, 1.29 M Ammonium sulphate, 0.518 % (v/v) Phosphoric acid, and 0.8 mM CBB G250) for 72 hours at room temperature with continuously shaking. Proteins were cut out of the gel and dried using the vacuum centrifugation.

Amh directed antibodies

Two rabbit antisera were produced. Anti-N was raised against aa 53-67 –

CVHRQQPTDQHATED- (AY721604) and anti-C, against aa 443-456 – AARADEDGPSASNQ located immediately downstream of the predicted proteolytic cleavage site. Antiserum and purified IgG were obtained from BioGenes, Germany. Western blot analysis were performed with zebrafish Amh anti-N and anti-C diluted primary antibodies 1:200 and mouse monoclonal anti-polyHis (H1029, Sigma) 1:3000. Secondary antibodies were horse peroxidase conjugated goat anti-rabbit IgG antibody (NA934V, Amersham) and sheep anti-mouse IgG (NA931V, Amersham) both diluted 1:2000. All blots were developed using Enhanced Chemiluminisence kit (ECL), Amersham. Silver staining of gels were performed as described in (3).

Immunocytochemistry of transfected HEK293 cells

HEK cells were transferred to cover slips pre-incubated with collagen (Sigma), 25 μg/ml in 0.1 M acetic acid. Immunocytochemistry was performed as described in (4). Antibodies were diluted in ordinary complete medium. The anti-C Amh specific primary antibody was diluted 1:100. The Alexafluor 594 goat anti-rabbit IgG secondary antibody (A11012, Invitrogen Molecular probes) was diluted 1:500. In addition, primary antibody against Protein Disulphide Isomerase (ab2792, Abcam) was diluted 1:200 and secondary antibody Alexafluor 488-conjugated anti-mouse IgG (A11029, Invitrogen Molecular probes) was diluted 1:1000. Nuclei were stained with DAPI present in the mounting solution (Vectashield).All samples were analysed using a Leica DMI6000 B, inverse fluorescence microscope using the Leica Application suite software.

Immunocytochemical detection of endogenous Amh protein in adult zebrafish testes

Testes of adult males were dissected and fixed in 4% buffered paraformaldehyde for 4 h, dehydrated in ethanol, embedded in paraffin and sectioned as described previously (5). Sections were submitted to standard immunocytochemistry procedures as described before (6). Before over night incubation with the primary antibody (Amh anti C, purified 1 mg/ml used in dillution 1:200 in 1% bovine serum albumin), slides were subjected to antigen retrieval in 10mM citrate buffer (pH 6.0) for 10 min (slides in 200 ml buffer, microwave set to 700W). The sections were counterstained with haematoxylin Gills #3 (Sigma). To evaluate the specificity of the immunocytochemistry reaction, the primary antibody (1mg/ml) was pre-incubated over night at 4 ºC with the peptide (5mg/ml) used to generate the antibody (Supplemental Fig. 4).

Biological activity of recombinant zebrafish Amh: effects on androgen release, and spermatogenesis in testis tissue culture

To study androgen release, both testes of 8 outbred males per condition were dissected and pre-incubated for 6 or 24 hrs with or without 10 µg/ml recombinant, plasmin-treated zebrafish His-Amh-Q441R. Then, to half of the testes (right or left of a given individual) incubations, recombinant zebrafish Fsh (100 ng/ml) was added to stimulate androgen release and the incubation was continued for another 18 hrs (as described in 7). This set-up resulted in the following conditions: 1. No Amh + no Fsh; 2. No Amh + Fsh; 3. Amh + no Fsh; 4. Amh + Fsh, where Amh had been present for either 6 or 24 hrs before Fsh was added. Eighteen hours after adding Fsh, incubation media were collected and analysed for 11-KT by radio-immuno assay as described before (7). Testis tissue was weighed to calculate 11-KT release as ng 11-KT/mg of testis tissue. The stimulatory effect of Fsh was calculated as fold-increase above basal androgen release (i.e. comparing androgen release from the two testes of one animal) and assessed statistically by a one sample paired t-test against the hypothetical value 1 (i.e. no stimulation), using Graph Pad Prism 4.0 (Graph Pad Software, Inc., San Diego, CA, USA, http://www.graphpad.com). The Fsh-induced fold-increases obtained in the presence or in the absence of Amh were compared by unpaired Student t-test. Next to plasmin-treated His-Amh-Q441R, we also tested His-Amh-Q441R before plasmin treatment with, however, only a single period (24 hrs) of His-Amh-Q441R pre-incubation before addition of Fsh.

To study spermatogenesis in tissue culture, testes were dissected from outbred adult zebrafish (n = 5-7) and cultured in parallel (i.e. one testis incubated under control, the contralateral one under experimental conditions), using a tissue culture system on agar blocks, as described previously (8). Two experiments were carried out. In the first experiment, one testis of each fish was incubated with 200 nM 11-KT (control condition), while the contralateral testis was incubated with 200 nM 11-KT and 10 µg/ml of plasmin-cleaved His-Amh-Q441R for 7 days. For the second experiment, adult males were exposed *in vivo* for three weeks to 10 nM of 17β-estradiol, as described previously (9) to reduce the spermatogonial proliferation and differentiation activity. The two testes of the oestrogen-treated males were then incubated in parallel in basal medium (control) as described previously, or in medium containing 10 µg/ml of plasmin-cleaved His-Amh-Q441R for 7days. During the last 6 hours of incubation, 50 µg/ml of 5-bromo-2-deoxyuridine (BrdU) was added to the medium. Testis tissue was fixed in methacarn or 4% buffered paraformaldehyde, dehydrated, sectioned and embedded in Technovit 7100 as described before (8). Sections were either stained with toluidine blue, or subjected to antigen retrieval and peroxidase blocking, before BrdU immunodetection, as previously described (10). In the first experiment, we counted spermatogenic cysts containing single, undifferentiated type A spermatogonia (Aund), differentiated type A spermatogonia (Adiff), type B spermatogonia (B), spermatocytes (SPC) or spermatids (ST) (see 5). Normalization took place by expressing the results as number of cysts per mm^2 of counted testis section surface. Moreover, we determined the BrdU-labelling index of

spermatogonia type Aund. In the second experiment, we also determined the BrdU-labelling index of spermatogonia type Aund, while testis morphology and BrdU incorporation in further advanced stages of germ cell development were examined qualitatively. Where appropriate, paired t-tests (GraphPad Prism 4.0) were carried out to calculate the statistical significance between the testes incubated with or without Amh, respectively.

Bioinformatic analyses

A leader sequence was predicted with SignalP version 3.0 (web-site: http://www.cbs.dtu.dk/services/SignalP/) using the hidden markov model (11). Glycosylation sites were predicted using NetNGlyc version 1.0 (web-site: http://www.cbs.dtu.dk/services/NetNGlyc/).
Theoretical molecular weights were estimated with ProtParam tool (web-site: http://au.expasy.org/tools/protparam.html). Alignment was conducted with the Cobalt Multiple Alignment tool, NCBI and T-COFFEE at Swiss Institute of Bioinformatics (http://tcoffee.vital-it.ch/cgi- bin/Tcoffee/tcoffee_cgi/index.cgi)

References

1. Weenen C, Laven JS, Von Bergh AR, Cranfield M, Groome NP, Visser JA, Kramer P, Fauser BC, Themmen AP 2004 Anti-Mullerian hormone expression pattern in the human ovary: potential implications for initial and cyclic follicle recruitment. Mol Hum Reprod 10:77-83

2. Dunn MJ 1999 Detection of Total Proteins on Western Blots of 2-D Polyacrylamide gels In: Link AJ ed. 2-D Proteome Analysis Protocols. Totowa, New Jersey: Humana Press; 319-329 Heukeshoven J, Dernick R 1985 Simplified method for silver staining of proteins in polyacrylamide gels and the mechanism of silver staining. Electrophoresis 6:103-112

3. Heukeshoven J, Dernick R 1985 Simplified method for silver staining of proteins in polyacrylamide gels and the mechanism of silver staining. Electrophoresis 6:103-112

4. Dolle C, Niere M, Lohndal E, Ziegler M 2010 Visualization of subcellular NAD pools and intra-organellar protein localization by poly-ADP-ribose formation. Cell Mol Life Sci 67:433-443

5. Leal MC, Cardoso ER, Nobrega RH, Batlouni SR, Bogerd J, Franca LR, Schulz RW 2009 Histological and stereological evaluation of zebrafish (Danio rerio) spermatogenesis with an emphasis on spermatogonial generations. Biol Reprod 81:177-187

6. Almeida FF, Kristoffersen C, Taranger GL, Schulz RW 2008 Spermatogenesis in Atlantic cod (Gadus morhua): a novel model of cystic germ cell development. Biol Reprod 78:27-34

7. Garcia-Lopez A, de Jonge H, Nobrega RH, de Waal PP, van Dijk W, Hemrika W, Taranger GL, Bogerd J, Schulz RW 2010 Studies in zebrafish reveal unusual cellular expression patterns of gonadotropin receptor messenger ribonucleic acids in the testis and unexpected functional differentiation of the gonadotropins. Endocrinology 151:2349-2360

8. Leal MC, de Waal PP, Garcia-Lopez A, Chen SX, Bogerd J, Schulz RW 2009 Zebrafish primary testis tissue culture: an approach to study testis function ex vivo. Gen Comp Endocrinol 162:134-138

9. de Waal PP, Leal MC, Garcia-Lopez A, Liarte S, de Jonge H, Hinfray N, Brion F, Schulz RW, Bogerd J 2009 Oestrogen-induced androgen insufficiency results in a reduction of proliferation and differentiation of spermatogonia in the zebrafish testis. J Endocrinol 202:287-297

10. van de Kant HJ, de Rooij DG 1992 Periodic acid incubation can replace hydrochloric acid hydrolysis and trypsin digestion in immunogold--silver staining of bromodeoxyuridine incorporation in plastic sections and allows the PAS reaction. Histochem J 24:170-175

11. Emanuelsson O, Brunak S, von Heijne G, Nielsen H 2007 Locating proteins in the cell using TargetP, SignalP and related tools. Nat Protoc 2:953-97

Legends to supplemental figures.

Supplemental Figure 1: Signal peptide, N-glycosylation and cleavage site predictions in zebrafish Amh with comparison of zebrafish and human recombinant proteins.

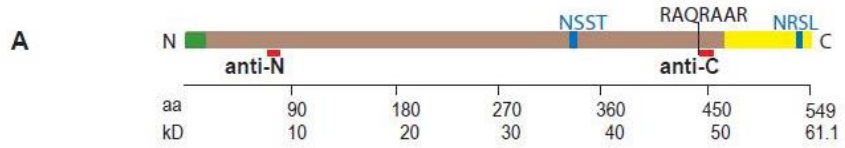

B

```
Dr    1  MLFQTRFGLMLMMTVAIGSYCATVRHEEQDNNPKVNPL---SELNGDQLEVRDLACVHRQQPTDQRATEDTPFNKEQKTL  77
Hs    1  MRDLPLTSLALVLS-ALGALLGTEALRAEEPAVGTSGLIFREDLDWPPGIPQEPLCLVALGGDSNGSSSPLRVVGALSAY  79

Dr   78  NE-FLSALKSAG-ELGKMDFLGTCSSETQSSQVSHLVQSVLQKQSGLKG------VHATEDIWDADNEEGITLTLTFPKH  149
Hs   80  EQAFLGAVQRARWGPRDLATFGVCNTGDRQAALPSLRR--LGAWLRDPGGQRLVVLHLEEVTWEP------TPSLRFQEP  151

Dr  150  SLPAGPASVMLLFSVNPVKGDSLRVQFNSQSIHPNTQTVCISESTRFLIVT-----GGWSHGHIHLKLKTMVETSMDDNR  224
Hs  152  PPGGAGPPELALLVLYPGPGPEVTV---TRAGLPGAQSLCPSRDTRYLVLAVDRPAGAWRGSGLALTLQPRGEDS-----  223

Dr  225  RKLSVSELNEVLMRKVDGSSTTIKPVLLFLSDLDEPHLKRH------------RIPQDERLPSRTYLFLCELQKFLRDIL  292
Hs  224  -RLSTARLQALLFGDDHRCFTRMTPALLLLPRSEPAPLPAHGQLDTVPFPPPRPSAELEESPPSADPFLETLTRLVRALR  302

Dr  293  -PQSKSTTPQDDPSAVSLDTLHSLPPLRLGVSSTESLLSGLVNSSTPTVFVFPQRQQGLQTHRVEVTLDSPLLSVLRMRL  371
Hs  303  VPPARASAPR---LALDPDALAGFPQGLVNLSDPAAL-ERLLDGEEPLLLLLRPTAA---TTGDPAPLHDPTSAPWATAL  375

Dr  372  DEAMAQVKQQEAGR-KMIDRLQK-----LTELSALSPDGEDSEAATKDHKEAQYRSVLLLKALQMVLSNWE------SER  439
Hs  376  ARRVAAELQAAAAELRSLPGLPPATAPLLARLLALCPGGPGGLGDP-------LRALLLLKALQGLRVEWRGRDPRGPGR  448

Dr  440  AQRAARADEDGPSASNQCHLQSLSVSLR--KFFLEPSRANINNCEGTCGFPLNNAN----NHAVLLNSHIQSGQPVNRSL  513
Hs  449  AQRSAGAT----AADGPCALRELSVDLRAERSVLIPETYQANNCQGVCGWPQSDRNPRYGNHVVLLLKMQARGAALARPP  524

Dr  514  CCVPVEYDDLCVIELESETTNISYKTNVVAIKCECR  549
Hs  525  CCVPTAYAGKLLISLSEERISAHHVPNMVATECGCR  560
```

C

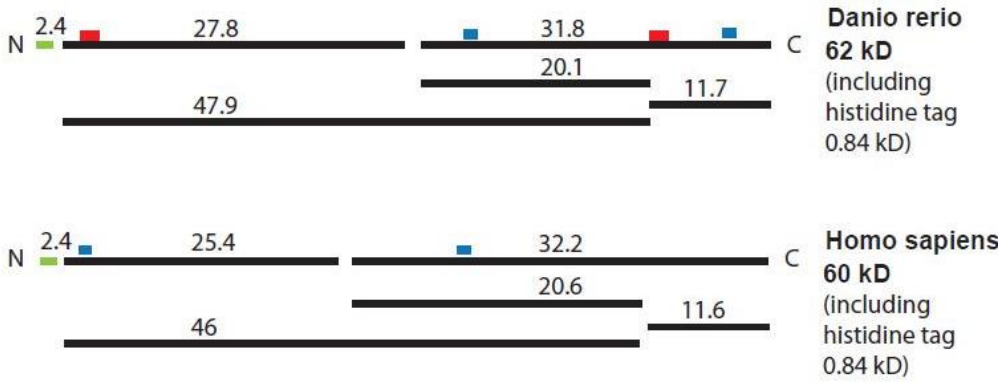

The amino acid sequence of zebrafish (Dr) is shown schematically in **A**, aligned against the amino acid sequence of human (Hs) AMH in **B** and recombinant proteins are compared schematically in **C**. Antigen peptides used to generate Zebrafish Amh-specific antibodies anti-N (near N-terminal) and anti-C (near C-terminal) are coloured red in **A-C** at amino acid positions 53-67 and 443-456, respectively. The N-terminal signal peptides, amino acids 1-21 in zebrafish and 1-24 in human Amh, are coloured green in **A-C**. N-glycosylation sites, zebrafish N334 in NSST and N510 in NRSL and human sites N64 in NGSS and N329 in NLSD, are coloured blue in **B** and **C**. The conserved TGFß-domain predicted at amino acids 457-549 in zebrafish Amh is indicated in yellow in **A** and the seven conserved cysteines **are** indicated in light grey in **B**. The human cleavage motif RAQR at position 448-451 is in bold and underlined in human sequence in **B** while

the homologous putative protease cleavage site in zebrafish Amh at amino acids 439-445 is indicated in **A** (RAQRAAR) and underlined in **B.** A second cleavage site in human AMH behind R254 and the cleavage site demonstrated in this paper for recombinant zebrafish Amh (after K263 or R264) are shown in bold and underlined in **B**. Expected N- and C- fragmens after cleavage are shown in **C** with molecular weights without considering glycosylation and including histidine tag. Other possible plasmin cleavage sites in zebrafish Amh that are in close proximity to the verified cleavage site are indicated in dark grey in **B**. Histidine tag insertion points at amino acid proline, positions 33 and 30 in zebrafish and human recombinant AMH, respectively, are coloured purple in **B**. The number of amino acids (aa) and molecular weight (kD) are indicated. N- and C-termini are indicated.

Supplemental Figure 2: Proteolytic processing of recombinant zebrafish Amh

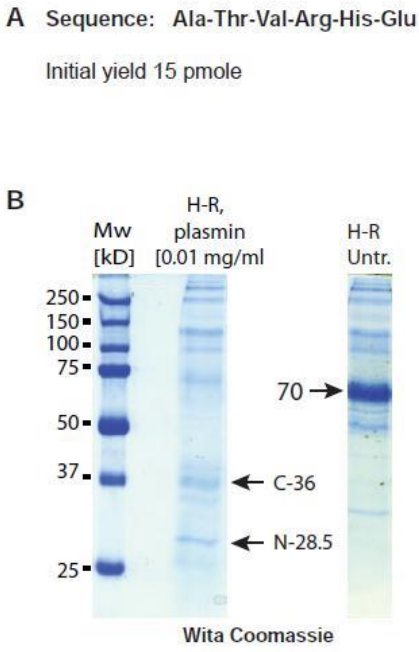

Purified recombinant His-Amh-Q441R precursor protein subjected to N-terminal sequencing of the six most N-terminal amino acids showed that signal peptide had been cleaved off before secretion. The alanine is corresponding to amino acid number 22 of the primary amino acid sequence (**A**). The 70 kD, N-28,5 and C-36 fragments of plasmin-treated (0,01 mg/ml) His-Amh-Q441R-protein were cut out from a Wita Coomassie- stained polyacrylamide gel and subjected to trypsin digestion and mass spectrometry (**B**). Molecular weight Precision plus protein standard was used and the molecular weights are given in kD. Mass spectrometry peptide fragment distribution revealed plasmin cleavage at KRH263-265 behind Lysine or Arginine. Expected molecular weights after cleavage behind R264 without signal peptide and including histidine tag would have been 27.8 and 31.8 kD for the N- and C-fragments after cleavage, respectively (Fig. 1B and 1C).

Supplemental Figure 3: Recombinant Amh is located to ER.

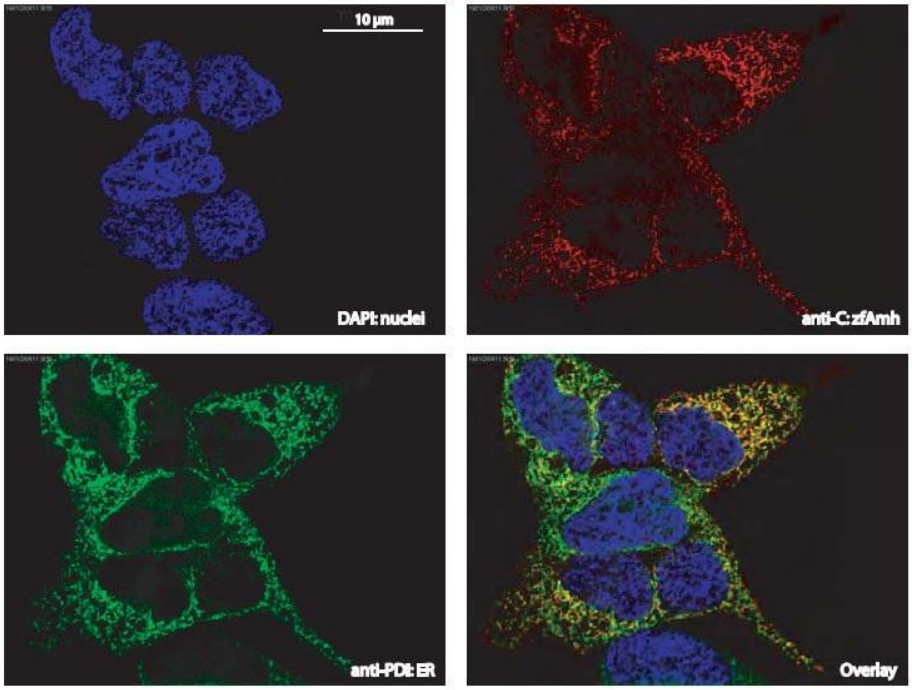

Immunocytochemistry of HEK cells producing His-Amh-Q441R co-localised Amh to ER with protein disulphide isomerase (PDI). Primary antibodies were rabbit anti-C and mouse anti-PDI (**C**). Secondary antibodies were Alexafluor 594-conjugated anti-rabbit IgG (red) and Alexafluor 488-conjugated anti-mouse IgG (green). DAPI stained nuclei blue. Yellow colouring indicates co-localisation in the merged image.

Supplemental Figure 4.

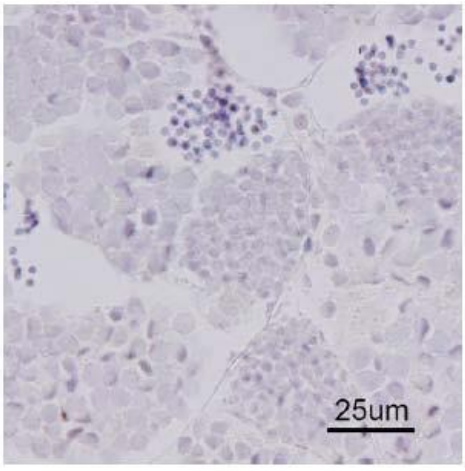

Zebrafish testis section used as a negative control for the immunocytochemical detection of Amh. The primary antibody was first incubated over night at a concentration of 1 mg/ml with the 5mg/ml peptide used to generate the antibody.

Supplemental Figure 5.

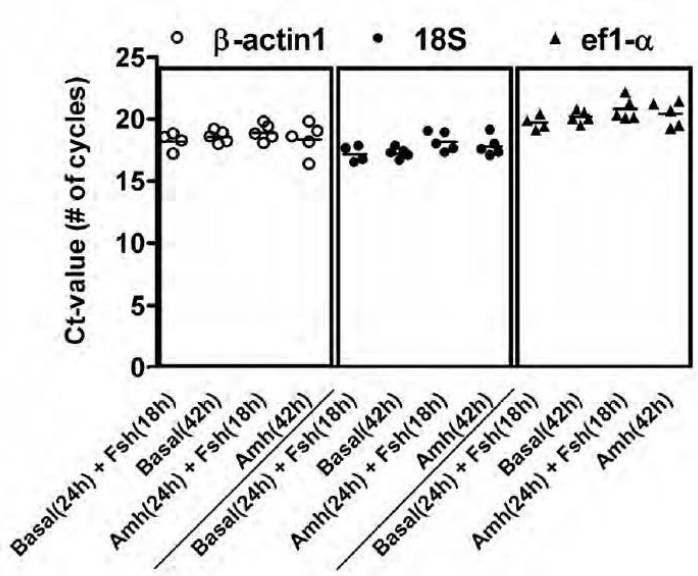

Scatter plot to check for the stability of *β-actin1* (○), *18S rRNA* (●), and *ef1-α* (▲) mRNAs as housekeeping genes for the normalization of the expression of the selected testicular genes (*cyp17a1*, *star*, *insl3*, and *ar*) in the different experimental conditions. Each dot in the scatter plot represents the average Ct-value of duplicate measurements for each testis per condition. No significant differences (P>0.05) were found for the Ct-values between the different experimental groups.

CHAPTER 6

Fsh Promotes Zebrafish Spermatogonial Proliferation and Differentiation Through Igf3, a New Igf Family Member

Rafael Henrique Nóbrega[*], Roberto Daltro Vidal de Souza Morais[*], Paul de Waal, Luiz Renato de França, Rüdiger W Schulz[#], Jan Bogerd[#]

**contributed equally to this work.*
#corresponding authors

in preparation

SUMMARY

Background

The balance between spermatogonial stem cell (SSC) self-renewal and differentiation is determined by the availability of SSC niche space. Signaling molecules released from testicular somatic cells can contribute to the niche characteristics. Here we report that a recently described, new member of the Igf family, Igf3, shifts the balance towards differentiation in the spermatogonial stem cell niche under the influence of Fsh.

Results

In primary testis tissue culture experiments, Fsh increased in a steroid-independent manner the number and mitotic index of type A undifferentiated and of type A differentiating spermatogonia in adult zebrafish. All four *igf* gene family members are expressed in the testis but only *igf3* mRNA (and protein) levels increased in response to recombinant zebrafish Fsh. This occurred in a cAMP/PKA-dependent manner, in line with the results of studies on the *igf3* gene promoter. Igf3 protein was detected in Sertoli cells contacting type A undifferentiated and differentiating spermatogonia, and recombinant zebrafish Igf3 increased the mitotic index of these spermatogonia and up-regulated the expression of genes related to germ cell differentiation and entry into meiosis. Finally, an Igf receptor inhibitor blocked Igf3- and, importantly, also Fsh-induced spermatogonial proliferation.

Conclusions

Fsh stimulates in a PKA-dependent but steroid-independent manner Sertoli cell production of Igf3, which then stimulates via Igf receptor signaling, the proliferation and differentiation of spermatogonia and their entry into meiosis in the adult zebrafish testis. Previous work showed that stimulatory effects on spermatogenesis are also exerted via gonadotropin-induced androgen production. On the other hand, Fsh also released spermatogonia from inhibitory signals, such as the previously reported down-regulation of anti-Müllerian hormone (Amh) transcript levels in Sertoli cells. We present a model, in which Fsh regulates stimulatory (Igf3, androgens) and inhibitory (Amh) signals to promote spermatogenesis.

GRAPHICAL ABSTRACT

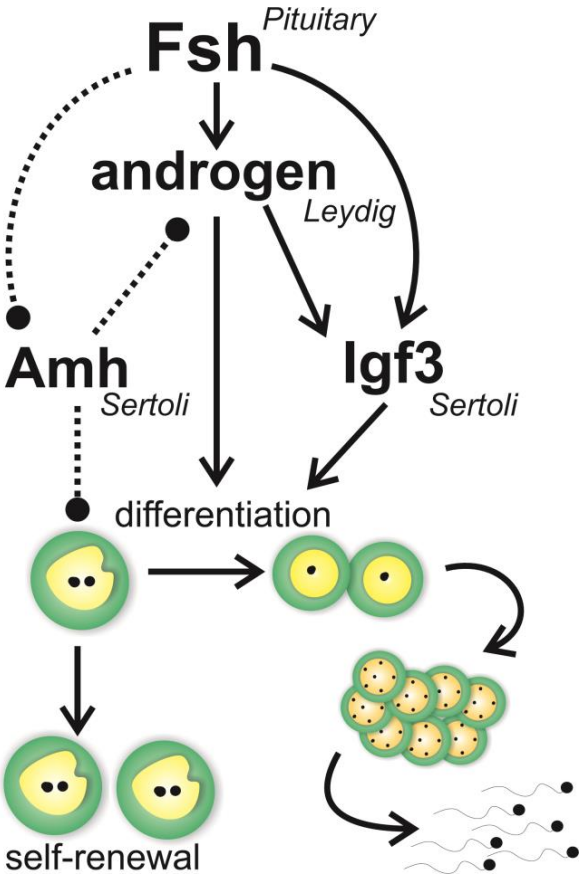

HIGHLIGHTS

1. *Follicle-stimulating hormone (Fsh) promotes zebrafish spermatogenesis and stimulates Sertoli cell production of insulin-like growth factor 3 (Igf3).*
2. *Both Fsh and Igf3 stimulate germ cell proliferation and differentiation in adult zebrafish testis tissue culture in an androgen-independent manner.*
3. *Since Fsh-induced spermatogonial proliferation is blocked by an Igf receptor inhibitor, we conclude that Fsh stimulation of spermatogenesis involves increased Sertoli cell production of Igf3 that then promotes germ cell development.*

INTRODUCTION

Spermatogenesis relies on the continuous proliferation of spermatogonial stem cells (SSC), the male germ line stem cells in the testis. SSCs either self-renew, producing more stem cells or differentiate into committed progenitor cells ultimately generating spermatozoa. In different vertebrate models, the location of SSCs, also referred to as niche, is preferentially found close to areas of the seminiferous tubules neighboring the interstitium and blood vessels (Chiarini-Garcia et al., 2001; 2003; Yoshida et al., 2007; Nóbrega et al., 2011; De Rooij and Griswold, 2012). In the niche, SSCs are able to retain their undifferentiated state (De Rooij, 2009; De Rooij and van Beek, 2013). When germ cells leave the niche, or when signaling characteristics change in the niche, SSCs are likely to produce differentiating progenitor cells (Russell et al., 1990; De Rooij and Griswold, 2012).

Growth factors released from somatic elements, such as Sertoli, Leydig, peritubular myoid, and endothelial cells, contribute to the niche characteristics, and influence the balance between SSC self-renewal and differentiation (De Rooij and Griswold, 2012). For example, colony-stimulating factor 1 (CSF1) secreted by Leydig and some peritubular myoid cells (Oatley et al., 2009) and the glial cell line-derived neurotrophic factor (GDNF) produced by Sertoli cells (Meng et al., 2000; Yomogida et al., 2003; Savitt et al., 2012) stimulate self-renewal, while activin A and bone morphogenetic protein 4 (BMP4), also produced by Sertoli cells (Loveland and Robertson, 2005), promote differentiation (Nagano et al., 2003). It is possible that yet unknown factors participate in regulating germ cell proliferation/differentiation or that known factors exert yet unknown functions in the testis. In this regard, fish are excellently suited experimental

models. For example, fish express anti-Müllerian hormone (Amh), while Müllerian ducts are absent in teleost fish, suggesting evolutionary older functions of this molecule. Indeed, Amh inhibited differentiation of type A spermatogonia in juvenile eel (Miura et al., 2002) and adult zebrafish, where it also inhibited gonadotropin-stimulated androgen production (Skaar et al., 2011).

Follicle-stimulating hormone (FSH) and luteinizing hormone (LH) regulate Sertoli and Leydig cell functions, thereby also modulating SSC fate. In rodents, for example, FSH stimulates Sertoli cell GDNF secretion which promotes SSC self-renewal (Tadokoro et al., 2002). Androgens do not seem to be required for SSC self-renewal or differentiation in rodents (Zhou and Griswold, 2008), but can inhibit spermatogonial differentiation under certain conditions (Shetty et al., 2001; 2006). On the other hand, androgens are required for the completion of meiosis (Johnston et al., 2001) and spermiogenesis in rodents (De Gendt et al., 2004). To distinguish between androgen and FSH action is complicated by indirect stimulatory FSH effects on Leydig cell androgen production in rodents (Abel et al., 2009; O'Shaughnessy et al., 2009); piscine Fsh even exerts direct stimulatory effects on Leydig cells (see below).

Analysis of mice models lacking FSH or its receptor (Kumar et al., 1997; Dierich et al., 1998; Abel et al., 2000) showed that puberty was delayed, Sertoli cell number and testis weight were clearly reduced, and the percentage of misshaped sperm with compromised mobility was increased but the males were still able to sire offspring albeit at a reduced rate. On the other hand, deleting the androgen receptor ubiquitously (ARKO) or selectively in Sertoli cell (SCARKO), arrested spermatogenesis at the meiotic phase and resulted in complete infertility (De Gendt et al., 2004).

Injections of FSH in gonadotropin-deficient and androgen-insensitive mice showed that FSH increased the number of spermatogonia and stimulated their entry into meiosis, but the germ cells failed to complete meiosis, which is entirely dependent on androgen action (O'Shaughnessy et al., 2009). Therefore, it is reasonable to assume that FSH modulated the balance among stimulatory and inhibitory growth factors that mainly target the spermatogonial generations and their entry into meiosis.

To unravel the effects of a given growth factor, the mammalian testis with its multi-layered germinal epithelium is a comparatively complex structure, in which a Sertoli cell is associated with several different stages of germ cell development at any given time (Hess and França, 2008). Here, we propose to make use of the cystic mode of spermatogenesis in fish (Schulz et al., 2010) as an alternative model to study this question, mainly because a fish Sertoli cell usually contacts only one or two different germ cell clones. In cystic spermatogenesis, a SSC is completely enveloped by Sertoli cells. Upon differentiation, germ cells develop clonally as seen in animals in general, clone members stay interconnected by cytoplasmic bridges, and the developing germ cell clone remains enveloped by and accompanied through spermatogenesis by a group of Sertoli cells that also proliferate in a predictable manner (Schulz et al., 2005; Leal et al., 2009), to provide space and support for the proliferating/differentiating germ cell clone. Thus, piscine Sertoli cells do not contact several but only one or two germ cell clones at a time in the postpubertal testis, i.e. show a much less complex Sertoli/germ cell relation than mammals.

We sought to further simplify the situation in our search for testicular factors regulating spermatogonial development by investigating a species showing clear reproductive seasonality. Focusing on the transition

from a quiescent, immature testis towards an activation of spermatogonial proliferation, we analyzed differentially expressed genes in Atlantic salmon testis tissue samples using microarrays (manuscript in preparation). Among the differentially expressed genes, an inhibitory and a stimulatory growth factor have been identified. The identity and biological activity of the inhibitory factor Amh has been described previously in juvenile eel (Miura et al., 2002) and adult zebrafish (Skaar et al., 2011). Here we report the identity and biological activity of a stimulatory factor, a recently described new member of the Igf family, Igf3 (Wang et al., 2008; Zou et al., 2009). An evolutionary interesting aspect is that this gene seems to have arisen during the teleost-specific genome duplication and then has evolved to be expressed predominantly in the gonads (Wang et al., 2008; Zou et al., 2009). Here, we show that Fsh stimulates spermatogonial proliferation and differentiation in an androgen-independent manner by stimulating Sertoli cell Igf3 production; importantly, inhibiting Igf receptor activity abolished the stimulatory effects of Fsh on spermatogonial proliferation. Together with the previously reported Fsh-mediated stimulation of Leydig cell androgen production, and the also Fsh-mediated down-regulation of *amh* transcript levels, we conclude that Fsh orchestrates Sertoli and Leydig cell signaling to stimulate spermatogenesis by increasing stimulatory and by decreasing inhibitory signaling.

RESULTS

Fsh triggers zebrafish spermatogenesis in an androgen-independent manner

We have previously produced recombinant zebrafish Fsh and Lh (García-López et al., 2010). To confirm the biological activity of a new,

similarly produced batch of Fsh, we analyzed androgen release and the expression of selected genes after 20 h of incubation in a zebrafish testis tissue culture system (Leal et al., 2009). As observed previously (García-López et al., 2010), Fsh increased androgen release and transcript levels of steroidogenesis-related genes (Fig. 1A), such as *cyp17* and *star* and reduced mRNA levels of *amh* (Skaar et al., 2011; Fig. 1A).

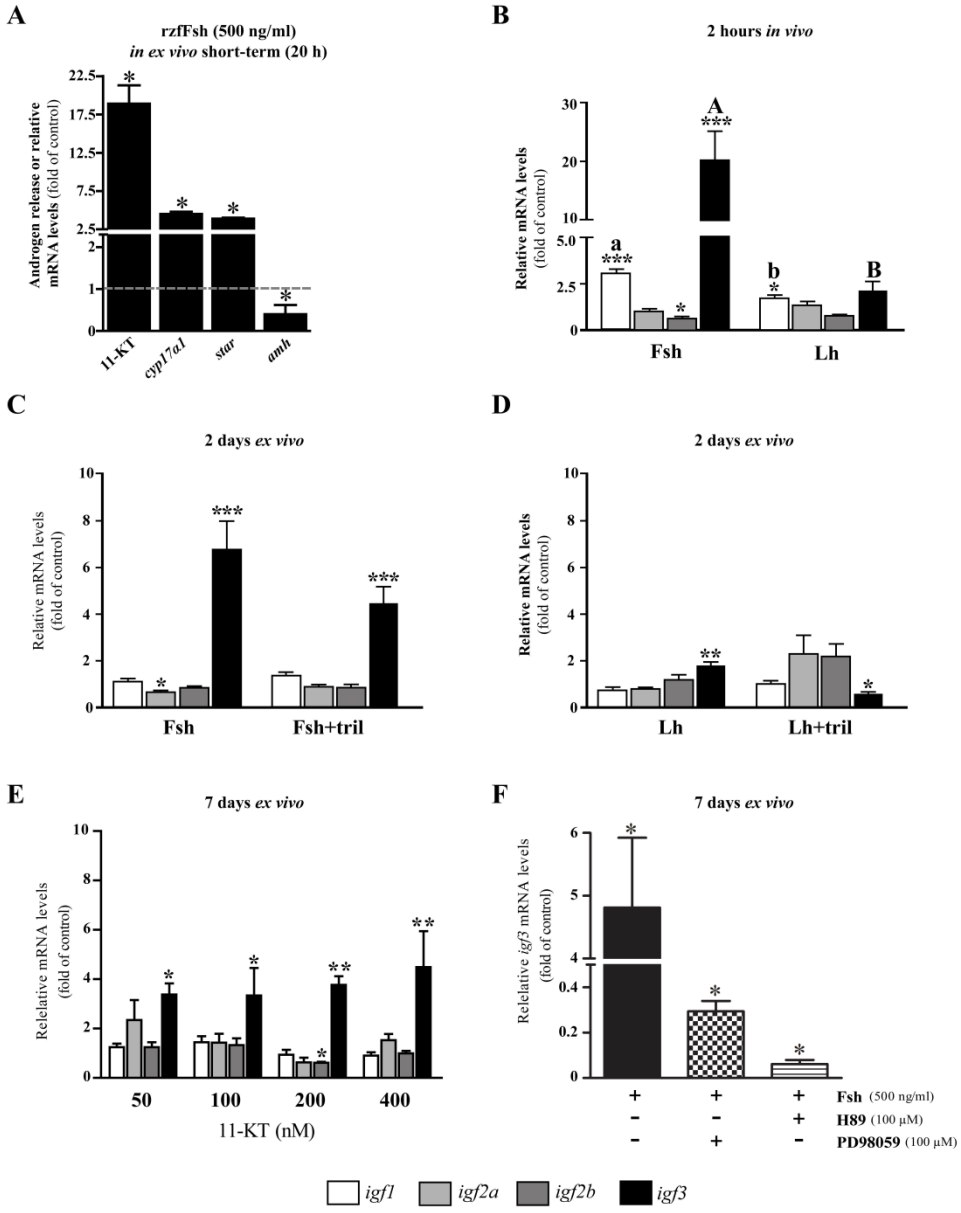

Figure 1. Androgen release and gene expression analyses under the influence of gonadotropins and sex steroids.

(A) Androgen release and mRNA levels of Sertoli cell- and Leydig cell-specific genes in response to 500 ng/mL recombinant zebrafish Fsh (rzfFsh). **(B)** Gene expression patterns of *igf1*, *igf2a*, *igf2b* and *igf3*, two hours after injection into the coelomic cavity of rzfFsh or recombinant zebrafish Lh (rzfLh) (100 ng/g body weight; n = 6-8 fish per treatment). Gene expression of selected *igf* genes, two days after culture under the influence of rzfFsh **(C)** or

rzfLh **(D)** in the absence or presence of 25 µg/mL trilostane (tril; n = 6-8 per treatment). **(E)** Testicular explants treated with increasing concentrations of 11-KT *ex vivo* (n = 4-7 explants per dose) for 7 days. **(F)** Relative mRNA levels of *igf3* after testicular explants treated with rzfFsh in the presence or absence of the PKA inhibitor, H89 or the MAPK inhibitor, PD98059 (n = 4-7 explants per dose) for 7 days. All columns are expressed as the fold change of the relative mRNA levels of the treated group over its respective control (mean ± SEM). Respectively, asterisks and different letters indicate significant differences ($p < 0.05$) between treated and control groups or when comparisons were made between treatments (i.e. Fsh versus Lh).

Previous work (Baudiffier et al., 2012) and other laboratories suggested that insulin-like growth factor (Igf) family members could mediate directly (Loir, 1994) or in a permissive manner (Nader et al., 1999) gonadotropin stimulation of on fish spermatogenesis. Therefore, we examined if exposure to Fsh resulted in changes in the testicular transcript levels of the four zebrafish Igf family members (*igf1*, *igf2a*, *igf2b*, *igf3*) (Fig. 1B-C). We found that Fsh strongly increased testicular transcript levels of *igf3 in vivo* (2h; ~20-fold; Fig. 1B) and ~7-fold after 2 days of tissue culture (Fig. 1C). Other Igf family members showed no or much less prominent changes in transcript levels. The responses to Lh were clearly distinct (Fig. 1B, D): *in vivo*, only a slight stimulatory effect on *igf1* mRNA levels was observed, while *ex vivo* the *igf3* mRNA levels were increased slightly. Since both gonadotropins stimulated Leydig cell steroid release in zebrafish (García-López et al., 2010), we examined in tissue culture if part of the stimulatory response was attributable to the steroidogenic potency of the gonadotropins. To this end, we blocked the production of biologically active steroids using the 3β-hydroxysteroid dehydrogenase inhibitor, trilostane. The Fsh-induced increase in the *igf3* mRNA level was somewhat reduced but did not reach statistical significance (Fig. 1C). Blocking Lh-induced steroid production also blocked the Lh-mediated increase in *igf3* mRNA levels (Fig. 1D), so that we analyzed the *igf* transcript levels under

the influence of androgens. Indeed, the *igf3* transcript was up-regulated at all concentrations of 11-KT, although less prominently than in response to Fsh, and *igf2b* transcript levels were reduced at 200 nM 11-KT (Fig. 1E).

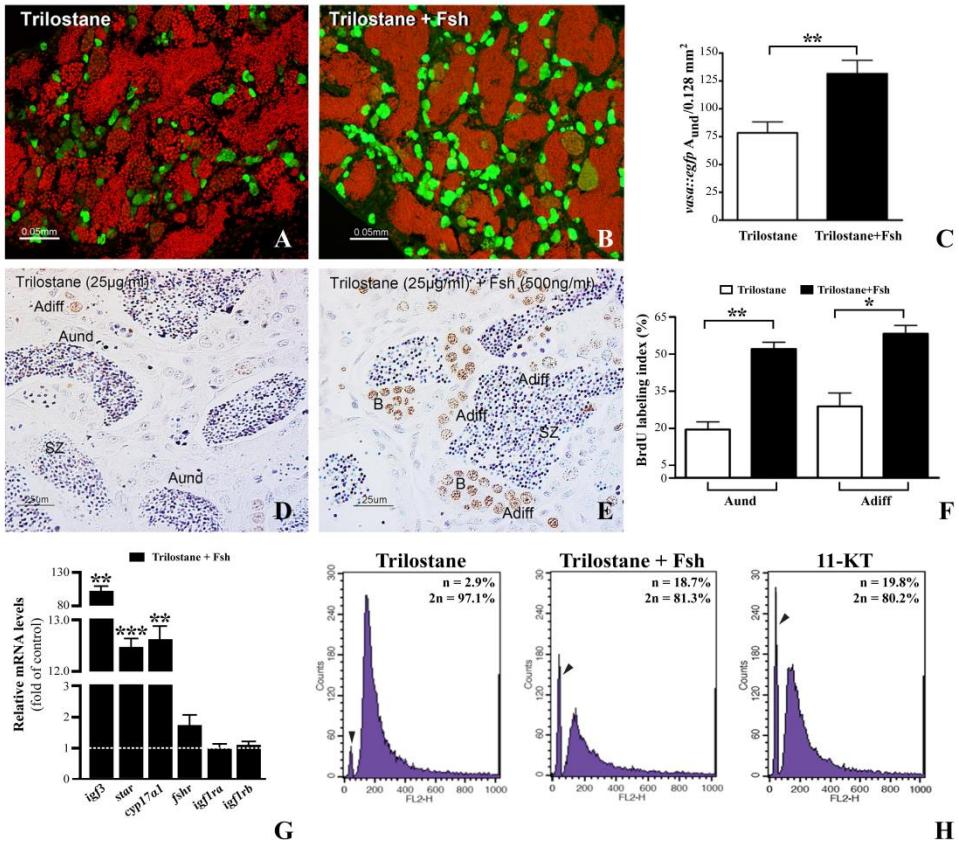

Figure 2. Effects of recombinant zebrafish Fsh in spermatogonial proliferation in the zebrafish in testes. (A-C) Morphological analysis and quantitative evaluation of A_{und} in *vasa::egfp* zebrafish testes treated with 25 g/mL trilostane in the absence or presence of 500 ng/mL rzfFsh (n=8). **(D-F)** Morphological analysis and BrdU labelling index of A_{und} and A_{diff} in zebrafish testis, pre-exposed to E_2 *in vivo* for 21 days, and cultured for 7 days with 25 µg/mL trilostane in the absence or presence of 500 ng/mL rzfFsh (n = 8 fish). **(G)** Proportion of haploid cells (spermatids/spermatozoa), indicated by arrowheads, after testicular cell suspension treated with 25 µg/mL trilostane (negative control), 400 nM 11-KT (positive control) or with 100 ng/mL rzfFsh+trilostane (n = 4) per 7 days. **(H)** Gene expression patterns of selected genes in zebrafish testes, pre-exposed to E_2 *in vivo* for 21 days and next incubated *ex vivo* with 25 µg/mL trilostane in the absence or presence of 500 ng/mL rzfFsh (n = 8). The columns are expressed as the fold change of the mRNA levels of the treated group compared with its respective control (mean ± SEM). The asterisks indicate significant differences ($p < 0.05$; n=8) between the treated and control groups. SPG

A_{und}, undifferentiated type A spermatogonia; SPG A_{diff}, spermatogonia type A differentiating; SPG B, spermatogonia type B, and SZ, spermatozoa.

We then examined if Fsh stimulated spermatogenesis *ex vivo*. In the light of the steroidogenic activity of Fsh, we included trilostane to block the production of biologically active steroids (see Figs. 2 A-C, G); for some experiments, we also used testis tissue from an androgen-insufficiency model that is based on *in vivo* exposure of adult males to 10 nM estradiol (E_2) for 3 weeks, greatly reducing the androgen production capacity (de Waal et al., 2009). Testis tissue from these animals is enriched in type A spermatogonia that accumulate in the testis since their differentiation is inhibited when androgen production is strongly reduced.

In *vasa::gfp* transgenic animals, the single type A undifferentiated (A_{und}) spermatogonia and the first generations of type A differentiating (A_{diff}) spermatogonia are particularly rich in Gfp protein. Analyzing testis tissue from this transgenic line by fluorescence microscopy (Fig. 2 A,B) showed a clear increase in the frequency of strongly Gfp-positive spermatogonia when incubated in the presence of Fsh (500 ng/ml). In parallel experiments, tissue was fixed and prepared for immunocytochemical detection of Gfp protein to quantify the number of strongly Gfp-positive, single type A_{und} spermatogonia (see supplemental data). This approach provided quantitative and statistically significant confirmation for the increase in the number of type A_{und} cells in response to 500 ng Fsh/ml (Fig. 2C). Using the androgen-insufficiency model and the associated enrichment of type A spermatogonia, we examined Fsh effects on BrdU-incorporation and found increased mitotic indices of both type A_{und} and type A_{diff} spermatogonia (Fig. 2 D-F). Also type B spermatogonia,

absent or rarely seen in control incubations in this androgen-insufficiency model, were present and proliferated in the presence of Fsh (Fig 2E). We conclude that Fsh can stimulate spermatogonial development in an androgen-independent manner. Moreover, analyzing gene expression under the same conditions, we found an ~100-fold increase in testicular *igf3* mRNA and an ~13-fold increase in mRNA levels of the steroidogenic enzyme genes, *star* and *cyp17a1* (Fig. 2G). No changes were observed in testicular mRNA levels of *fshr*, *igfr1a* and *igfr1b*.

To examine if Fsh can also promote the development of haploid cells, aliquots of a testicular cell suspension (~10^5 cells) prepared from adult males and containing about 3% of haploid cells, were incubated for 7 days in the absence or presence of 100 ng Fsh/ml in medium containing trilostane. Incubations with 11-ketotestosterone (400 nM) served as positive control, which was previously shown to result in the production of BrdU-positive spermatids and spermatozoa in tissue culture (Leal et al., 2009).

After 7 days, the cells were DNA-stained with propidium iodine and analyzed using a flow cytometer (Fig. 2H). Both, Fsh and androgen clearly increased the proportion of haploid cells from 3% to ~19%. Further work focused on the cellular localization of Igf3 peptide in the zebrafish testis and the biological activity of recombinant zebrafish Igf3 (rzfIgf3), the production of which is described in the supplemental material.

Igf3 is expressed in Sertoli cells contacting type A spermatogonia

Analyzing the expression of *igf* gene family members in the germ cell-free homozygous *piwil1* (formerly known as *ziwi*) mutant [*piwil1*$^{(-/-)}$] (Houwing *et al*. 2007) in comparison with wild type fish, revealed that only *igf2b* mRNA levels were reduced significantly. *In situ* hybridization

experiments then showed that injecting 100 ng Fsh/g body weight 2 h before collecting testis tissue (resulting in a 20-fold increase in testicular *igf3* mRNA levels, see Fig. 1B) allowed localization of *igf3* mRNA expressing cells (Fig. 3A,B). Typically, *igf3* mRNA was localized in the cytoplasm of cells with elongated nuclei that were situated close to single germ cells or to small groups of germ cells with round, large nuclei, suggesting the *igf3* mRNA-positive cells are Sertoli cells contacting type A spermatogonia.

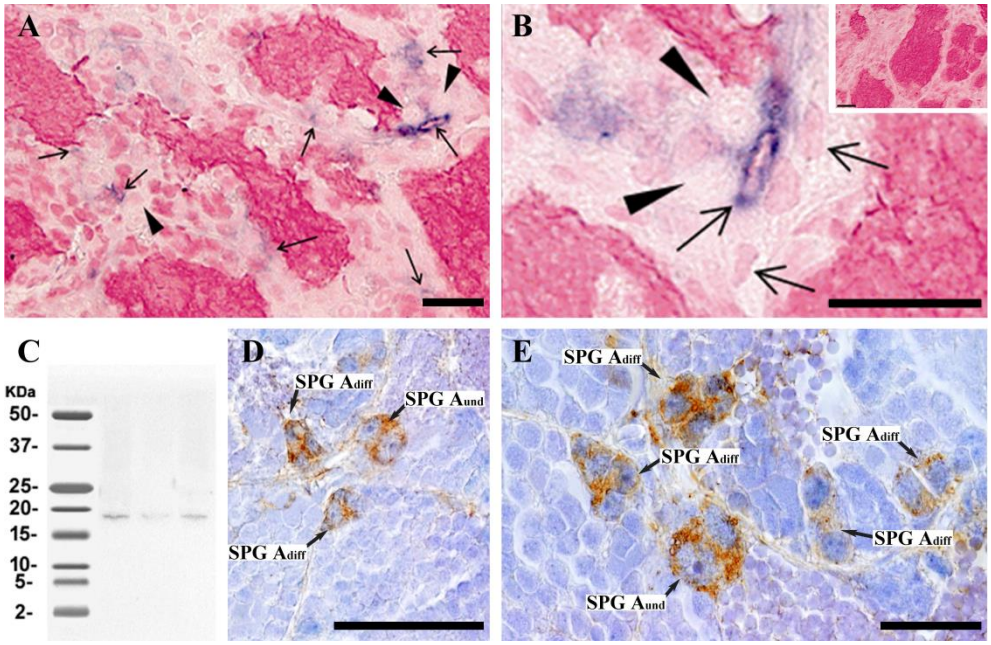

Figure 3. Localization of *igf3* mRNA (ISH) and Igf3 protein (IHC) in the zebrafish testis collected after injections into the coelomic cavity with rzfFsh. (A-B) Localization of testicular *igf3* mRNA expression by ISH (indicated by arrows) in the zebrafish testis, while the arrowheads indicate nuclei of type A spermatogonia. No specific staining was obtained with the sense cRNA probes (inset in B). **(C)** Testicular-specific expression of *igf3* mRNAs by western blot showing the specificity of the antibody produced against the zebrafish Igf3. **(D-E)** Small and higher magnification of zebrafish testis sections showing the testicular expression sites of Igf3 by IHC. SPG A_{und}, undifferentiated type A spermatogonia; SPG A_{diff}, spermatogonia type A differentiating.

Igf3 protein was localized with an antibody raised against the E domain of Igf3 (Supplemental Material), which detected a single band at the

expected molecular weight of ~17 kDa in Western blots (Fig. 3C). Using again testis tissue from Fsh-treated adult males, Igf3 protein was localized in cytoplasmic extensions of Sertoli cells contacting type A_{und} and type A_{diff} spermatogonia (Fig. 3D,E). Sertoli cells contacting more advanced germ cells (type B spermatogonia, meiotic and post-meiotic cysts) or Leydig cells were not stained. Pre-treatment with Fsh was required to be able to detect *igf3* mRNA while Igf3 protein detection was possible in non-pretreated fish, although Fsh injection enhanced Igf3 protein detection. Collectively, our observations show that *igf3* mRNA and Igf3 protein are localized to Sertoli cells contacting type A spermatogonia and that their expression is enhanced by Fsh.

Initial PCR studies showed that the two Igf receptor genes present in the zebrafish genome, *igf1ra* and *igf1rb*, are both expressed in the testis (data not shown). We then compared their testicular mRNA levels in wild type and germ cell-free *piwil1*$^{(-/-)}$ mutant males (Houwing et al., 2007). The *piwil2* mRNA levels in the mutant were very low, compatible with the germ cell depletion. While *igf1ra* transcript levels were partially reduced, *igf1rb* mRNA levels remained unchanged in the mutant (supplemental data). One possible explanation for this pattern is that *igfr1a* mRNA is expressed by germ and somatic cells, while *igf1rb* is mainly expressed by somatic cells.

Cyclic AMP response element-binding protein and activating transcription factor 1 response elements in the *igf3* promoter are involved in regulating *igf3* gene expression.

The PKA inhibitor H89 (100 µM) and the MAPK inhibitor PD98059 (50 µM) clearly reduced the Fsh-induced (500 ng/mL) increases in testicular

igf3 mRNA levels (Fig. 1F), suggesting that the cAMP pathway is involved in regulating *igf3* gene expression.

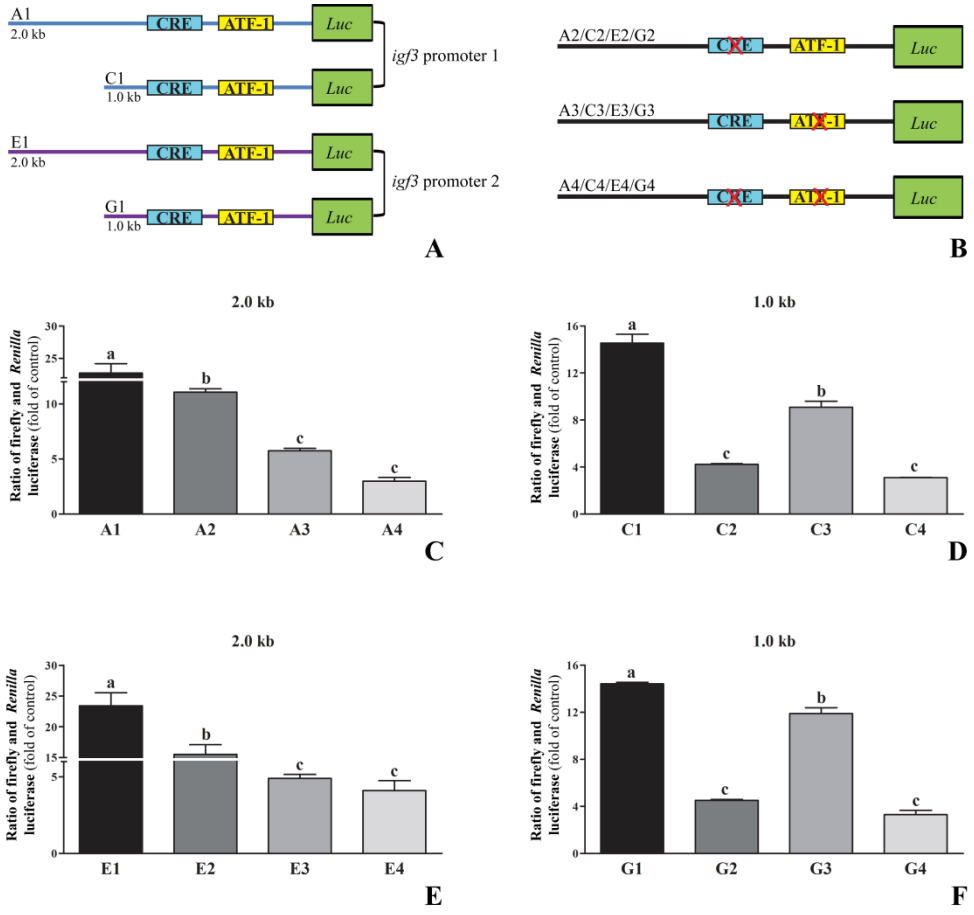

Figure 4. The *igf3* promoter activity in HEK 293T cells. (A-B) Schematic representation of two different, probably polymorphic (A and C *versus* E and G) promoter regions of 2.0 kb (A1 and E1) and 1.0 kb (C1 and G1) of the zebrafish *igf3* gene, with presumed CRE and ATF-1 transcription factor-binding sites indicated, as well as mutant promoter regions with inactivating point mutations in CRE (A2, C2, E2 and G2), ATF-1 (A3, C3, E3 and G3) or both CRE and ATF-1 (A4, C4, E4 and G4) transcription factor-binding sites**. (C-F)** Luciferase activity of the different promoter constructs, in cells treated with 10 µM forskolin compared with untreated cells. The columns in **C-F** are expressed as arbitrary units of luciferase activity, normalized by TK *Renilla* activity. Data are represented as mean ± SEM from one representative experiment out of two independent experiments, each of which was performed in triplicate. Different letters represent significant differences ($p < 0.05$) among the different constructs transfected.

To study the regulation of *igf3* gene expression in more detail, two distinct (i.e. polymorphic) zebrafish *igf3* promoter sequences (see Supplemental Information) as well as truncated and mutated versions (Fig. 4A,B) were cloned in front of a luciferase reporter gene and investigated after transfection in human embryonic kidney 293T cells. Luciferase activity was reduced in the truncated versions of the *igf3* promoter (Fig. 4C-F), suggesting that sequences upstream of the 1.0 kb promoter region are relevant for enhancing *igf3* expression. Mutation of the CRE and ATF-1 motifs (~-610 bp and ~-260 bp, respectively), present in the ~1.0 kb promoter, individually or in combination, substantially reduced luciferase activity, indicating that regulation of *igf3* gene expression involves also these motifs (Fig. 4C-F).

Taken together, our results show that Sertoli cells contacting type A spermatogonia respond to Fsh by up-regulating *igf3* expression in a cAMP-/PKA-/MAPK-dependent manner.

Recombinant Igf3 stimulates zebrafish spermatogenesis

Using testis tissue from adult males rendered androgen insufficient by *in vivo* E_2 exposure (de Waal et al., 2009), we carried out a dose-finding experiment with 10, 100 or 1000 ng/ml of rzfIgf3 for 7 days. A clear stimulation of spermatogenesis was observed at a concentration of 100 ng/ml, as revealed by morphological and gene expression analyses (Figs. 5,6A-D). Examining the mRNA amounts of the *dazl* gene, expressed in type B spermatogonia and leptotene/zygotene spermatocytes in zebrafish (Chen et al., 2013), or of the *piwil2* (formerly *zili*) gene expressed in all germ cells except spermatozoa (Houwing et al., 2008), we found 2- to 4-fold increases, respectively, in response to 100 ng/mL Igf3 (Fig. 5). No changes were found

for the mRNA level of a gene expressed in type A spermatogonia (*piwil1*; Houwing et al., 2007), in pachytene spermatocytes (*sycp3l*; Chen et al., 2013), or in spermatids (*shippo1*; Yano et al., 2008). Also the mRNA levels of 10 genes (preferentially) expressed in testicular somatic cells (*amh, ar, cyp17a1, fgf8, fshr, gsdf, insl3, lhcgr, pgr, star*) as well as *igfr1a* and *b* mRNA (expressed in somatic and germ cells) did not change in response to Igf3 (data not shown).

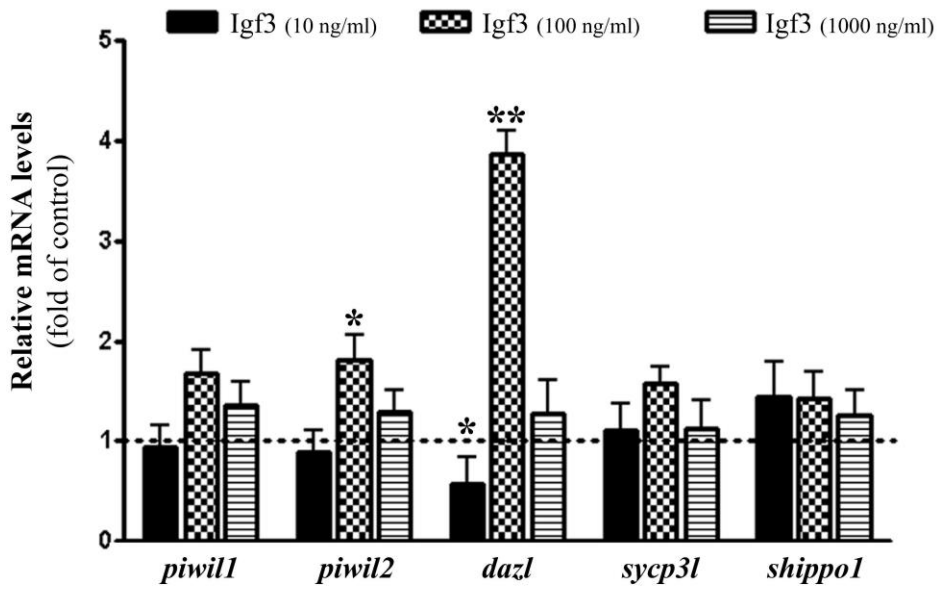

Figure 5. Gene expression after Igf3-dose response. The mRNA levels of selected genes after 7 days of zebrafish testis cultured with different doses of recombinant zebrafish Igf3 (10, 100 and 1000 ng/mL). The columns are expressed as the fold change of the mRNA levels of the treated group compared with its respective control (mean ± SEM).

Morphological analysis of testis tissue incubated in the absence of Igf3 showed the typical appearance of androgen insufficiency: the tissue contains mainly type A_{und} and some type A_{diff} spermatogonia (Fig. 6A); intermediate germ cell stages (type B spermatogonia, spermatocytes and

spermatids) were rare or missing, while spermatozoa that were in the testis at the beginning of the treatment stayed in the tubular lumen. Tissue incubated with 100 ng/mL Igf3 showed a clearly different germ cell composition (Fig. 6B). Type A_{diff} spermatogonia were more prominent, type B spermatogonia and also spermatocytes, both rare or absent from control tissue samples, were regularly found in Igf3-exposed tissue.

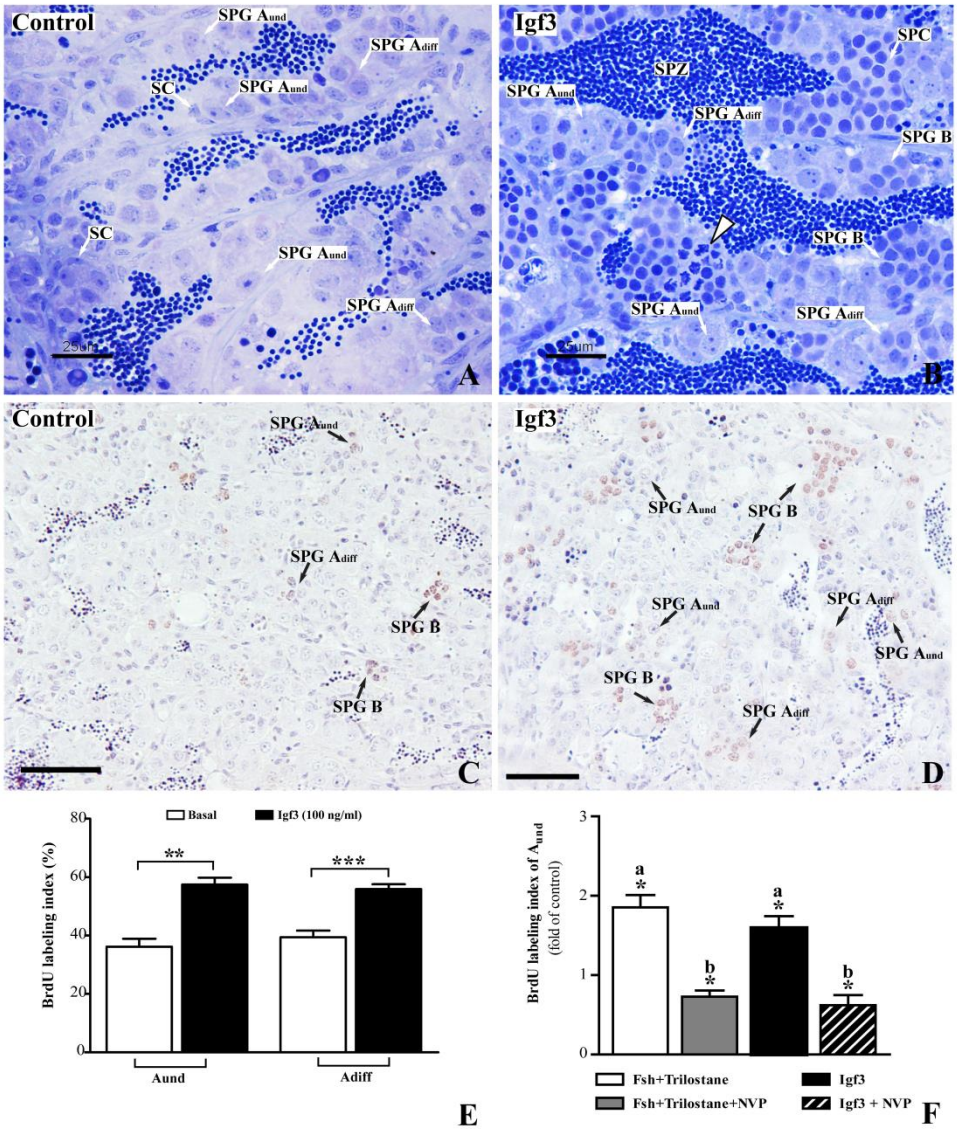

Figure 6. Effects *in vitro* and *in vivo* of recombinant zebrafish Igf3 in the zebrafish testis. **(A-B)** Morphological analysis of zebrafish testis, after 7 days in culture in the absence (control) or presence of recombinant zebrafish Igf3 (rzfIgf3), which shows the recovery of spermatogenesis after depletion induced by E_2 treatment *in vivo*. **(C-D)** BrdU immunodetection in zebrafish testis sections, after 7 days in culture in the absence (control) or presence of rzfIgf3, which demonstrates a higher proliferative activity while in the presence of rzfIgf3. **(E)** BrdU labelling index of A_{und} and A_{diff} in zebrafish testis, pre-exposed to E_2 *in vivo* for 21 days, and cultured for 7 days with 25 µg/mL trilostane in the absence or presence of 500 ng/mL rzfFsh (n = 8 fish). **(F)** BrdU labelling index of A_{und} spermatogonia under different conditions: Fsh+Tril; Fsh+Tril+NVP; Igf3 and Igf3+NVP, showing that while in the presence of the Igf1R inhibitor (NVP) the proliferation of A_{und} was suppressed. SC, Sertoli cells; SPG A_{und}, spermatogonia type A undifferentiated; SPG A_{diff}, spermatogonia type A differentiated; SPG B, spermatogonia type B; SPC, spermatocyte; SPZ, spermatozoa; NVP, the Igf receptor-specific inhibitor NVP-AEW541.

To examine if the biological activity of Igf3 includes modulation of testicular androgen release in zebrafish, we quantified basal and Fsh-stimulated 11-ketotestosterone release in the absence and presence of Igf3, as described previously (García-López et al., 2010). We did not detect statistically significant changes in androgen release (supplemental figure X), which is in line with the absence on Igf3 effects on mRNA levels of genes involved in steroidogenesis (*star* and *cyp17a1*; see above). Thus, Igf3 directly stimulated the proliferation and differentiation of spermatogonia and entry into meiosis in tissue culture, which was not associated with a change of mRNA levels for several somatic genes (growth factors, receptors, steroidogenesis genes) or with a change in androgen release.

Fsh-induced proliferation of type A spermatogonia is blocked by an Igf receptor inhibitor

Next, we examined if the stimulatory effect of Fsh on proliferation type A spermatogonia (see Fig. 2A-F) is mediated by Igf3. To this end, we quantified BrdU-incorporation into testis tissue cultures from males rendered androgen-insufficient. In line with previous experiments, we first

showed that Fsh (500 ng/ml) led to an ~2-fold increase of the mitotic index of type A_{und} spermatogonia (Fig. 6F). We then found that also Igf3 (100 ng/ml) resulted in a similar increase of the proliferation activity (Fig. 6F). This effect of Igf3 was blocked by adding an Igf receptor kinase inhibitor (NVP), and most importantly, also the Fsh-mediated stimulation of the mitotic index of type A_{und} spermatogonia was blocked by the addition of NVP (Fig. 6F).

Collectively, our data show that Fsh stimulates in a cAMP-dependent manner Sertoli cell production of Igf3, which then stimulates via Igf receptor signaling but independent of androgen release, the proliferation and differentiation of spermatogonia and their entry into meiosis in the adult zebrafish testis. While Fsh could still effectively stimulate *igf3* transcript levels when androgen production was blocked, androgens also exerted a weak stimulatory effect on igf3 transcript levels.

Experimental Procedures

Zebrafish stocks

In the present study sexually adult males (~100-300 days post fertilization) were used. Fish were either outbred wild-type, transgenic expressing enhanced green fluorescent protein under the control of the germ cell-specific *vasa* promoter (*vasa::egfp*) (Krøvel and Olsen, 2002), or *piwil1* (formerly known as *ziwi*) mutant [$piwil1^{(-/-)}$] zebrafish (Houwing et al. 2007). In some experiments, an androgen insufficiency zebrafish model (de Waal et al. 2009) was used. Animal culture was done using standard conditions for this species (Westerfield et al., 2000). Handling and experimentation were consistent with the Dutch national regulations; the

Life Science Faculties Committee for Animal Care and Use in Utrecht (The Netherlands) approved the experimental protocols.

Testicular androgen release

The androgen release capacity of zebrafish testicular tissue into culture medium was measured after a short-term (20 hours) *ex vivo* culture system as described by García-López et al. (2010). This technique was used to examine the steroidogenic activity of the new batch of recombinant zebrafish Fsh (Figure 1A) and to study if recombinant zebrafish Igf3 modulates basal or Fsh-stimulated androgen release (Figure S2 B).

Testis tissue culture.

A previously described *ex vivo* organ culture system for zebrafish testis (Leal et al., 2009) was used. This technique was used for short-term (20 hours for steroid release and gene expression as in Fig. 1A), medium-term (2 days as in Fig. 1C and D), or long-term (7 days in all other cases) incubations. The zebrafish testis was challenged either by recombinant zebrafish Fsh and Lh (both at 500 ng/ml), in the presence or absence of trilostane (25 µg/ml), androgen (11-ketotestosterone; 400 nM) or recombinant zebrafish Igf3 (100 ng/ml; see supplemental information for details on Igf3 production). In addition, an IGF 1 receptor (IGF1R) kinase inhibitor, NVP-AEW541 (Selleckchem; 10 µM), or cAMP pathway inhibitors, the PKA inhibitor H89 (100 µM) and the MAPK inhibitor PD98059 (50 µM) were added to the culture medium when proliferation (Figure 5F) or *igf3* gene expression (Figure 1F) were studied. BrdU (50 µg/ml; 5-bromo-2-deoxyuridine; Sigma-Aldrich) was added in the last 6 hours of incubation (long-term) to investigate the proliferation activity in

the testis. Zebrafish testis was either harvested for gene expression studies (see testicular gene expression section) or for morphological analyses.

Testicular gene expression

Testes collected for gene expression analysis were snap frozen in liquid nitrogen and stored at -80ºC until RNA isolation. Total RNA extraction was performed using RNAqueous-Micro Kit (Ambion, Austin, TX, USA), following the manufacturers' instructions. To estimate the relative mRNA expression levels of a number of selected genes (Table S1) by real-time, quantitative qPCR (qPCR), samples were processed as described by de Waal et al. (2008). Primers were tested before use for specificity and amplification efficiency on serial dilutions of testis cDNA as described previously (Bogerd et al., 2001). All qPCRs were performed in 20 µl reactions and Cq values determined in a 7900HT Real-Time PCR system (Applied Biosystems) using default settings. Relative mRNA levels were calculated as reported previously (Bogerd et al., 2001; de Waal et al., 2008).

Morphological analysis

Testis was fixed either in 4% glutaraldehyde (Fig. 5A,B), freshly prepared methacarn for BrdU detection (Fig. 5C,D), or in phosphate-buffered 4% paraformaldehyde for Igf3 and Gfp immunohistochemistry (Fig. 3D,E). After dehydration, samples were embedded either in Technovit 7100 (Heraeus Kulzer, Wehrheim, Germany) when glutaraldehyde/methacarn were used as fixatives, or in paraplast (Sigma-Aldrich) when tissue was fixed in paraformaldehyde. Sections of 3 µm (Technovit 7100) or 5 µm (paraplast) thickness were used. The detection of Igf3 or Gfp by immunohistochemistry has been carried out as described

previously (Almeida et al., 2008). Rabbit anti-Igf3 (2 µg/ml of affinity purified) or rabbit anti-Gpf (1:1000) were applied, after which sections were incubated with avidin-biotin complex (ABC; Vector laboratories) and DAB staining was performed. Counterstaining was done with hematoxylin (Igf3/Gfp) and PAS (Gfp). Evaluation of BrdU incorporation into type A undifferentiated and differentiated spermatogonia was carried out as described by Skaar et al. (2011). The E domain of zebrafish Igf3 was selected for the antibody production and its specificity was confirmed by Western blot as established previously by de Waal et al. (2009).

Igf3 mRNA Localization and Western blot

To visualize the cellular expression sites of *igf3* mRNA in zebrafish testis, a whole mount in situ hybridization (ISH) was performed as described previously (Morais et al., 2013), using zebrafish *igf3*-specific PCR products generated with primers 2878–2879 (Table S2), containing either T3 (primer 2878) or T7 (primer 2879) RNA polymerase-promoter sequences attached at their 5'–ends.

Testicular cell suspension and cell sorting

Testis tissue fragments from wild-type zebrafish were digested with 0.2% collagenase and 0.12% dispase as described previously (Nóbrega et al., 2010). The resulting cell suspension was aliquoted (10^5 cells/treatment) and incubated for 7 days in the absence or presence of 100 ng Fsh/ml in medium containing trilostane (25 µg/ml). As positive control, 11-ketotestosterone (400 nM) was used, which resulted in the production of BrdU-positive spermatids and spermatozoa in tissue culture (Leal et al., 2009). After 7 days, cells were collected and stained with propidium iodine

(PI) for DNA quantification according to previous studies (Saito et al., 2011). Flow cytometry was carried out using the BD FACS Calibur (BD Biosciences, San Jose, CA, USA) where the proportion of haploid cells (spermatids/spermatozoa) were evaluated by DNA histograms for each condition (Fig. 2G).

Transfection assays

Human embryonic kidney (HEK 293T cells were grown under 5% CO_2 in Dulbecco's modified Eagle's medium (DMEM), supplemented with antibiotic solution (100 IU/ml), 2 mM glutamine and 10% fetal bovine serum (FBS; all from Life technologies). One day prior to transfection in 24-well plates, 1.5 x 10^5 cells were seeded per well. Cells were transiently co-transfected by polyethylenimine (PEI) with a total of 850 ng plasmid DNA, consisting of 500 ng *igf3* promoter construct, 100 ng TK-*Renilla* luciferase plasmid and 250 ng empty pcDNA3 vector. For each *igf3* promoter construct (see supplemental information), transfection was performed in triplicate. Twenty-four h after transfection, the medium was replaced by medium without (basal) or with (stimulation) 10 µM forskolin (Sigma-Aldrich, Saint Louis, MO, USA). After 8 h, cells were washed with phosphate-buffered saline (PBS; Life technologies) and lysed in 200 µl passive lysis buffer (Dual-Luciferase Reporter Assay System, Promega). Twenty-five µl lysate was used to measure the firefly as well as *Renilla* luciferase activities (Dual-Luciferase Reporter Assay System, Promega) in a Centro XS LB 960 microplate luminometer (Berthold Technologies GmbH, Germany). Data were expressed as the ratio of firefly and *Renilla* luciferase activities (fold induction of basal).

Statistical analysis

All data are represented as mean ± SEM (standard error of the mean). Significant differences between two groups were identified using Student's **t** test (paired and unpaired) (**P** < 0.05). Comparisons of more than two groups were performed with one-way ANOVA followed by Student-Newman-Keuls test (**P** < 0.05). GraphPad Prism 4.0 (GraphPad Software, Inc., San Diego, CA) was used for all statistical analysis.

Discussion

We report that Fsh stimulates, via PKA, Sertoli cell Igf3 production, which then promotes germ cell proliferation/differentiation in the adult zebrafish testis in a steroid-independent manner. In vertebrates, the pituitary gonadotropins Fsh and Lh control testicular development and function by regulating the activity of local signaling systems, involving sex steroids and growth factors (Pierce and Parson, 1981; McLachlan et al., 1996), small RNAs (van den Driesche et al., 2014; ; Panneerdoss et a., 2012) and epigenetic switches (Shirakawa et al., 2013). Fish are an interesting model in this regard (Schulz et al., 2010). Despite an overall similarity among vertebrates, evolution seems to have taken a different path in teleost fish with respect to the gonadotropic hormones and their biological activities. Early in teleost evolution, the genomic environment of the hormone-specific *lhb* gene has changed and syntenic homology was lost to tetrapod gonadotropins but also to teleost *fshb* genes (Kanda et al., 2011). Moreover, the spectrum of biological activity of teleost gonadotropins deviates from the tetrapod scheme: Leydig cells express not only the receptor for Lh (typically seen in all vertebrates) but also the receptor for Fsh (Ohta et al., 2007; García-López et al., 2009 and 2010; Chauvigné et al., 2012). Finally,

information on circulating gonadotropin levels in salmonid species showed that during the several months long testicular growth period, plasma Fsh (and androgen) levels were elevated while plasma Lh levels remained very low or undetectable and did not increase clearly until approaching the actual spawning season (Gomez et al., 1999; Campbell et al., 2003); also in juvenile sea bass, a perciform fish, Fsh is sufficient to trigger full spermatogenesis and androgen production (Mazón et al., 2014). Taken together, this information suggests that Fsh is the main gonadotropin driving the initial stages of spermatogenesis in fish by regulating both Leydig and Sertoli cell activities (Planas et al., 1993; Schulz et al., 2010). We focused our experimental approach for the present study on the Sertoli cell-mediated effects of Fsh by neutralizing its steroidogenic activity.

In rodents, FSH can modulate the production of Sertoli cell growth factors that are relevant either for SSC self-renewal (e.g. GDNF, Meng et al., 2000; FGF2, Kubota et al., 2004), or for SSC differentiation (e.g. activin, Nagano et al., 2003). We became interested in the insulin/Igf signaling system in this regard in zebrafish since this system appears to have an evolutionary conserved role in regulating male germ line stem cell proliferation, while relatively little is known about this role in the vertebrate testis. Moreover, an additional genome duplication in the vertebrate branch leading towards teleost fish generated a new paralogue of the Igf family, Igf3, showing a preferential or exclusive expression in gonadal tissue (Wang et al., 2008; Zou et al., 2009; Li et al., 2011, 2012), hence rendering fish excellently suited models for studying this question.

In *C. elegans* expression of insulin/Igf ligand occurs in somatic cells while receptor signaling is crucial in germ cells (Michaelson et al., 2010; Hubbard, 2011). In *D. melanogaster*, receptor signaling is relevant in both

germ and somatic cells (McLeod et al., 2010). In mice, receptors are also expressed in germinal and somatic compartments of the testis, but receptor ablation is only dispensable in the germ cell compartment, while Sertoli cell-specific loss of the IGF receptor alone or in combination with losing the insulin receptor, compromises Sertoli cell proliferation and hence adult testis size and sperm output (Pitetti et al., 2013). Also in fish, Igf receptors were found in both the somatic and the germinal compartment in trout (LeGac et al., 1996) and seabream (Perrot et al., 2000). This is consistent with our conclusion based on analyzing Igf receptor gene expression in wild type and germ cell-free mutant zebrafish. Genetic evidence as regards the cell type-specific effects of receptor gene ablation is missing in zebrafish, but recent work showed that thyroid hormone-induced proliferation of Sertoli cells involved elevated *igf3* transcript levels that was compromised (but not fully blocked) by the Igf receptor antagonist NVP-AEW541 (Morais et al., 2013). One way of understanding the results on Igf3-stimulated germ cell development presented here is assuming a direct stimulatory effect of Igf3 on germ cells, as has been shown for Igf1 in primary spermatogonial cell culture studies of trout (Loir et al., 1999). In the eel however, on the other hand, Igf does not have stimulatory effects on germ cell proliferation *per se* but is required as permissive factor for androgen-mediated stimulation of spermatogenesis (Nader et al., 1999), so that in eel Igf signaling might regulate Sertoli cell functions relevant for facilitating androgen action.

In mammals, Igf ligands can reach the testes from extratesticular sites via the circulation but can also be derived from different testicular cell types, such as Sertoli and Leydig cells in mice (Villalpando et al., 2008) or different germ cell types in stallion (Yoon et al., 2010). Both somatic

(Leydig and Sertoli cells) and germ cells (mainly spermatogonia and spermatocytes) have been identified as Igf1 sources also in fish (LeGac et al., 1996; Perrot et al., 2000; Berishvili et al., 2006). However, the gonads appear to be the main site of *igf3* gene expression in adult fish (see above). In tilapia, Igf3 protein was described as interstitial (Li et al., 2012) whereas in zebrafish, we detected both mRNA and protein exclusively in Sertoli cells. Moreover, comparative expression analysis revealed that *igf3* is the only igf family member significantly stimulated by Fsh in zebrafish testis. This effect is suppressed in the presence of protein kinase A (PKA) inhibitor H89, indicating that Fsh increased *igf3* transcript levels via the PKA pathway. Similarly, human chorionic gonadotropin (hCG) increased via PKA/cAMP *igf3* transcript levels in zebrafish ovarian tissue (Li et al., 2010; Irwin and van der Kraak, 2012), and purified salmonid Fsh also increased igf3 expression in rainbow trout testes (Sambroni et al., 2013). One puzzling aspect of results obtained for rainbow trout is the observation that androgens inhibited basal and Fsh-stimulated increases in *igf3* transcript levels (Sambroni et al., 2013). This is puzzling since also in trout, both Fsh (Sambroni et al., 2013) and androgens (Rolland et al., 2013) stimulated spermatogenesis, and Fsh is a potent steroidogenic hormone that stimulated androgen production (Sambroni et al., 2013). In zebrafish, on the other hand, the Fsh-induced increase in *igf3* transcript levels was slightly reduced when androgen production was blocked by trilostane, suggesting a mild, positive influence of androgens on *igf3* transcript levels, which was confirmed experimentally (Fig. 1E). The reason for this discrepancy between trout and zebrafish is not clear at present but might be related to the fact that trout testis was studied at the beginning of pubertal development while we used testis tissue from adult males. Also in adult tilapia, androgen-

insufficiency following estrogen exposure led to reduced *igf3* transcript levels (Berishvili et al., 2010), while exposure of adult male zebrafish to clotrimazole, a fungicide up-regulating testicular transcript levels for steroidogenic genes and the Fsh receptor (Baudiffier et al., 2012) reduced *igf3* mRNA levels. Altogether, these data suggest that Fsh (and to a lesser extent also androgens, at least in adults) is a major stimulator of testicular *igf3* transcript levels.

Considering that (i) growth hormone (Gh) increased testicular *igf1* transcript levels in trout in Sertoli cells, spermatogonia and spermatocytes (LeGac et al., 1996), that (ii) Gh receptors were found in trout testis tissue, in particular in Sertoli cell-enriched fractions (Gomez et al., 1998), and that (iii) recombinant human IGF1 stimulated the proliferation of trout spermatogonia in primary cell culture experiments (Loir, 1999), it seemed possible that piscine Gh may have an effect on testicular *igf3* transcript levels as well. However, since Gh did not change *igf3* mRNA levels in zebrafish ovarian tissue (Irwin and van der Kraak, 2012), and since overexpression of Gh had no effect on *igf3* transcript levels in tilapia testes (Berishvili et al., 2010), we did not study this aspect in adult zebrafish testis.

Treatment with Fsh acutely increased Igf3 transcript and protein levels in Sertoli cells contacting type A spermatogonia in zebrafish testes. Similarly, FSH increased IGF1 secretion in immature rat Sertoli cells (Cailleau et al., 1990), hCG elevated zebrafish ovarian *igf3* transcript levels (Li et al., 2010; Irwin and van der Kraak, 2012), and Fsh elevated testicular *igf3* transcript levels in zebrafish (Baudiffier et al., 2012) and trout (Sambroni et al., 2013). The localization of Igf3 suggests that next to potential autocrine functions to stimulate Sertoli cell proliferation (Morais et al., 2013), Igf3 could stimulate the proliferation of type A_{und} and type A_{diff}

spermatogonia in zebrafish. However, we also found evidence for stimulatory effects of Igf3 on later germ cell stages: the appearance of type B spermatogonia and of primary spermatocytes was induced (Fig. 5B) and elevated transcript levels of *dazl* were found (Fig. 4), a gene typically expressed by type B spermatogonia and leptotene/zygotene spermatocytes (Chen et al., 2013). Future studies will have to show what germ cell stage(s) can respond directly to Igf3; some of the effects observed with regard to type B spermatogonia and spermatocytes might be indirect consequences of Igf3 actions on type A spermatogonia. Moreover, Igf binding proteins might modulate Igf effects (e.g. Loir and LeGac, 1994), and our preliminary work has shown that several Igf binding proteins are expressed in the zebrafish testis. Hence, the physiological system determining the biological activity of Igf3 in the testis is most likely composed of additional players not yet studied.

While recombinant zebrafish Igf3 showed clear biological activity at 100 ng/ml, we noted a bell-shaped dose-response curve when studying gene expression (Fig. 4). It is possible that the reduced biological activity at high Igf3 concentrations is related to observations made at high insulin concentrations that led to ligand self-association; the resulting dimers then compromised receptor signaling (Knudsen et al., 2013). As regards the IGF receptor, high ligand concentrations were reported to induce a negative co-operativity at the receptor (De Meyts, 1994).

In the experiments with recombinant Fsh, we noted that not only spermatogonial and meiotic stages were stimulated but that – different from effects observed after incubations with recombinant Igf3 – also post-meiotic stages were induced by Fsh while the production of biologically active steroids was blocked by trilostane. This is remarkable in two ways. First,

previous work using immature Japanese eel (*Anguilla japonica*) testis tissue suggested that the stimulatory effect of Fsh on spermatogenesis can be fully explained by the Fsh-triggered production of androgens in Leydig cells (Ohta et al., 2007). Clearly, this is different in adult zebrafish testes, where the stimulatory effects of Fsh are not compromised by an inhibitor of androgen production but by an inhibitor of Igf receptor signaling. As discussed above, this might reflect species-specific differences in the cellular site of Igf action that, in eel, seems to be of a permissive, potentially autocrine manner on Sertoli cells facilitating androgen action. The second aspect of interest is the conclusion that Fsh has a broader range of stimulatory actions on spermatogenesis (e.g. including stimulation of post-meiotic stages) than Igf3, suggesting that other, non-steroidal mediators of Fsh action may be responsible for the transition through the two meiotic divisions and entrance into spermiogenesis. In this regard, zebrafish Fsh shows a broader range of biological activity than in rodents where androgen but not FSH action is required to complete meiosis and spermiogenesis (De Gendt et al., 2004; O'Shaughnessy et al, 2009)

When activating type A_{und} spermatogonia by exposing zebrafish to a cytostatic drug that depleted spermatogenesis, transcript levels of *igf3* were up-regulated and those of *amh* (anti-Müllerian hormone) were down-regulated during the initial recovery phase (Nóbrega et al., 2010). Moreover, other experiments showed that Fsh suppressed testicular *amh* transcript levels in adult zebrafish, thereby preventing inhibitory effects Amh would otherwise have exerted on androgen production and, independent of androgen action, also preventing inhibitory effects of Amh on proliferation and differentiation of type A spermatogonia (Skaar et al., 2011). It therefore appears that Fsh stimulates zebrafish spermatogenesis by controlling the

balance between inhibitory (e.g. Amh) and stimulatory (e.g. Igf3, sex steroids) signals. However, additional, yet to be described factors and components, including those mediating stimulatory effects on meiotic and post-meiotic stages will probably be involved in mediating Fsh action on spermatogenesis. Transcriptomic analyses are ongoing to identify potential testicular Fsh target genes in zebrafish. Finally, we conclude that the main progress realized in this thesis is that Fsh effects shown to be mediated by growth factors, and not only by steroids, as it was previously reported. Moreover, there is very little knowledge in vertebrates in general about the local "translation" of the Fsh and androgen signals into paracrine signals/cell-cell signals that modulate germ cell behaviour. The new paralogue of Igf gene, Igf3, seems to represent an evolutionary conserved insulin/Igf signaling, while Amh effects on SSC behavior described first time in fish should be tested in mammals (or other tetrapods) as it might be a conserved but yet undetected effect.

Supplemental Figures Legend

Figure S1. mRNA expression of Igfs and type 1 Igf receptors in zebrafish testis.

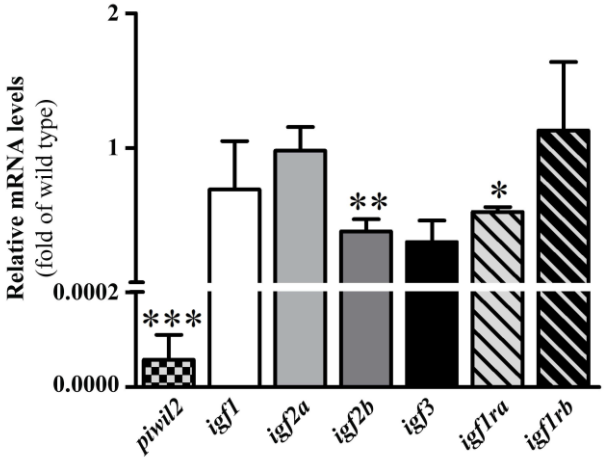

Relative mRNA levels of Igf ligands and Igf receptors in *piwil1*$^{(-/-)}$ zebrafish testis.The columns represent the fold change of the relative mRNA levels (mean ± SEM) in the *piwil1*$^{(-/-)}$ zebrafish over wild type zebrafish.
Bars marked with * ($p < 0.05$), ** ($p < 0.01$), or *** ($p < 0.001$) indicate significant differences between the different outbred fish.

Figure S2. Steroidogenic capacity of zebrafish testis under different treatments.

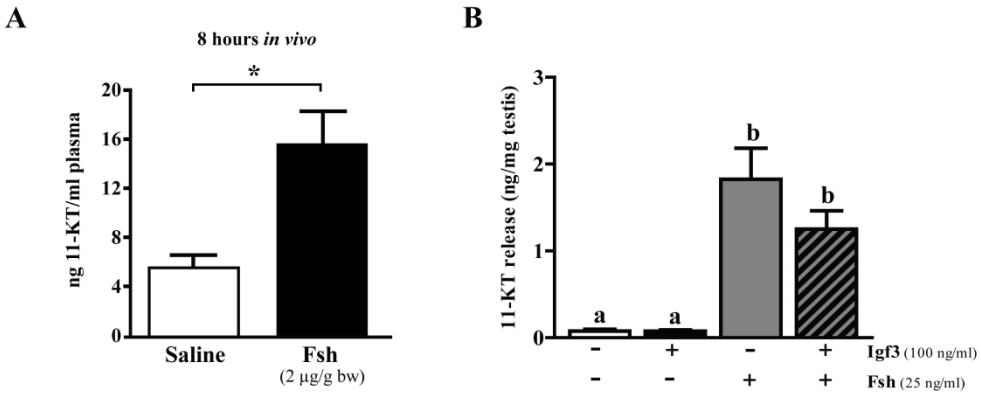

(A) Androgen release and mRNA levels of Sertoli cell- and Leydig cell-specific genes in response to 500 ng/mL recombinant zebrafish Fsh (rzfFsh). (**B)** Increased 11-KT plasma levels (ng/mL) 8 hours after injection with saline or rzfFsh (100 ng/g of body weight) into the coelomic cavity. **(C)** 11-KT released (ng/mg of testis weight) by the zebrafish testis treated with rzfIgf3, in the absence or presence of rzfFsh in cultured for 1 day. The columns in **A** represent the fold change of the relative mRNA levels in the treated group over its respective control (mean ± SEM). Asterisks indicate significant differences ($p < 0.05$) between treated and control groups, different letters indicate significant differences ($p < 0.05$) between different treatment conditions.

Figure S3. Immunohistochemistry analyses in *vasa::egfp*zebrafish testis treated with rzfFsh.

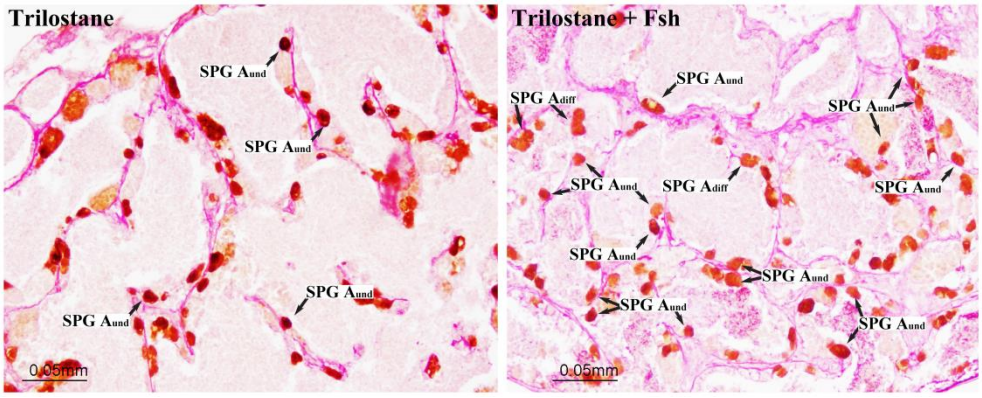

Immunostaining of Gfp in *vasa::egfp* zebrafish testis after incubation for 7 days with trilostane (25 µg/ml) in the absence or presence of rzfFsh (500 ng/mL) showing an increased number (see Fig. 2C) of type A SPG while in the presence of rzfFsh. Periodic acid–Schiff (PAS) reaction was used as a counterstained. SPG A_{und}, spermatogonia type A undifferentiated.

Table S1: Primers used for gene expression studies by real-time, quantitative PCR.

Target gene	References	Primers	Sequences (5'→3')
amh	Schulz et al., 2007	AD (Fw) AE (Rv) AF (probe)	CTCTGACCTTGATGAGCCTCATTT GGATGTCCCTTAAGAACTTTTGCA FAM-ATTCCACAGGATGAGAGGCTCCCATCC-TAMRA
gsdf	Leal et al., 2009	2366 (Fw) 2367 (Rv)	CATCTGCGGGAGTCATTGAAA CAGAGTCCTCCGGCAAGCT
efl1α	Schulz et al., 2007	AG (Fw) AH (Rv) AI (probe)	GCCGTCCCACCGACAAG CCACACGACCCACAGGTACAG FAM-CTCCAATTTTGTACACATCCTGAAGTGGCA-TAMRA
igf1	Chen et al., 2013	2394 (Fw) 2395 (Rv)	CCCAGGACACCAAAGAAACCTA CGGCTCGAGTTCTTCTGATGA
igf2a	De Waal, 2009	3079 (Fw) 3080 (Rv)	GGCTTCTATTTCAGTCGACCAACTAG ACTAAAACAACACTCCTCCACAATCC
igf2b	De Waal, 2009	3077 (Fw) 3078 (Rv)	CTGCCATGGATGATTACCATGTATT CATGGACAATGACAGAACGAAGAC
igf3	Morais et al., 2013	2680 (Fw) 2681 (Rv)	TGTGCGGAGACAGAGGCTTT CGCCGCACTTTCTTGGATT
igf1ra	Morais et al., 2013	2362 (Fw) 2363 (Rv)	TACATCGCTGGCAACAAGCA TCATTGAAACTGGTCCTTATGCAAT
igf1rb	Morais et al., 2013	2595 (Fw) 2596 (Rv)	GTGCTGGTCCTCTCCACACTCT TTACCGATGTCGTTGCCAATATC
shippo1	Leal et al., 2009	2791 (Fw) 2792 (Rv)	GATGCCTGGAGACATGACCAA CAAAGGAGAAGCTGGGAGCTTT
sycp3l	Leal et al., 2009	2730 (Fw) 2731 (Rv)	AGAAGCTGACCCAAGATCATTCC AGCTTCAGTTGCTGGCGAAA
fshr	De Waal et al., 2009	2552 (Fw) 2553 (Rv)	GAGGATTCCCAGTAATGCTTTCCT TCTATCTCACGAATCCCGTTCTTC
lhr	De Waal et al., 2009	2548 (Fw) 2549 (Rv)	CGCTCAGTACCATCCAATGCT TTGAAGGCATGGCTCTCTATTTCT
pgr	Chen et al., 2009	2901 (Fw) 2902 (Rv)	GGATTGTCAGATGGTCCAAATCTC GCCCATCCAGGAATACTGAATTAGT
fgf8	Present work	2470 (Fw) 2471 (Rv)	TTTTGCTACTATGCTCAGGTAACCA GTCCGTCACCTTACTTTGCTCACT
ar	De Waal et al., 2008	2412 (Fw) 2413 (Rv)	ACGTGCCTGGCGTGAAAA CAAACCTGCCATCCGTGAAC
star	Leal et al., 2009	2546 (Fw) 2547 (Rv)	CCTGGAATGCCTGAGCAGAA ATCTGCACTTGGTCGCATGAC
cyp17a1	Leal et al., 2009	2773 (FW) 2774 (Rv)	GGGAGGCCACGGACTGTTA CCATGTGGAACTGTAGTCAGCAA
dazl	Chen et al., 2013	3104 (Fw) 3105 (Rv)	AGTGCAGACTTTGCTAACCCTTATGTA GTCCACTGCTCCAAGTTGCTCT
piwil1	Chen et al., 2013	2542 (Fw) 2543 (Rv)	GATACCGCTGCTGGAAAAAGG TGGTTCTCCAAGTGTGTCTTGC
piwil2	Morais et al., 2013	2994 (Fw) 2995 (Rv)	TGATACCAGCAAGAAGAGCAGATCT ATTTGGAAGGTCACCCTGGAGTA

Table S2: Primers use to generate DNA templates for DIG-labeled cRNA probe syntheses for *in situ* hybridization and to amplify and mutate the zebrafish *igf3* promoter sequences

Target gene	References	Primers	Sequences (5'→3')
igf3 – ISH	Present work	2878[a] (Fw) 2879[b] (Rv)	T3Rpps-GGGCCAGAGCACGCTGCG T7Rpps-GGATGTGAGAGATGAATGTTGGCGT
igf3 – promoter (2.0 kb)	Present work	3482[c] (Fw) 3486[d] (Rv)	5'-GCGGTACCGGTGTTACTATGTAACCAGCTCTCCTA-3' 5'-CCCATGGTGGCGGCGTCTGATGGCATGTCTTTTT-3'
igf3 – promoter (1.0 kb)	Present work	3484[c] (Fw) 3486[d] (Rv)	5'-GCGGTACCGGCTGTGTAAAAACGTGCTGGAT-3' 5'-CCCATGGTGGCGGCGTCTGATGGCATGTCTTTTT-3'
CRE – site mutagenesis	Present work	3770 (Fw) 3771 (Rv)	5'- CACAGTATCCATATCACAAAACTCAAATGGAGCCAAACTGCTTTCA TGAACGAGACAATG-3' 5'-CATTGTCTCGTTCATGAAAGCAGTTTGGCTCCATTTGAGTTTTGT GATATGGATACTGTG-3'
ATF-1 – site mutagenesis	Present work	3775 (Fw) 3776 (Rv)	5'-CTCTAATTTAAGATGGATAACATCAGTAATGAAGTTTTGGTTTGT TGATGTTTAAT-3' 5'-ATTAAACATCAACAAACCAAAACTTCATTACTGATGTTATCCATCTT AAATTAGAG-3'

[a]Primer 2878 contain the T3 RNA polymerase promoter sequence (underlined) at its 5'-end (T3Rpps; 5'-GGGCGGGT GTTATTAACCCTCACTAAAGGG-3').

[b]Primer 2879 contain the T7 RNA polymerase promoter sequence (underlined) at its 5'-end (T7Rpps;5'-CCGGGGGG TGTAATACGACTCACTATAGGG-3').

[c]The underlined GGTACC sequence in primers 3482 and 3484 represent a *Kpn* I restriction enzyme site.

[d]The underlined CCATGG in primer 3486 represents a *Nco* I restriction enzyme site.

Production of recombinant zebrafish Igf3

The expression construct for recombinant zebrafish Igf3 (rzfIgf3) production comprised the entire coding sequence of *igf3* (GenBank accession number: HQ241070) lacking the signal peptide sequence. The relevant sequence was amplified with primers introducing a 5' *Bam* HI and a 3' *Not* I restriction site, digested with these enzymes and ligated into a *Bam* HI-*Not* I compatible proprietary mammalian expression vector introducing three C-terminal Strep II tags (U-Protein Express B.V., Utrecht, The Netherlands). Recombinant zebrafish Igf3 was transiently produced in HEK293 cells (U-Protein Express B.V., Utrecht, The Netherlands). After five days, the medium was harvested by centrifugation, concentrated over a Quixstand hollow fiber (GE Healthcare, Eindhoven, the Netherlands) with a 5 kDa molecular weight cut-off cartridge (GE Healthcare) to ~250 ml, and diafiltrated against 1 l phosphate-buffered saline containing 500 mM NaCl. The concentrated and diafiltrated medium (~210 ml) was collected and aggregates were removed by centrifugation (at 5252 g for 5 minutes). The recombinant protein solution was incubated with 3 ml Strep-tactin Sepharose HP (GE Healthcare) at 11^{o}C for 2 h, which was then loaded into a 3 ml Tricorn column (GE Healthcare) and eluted with a gradient of desthiobiotin (0 - 2.5 mM) in phosphate-buffered saline containing 500 mM NaCl. The peak fraction was further purified by gelfiltration using a Superdex 75 26/600 prep grade column, which was equilibrated in PBS. Peak fractions were analyzed using SDS PAGE and fractions containing hormone were pooled and concentrated to 1.31 ml recombinant zebrafish Igf3 solution (1.28 mg/ml) using a Vivaspin 20 ml (10 kDa MW cut-off) centrifugal concentrators (Sartorius, Göttingen, Germany).

Analysis of the putative promoter sequence of the zebrafish *igf3* gene

The sequence upstream of the *igf3* translation site was obtained from ENSEMBL (http://www.ensembl.org/Danio_rerio/Info/Index). Promoter constructs of ~2.0 kb and ~1.0 kb were PCR amplified with zebrafish genomic DNA as template using forward primers 3482 and 3484 in combination with reverse primer 3486 (see Suppl. Table S2). PCR products were cloned into pGL3 basic vector preceding the firefly luciferase gene (Promega, Leiden, The Netherlands). Two distinct but homologous versions of *igf3* promoter sequences, most likely originating from DNA polymorphism in the zebrafish population, were obtained. Putative transcription factor-binding sites involved in the transcriptional control of *igf3* gene expression were identified by TESS software (www.cbil.upenn.edu/tess), and presumed CRE and ATF-1 transcription factor-binding sites (at ~-610 bp and ~-260 bp) identified in the *igf3* promoter constructs were scrambled by site-directed mutagenesis using primers 3770-3771 and 3775-3776 (see Suppl. Table S2). All cloned DNA fragments were sequence verified.

Human embryonic kidney (HEK 293T cells were grown under 5% CO_2 in Dulbecco's modified Eagle's medium (DMEM), supplemented with antibiotic solution (100 IU/ml), 2 mM glutamine and 10% fetal bovine serum (FBS; all from Life technologies). One day prior to transfection in 24-well plates, 1.5 x 10^5 cells were seeded per well. Cells were transiently co-transfected by polyethylenimine (PEI) with a total of 850 ng plasmid DNA, consisting of 500 ng *igf3* promoter construct, 100 ng TK-*Renilla* luciferase plasmid and 250 ng empty pcDNA3 vector. For each *igf3* promoter construct, transfection was performed in triplicate. Twenty-four h after transfection, the medium was replaced with or without 10 µM

forskolin (Sigma-Aldrich, Saint Louis, MO, USA). After 8 h, cells were washed with phosphate-buffered saline (PBS; Life technologies) and lysed in 200 µl passive lysis buffer (Dual-Luciferase Reporter Assay System, Promega). Twenty-five µl lysate was used to measure the firefly as well as *Renilla* luciferase activities (Dual-Luciferase Reporter Assay System, Promega) in a Centro XS LB 960 microplate luminometer (Berthold Technologies GmbH, Germany). Data were expressed as the ratio of firefly and *Renilla* luciferase activities (fold induction of basal).

Reference List

Abel, M.H., Baban, D., Lee, S., Charlton, H.M., and O'Shaughnessy, P.J. (2009). Effects of FSH on testicular mRNA transcript levels in the hypogonadal mouse. J Mol Endocrinol *42*, 291-303.

Abel, M.H., Wootton, A.N., Wilkins, V., Huhtaniemi, I., Knight, P.G., and Charlton, H.M. (2000). The effect of a null mutation in the follicle-stimulating hormone receptor gene on mouse reproduction. Endocrinology *141*, 1795-1803.

Almeida, F.F., Kristoffersen, C., Taranger, G.L., and Schulz, R.W. (2008). Spermatogenesis in Atlantic cod (Gadus morhua): a novel model of cystic germ cell development. Biol Reprod *78*, 27-34.

Baudiffier, D., Hinfray, N., Ravaud, C., Creusot, N., Chadili, E., Porcher, J.M., Schulz, R.W., and Brion, F. Effect of in vivo chronic exposure to clotrimazole on zebrafish testis function. Environ Sci Pollut Res Int *20*, 2747-2760.

Baudiffier, D., Hinfray, N., Vosges, M., Creusot, N., Chadili, E., Porcher, J.M., Schulz, R.W., and Brion, F. A critical role of follicle-stimulating hormone (Fsh) in mediating the effect of clotrimazole on testicular steroidogenesis in adult zebrafish. Toxicology *298*, 30-39.

Berishvili, G., Baroiller, J.F., Eppler, E., and Reinecke, M. (2010) Insulin-like growth factor-3 (IGF-3) in male and female gonads of the tilapia: development and regulation of gene expression by growth hormone (GH) and 17alpha-ethinylestradiol (EE2). Gen Comp Endocrinol *167*, 128-134.

Berishvili, G., Shved, N., Eppler, E., Clota, F., Baroiller, J.F., and Reinecke, M. (2006). Organ-specific expression of IGF-I during early development of bony fish as revealed in the tilapia, Oreochromis niloticus, by in situ hybridization and immunohistochemistry: indication for the particular importance of local IGF-I. Cell Tissue Res *325*, 287-301.

Bogerd, J., Blomenrohr, M., Andersson, E., van der Putten, H.H., Tensen, C.P., Vischer, H.F., Granneman, J.C., Janssen-Dommerholt, C., Goos, H.J., and Schulz, R.W. (2001). Discrepancy between molecular structure and ligand selectivity of a testicular follicle-stimulating hormone receptor of the African catfish (Clarias gariepinus). Biol Reprod *64*, 1633-1643.

Cailleau, J., Vermeire, S., and Verhoeven, G. (1990). Independent control of the production of insulin-like growth factor I and its binding protein by cultured testicular cells. Mol Cell Endocrinol *69*, 79-89.

Campbell, B., Dickey, J.T., and Swanson, P. (2003). Endocrine changes during onset of puberty in male spring Chinook salmon, Oncorhynchus tshawytscha. Biol Reprod *69*, 2109-2117.

Chauvigne, F., Verdura, S., Mazon, M.J., Duncan, N., Zanuy, S., Gomez, A., and Cerda, J. Follicle-stimulating hormone and luteinizing hormone mediate the androgenic pathway in Leydig cells of an evolutionary advanced teleost. Biol Reprod *87*, 35.

Chen, S.X., Bogerd, J., Schoonen, N.E., Martijn, J., de Waal, P.P., and Schulz, R.W. A progestin (17alpha,20beta-dihydroxy-4-pregnen-3-one) stimulates early stages of spermatogenesis in zebrafish. Gen Comp Endocrinol *185*, 1-9.

Chiarini-Garcia, H., Hornick, J.R., Griswold, M.D., and Russell, L.D. (2001). Distribution of type A spermatogonia in the mouse is not random. Biol Reprod *65*, 1179-1185.

Chiarini-Garcia, H., Raymer, A.M., and Russell, L.D. (2003). Non-random distribution of spermatogonia in rats: evidence of niches in the seminiferous tubules. Reproduction *126*, 669-680.

De Gendt, K., Swinnen, J.V., Saunders, P.T., Schoonjans, L., Dewerchin, M., Devos, A., Tan, K., Atanassova, N., Claessens, F., Lecureuil, C., et al. (2004). A Sertoli cell-selective knockout of the androgen receptor causes spermatogenic arrest in meiosis. Proc Natl Acad Sci U S A *101*, 1327-1332.

De Meyts, P. (1994). [Insulin receptors and mechanism of action of insulin and of insulin-like growth factors]. Bull Mem Acad R Med Belg *149*, 181-190; discussion 190-184.

de Rooij, D.G. (2009). The spermatogonial stem cell niche. Microsc Res Tech *72*, 580-585.

de Rooij, D.G., and Griswold, M.D. Questions about spermatogonia posed and answered since 2000. J Androl *33*, 1085-1095.

de Rooij, D.G., and van Beek, M.E. Computer simulation of the rodent spermatogonial stem cell niche. Biol Reprod *88*, 131.

de Waal, P.P., Leal, M.C., Garcia-Lopez, A., Liarte, S., de Jonge, H., Hinfray, N., Brion, F., Schulz, R.W., and Bogerd, J. (2009). Oestrogen-induced androgen insufficiency results in a

reduction of proliferation and differentiation of spermatogonia in the zebrafish testis. J Endocrinol *202*, 287-297.

de Waal, P.P., Wang, D.S., Nijenhuis, W.A., Schulz, R.W., and Bogerd, J. (2008). Functional characterization and expression analysis of the androgen receptor in zebrafish (Danio rerio) testis. Reproduction *136*, 225-234.

Dierich, A., Sairam, M.R., Monaco, L., Fimia, G.M., Gansmuller, A., LeMeur, M., and Sassone-Corsi, P. (1998). Impairing follicle-stimulating hormone (FSH) signaling in vivo: targeted disruption of the FSH receptor leads to aberrant gametogenesis and hormonal imbalance. Proc Natl Acad Sci U S A *95*, 13612-13617.

Garcia-Lopez, A., Bogerd, J., Granneman, J.C., van Dijk, W., Trant, J.M., Taranger, G.L., and Schulz, R.W. (2009). Leydig cells express follicle-stimulating hormone receptors in African catfish. Endocrinology *150*, 357-365.

Garcia-Lopez, A., de Jonge, H., Nobrega, R.H., de Waal, P.P., van Dijk, W., Hemrika, W., Taranger, G.L., Bogerd, J., and Schulz, R.W. Studies in zebrafish reveal unusual cellular expression patterns of gonadotropin receptor messenger ribonucleic acids in the testis and unexpected functional differentiation of the gonadotropins. Endocrinology *151*, 2349-2360.

Gomez, J. M., Weil, C., Ollitrault, M., Lebail, P.Y., Breton, B., LeGac, F., 1999. Growth hormone (GH) and gonadotropin subunit gene expression and pituitary and plasma changes during spermatogenesis and oogenesis in rainbow trout (*Oncorhynchus mykiss*). Gen. Comp Endocrinol. 113**,** 413-428.

Gomez, J.M., Loir, M., and Le Gac, F. (1998). Growth hormone receptors in testis and liver during the spermatogenetic cycle in rainbow trout (Oncorhynchus mykiss). Biol Reprod *58*, 483-491.

Hess, R.A., and Renato de Franca, L. (2008). Spermatogenesis and cycle of the seminiferous epithelium. Adv Exp Med Biol *636*, 1-15.

Houwing, S., Berezikov, E., and Ketting, R.F. (2008). Zili is required for germ cell differentiation and meiosis in zebrafish. EMBO J *27*, 2702-2711.

Houwing, S., Kamminga, L.M., Berezikov, E., Cronembold, D., Girard, A., van den Elst, H., Filippov, D.V., Blaser, H., Raz, E., Moens, C.B., et al. (2007). A role for Piwi and piRNAs in germ cell maintenance and transposon silencing in Zebrafish. Cell *129*, 69-82.

Hubbard, E.J. Insulin and germline proliferation in Caenorhabditis elegans. Vitam Horm *87*, 61-77.

Irwin, D.A., and Van Der Kraak, G. Regulation and actions of insulin-like growth factors in the ovary of zebrafish (Danio rerio). Gen Comp Endocrinol *177*, 187-194.

Johnston, D.S., Russell, L.D., Friel, P.J., and Griswold, M.D. (2001). Murine germ cells do not require functional androgen receptors to complete spermatogenesis following spermatogonial stem cell transplantation. Endocrinology *142*, 2405-2408.

Kanda, S., Okubo, K., and Oka, Y. Differential regulation of the luteinizing hormone genes in teleosts and tetrapods due to their distinct genomic environments--insights into gonadotropin beta subunit evolution. Gen Comp Endocrinol *173*, 253-258.

Knudsen, L., Hansen, B.F., Jensen, P., Pedersen, T.A., Vestergaard, K., Schaffer, L., Blagoev, B., Oleksiewicz, M.B., Kiselyov, V.V., and De Meyts, P. Agonism and antagonism at the insulin receptor. PLoS One *7*, e51972.

Krovel, A.V., and Olsen, L.C. (2002). Expression of a vas::EGFP transgene in primordial germ cells of the zebrafish. Mech Dev *116*, 141-150.

Kubota, H., Avarbock, M.R., and Brinster, R.L. (2004). Growth factors essential for self-renewal and expansion of mouse spermatogonial stem cells. Proc Natl Acad Sci U S A *101*, 16489-16494.

Kumar, T.R., Wang, Y., Lu, N., and Matzuk, M.M. (1997). Follicle stimulating hormone is required for ovarian follicle maturation but not male fertility. Nat Genet *15*, 201-204.

Leal, M.C., Cardoso, E.R., Nobrega, R.H., Batlouni, S.R., Bogerd, J., Franca, L.R., and Schulz, R.W. (2009). Histological and stereological evaluation of zebrafish (Danio rerio) spermatogenesis with an emphasis on spermatogonial generations. Biol Reprod *81*, 177-187.

Leal, M.C., de Waal, P.P., Garcia-Lopez, A., Chen, S.X., Bogerd, J., and Schulz, R.W. (2009). Zebrafish primary testis tissue culture: an approach to study testis function ex vivo. Gen Comp Endocrinol *162*, 134-138.

Legac, E., Vaugier, G.L., Bousquet, F., Bajelan, M., and Leclerc, M. (1996). Primitive cytokines and cytokine receptors in invertebrates: the sea star Asterias rubens as a model of study. Scand J Immunol *44*, 375-380.

Li, J., Liu, Z., Wang, D., and Cheng, C.H. Insulin-like growth factor 3 is involved in oocyte maturation in zebrafish. Biol Reprod *84*, 476-486.

Li, M., Wu, F., Gu, Y., Wang, T., Wang, H., Yang, S., Sun, Y., Zhou, L., Huang, X., Jiao, B., et al. Insulin-like growth factor 3 regulates expression of genes encoding steroidogenic enzymes and key transcription factors in the Nile tilapia gonad. Biol Reprod *86*, 163, 161-110.

Loir, M. (1994). In vitro approach to the control of spermatogonia proliferation in the trout. Mol Cell Endocrinol *102*, 141-150.

Loir, M. (1999). Spermatogonia of rainbow trout: III. In vitro study of the proliferative response to extracellular ATP and adenosine. Mol Reprod Dev *53*, 443-450.

Loir, M., and Le Gac, F. (1994). Insulin-like growth factor-I and -II binding and action on DNA synthesis in rainbow trout spermatogonia and spermatocytes. Biol Reprod *51*, 1154-1163.

Loveland, K.L, and Robertson, D.M. (2005). The TGF b superfamily in Sertoli cell biology. In: Griswold, M and M Skinner. (Eds.),. *Sertoli Cell Biology*. Maryland Heights, Missouri: Elsevier Science: 227–247.

Mazón, M.J, Gómez, A., Yilmaz, O., Carrillo, M., Zanuy, S. (2014). Administration of Follicle-Stimulating Hormone In Vivo Triggers Testicular Recrudescence of Juvenile European Sea Bass (*Dicentrarchus labrax*)*Biol Reprod* January 2014 90 (1) 6, 1-10; published ahead of print November 20, 2013,doi:10.1095/biolreprod.113.110569

Mclachlan, R.I, Wreford, N.G, O'Donnell, L., De Kretser, D.M, Robertson, D.M. (1996) The endocrine regulation of spermatogenesis: independent roles for testosterone and FSH. J *Endocrinol.;*148:1–9.

McLeod, C.J., Wang, L., Wong, C., and Jones, D.L. Stem cell dynamics in response to nutrient availability. Curr Biol *20*, 2100-2105.

Meng, X., Lindahl, M., Hyvonen, M.E., Parvinen, M., de Rooij, D.G., Hess, M.W., Raatikainen-Ahokas, A., Sainio, K., Rauvala, H., Lakso, M., et al. (2000). Regulation of cell fate decision of undifferentiated spermatogonia by GDNF. Science *287*, 1489-1493.

Michaelson, D., Korta, D.Z., Capua, Y., and Hubbard, E.J. Insulin signaling promotes germline proliferation in C. elegans. Development *137*, 671-680.

Miura, T., Miura, C., Konda, Y., and Yamauchi, K. (2002). Spermatogenesis-preventing substance in Japanese eel. Development *129*, 2689-2697.

Morais, R.D., Nobrega, R.H., Gomez-Gonzalez, N.E., Schmidt, R., Bogerd, J., Franca, L.R., and Schulz, R.W. Thyroid Hormone Stimulates the Proliferation of Sertoli Cells and Single Type A Spermatogonia in Adult Zebrafish (Danio rerio) Testis. Endocrinology.

Nader, M.R., Miura, T., Ando, N., Miura, C., and Yamauchi, K. (1999). Recombinant human insulin-like growth factor I stimulates all stages of 11-ketotestosterone-induced spermatogenesis in the Japanese eel, Anguilla japonica, in vitro. Biol Reprod *61*, 944-947.

Nagano, M., Ryu, B.Y., Brinster, C.J., Avarbock, M.R., and Brinster, R.L. (2003). Maintenance of mouse male germ line stem cells in vitro. Biol Reprod *68*, 2207-2214.

Nobrega, R.H., Greebe, C.D., van de Kant, H., Bogerd, J., de Franca, L.R., and Schulz, R.W. Spermatogonial stem cell niche and spermatogonial stem cell transplantation in zebrafish. PLoS One *5*.

Oatley, J.M., Oatley, M.J., Avarbock, M.R., Tobias, J.W., and Brinster, R.L. (2009). Colony stimulating factor 1 is an extrinsic stimulator of mouse spermatogonial stem cell self-renewal. Development *136*, 1191-1199.

Ohta, T., Miyake, H., Miura, C., Kamei, H., Aida, K., and Miura, T. (2007). Follicle-stimulating hormone induces spermatogenesis mediated by androgen production in Japanese eel, Anguilla japonica. Biol Reprod *77*, 970-977.

O'Shaughnessy, P.J., Monteiro, A., Verhoeven, G., De Gendt, K., and Abel, M.H. Effect of FSH on testicular morphology and spermatogenesis in gonadotrophin-deficient hypogonadal mice lacking androgen receptors. Reproduction *139*, 177-184.

Panneerdoss, S., Chang, Y.F., Buddavarapu, K.C., Chen, H.I., Shetty, G., Wang, H., Chen, Y., Kumar, T.R., and Rao, M.K. Androgen-responsive microRNAs in mouse Sertoli cells. PLoS One *7*, e41146.

Perrot, V., Moiseeva, E.B., Gozes, Y., Chan, S.J., and Funkenstein, B. (2000). Insulin-like growth factor receptors and their ligands in gonads of a hermaphroditic species, the gilthead seabream (Sparus aurata): expression and cellular localization. Biol Reprod *63*, 229-241.

Pierce, J.G, Parsons, T.F. (1981). Glycoprotein hormones: structure and function. *Annu Rev Biochem.*;50:465–495.

Pitetti, J.L., Calvel, P., Zimmermann, C., Conne, B., Papaioannou, M.D., Aubry, F., Cederroth, C.R., Urner, F., Fumel, B., Crausaz, M., et al. An essential role for insulin and IGF1 receptors in regulating sertoli cell proliferation, testis size, and FSH action in mice. Mol Endocrinol *27*, 814-827.

Planas, J. V., Swanson, P., Dickhoff, W. W. (1993). Regulation of testicular steroid production in vitro by gonadotropins (GTH I and GTH II) and cyclic AMP in Coho salmon (*Oncorhynchus kisutch*). Gen. Comp. Endocrinol. 91**,** 8-24.

Rolland, A.D., Lardenois, A., Goupil, A.S., Lareyre, J.J., Houlgatte, R., Chalmel, F., and Le Gac, F. Profiling of androgen response in rainbow trout pubertal testis: relevance to male gonad development and spermatogenesis. PLoS One *8*, e53302.

Russell, L.D., Ren, H.P., Sinha Hikim, I., Schulze, W., and Sinha Hikim, A.P. (1990). A comparative study in twelve mammalian species of volume densities, volumes, and numerical densities of selected testis components, emphasizing those related to the Sertoli cell. Am J Anat *188*, 21-30.

Sambroni, E., Lareyre, J.J., and Le Gac, F. Fsh controls gene expression in fish both independently of and through steroid mediation. PLoS One *8*, e76684.

Sambroni, E., Rolland, A.D., Lareyre, J.J., and Le Gac, F. FSH and LH have common and distinct effects on gene expression in rainbow trout testis. J Mol Endocrinol *50*, 1-18.

Savitt, J., Singh, D., Zhang, C., Chen, L.C., Folmer, J., Shokat, K.M., and Wright, W.W. The in vivo response of stem and other undifferentiated spermatogonia to the reversible inhibition of glial cell line-derived neurotrophic factor signaling in the adult. Stem Cells *30*, 732-740.

Schulz, R.W., de Franca, L.R., Lareyre, J.J., Le Gac, F., Chiarini-Garcia, H., Nobrega, R.H., and Miura, T. Spermatogenesis in fish. Gen Comp Endocrinol *165*, 390-411.

Schulz, R.W., Menting, S., Bogerd, J., Franca, L.R., Vilela, D.A., and Godinho, H.P. (2005). Sertoli cell proliferation in the adult testis--evidence from two fish species belonging to different orders. Biol Reprod *73*, 891-898.

Schulz, R.W., van Dijk, W., Chaves-Pozo, E., Garcia-Lopez, A., de Franca, L.R., and Bogerd, J. Sertoli cell proliferation in the adult testis is induced by unilateral gonadectomy in African catfish. Gen Comp Endocrinol *177*, 160-167.

Shetty, G., Weng, C.C., Meachem, S.J., Bolden-Tiller, O.U., Zhang, Z., Pakarinen, P., Huhtaniemi, I., and Meistrich, M.L. (2006). Both testosterone and follicle-stimulating hormone independently inhibit spermatogonial differentiation in irradiated rats. Endocrinology *147*, 472-482.

Shetty, G., Wilson, G., Huhtaniemi, I., Boettger-Tong, H., and Meistrich, M.L. (2001). Testosterone inhibits spermatogonial differentiation in juvenile spermatogonial depletion mice. Endocrinology *142*, 2789-2795.

Shirakawa, T., Yaman-Deveci, R., Tomizawa, S., Kamizato, Y., Nakajima, K., Sone, H., Sato, Y., Sharif, J., Yamashita, A., Takada-Horisawa, Y., et al. An epigenetic switch is crucial for spermatogonia to exit the undifferentiated state toward a Kit-positive identity. Development *140*, 3565-3576.

Skaar, K.S., Nobrega, R.H., Magaraki, A., Olsen, L.C., Schulz, R.W., and Male, R. Proteolytically activated, recombinant anti-mullerian hormone inhibits androgen secretion, proliferation, and differentiation of spermatogonia in adult zebrafish testis organ cultures. Endocrinology *152*, 3527-3540.

Tadokoro, Y., Yomogida, K., Ohta, H., Tohda, A., and Nishimune, Y. (2002). Homeostatic regulation of germinal stem cell proliferation by the GDNF/FSH pathway. Mech Dev *113*, 29-39.

van den Driesche, S., Sharpe, R.M., Saunders, P.T., and Mitchell, R.T. Regulation of the germ stem cell niche as the foundation for adult spermatogenesis: a role for miRNAs? Semin Cell Dev Biol *29*, 76-83.

Villalpando, I., Lira, E., Medina, G., Garcia-Garcia, E., and Echeverria, O. (2008). Insulin-like growth factor 1 is expressed in mouse developing testis and regulates somatic cell proliferation. Exp Biol Med (Maywood) *233*, 419-426.

Wang, D.S., Jiao, B., Hu, C., Huang, X., Liu, Z., and Cheng, C.H. (2008). Discovery of a gonad-specific IGF subtype in teleost. Biochem Biophys Res Commun *367*, 336-341.

Yano, A., Suzuki, K., and Yoshizaki, G. (2008). Flow-cytometric isolation of testicular germ cells from rainbow trout (Oncorhynchus mykiss) carrying the green fluorescent protein gene driven by trout vasa regulatory regions. Biol Reprod *78*, 151-158.

Yomogida, K., Yagura, Y., Tadokoro, Y., and Nishimune, Y. (2003). Dramatic expansion of germinal stem cells by ectopically expressed human glial cell line-derived neurotrophic factor in mouse Sertoli cells. Biol Reprod *69*, 1303-1307.

Yoon, M.J., Berger, T., and Roser, J.F. Localization of insulin-like growth factor-I (IGF-I) and IGF-I receptor (IGF-IR) in equine testes. Reprod Domest Anim *46*, 221-228.

Yoshida, S., Sukeno, M., and Nabeshima, Y. (2007). A vasculature-associated niche for undifferentiated spermatogonia in the mouse testis. Science *317*, 1722-1726.

Zhou, Q., and Griswold, M.D. (2008). Regulation of spermatogonia. StemBook [Internet]. Cambridge (MA): Harvard Stem Cell Institute.

Zou, S., Kamei, H., Modi, Z., and Duan, C. (2009). Zebrafish IGF genes: gene duplication, conservation and divergence, and novel roles in midline and notochord development. PLoS One *4*, e7026.

CHAPTER 7

SUMMARIZING DISCUSSION

Summarizing Discussion

Spermatogonial Stem Cell and their niche in teleosts

Spermatogenesis relies on the continuous proliferation of spermatogonial stem cells (SSCs), the male germ line stem cells in the testis. Two modes of SSC proliferation are predicted in the testis: one, when a SSC divides to produce two new, individual stem cells (self-renewal), and another, in which two differentiated cells are formed (differentiation). In the differentiation pathway, an interesting behavior is seen in all animals. At the end of the first mitosis, the two daughter cells remain interconnected by a cytoplasmic bridge. These bridges are also formed during all subsequent germ cell divisions. In this way, the germ cells derived from a given SSC form a clone of interconnected cells. All members of the same clone are in the same stage of development, synchronised in their activities via the cytoplasmic bridges (Schulz et al., 2010). Therefore, SSCs are found among the single germ cells present in the seminiferous tubules. In the rodent testes, type A undifferentiated spermatogonia (As) are the single spermatogonia in the seminiferous epithelium (De Rooij and Russell, 2000; De Rooij and Griswold, 2012), contacting the basement membrane at the their basal part, and Sertoli cells at their latero-apical part (Hess and França, 2007). In fish, type A undifferentiated spermatogonia are also the single germ cells in the testis (Chapter 2). However, these cells are completely enveloped by cytoplasmic projections of Sertoli cells, forming the morpho-functional unit of fish spermatogenesis, the spermatogenic cyst. In this context, Chapter 2 proposed a new nomenclature for spermatogonial generations in fish based on high-resolution microscopy criteria also used for rodents (Chiarini-Garcia and Meistrich, 2008), thereby allowing a unifying nomenclature for the spermatogonia in mammals and fish (and

potentially in vertebrates in general). In the past, two types of spermatogonia were described in fish; primary or type A spermatogonia to designate the larger and single spermatogonia; and secondary or B spermatogonia to the subsequent generations of spermatogonia (smaller and grouped cells) (Billard, 1984; Selman and Wallace, 1986). Apart from the significant differences in morphology among the several spermatogonial generations, the previous classification did not take in account the presence of SSCs in fish. Using high resolution microscopy, and criteria mainly based on nuclear morphology also used for rodent spermatogonia (shape, size, characteristics of nuclear envelope, amount of chromatin), 4 types of spermatogonia were proposed for (zebra)fish: type A undifferentiated spermatogonia (A_{und}) (single cells), type A differentiated spermatogonia (A_{diff}), type B early spermatogonia (B early), and type B late spermatogonia (B late) (Chapter 2).

Interestingly, two subtypes were found among type A undifferentiated spermatogonia: one larger with an irregular nuclear membrane and clear chromatin referred to as A_{und}*, and another smaller type, with a smoothly shaped nuclear membrane and dark chromatin referred to as A_{und} (Chapter 2). Further studies are necessary to clarify if these cells are separated from each other by mitosis or by a differentiation process. Also the degree of stemness and the gene expression of these cells still remain unknown. However, throughout vertebrate species, morphologically and/or functionally different types of single spermatogonia have been described, and in some cases differences in their characteristics have been described. In the human testis, for example, two types (designated pale and dark [A_{pr} and A_{al}], based on tinctorial properties) of single type A spermatogonia are present and can play distinct roles as “reserve” and

"active" stem cell, respectively (Schulze, 1979; 1988). Also, recent experiments suggested the existence of "true" and "potential" spermatogonial stem cells in mice testes, since after severe testicular damage (e.g. after chemo- or radiotherapy), both types of undifferentiated spermatogonia (A_{pr} and A_{al}) can act as stem cells (Nakagawa et al., 2007). Alternatively, recent studies showed that among the single spermatogonia, few are considered stem cells in the rodent testis, and the stemness is not strictly associated with single cells only (Nakagawa et al., 2010). For example, clones of A_{al} can fragment to form new single type A spermagonia (stem cells) (Nakagawa et al., 2010).

To study the stemness of type A undifferentiated (A_{und}*/A_{und}) spermatogonia in zebrafish, two approaches were applied (Chapter 3). Adult stem cells are characterized by long-term retaining labels used to study S-phase DNA duplication, the background being that stem cells are quiescent or at least much slower cycling cells than more differentiated cells in their surroundings. Hence, techniques to localize these "long-term label retaining cells" (LRCs) have been used to locate putative stem cells (Potten et al., 2002; Zhang et al., 2003). For that purpose, BrdU (bromodeoxyuridine) is commonly used that can be traced by immunohistochemistry. S-phase cells incorporate the label, but this labelling is diluted and eventually lost during subsequent cell divisions. Therefore, cells quiescent after the last S-phase or slowly cycling cells, i.e. stem cell candidates, retain BrdU over a long period. Using the LRC approach in zebrafish testes showed that only the single type A undifferentiated spermatogonia (both, A_{und}* and A_{und}) were able to retain BrdU over a long period (3 weeks) (Chapter 3). Two kinetic patterns of BrdU dilution were seen among these cells: the BrdU label remained constant for A_{und}* over a long period, while for A_{und}, the BrdU

label was diluted/lost faster (Chapter 3). Therefore, it is suggested that both, A_{und}* and A_{und}, can be candidates of SSCs in zebrafish testes, with A_{und}* potentially acting as "reserve", and A_{und} as "active" SSC.

The second approach to study stem cells is based on their capacity to regenerate after transplantation in injured or damaged tissue (Brinster & Zimmermann, 1994; Brinster & Avarbock, 1994), exploiting the fact that only stem cells are able to recover tissue functionality after transplantation. For SSCs, Brinster and colleagues (1994) have developed this germ cell transplantation technique for rodents, and showed donor-derived spermatogenesis in animals, in which endogenous spermatogenesis had been depleted. In zebrafish, germ cell transplantation using large, single *vasa::egfp*-expressing type A spematogonia donor cells has been developed (Chapter 3), demonstrating donor-derived spermatogenesis in recipient fish where endogenous spermatogenesis was depleted with a cytotastic agent (busulfan). Moreover, sexual plasticity of the SSCs has been shown using this technique, since SSCs were able to differentiate into female germ line cells after transplantation into zebrafish ovaries (Chapter 3). Taken together, LRC and transplantation studies indicate that single type A undifferentiated spermatogonia show SSC characteristics in the zebrafish testes.

After demonstrating the stemness among single type A spermatogonia, LRCs were localized to examine if they show a preferential location in the testes, compatible with the concept of a stem cell niche. LRC (A_{und}*/A_{und}) were – of course enveloped by Sertoli cells – preferentially distributed near the interstitial compartment, where Leydig cells, peritubular myoid cells and blood vessels are located (Chapter 3). Similarly, studies in rodents have demonstrated that SSCs are preferentially located to areas of the seminiferous tubules neighboring the interstitium and blood vessels, also

referred to as niche (Chiarini-Garcia et al., 2001; 2003; Yoshida et al., 2007). In the niche, SSCs are able to retain their undifferentiated state (De Rooij, 2009; De Rooij and van Beek, 2013). When germ cells leave the niche, or when signaling characteristics change in the niche, SSCs are likely to produce differentiating progenitor cells (De Rooij, 2009; De Rooij and Griswold, 2012). In zebrafish, the niche conditions may provide the structural and molecular environment to sustain undifferentiated SSCs over long periods, and to regulate stem cell-specific properties, including the decision to be quiescent, or – when cell cycling – to self-renew, or to differentiate. This is clearly seen when exposing zebrafish to a cytotastic drug (busulfan) that depletes spermatogenesis (Chapter 3). The quick recovery of spermatogenesis that is seen within a few days indicates a change in the microenvironment of the SSCs now favoring differentiation instead of self-renewal or quiescence (Chapter 3). Growth factors produced by testicular somatic cells are considered important players for this microenvironment. Amh (anti-Müllerian hormone) and Igf3 (insulin-like growth factor 3) have emerged as potential growth factor candidates, since a remarkably change in their expression is seen during the initial recovery phase of zebrafish spermatogenesis (Chapter 3). The next chapters (4, 5, 6) were dedicated to unravel the endocrine and paracrine regulation of SSC niche, focussing on the roles of these growth factors.

Endocrine and Paracrine Regulation of SSC niche

In vertebrates, the pituitary gonadotropins Fsh and Lh control testicular development and function by regulating the activity of local signaling systems, involving sex steroids and growth factors (Pierce and Parson, 1981; McLachlan et al., 1996), small RNAs (Panneerdoss et al.,

2012) and epigenetic switches (Shirakawa et al., 2013). Despite an overall similarity among vertebrates, evolution seems to have taken a different path in teleost fish with respect to the gonadotropic hormones and their biological activities. Early in teleost evolution, the genomic environment of the hormone-specific *lhb* gene has changed and syntenic homology was lost to tetrapod gonadotropins but also to teleost *fshb* genes (Kanda et al., 2011). Since differences in the regulation of Lh synthesis and secretion may have resulted in differences in gonadotropin functions, experiments were carried out to examine the biological roles of zebrafish Fsh and Lh on testis function (Chapter 4), using recombinant zebrafish hormones that were tested in a zebrafish testis tissue culture system (Leal et al., 2009). Gene expression analysis showed that Fsh and Lh have different downstream mechanisms in zebrafish testes. For example, Fsh increased the expression of a number of steroidogenesis-related genes, while Lh did not (Chapter 4). Still, both gonadotropins are potently stimulating androgen release *in vitro* and *in vivo*, although Fsh seems somewhat more active than Lh (Chapter 4). This is explained because Leydig cells express not only the receptor for Lh (typically seen in all vertebrates) but also the receptor for Fsh (Ohta et al., 2007; García-López et al., 2009, 2010; Chauvigné et al., 2012). Therefore, piscine Fsh exerts its role through Leydig and Sertoli cells, in contrast to the mammalian Fsh, which acts only on Sertoli cell functions. These differences led us to speculate the capacity of Fsh to support both steroidogenesis and spermatogenesis on a long-term basis in fish, whereas Lh-stimulated steroidogenesis might be a short-term process, possibly restricted to periods during which peak steroid levels are required, while Fsh-stimulated steroidogenesis might be a sustained process (Chapter 4). In this context, it is interesting to note that elevated circulating levels of androgens and Fsh

coincided with active spermatogonial proliferation in Chinook salmon, and Fsh is stimulates spermatogonial proliferation in juvenile Japanese eel (Ohta et al., 2007) and androgen production in several fish species (Planas et al., 1993; Ohta et al., 2007; García-López et al., 2009,2010; Mazón et al., 2014). Taken together, this information suggests that Fsh might be the main gonadotropin driving spermatogonial proliferation in fish through androgen release in Leydig cells, and through growth factor production in Sertoli cell (Schulz et al., 2010). We focused our experimental approach on the Sertoli cell-mediated effects of Fsh by neutralizing its steroidogenic activity (Chapters 5,6). Neutralizing the androgens effects, we showed that recombinant Fsh promoted not only spermatogonial proliferation, but also meiotic and post-meiotic phases of zebrafish spermatogenesis (Chapter 6). This is a remarkable observation, because previous work using immature Japanese eel (*Anguilla japonica*) testis tissue suggested that the stimulatory effect of Fsh on spermatogenesis can be fully explained by the Fsh-triggered production of androgens in Leydig cells (Ohta et al., 2007). Clearly, this is different in adult zebrafish testes, where stimulatory effects of Fsh are not compromised by inhibiting the production of biologically active androgens. This led us to search for growth factors possibly involved in Fsh-induced but androgen-independent spermatogenesis. To further simplify the experimental situation for our search for testicular factors regulating spermatogonial development, a side-step was made to a species showing clear seasonal reproductive cycles. We focused on the first developmental steps, the transition from a quiescent, immature testis towards an activation of spermatogonial proliferation, by analyzing differentially expressed genes in Atlantic salmon testis tissue samples just before versus just after the start of the seasonal testis growth period using microarrays (Bogerd and Schulz,

in preparation). Among the differentially expressed genes, an inhibitory and a stimulatory growth factor were identified. The identity and biological activity of the inhibitory factor, anti-Müllerian hormone (Amh) has been described previously in juvenile eel (Miura et al., 2002) and adult zebrafish (Chapter 5). The identity and biological activity of a stimulatory factor, a recently described new member of the Igf (insulin-like growth factor) family, named Igf3 (Wang et al., 2008; Zou et al., 2009) has been evaluated in zebrafish spermatogenesis for the first time here (Chapter 6).

Anti-Müllerian hormone (Amh) has been characterized as a glycoprotein in mammals, and is a member of the transforming growth factor beta (TGF-β). The namesake function of Amh is to induce regression of the Müllerian ducts during male sex differentiation in tetrapod vertebrates (Josso, 1986, 2008). However, fish do not have Müllerian ducts, and Amh might exert different, evolutionary older functions in fish. Experiments using zebrafish testes tissue cultures showed that plasmin-cleaved, but not uncleaved, Amh inhibited gonadotropin-stimulated androgen production (Chapter 5). Moreover, we found higher Amh protein levels in Sertoli cells contacting type A spermatogonia than in Sertoli cells contacting more advanced stages of germ cells, and that recombinant Amh inhibited the proliferation as well as differentiation of type A spermatogonia (Chapter 5); this inhibitory effect of Amh on spermatogonial development was also found in the presence of exogenous androgens, i.e. is exerted independent of Amh's inhibitory effect on androgen production. Interestingly, recombinant zebrafish Fsh decreased *amh* transcript levels. In conclusion, zebrafish Amh inhibited both steroidogenesis and spermatogenesis by independent mechanisms, and was down-regulated by Fsh .

Finally, Chapter 6 showed that insulin/Igf ligands are crucial signals for germ cell survival and development in zebrafish. This seems to be an evolutionary conserved function of this family of growth factors. Fish are particularly interesting in this regard since the additional round of genome duplication that has occurred in the branch leading to teleost fish resulted in the appearance of a new paralogue of the Igf family, Igf3 (Wang et al., 2008; Zou et al., 2009). Interestingly, Igf3 has assumed a preferential or exclusive expression in gonadal tissue in fishes (Wang et al., 2008; Li et al., 2011). Moreover, comparative expression analysis revealed that *igf3*, expressed in Sertoli cells contacting type A spermatogonia, is the only Igf family member significantly stimulated by Fsh in zebrafish testis. This effect is suppressed in the presence of the protein kinase A (PKA) inhibitor H89, indicating that Fsh increased *igf3* transcript levels via the PKA pathway. Recombinant zebrafish Igf3 promoted the proliferation of type A_{und} and type A_{diff} spermatogonia in zebrafish. Moreover, stimulatory effects of Igf3 on later germ cell stages were also evident: the appearance of type B spermatogonia and of primary spermatocytes was induced and elevated transcript levels of *dazl* were found, a gene typically expressed by type B spermatogonia and leptotene/zygotene spermatocytes (Chen et al., 2013). Further, stimulatory effects of Igf3 and Fsh on spermatogonial proliferation and differentiation were compromised when interfering with Igf receptor signaling in the zebrafish testes. Altogether, we conclude in Chapter 6 that one aspect of Fsh-stimulated spermatogenesis is to increase Sertoli cell production of Igf3 that then promoted germ cell development in zebrafish testes.

Figure 1 summarizes our main findings, and presents an overview of the most recent data on endocrine and paracrine regulation of zebrafish spermatogenesis, focusing in the spermatogonial phase. In this summarizing scheme, Fsh is the key endocrine signal that modulates the balance between stimulatory (Igf3) and inhibitory (Amh) growth factors in Sertoli cells, which together with androgens produced by Leydig cells, regulate the spermatogonial activity in zebrafish testis. Future work will likely provide information that will further increase the complexity of this scheme.

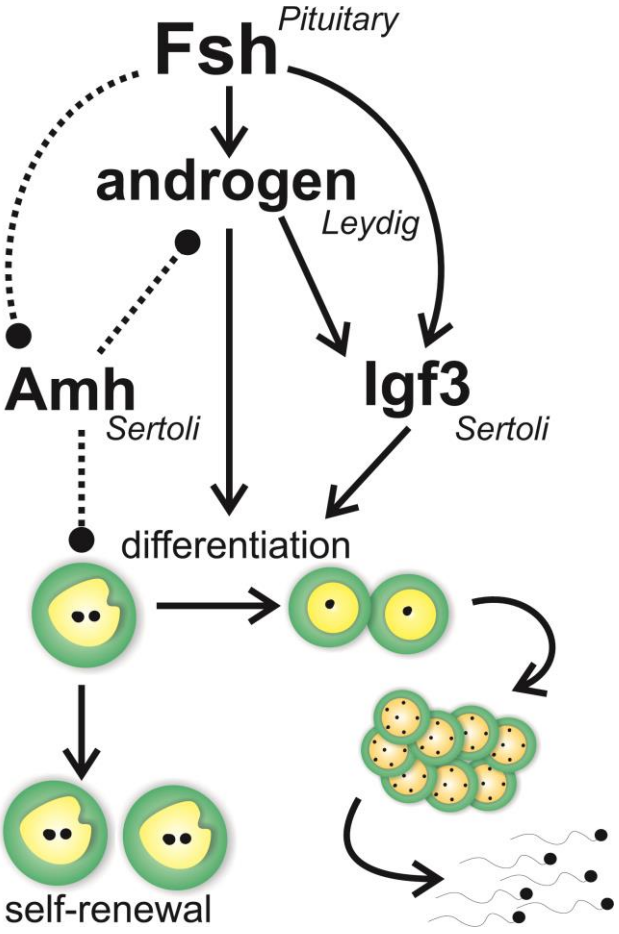

Figure 1. Fsh stimulates Leydig cell androgen production, which in turn promotes germ cell differentiation. At the same time, Fsh reduces (stippled line) Sertoli cell expression of anti-Müllerian hormone (Amh) that would otherwise inhibit Leydig androgen production and differentiation of spermatogonia. Fsh also stimulates Sertoli cell expression of insulin-like 3 (Igf3), which promotes germ cell differentiation; androgens also (weakly) stimulate Igf3 production.

Final Remarks

Fsh is one of the main endocrine signals, which stimulates zebrafish spermatogenesis by controlling the balance between inhibitory (e.g. Amh) and stimulatory (e.g. Igf3, sex steroids) signals. However, additional, yet to be described factors and components, including those mediating stimulatory effects on meiotic and post-meiotic stages, are likely to be involved in mediating the stimulatory effects of Fsh on spermatogenesis. Transcriptomic studies are now ongoing in zebrafish and can be useful to identify potential testicular Fsh target genes involved in meiotic and post-meiotic phases, but also in identifying additional factors regulating the spermatogonial phase. Next to the growth factor regulation, it has become evident that small RNA molecules can control several biological processes. No information in this regard is available for zebrafish spermatogenesis so far. Taking in account the advantageous of mirRNAomics and the *in silico* analysis to predict the target genes, it seems a promising aspect to evaluate the role of miRNAs on zebrafish spermatogenesis.

Another interesting aspect for future work refers to the signaling systems used by Amh to modulate steroidogenesis via Leydig cells, and spermatogenesis via Sertoli cells; and the integration of the apparently predominating inhibitory Amh signaling with presumably existing, stimulatory signaling, such as in the case of Igf3, for example. In this regard, ongoing experiments with zebrafish testis tissue cultures incubated with androgens in the presence or absence of Amh are analyzed by RNA sequencing. Previous work (Chapter 5) has shown that Amh blocks androgen-induced spermatogonial proliferation, an experimental condition suitable to identify candidate genes involved in Amh-regulated spermatogenesis via Sertoli or Leydig cells. Interestingly, one of the

transcripts down-regulated by Amh is *igf3*, suggesting that future work should examine also the interaction of stimulatory and inhibitory factors. Finally, we conclude that the main progress realized in this thesis is that Fsh effects shown to be mediated by growth factors, and not only by steroids, as it was previously reported. Moreover, there is very little knowledge in vertebrates in general about the local "translation" of the Fsh and androgen signals into paracrine signals/cell-cell signals that modulate germ cell behaviour. The new paralogue of Igf gene, Igf3, seems to represent an evolutionary conserved insulin/Igf signaling, while Amh effects on SSC behavior described first time in fish should be tested in mammals (or other tetrapods) as it might be a conserved but yet undetected effect.

Reference List

BILLARD R. (1984). Ultrastructural changes in the spermatogonia and spermatocytes of *Poecilia reticulata* during spermatogenesis. *Cell Tissue Res*; 237:219–226.

BRINSTER RL, AVARBOCK MR. (1994). Germline transmission of donor haplotype following spermatogonial transplantation. *Proc Natl Acad Sci USA* 91:11303-11307.

BRINSTER RL, ZIMMERMANN JW. (1994). Spermatogenesis following male germ-cell transplantation. *Proc Natl Acad Sci USA* 91:11298-11302.

CHAUVIGNÉ F, ZAPATER C, GASOL JM, CERDÀ J. (2014). Germ-line activation of the luteinizing hormone receptor directly drives spermiogenesis in a nonmammalian vertebrate. *Proc Natl Acad Sci U S A. 2014* Jan 28;111(4):1427-32. doi: 10.1073/pnas.1317838111. Epub 2014 Jan 13.

CHEN SX, BOGERD J, SCHOONEN NE, MARTIJN J, DE WAAL PP, SCHULZ RW. (2013) A progestin (17alpha,20beta-dihydroxy-4-pregnen-3-one) stimulates early stages of spermatogenesis in zebrafish. *Gen. Comp. Endocrinol.* 185: 1-9.

CHIARINI-GARCIA H, HORNICK JR, GRISWOLD MD, RUSSELL LD. (2001). Distribution of type A spermatogonia in the mouse is not random. *Biol Reprod* 65:1179-1185.

CHIARINI-GARCIA H, RAYMER A, RUSSELL L. (2003). Non-random distribution of spermatogonia in rats: evidence of niches in the seminiferous tubules. *Reprod* 126:669-680.

CHIARINI-GARCIA H, MEISTRICH ML. (2008). High-resolution light microscopic characterization of spermatogonia. *Methods in Molecular Biology*, 450: 95-107.

DE ROOIJ DG AND GRISWOLD MD. (2012). Questions about spermatogonia posed and answered since 2000. *J Androl* 33, 1085-1095.

DE ROOIJ DG AND GRISWOLD MD. (2012). Questions about spermatogonia posed and answered since 2000. *J Androl* 33, 1085-1095.

DE ROOIJ DG AND VAN BEEK ME. (2013). Computer simulation of the rodent spermatogonial stem cell niche. *Biol Reprod* 88, 131.

DE ROOIJ DG, RUSSELL LD. (2000). All you wanted to know about spermatogonia but were afraid to ask. *J Androl* 21:776-798.

DE ROOIJ DG. (2009). The spermatogonial stem cell niche. *Microsc Res Tech* 72(8):580-5.

GARCIA-LOPEZ A, BOGERD J, GRANNEMAN JC, VAN DIJK W, TRANT JM, TARANGER GL, SCHULZ RW. (2009). Leydig cells express follicle-stimulating hormone receptors in African catfish. *Endocrinol* 150(1):357-65.

GARCIA-LOPEZ A, DE JONGE H, NOBREGA RH, DE WAAL PP, VAN DIJK W, HEMRIKA W, TARANGER GL, BOGERD J, SCHULZ RW. (2010). Studies in zebrafish reveal unusual cellular expression patterns of gonadotropin receptor messenger ribonucleic acids in the testis and unexpected functional differentiation of the gonadotropins. *Endocrinol* 151(5):2349-60.

HESS RA, FRANÇA LR. (2007). Spermatogenesis and cycle of the seminiferous epithelium. In: Cheng CY (ed). Molecular mechanisms in spermatogenesis, Landes Bioscience, pp. 1-15.

JOSSO N. (1986). Anti-mullerian hormone. *Clin Endocrinol* (Oxf) 25:331-345.

JOSSO N. (2008). Professor Alfred Jost: the builder of modern sex differentiation. *Sex Dev* 2:55-63.

KANDA S, OKUBO K, OKA Y. (2011). Differential regulation of the luteinizing hormone genes in teleosts and tetrapods due to their distinct genomic environments--insights into gonadotropin beta subunit evolution. *Gen Comp Endocrinol.* 173:253-258.

LEAL MC, DE WAAL PP, GARCIA-LOPEZ A, CHEN SX, BOGERD J, SCHULZ RW. (2009). Zebrafish primary testis tissue culture: An approach to study testis function ex vivo. *Gen Comp Endocrinol* 162(2):134-8.

LI J, LIU Z, WANG D, CHENG CH. (2011). Insulin-like growth factor 3 is involved in oocyte maturation of zebrafish. *Biol Reprod* 2011. 84:476–486.

MAZÓN MJ, GÓMEZ A, YILMAZ O, CARRILLO M, ZANUY S. (2014). Administration of Follicle-Stimulating Hormone In Vivo Triggers Testicular Recrudescence of Juvenile European Sea Bass (*Dicentrarchus labrax*)*Biol Reprod* January 2014 90 (1) 6, 1-10; published ahead of print November 20, 2013,doi:10.1095/biolreprod.113.110569

MCLACHLAN RI, WREFORD NG, O'DONNELL L, DE KRETSER DM, ROBERTSON DM. (1996) The endocrine regulation of spermatogenesis: independent roles for testosterone and FSH. J *Endocrinol.;*148:1–9.

MIURA T, MIURA C, KONDA Y, YAMAUCHI K. (2002). Spermatogenesis-preventing substance in Japanese eel. *Development* 129:2689-2697.

NAKAGAWA T, NABESHIMA Y, YOSHIDA S. (2007). Functional identification of the actual and potential stem cell compartments in mouse spermatogenesis. *Dev Cell* 12(2):195-206.

NAKAGAWA T, SHARMA M, NABESHIMA Y, BRAUN RE, YOSHIDA S. (2010). Functional hierarchy and reversibility within the murine spermatogenic stem cell compartment. *Science* 2;328(5974):62-7.

OHTA T, MIYAKE H, MIURA C, KAMEI H, AIDA K, MIURA T. (2007). Follicle-stimulating hormone induces spermatogenesis mediated by androgen production in Japanese eel, *Anguilla japonica*. *Biol Reprod* 77(6):970-7.

PANNEERDOSS S, CHANG YF, BUDDAVARAPU KC, CHEN HI, SHETTY G, WANG H, CHEN Y, KUMAR TR, RAO MK. (2012) Androgen-Responsive MicroRNAs in Mouse Sertoli Cells. PLoS ONE 7(7): e41146. doi:10.1371/journal.pone.0041146

PIERCE JG, PARSONS TF. (1981). Glycoprotein hormones: structure and function. *Annu Rev Biochem.*;50:465–495.

PLANAS JV, SWANSON P, DICKHOFF WW. (1993). Regulation of testicular steroid production in vitro by gonadotropins (GTH I and GTH II) and cyclic AMP in coho salmon (*Oncorhynchus kisutch*). *Gen Comp Endocrinol* 91(1):8-24.

POTTEN CS, OWEN G, BOOTH D. (2002). Intestinal stem cells protect their genome by selective segregation of template DNA strands. *J. Cell Sci.*115:2381–2388.

SCHULZ RW, DE FRANÇA LR, LAREYRE JJ, LEGAC F, CHIARINI-GARCIA H, NÓBREGA RH & MIURA T (2010). Spermatogenesis in fish. *Gen Comp Endocrinol* 165, 390-411.

SCHULZE C. (1979). Morphological characteristics of the spermatogonial stem cells in man. *Cell Tiss. Res.* 198, 191-199.

SCHULZE C. (1988). Response of the human testis to long-term estrogen treatment: morphology of Sertoli cells, Leydig cells and spermatogonial stem cells. *Cell Tissue Res*. 251, 31-43.

SELMAN K, WALLACE RA. (1986). Gametogenesis in *Fundulus heteroclitus*. Am Zool; 26:173–192.

SHIRAKAWA T, YAMAN-DEVECI R, TOMIZAWA S, KAMIZATO Y, NAKAJIMA K, SONE H, SATO Y, SHARIF J, YAMASHITA A, TAKADA-HORISAWA Y, YOSHIDA S, URA K, MUTO M, KOSEKI H, SUDA T AND OHBO K. (2013). An epigenetic switch is crucial for spermatogonia to exit the undifferentiated state toward a Kit-positive identity. *Development*140, 3565-3576.

WANG DS, JIAO B, HU C, HUANG X, LIU Z, CHENG CHK. (2008). Discovery of a gonad-specific IGF subtype in teleost. *Biochemical and Biophysical Research Communications* 367 336–341. (doi:10.1016/j.bbrc.2007.12.136).

YOSHIDA S, SUKENO M, NABESHIMA Y. (2007). A vasculature-associated niche for undifferentiated spermatogonia in the mouse testis. *Science* 21;317(5845):1722-6.

ZHANG J, NIU C, YE L, HUANG H, HE X, TONG WG, ROSS J, HAUG J, JOHNSON T, FENG JQ. (2003). Identification of the haematopoietic stem cell niche and control of the niche size. *Nature* **425**, 836 841.10.1038/nature02041.

ZOU S, KAMEI H, MODI Z, DUAN C. (2009). Zebrafish IGF genes: gene duplication, conservation and divergence, and novel roles in midline and notochord development. *PLoS ONE* 4 e7026. (doi:10.1371/journal.pone.0007026).

SUMMARY

In stem cell biology, the term niche refers to anatomical and functional dimensions where stem cell populations are established and can be maintained. In these specific places, stem cells are protected from differentiating signals that otherwise might lead to their depletion, and also protected from overproliferation. To achieve this, the cells forming the niche (in the testis: Sertoli cells and interstitial cell types) integrate signals from different sources and produce regulatory output modulating stem cell behavior as necessary for sustaining tissue homeostasis. In this thesis, we studied spermatogonial stem cell (SSC) candidates, their niche, and endocrine and paracrine signals modulating SSC activity in zebrafish. In zebrafish testis, the anatomical location of SSCs was identified by the "label retaining cell" approach. Two populations of SSC candidates ("active" and "reserve") were found surrounded by Sertoli cells near the interstitial compartment. It is assumed that the vertebrate SSC niche integrates signals from Sertoli cells, and from interstitial elements (Leydig cell, myoid, blood vessels) to regulate the SSC activity, also in the zebrafish testes. The stemness and sexual plasticity of these SSC candidates was confirmed by transplantation assays, showing colonization and donor-derived spermatogenesis as well as oogenesis in recipient testis and ovaries. To broaden our knowledge about the functional aspects of the niche (signals), SSCs were activated by treating adult males with a cytostatic agent, and gene expression studies revealed an opposing effect on two growth factors expressed in Sertoli cells, the TGFβ family member Amh (anti-Müllerian hormone), and Igf3 (insulin-like growth factor 3). Recombinant Amh and Igf3 were produced and tested on zebrafish testis explants: Amh blocked spermatogonial differentiation, decreased the proliferation of type A

spermatogonia, and moreover compromised Leydig cell androgen release activated by follicle-stimulating hormone (Fsh). Igf3, on the other hand, stimulated spermatogonial proliferation and differentiation towards meiosis. Finally, this these showed that Fsh reduces Sertoli cell expression of Amh, and at the same time, stimulates Igf3, which promotes germ cell differentiation. Therefore, the main progress realized in this thesis is that the Fsh effects on spermatogenesis are shown to be mediated by growth factors, and not only by steroids, as it was believed previously. Moreover, there is very little knowledge in vertebrates in general about the local "translation" of the Fsh and androgen signals into paracrine signals/cell-cell signals that modulate germ cell behaviour. Igf3, derived from a new paralogue of the *igf1* gene, seems to function via an evolutionary conserved insulin/Igf signaling mechanism, while the Amh effects on SSC behavior, described for the first time in fish, should be tested in mammals (or other tetrapods), as it might be a conserved but yet undetected effect.

SAMENVATTING

In de stamcel biologie, wordt het woord 'niche' gebruikt voor de anatomische en functionele karakteristieken waar stamcelpopulaties zich bevinden en in stand kunnen worden gehouden. Hier worden stamcellen door signaalstoffen afkomstig vanuit de niche beschermd tegen overproliferatie maar ook tegen (te veel) differentierende signalen wat anders tot hun depletie zou kunnen leiden. Daartoe integreren de cellen, die de genoemde niche vormen (in de testis: Sertoli cellen en interstitiele celtypen) diverse signalen vanuit verschillende bronnen, en produceren zo - voor het behoud van de homeostase van het kiemepitheel – een bouquet van regulerende signaalstoffen die het uiteindelijke stamcelgedrag moduleren. In

dit proefschrift hebben we de (kandidaat) spermatogoniale stamcellen (SSC) onderzocht, alsmede hun niche, en endocriene en paracriene signalen die de SSC activiteit in de zebravis moduleren. In de zebravis testis, werd de anatomische locatie van SSCs geïdentificeerd gebruikmakend van een "label-retaining cell" aanpak. Twee populaties van SSC kandidaten ("actief" en "reserve") werden onderscheiden, welke - omringd door Sertoli cellen - zich in de buurt van het interstitiële compartiment bevinden. Aangenomen wordt dat de vertebraten SSC niche signalen afkomstig van Sertoli cellen en van de interstitiële elementen (Leydig cel, myoide, bloedvaten) integreert om de SSC activiteit te reguleren, en dat dit ook zo in de zebravis testes plaatsvindt. De ‘stemness’ en seksuele plasticiteit van deze SSC kandidaten in zebravissen werd bevestigd door transplantatie experimenten, waarbij we zowel kolonisatie als donor afgeleide spermatogenese en oogenese in de respectievelijke ontvangende testis en ovaria konden aantonen. Om onze kennis over functionele aspecten van de niche (en signaalstoffen uit de niche) te verbreden, werden SSCs geactiveerd door volwassen mannetjes met een cytostaticum te behandelen. Met genexpressie studies lieten we vervolgens een antagonistisch e werking zien op twee groeifactoren die in Sertoli cellen tot expressie komen: het TGFβ familielid Amh (anti-Müllerian hormoon) en het Igf3 (insuline-like growth factor 3). Recombinant Amh en Igf3 werden geproduceerd en getest op zebravissen testis *ex vivo*: Amh blokkeerde de differentiatie van spermatogonia, verminderde de proliferatie van type A spermatogonia, en remde bovendien de door follikel-stimulerend hormoon (Fsh) gestimuleerde Leydig cel androgeen afgifte. Igf3, anderzijds, stimuleerde juist de proliferatie, en differentiatie richting meiose, van de spermatogonia. Tenslotte lieten we zien dat Fsh de expressie van Amh in Sertoli cellen vermindert, en tegelijkertijd de expressie van Igf3, dat de

kiemceldifferentiatie bevordert, stimuleert. De belangrijkste bevinding van dit proefschrift is dan ook dat de Fsh effecten op de spermatogenese worden gemedieerd door groeifactoren, en niet alleen door steroïden, zoals voorheen werd gedacht. Bovendien draagt dit proefschrift bij aan het verbreden van de tot nu toe bij vertebraten in het algemeen vrij beperkte kennis over de lokale "vertaling" van Fsh en androgeen signalen in paracriene signalen die het kiemcelgedrag moduleren. Het Igf3, afkomstig van een nieuwe paraloog van het zebravissen *igf1* gen, lijkt via een evolutionair geconserveerd insuline/Igf signaleringsmechanisme op de spermatogenese in te werken, terwijl de Amh effecten op het SSC gedrag, voor het eerst beschreven voor vissen, in zoogdieren (of andere viervoeters) getest zouden moet worden omdat Amh ook bij hogere vertebraten een geconserveerde, maar nog niet ontdekte functie bij de regulatie van het SSC gedrag zou kunnen vertonen.

ACKNOWLEDGEMENTS

I would like to thank Dr. Rüdiger W Schulz for all guidance during all these years. I am extremely grateful for everything I have learnt with you; you are the BEST supervisor ever!! Your enthusiasm, support and confidence were very important to develop this work. THANK YOU FOR ALL!!! Apart of the work, I have to confess that I spent a great time with you, including Irish pub, Caipirinha drinks after work, travel to Conferences, Xmas's parties and our travel to Brazil.

Next to "Rüdiger", my other mentor, who I'm very glad to have met, Dr. Jan Bogerd. As I used to say, Jan is the pope of the molecular biology, and he helped me a lot with molecular things, which I did not know when I started my Phd. Apart of that, it was very nice our talks about science, life, and all the rest during lunch table!! We spent very nice time in Brazil which I will not forget!! Also I will not forget his kind present, the "ei warmer"… THANK YOU FOR ALL!!

I would like to thank my Brazilian mentor, Dr. Luiz Renato de França, a person who I admire and I'm extremely grateful to have indicated me to do the Phd in the Netherlands. Without doubts, "Luiz" have influenced significantly my scientifical life and I'm really glad for that. Thank you very much!!

I also have to thank my promoter, Dr. Sander van den Heuvel, head of the Developmental Biology Division at Utrecht University, who gave me the chance to perform my Phd in his group. Thank you for everything and for the given support.

Dr. Dick van der Horst, the former head of the "Endocrinology and Metabolism" group, the group in which I started my Phd. Thank you "Dick" for being my promoter in the first year and thank you for your kindness and all your help. Also I would like to thank your wife (Bernadette) for the nice French "crepes"!!

All the other members of the "Endocrinology and Metabolism" group, Kees, Koert, Rob, Jana, Antoinette, I'm very glad to have met you, and it was very to share nice moments together.

Dr. Dick de Rooij, a person who I only knew from the papers. Thank you very much for the talks, suggestions in the work and for the nice "laughs" during lunch time.

Dr. Rune Male and his student Katrine Skaar, for the collaboration in test the biological functions of the recombinant zebrafish Amh, which they produced in Bergen.

Three people are really special for me. Henk van de Kant, Joke, and Wytske.

Henk was always beside me, being a technician, a friend, and a father while I was in the Netherlands. I have learnt a lot with you about immunohistochemistry! You "rock" in the lab with your radio/music and immunos!!

Joke, you were so so helpful in everything in the lab, in orderings and I really enjoyed to talk with you during lunch, drinks and parties. And it was very nice to hear about your trips around the world.

Finally, Wytske. I really enjoyed to work with you in the RIA lab, your talks about your grandchildren, Frisland, and your trips. I enjoyed a lot, and I missed when you left the lab!

I also want to thank people from "Aquarium" for taking care of the animals. Henk Schriek, Ko, Cor, Henk my BIG THANK for all. And of course for the nice music!!!

All the master students who helped me with the work: Caaj, Joana, Natasha, Joran, Sergio, Laura, Aristea, Maryvonne, Pieter, and the last one Marina. Thank you for all!!!! Everyone is special and without you I could not do all the experiments by myself.

The former Phd students and PostDocs from the group "Endocrinology and Metabolism": Fernanda, Paul, Chen, Ángel, Hugo, Rob.

In special, I have to thank, Paul de Waal, who showed me everything in the beginning and with patience taught me his "secrets" in the lab!! THANK YOU!!

The current Phd students and PostDoc in the group: Roberto, Michelle, Luiz Henrique, Lazaro, Diego Safian, and Diego Crespo. It has been really nice to work with you!!! In special, I have to thank Roberto, who nowadays I admire as person and scientist!! Without his efforts, Igf3 chapter will not be the same!!

Miriam van Hattum, thank you for the help in many aspects, like bringing me to the City Hall to register until advices about life!! Thank you for your friendship!!

My friend, Rosen, who was my landlord but now a big friend!! Thank you for all your patience with me, especially after almost burning and flooding your house. Stay friend forever!!

My church friends from the choir, A BIG THANK to all of you!! (Renza, Giu, Ratna, Emmy, Oscar, André, Claudia, Bart, Rosa, Rohan, Thais, Ariadne, and all!!!) Life in the Netherlands would not be the same without you. We are one!!

To my brazilian students; Emanuel, Melanie, Andrés, Aldo, Marcos, Juliana, Arno, Sheryll, Elisandra, Charles, Lucas, Gabi, Mirella. Thank you for your support and help!!

My parents, Luiz and Eliane, who gave me life and with all efforts educated me to be this person who I'm. I'm eternally grateful for understanding my absence, during almost 4 years, and for all given support. I love you!!

In this family context, I want to thank my little brother, Juliano, who is following my steps in the academic field but in the pathology field. I love you so much!!

Finally, I would like to thank the financial support to develop this work: Utrecht University, the Brazilian funding agencies (CNPq/FAPESP), LIFE cycle project (European Union), and the Norwegian grants.

Rafael Henrique Nóbrega

CURRICULUM VITAE

I was born on the 31st of May 1981 in Campinas (Brazil), one of the main cities in São Paulo State. I graduated in Biology (Bachelor) at São Paulo State University (UNESP), Botucatu at the end of 2003, receiving an award as best student in the academic record ranking (Diploma Horacio Passos). After that, I continued by master studies in the post-graduate program "Cellular and Structural Biology" at the University of Campinas (UNICAMP) under supervision of Prof. Dr. Irani Quagio-Grassiotto. The title of my master thesis was "Changes in the male germinal epithelium, interstitial cells and gonadotropic cells during the annual reproductive cycle of *Serrasalmus spilopleura* and *Pimelodus maculatus*." In 2006, I was honored to have in my master thesis defense, Prof. Dr. Luiz Renato de França, considered one of the most important researchers on male reproductive biology in Brazil. After finishing my master studies (2006), I moved to Belo Horizonte ("Beautiful Horizon", the capital city of Minas Gerais State), where I started my internship in Prof. de França's laboratory at the Federal University of Minas Gerais with an extensive training on male reproductive biology, focusing on spermatogonial stem cell transplantation. As scientific mentor, Prof. de França gave me many opportunities to learn and to develop self-confidence. One of these opportunities came with the possibility to do PhD studies in The Netherlands. In September 2008, I joined the Division Endocrinology and Metabolism, which is now part of the Division of Developmental Biology headed by Prof. Dr. Sander van den Heuvel, to start PhD studies under supervision of Dr. Rüdiger Schulz and Dr. Jan Bogerd.. After all these years, I'm very happy to have concluded my thesis presented here about spermatogonial stem cells and their endocrine and paracrine regulation in zebrafish.

Hinfray, N. ; **Nobrega, R. H.** ; Caulier, M. ; Baudiffier, D. ; Maillot-Marechal, E. ; Chadili, E. ; Palluel, O.; Porcher, J.-M. ; Schulz, R. ; Brion, F. Cyp17a1 and Cyp19a1 in the zebrafish testis are differentially affected by stradiol. Journal of Endocrinology JCR, v. 1, p. 1-3, 2013.

Morais, R. D. V. S. ; **Nobrega, R. H.** ; Gomez-Gonzalez, N. E. ; Schmidt, R. ; Bogerd, J.; Franca, L. R. ; Schulz, R. W. Thyroid Hormone Stimulates the Proliferation of Sertoli Cells and Single Type A Spermatogonia in Adult Zebrafish (*Danio rerio*) Testis. Endocrinology (Philadelphia) JCR, v. 1, p. 1, 2013.

Honji, Renato Massaaki ; **Nóbrega, Rafael Henrique** ; Pandolfi, Matias ; Shimizu, Akio ; Borella, Maria Inês ; Moreira, Renata Guimarães. Immunohistochemical study of pituitary cells in wild and captive *Salminus hilarii* (Characiformes: Characidae) females during the annual reproductive cycle. SpringerPlus, v. 2, p. 460, 2013.

Quagio-Grassiotto, Irani ; Grier, Harry ; Mazzoni, Talita Sarah ; **Nóbrega, Rafael Henrique** ; de Arruda Amorim, João Paulo . Activity of the ovarian germinal epithelium in the freshwater catfish, *Pimelodus maculatus* (Teleostei: Ostariophysi: Siluriformes): Germline cysts, follicle formation and oocyte development. Journal of Morphology (1931. Print) JCR, p. n/a-n/a, 2011.

Nobrega, R. H. ; Skaar, K. S. ; Magaraki, A. ; Olsen, L. C. ; Schulz, R. W. ; Male, R. . Proteolytically Activated, Recombinant Anti-Mullerian Hormone Inhibits Androgen Secretion, Proliferation, and Differentiation of Spermatogonia in Adult Zebrafish Testis Organ Cultures. Endocrinology (Philadelphia) JCR, v. 152, p. 1-14, 2011.

Schulz, Rüdiger W. ; de França, Luiz Renato ; Lareyre, Jean-Jacques ; LeGac, Florence ; Chiarini-Garcia, Helio ; **Nobrega, Rafael Henrique** ; Miura, Takeshi . Spermatogenesis in fish. General and Comparative Endocrinology (Print) JCR, v. 165, p. 390-411, 2010.

Garcia-Lopez, A. ; de Jonge, H. ; **Nobrega, R. H.** ; de Waal, P. P. ; van Dijk, W. ; Hemrika, W. ; Taranger, G. L. ; Bogerd, J. ; Schulz, R. W. . Studies in Zebrafish Reveal Unusual Cellular Expression Patterns of Gonadotropin Receptor Messenger Ribonucleic Acids in the Testis and Unexpected Functional Differentiation of the Gonadotropins. Endocrinology (Philadelphia) JCR, v. 151, p. 2349-2360, 2010.

Nóbrega, Rafael Henrique ; Greebe, Caaj Douwe ; van de Kant, Henk ; Bogerd, Jan ; de França, Luiz Renato ; Schulz, Rüdiger W. . Spermatogonial Stem Cell Niche and Spermatogonial Stem Cell Transplantation in Zebrafish. Plos One JCR, v. 5, p. e12808, 2010.

Leal, M. C. ; Cardoso, E. R. ; **Nobrega, R. H.** ; Batlouni, S. R. ; Bogerd, J. ; Franca, L. R. ; Schulz, R. W. Histological and Stereological Evaluation of Zebrafish (Danio rerio) Spermatogenesis with an Emphasis on Spermatogonial Generations. Biology of Reproduction JCR, v. 81, p. 177-187, 2009.

Nóbrega, R. H. ; Batlouni, S. R. ; França, L. R. . An overview of functional and stereological evaluation of spermatogenesis and germ cell transplantation in fish. Fish Physiology and Biochemistry JCR, v. 35, p. 197-206, 2009.

Batlouni, S. R. ; **Nóbrega, R. H.** ; França, L. R. . Cell junctions in fish seminiferous epithelium. Fish Physiology and Biochemistry JCR, v. 35, p. 207-217, 2009.

Nóbrega, R. H. ; Quagio-Grassiotto, I. Morphofunctional changes in Leydig cells throughout the continuous spermatogenesis of the freshwater teleost fish, *Serrasalmus spilopleura* (Characiformes, Characidae): an ultrastructural and enzyme study. Cell and Tissue Research (Print) JCR, v. 329, p. 339-349, 2007.

Book Chapters

Schulz, R. W. ; **Nóbrega, Rafael Henrique**. Anatomy and Histology of Fish Testis. In: Anthony P. Farrell. (Org.). Encyclopedia of Fish Physiology- From Genome to Environment. 2011.

Schulz, R. W. ; **Nóbrega, Rafael Henrique** . Regulation of Spermatogenesis. In: Anthony P. Farrell. (Org.). Encyclopedia of Fish Physiology - From Genome to Environment. 2011.

Leal, M. C. ; **Nóbrega, R. H.** ; Franca, L. R. . Spermatogenesis in fsh: structural and functional basis for applied research. In: Tiersch; Green. (Org.). (Org.). Cryopreservation of Aquatic Species. 2ed.: , 2009, v. , p. 1-5.